Quantum Phenomena in the Realm of Cosmology and Astrophysics

Christine Gruber

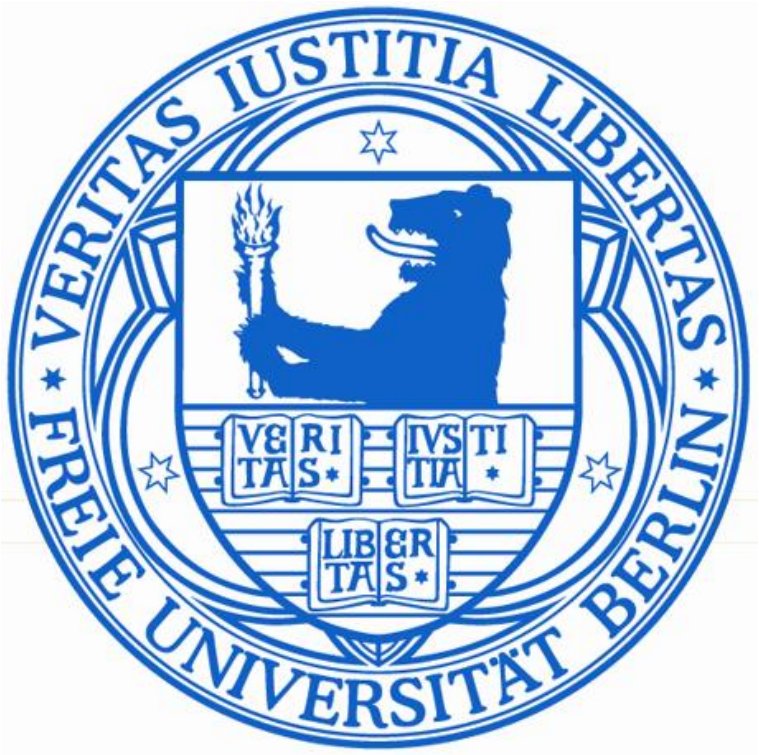

im Fachbereich Physik der Freien Universität Berlin
eingereichte Dissertation
Oktober 2013

Abgabe: 31.10.2013
Disputation: 11.12.2013

Erstgutachter: Prof. Dr. Dr. h.c. mult. Hagen Kleinert

Zweitgutachter: Prof. Dr. Dieter Breitschwerdt

Die in vorliegender Dissertation dargestellte Arbeit wurde in der Zeit zwischen September 2010 und Oktober 2013 im Fachbereich Physik an der Freien Universität Berlin unter Betreuung von Prof. Dr. Dr. h.c. mult. Hagen Kleinert durchgeführt.

Die Promotion wurde im Rahmen des Erasmus Mundus Joint Doctorate–Programms mit dem Grant Nummer 2010-1816 der EACEA der Europäischen Kommission unterstützt.

Selbstständigkeitserklärung

Hiermit versichere ich, die vorliegende Arbeit ohne unzulässige Hilfe Dritter und ohne Benutzung anderer als der angegebenen Hilfsmittel angefertigt zu haben. Die aus fremden Quellen direkt oder indirekt übernommenen Gedanken sind als solche kenntlich gemacht. Die Arbeit wurde bisher weder im In- noch im Ausland in gleicher oder ähnlicher Form einer anderen Prüfungsbehörde vorgelegt.

Berlin, 31.10.2013

Christine Gruber

Abstract

The success of modern physical theories is abundantly demonstrated by an impressive amount of examples, may it be in the small dimensions of the quantum world or on cosmologically large scales. Quantum mechanics and quantum field theories provide excellent descriptions for all kinds of quantum phenomena, while dynamics on the largest known scales can be well explained by Einstein's theory of General Relativity. However, attempts to unify these opposite ends of the spectrum into one ultimate physical theory have failed so far. Nevertheless, the physics on one scale can have considerable impact on others. In this dissertation, we will - in the framework of existing theories - consider scenarios where quantum effects have consequences on astrophysical or cosmological scales.

In one of these examples, we will develop a model for dark energy, i.e. the cause of the accelerated expansion of the universe, by calculating the vacuum fluctuations of quantum fields. We set up a scheme in which the divergent vacuum energy is tuned down to a finite small value by considering the opposite sign contributions of bosons and fermions. This vacuum energy can then explain the observed expansion behavior of the universe.

Experimentally, the magnitude of the cosmic acceleration can be obtained through the investigation of observational data like the luminosity of supernova events in the universe. Therefore, a part of this dissertation is dedicated to the analysis of experimental data in the framework of cosmography, a procedure to extract physical parameters from experimental data without assuming a particular model for the evolution of the universe a priori. As a result, we obtain kinematical constraints on the cosmic acceleration and therefore on the specific properties of its origin. We confirm the validity of the vacuum energy of quantum fields as a possible candidate to explain the behaviour of the cosmic expansion.

Ultimately, we turn our attention to a quantum phenomenon in astrophysics, i.e. the occurrence of a Bose-Einstein condensed phase of the matter within compact objects such as white dwarfs. Conditions in these environments allow for the formation of Bose-Einstein condensates due to a favourable combination of temperature and density, and thus it is of interest to study the condensation of bosonic particles under the influence of gravity in the framework of a Hartree-Fock theory. The resulting configurations are compared to observations via the predicted density profiles and macroscopic properties like the mass and size of the objects.

Zusammenfassung

Der Erfolg moderner physikalischer Theorien lässt sich anhand einer beeindruckenden Zahl an Beispielen von den kleinen Dimensionen der Quantenwelt bis zu kosmologischen Größenordnungen belegen. Die Quantenmechanik und Quantenfeldtheorien liefern hervorragende Beschreibungen für alle Arten von Quantenphänomenen, während die Dynamiken der größten Skalen von Einsteins allgemeiner Relativitäetstheorie weitgehend beschrieben werden können. Bisherige Bestrebungen, die beiden Theorien miteinander zu verknüpfen, scheiterten jedoch. Nichtsdestotrotz können physikalische Vorgänge in einem Bereich der Skala beträchtlichen Einflußauf andere Größenordnungen haben. In dieser Dissertation werden - im Rahmen existierender physikalischer Theorien - einige Beispiele untersucht, in denen Quanteneffekte in astrophysikalischen oder kosmologischen Situationen eine Rolle spielen. In einem dieser Szenarien wird ein Modell zur Erklärung der dunklen Energie entwickelt, die für die beschleunigte Ausdehnung des Universums verantwortlich ist, in dem Vakuumfluktuationen von Quantenfeldern berechnet werden. Berücksichtigt man die Beiträge von Bosonen und Fermionen zur Vakuumenergie, die entgegengesetzte Vorzeichen tragen, so kann die divergente Vakuumenergie auf einen kleinen endlichen Wert reguliert werden, der die beobachtete Größe der Expansion des Universums ergibt. Experimentell kann das Ausmaß der kosmischen Beschleunigung durch die Untersuchung von astrophyikalischen Daten abgeschätzt werden. Ein Teil dieser Dissertation wurde deshalb der Analyse von experimentellen Daten im Rahmen der Kosmographie gewidmet, einer Methode zur Extraktion physikalischer Parameter aus Daten, ohne ein bestimmtes Modell zur Erklärung der Daten vorauszusetzen. Die aus diesen Auswertungen erhaltenen kinematischen Randbedingungen für ein Modell der dunklen Energie befinden die Erklärung der kosmischen Expansion durch die Vakuumenergie von Quantenfeldern für gültig. Schließlich wird ein weiteres Quantenphänomen in astrophysikalischen Zusammenhängen untersucht, nämlich das Auftreten von Bose-Einstein-Kondensation im Inneren von kompakten Objekten wie weißen Zwergen. Die Formation eines derartigen Kondensats aufgrund einer günstigen Kombination von Temperatur und Dichte rechtfertigt die Untersuchung eines Systems aus bosonischen Teilchen unter dem Einfluß von Gravitation im Rahmen einer Hartree-Fock-Theorie. Die resultierenden Dichteprofile innerhalb des Sterns und makroskopische Größen wie die Masse oder den Radius der Konfigurationen werden anschließend mit Beobachtungen verglichen.

Contents

Part I.

Introduction

1. Basic Foundations and Outlook

This doctoral thesis is the result of three different projects pursued with the common aim of investigating quantum effects in cosmology and astrophysics. Two of them use theoretical models to deal with the occurrence of quantum phenomena in the context of cosmology and astrophysics, whereas the third provides an experimental background and motivation to one of them.

All work presented in this dissertation is based on the framework of the so-called ΛCDM model, the currently most accepted concordance model of cosmology, which - apart from a few open issues - describes well what we see in experiments and observations, and will be elaborated in detail in the following section. Even though the ΛCDM model is not completely successful in its description of the observable universe, and cannot be considered a fundamental theory by itself, it is assumed that any more fundamental model of physics would incorporate the ΛCDM as a limiting case. For cosmology it is the most viable and successful phenomenological model to work with, and thus provides a solid basis for the investigations carried out in this dissertation.

1.1. The ΛCDM model

The current concordance model of cosmology is based on the theory of general relativity as the underlying theory of gravity. In the present section, we will describe its most important aspects as well as some of its known weaknesses. Einstein's theory of General Relativity links the classical motion of massive objects in space and time to the geometry they are moving in, and draws a context between the mass of an object and its effect on the curvature of the spacetime it is embedded in. According to this theory, massive objects distort and curve spacetime, and thus the motion of an object appears curved when it actually follows the straightest path on a curved background [1]. Even though the limitations of the theory are well known by now, for instance the shortcomings in describing some of the large-scale phenomena in the universe, and obstacles to its quantization in analogy with other field theories, it is still regarded as a very successful theory. It is tested to work well

in a large range of situations, and it serves as a basic building block in constructing more advanced theories which eventually should be valid at both large and small length scales. The interplay between the energy content of the universe contained in massive (and massless) objects, and the global spacetime of the universe is described by Einstein's field equation,

$$G_{\mu\nu} = \frac{8\pi G_N}{c^4} T_{\mu\nu} \,. \tag{1.1}$$

In this tensor equation, $G_{\mu\nu}$ is the Einstein tensor describing the curvature of spacetime. The energy-momentum tensor $T_{\mu\nu}$ on the right hand side represents the energy content within that spacetime, G_N is Newton's gravitational constant, and c the speed of light. The equation links the properties of spacetime to the properties of matter and energy present in that spacetime.

Formally, the Ricci tensor is a contraction of the four-dimensional Riemann curvature tensor, which can be in turns expressed in general in terms of the affine connection ${\Gamma_{\mu\nu}}^{\lambda}$,

$${\Gamma_{\mu\nu}}^{\lambda} = \frac{1}{2} g^{\lambda\rho} (g_{\rho\mu,\nu} + g_{\rho\nu,\mu} - g_{\mu\nu,\rho}) \,, \tag{1.2}$$

defining the way vectors are parallel transported in different coordinate systems x^μ and x'^ν. The comma in $g_{\rho\mu,\nu}$ denotes covariant derivative, so that $g_{\rho\mu,\nu} = \partial_\nu \, g_{\rho\mu}$. The ${\Gamma_{\mu\nu}}^{\lambda}$ can be considered as the matrix elements of four 4×4-matrices, written as [2]

$${\Gamma_{\mu\nu}}^{\lambda} = (\Gamma_\mu)^\lambda_\nu = \mathbf{\Gamma}_\mu \,. \tag{1.3}$$

The Riemann curvature tensor $R_{\mu\nu\lambda}{}^{\kappa} = (\mathbf{R}_{\mu\nu})_\lambda{}^\kappa$ can be formulated in terms of the matrices $\mathbf{\Gamma}_\mu$ in a very intuitive form as

$$\mathbf{R}_{\mu\nu} = \partial_\mu \mathbf{\Gamma}_\nu - \partial_\nu \mathbf{\Gamma}_\mu - \left[\mathbf{\Gamma}_\mu, \mathbf{\Gamma}_\nu\right] , \tag{1.4}$$

where the square brackets denote the commutator. The Ricci tensor is then defined as a trace of the Riemann curvature tensor,

$$R_{\mu\nu} = -{R_{\sigma\mu\nu}}^{\sigma} \,, \tag{1.5}$$

from which the scalar curvature R is obtained by another contraction,

$$R = R^\mu_\mu = g^{\mu\nu} R_{\mu\nu} \,. \tag{1.6}$$

Note that in this notation the curvature of a sphere is positive, due to the additional negative sign which comes in due to the choice of co- and contravariant indices, whereas using the definition as given e.g. in Ref. [3] leads to a negative curvature of a sphere. The Einstein tensor is then given as

$$G_{\mu\nu} = R_{\mu\nu} - \frac{1}{2} g_{\mu\nu} \, R \,. \tag{1.7}$$

The metric tensor $g_{\mu\nu}$ contains all information about the geometry and causal structure of the universe. For flat spacetime, it is simply given by the Minkowski metric,

$$\eta_{\mu\nu} = \begin{pmatrix} -1 & 0 & 0 & 0 \\ 0 & 1 & 0 & 0 \\ 0 & 0 & 1 & 0 \\ 0 & 0 & 0 & 1 \end{pmatrix} . \tag{1.8}$$

The metric can also be formulated using the expression of an infinitesimal coordinate displacement ds^2 as

$$ds^2 = \eta_{\mu\nu} dx^\mu dx^\nu . \tag{1.9}$$

In the case of flat spacetime, the displacement is

$$ds^2 = -dt^2 + dx^2 + dy^2 + dz^2 , \tag{1.10}$$

which can be also written in spherical coordinates as

$$ds^2 = -dt^2 + dr^2 + r^2(d\theta^2 + \sin^2\theta d\phi^2) = -dt^2 + dr^2 + r^2 d\Omega^2 . \tag{1.11}$$

The most commonly used form of spacetime in cosmology is however not the Minkowski, but the Friedmann-Lemaître-Robertson-Walker (FLRW) metric [4],

$$ds^2 = -c^2 dt + a(t)^2 \left[dx^2 + dy^2 + dz^2\right] . \tag{1.12}$$

The time-dependence of the spatial part of the metric is parametrized by the so-called scale factor $a(t)$, a dimensionless scaling quantity, whereas the temporal part of the metric evolves linearly. This metric is an exact solution to the Einstein equation describing an isotropic and homogeneous universe with arbitrary but constant curvature. Curvature is accounted for by the factor k, incorporated in the metric (in the example of spherical symmetric coordinates) as

$$d\Sigma^2 = \frac{dr^2}{1 - kr^2} + r^2 d\Omega^2 . \tag{1.13}$$

For k assuming the values 1, 0 or -1 the asymptotic behaviour of the universe is open, flat or closed, i.e. the expansion of the universe after the big bang is approaching a constant velocity, slowing down to zero velocity or reversing itself to contract again.

The energy-momentum tensor describes the energy content of the system in question. It takes into account the microphysics determining the macroscopical behaviour of a substance, and contains information about its composition and structure. The simplest example is that of a non-interacting complex massive scalar field, for which the energy-momentum tensor reads

$$T_\phi^{\mu\nu} = \left(g^{\mu\alpha} g^{\nu\beta} + g^{\mu\beta} g^{\nu\alpha} - g^{\mu\nu} g^{\alpha\beta}\right) \partial_\alpha \bar{\phi}\, \partial_\beta \phi - m^2\, \bar{\phi}\, \phi . \tag{1.14}$$

It can be derived from the variation of the Lagrangian describing the system in question,

$$T_{\phi}^{\mu\nu} = \frac{2}{\sqrt{-g}} \frac{\partial \left(\mathcal{L}_{\phi}\sqrt{-g}\right)}{\partial g_{\mu\nu}} \,, \tag{1.15}$$

where the Lagrangian of a complex massive scalar field reads

$$\mathcal{L}_{\phi} = g^{\mu\nu}\partial_{\mu}\bar{\phi}\,\partial_{\nu}\phi - m^2\,\bar{\phi}\,\phi \,. \tag{1.16}$$

In cosmology, it is common to use perfect fluids to include various kinds of substances, such as e.g. radiation or matter. Perfect fluids are described by the energy-momentum tensor

$$T^{\mu\nu} = \left(\rho + \frac{p}{c^2}\right) u^{\mu}u^{\nu} + p\, g^{\mu\nu} \,, \tag{1.17}$$

where u^{μ} is the four-velocity, ρ is the energy density and p is the pressure of the fluid. In this context the equation of state of a perfect fluid is defined as

$$p = \omega\rho \,, \tag{1.18}$$

with ω being an equation of state (EoS) parameter that may take different values for different kinds of fluids.
Einstein's field equations can be derived from the Einstein-Hilbert action,

$$S_{\mathrm{EH}} = \frac{1}{2\kappa}\int d^D x\,\sqrt{-g}\,R \,, \tag{1.19}$$

using the principle of minimal action. Here, the abbreviation $\kappa = 8\pi G_N/3c^4$ was introduced. The principle of minimal action states that the classically followed path of a system is the one which minimizes the action. By varying the above action with respect to the metric $g_{\mu\nu}$, the Einstein equation in vacuum is obtained,

$$G_{\mu\nu} = 0 \,. \tag{1.20}$$

Including a Lagrangian function $\mathcal{L}_{\mathrm{m}}$ describing energy or matter content into the action,

$$S = \frac{1}{2\kappa}\int d^D x\,\sqrt{-g}\left[R + \mathcal{L}_{\mathrm{m}}\right] , \tag{1.21}$$

the commonly known Einstein equation with the energy-momentum tensor is recovered,

$$G_{\mu\nu} = \kappa\, T_{\mu\nu}^{(\mathrm{m})} \,, \tag{1.22}$$

where the energy-momentum tensor is given by

$$T_{\mu\nu}^{(\mathrm{m})} = \frac{2}{\sqrt{-g}} \frac{\partial \left(\mathcal{L}_{\mathrm{m}}\sqrt{-g}\right)}{\partial g_{\mu\nu}} \,. \tag{1.23}$$

The presence of a *negative* constant term Λ in the Einstein-Hilbert action leads to the ΛCDM action,

$$S_{\Lambda\mathrm{CDM}} = \frac{1}{2\kappa}\int d^D x\,\sqrt{-g}\left[R - 2\Lambda + \mathcal{L}_\mathrm{m}\right]. \tag{1.24}$$

The constant Λ results, after variation with respect to the metric, in an additive term on the left hand side of the Einstein equations,

$$G_{\mu\nu} + \Lambda g_{\mu\nu} = \kappa T^{(\mathrm{m})}_{\mu\nu}\,. \tag{1.25}$$

Such a term is generally named a cosmological constant term, and simulates a fluid with constant negative energy density, as we will see in the following. Eq. (1.24) is the action of the ΛCDM model, currently accepted to be the concordance model of cosmology. We will comment further on the matter content described by the Lagrangian $\mathcal{L}_\mathrm{m}$ at a later point. Eq. (1.25) can be adapted to depict the particular choice of a homogeneous and isotropic universe by employing the FLRW-metric with constant curvature k. Assuming the energy-momentum tensor Eq. (1.17), describing an ideal fluid with energy density ρ and pressure p, and the existence of the cosmological constant Λ, from the 00-component and the trace of Eq. (1.25), we end up with the Friedmann equations [4]:

$$H^2 = \left(\frac{\dot{a}}{a}\right)^2 = \frac{8\pi G_N}{3c^2}\rho - \frac{kc^2}{a^2} + \frac{\Lambda c^2}{3}\,, \tag{1.26a}$$

$$\dot{H} + H^2 = \frac{\ddot{a}}{a} = -\frac{4\pi G_N}{3c^2}\left(\rho + \frac{3p}{c^2}\right) + \frac{\Lambda c^2}{3}\,. \tag{1.26b}$$

Combining the two equations by using the Hubble parameter H defined by Eq. (1.26a) in Eq. (1.26b), we obtain an equation of mass-energy conservation in the universe,

$$\dot{\rho} = -3H\left(\rho + p\right)\,. \tag{1.27}$$

In general, the fluid can be anything - pure radiation, pure dust, or a mixture, i.e. energy density and pressure come from different components. If the fluid is solely assembled from one species of particles, the behaviour in an expanding background can be derived easily, and Eq. (1.27) can be restated as

$$\frac{1}{a^3}\frac{\partial(\rho a^3)}{\partial t} = -3\,\frac{\dot{a}}{a}\,p\,. \tag{1.28}$$

The equation of state for different species, $p = \omega\rho$, is known from thermodynamical derivations, with ω containing the ratio of specific heats for the fluid. For radiation, $\omega = 1/3$, while for nonrelativistic matter $\omega \simeq 0$. Using this information, it can be inferred that the energy density of radiation scales like $\rho_\mathrm{r} \propto a^{-4}$ in the expanding FLRW-background, while for matter the relation is $\rho_\mathrm{m} \propto a^{-3}$. Expressing the relation in a general form, and

solving Eq. (1.28) using Eq. (1.18), the energy density of a fluid with an equation of state parameter ω behaves like

$$\rho \propto a^{-3(1+\omega)} . \tag{1.29}$$

The Friedmann equation can thus be restated in terms of separate densities for radiation ρ_r and matter ρ_m as

$$H^2 = \kappa \left(\frac{\rho_\mathrm{r}}{a^4} + \frac{\rho_\mathrm{m}}{a^3} \right) - \frac{kc^2}{a^2} + \frac{\Lambda c^2}{3} . \tag{1.30}$$

Assuming the universe at a certain time to be dominated by a fluid with equation of state parameter ω, the Friedmann equation reduces to

$$H^2 = \left(\frac{\dot{a}}{a} \right)^2 = \kappa \, a^{-3(1+\omega)} . \tag{1.31}$$

Solving this differential equation for $a(t)$ is straightforward, and results in

$$a(t) \propto t^{\frac{2}{3(1+\omega)}} . \tag{1.32}$$

For a radiation-dominated universe, the scale factor expands like $a_r(t) \propto t^{1/2}$, while for matter-dominance, one finds $a_m(t) \propto t^{2/3}$.
Another situation worth investigating is the case of a negative equation of state parameter. Assuming an equation of state of $p = -\rho$ leads to a scaling of the energy density of such a fluid of

$$\rho \propto a^{-3(1+\omega)} = a^0 \sim \text{const.}, \tag{1.33}$$

i.e. the energy density of the fluid remains constant with the expansion of the universe. This is called de Sitter behaviour, and by solving Eq. (1.31) we see that the scale factor grows exponentially in this case,

$$a_{dS}(t) \propto e^t . \tag{1.34}$$

It corresponds to the behaviour of a cosmological constant in the Friedmann equation, and so Λ is equivalent to a fluid with $\omega = -1$.
In 1998 and 1999, the astrophysical observations of two separate groups of scientists, the *High-z Supernova Search Team* [5], and the *Supernova Cosmology Project* [6], were published indicating the fact that the universe is currently expanding at an accelerating pace. This conclusion was extracted from the observations of Type Ia supernovae events at various redshifts, measuring the luminosity of these supernovae as a function of their redshift. The findings made quite an impact on the astrophysical and cosmological community, since up to that point of time the universe was believed to be in a matter-dominated stage, which drives the expansion of the universe with a constant or decelerating pace, and depending on the total amount of matter and radiation admits an open, flat or closed evolution of

the universe. However, the data are hinting at an on-going transition from a matter-dominated into another stage of evolution, dominated by an as of yet unknown substance with constant energy density and a negative equation of state parameter $\omega = -1$, resulting in dynamics which a matter-dominated universe could not explain. In the years following the publications [5, 6], other experiments confirmed and consolidated the discoveries of the earlier analyses, and by today the acceleration of the expansion of the universe is an accepted feature of current cosmological models, including the ΛCDM. Evidence and discussions can be found in the publications [7–9], from the WMAP collaboration [10] or the Planck collaboration [11].

There are several works [12–16], which aim at quantitatively extracting the exact dynamics and kinematics of the accelerated expansion from data, within the framework of a branch of cosmology called cosmography. The analysis strives to describe the kinematical features of the expansion of the universe without the assumption of a particular model *a priori*; i.e. carrying out the analysis of data from a viewpoint which is as neutral as possible, and avoiding the need to choose an underlying model of cosmology. From such investigations, it is possible to obtain information on the equation of state of the universe, and constraining the specific properties of the underlying mechanism for the accelerated expansion.

From those cosmographic analyses, which are in detail described in Part III of this thesis, the current equation of state parameter of the total universe is predicted to be $\omega = -0.7174^{+0.0922}_{-0.0964}$ [15]. This is a value that describes the universe as one single ideal fluid, being a mixture of radiation, matter and some unknown, but, as it seems, pre-dominant, substance.

More model-dependent analyses, as e.g. the one of the Planck collaboration [11], predict similar values for the parameter ω, assuming the validity of the ΛCDM model. As already described, the ΛCDM model features a cosmological constant in order to explain the dark energy phenomenon, and matter contributions described by the Lagrangian $\mathcal{L}_{\mathrm{m}}$, containing the standard model particle content of the universe representing the small amount of baryonic matter and an unknown substance dubbed dark matter, whose existence was postulated in order to explain the observed rotation curves of galaxies and the acoustic peaks of the CMB temperature spectrum. Dark matter is, besides dark energy, yet another unexplained feature of the ΛCDM, introduced ad hoc to account for observations, but without microphysical motivation. It is assumed to consist of particles which are only weakly or non-interacting with normal matter, and is therefore hard to detect. It is postulated to form large lumps at the center of galaxies and large scale structures, thus explaining the observed innergalactic dynamics. Since both dark energy and dark matter seem to be needed on an observational level but are yet unknown in nature and origin, their combined existence is dubbed the dark sector of cosmology. The contributions of baryonic and dark

matter are estimated in the analysis of the Planck collaboration as $\Omega_M = 31.75\%$, and the cosmological constant is assumed to make up about $\Omega_\Lambda = 68.25\%$. The equation of state of the universe in the ΛCDM model can be given considering these contributions as

$$\omega = -\frac{1}{1 + \Omega_M/\Omega_\Lambda a^{-3}}\,, \tag{1.35}$$

which for the above values results in $\omega \simeq -0.68$.
The cosmological constant postulated in the ΛCDM model doesn't contain any information on its micro-physical background or origin, it is a phenomenological quantity motivated by observed features of the universe and requires yet to be derived and justified from a micro-physical theory. Some constraints on its physical nature can be obtained from experiments, but since the only information comes from indirect observations of its consequences, our knowledge about the origin of the effect stands on shaky grounds. Many theories put forward as its explaination are in accordance with observations, since the parameters to compare with the data are few, and this leads to a large degeneracy of models. Correspondingly, there has been an animated discourse and prosperous growth of the number of theories about the possible explaination to the phenomenon, and a fair evaluation of the models at hand and their success is definitely necessary, and may be provided by cosmography.

1.2. Contents

In this dissertation, we thus address some of the major concerns of modern cosmology. On the theoretical side, we successfully develop a model to explain dark energy by connecting it to a quantum theoretical phenomenon which has led to puzzles in quantum field theories. Among the abundance of models trying to explain this kinematic feature of the universe, one of them is to consider the vacuum fluctuations of quantum fields, an energy density constant in space as the origin of this expansion. The vacuum energy is a divergent quantity however, and is thus usually discarded as a possible explaination for dark energy. The huge discrepancy between an infinite value of the vacuum energy, or a very large finite value achieved by some kind of renormalization technique, and the tiny constant energy density driving the cosmic expansion, is termed the *hirarchy problem*. By balancing contributions of different quantum fields, a small finite value of the vacuum energy can be achieved, which can correctly account for the expansion of the universe. In this way, we find an explaination to the question of dark energy as well as manage to resolve the hirarchy problem in this context.

To complement this part of the work, we investigate the issue of the accelerated re-expansion of the universe from an observational point of view and improve conventional methods of data analysis to be able to extract the universe's kinematical properties from experimental results in the most independent way, in order to give the constraints that any viable theory of cosmology has to fulfill. We investigate observational data of the luminosity of type Ia supernovae events in order to obtain numerical fits for the parameters of the so-called cosmographic series, consisting of the Hubble parameter H_0, the acceleration parameter q_0, and further higher-order parameters describing the kinematical evolution of the universe. The conventional approach utilizes Taylor expansions of the relevant quantities for data fitting. We extend the existing analyses for several orders in the expansion, and suggest improvements to conventional cosmography by constructing alternatives to the commonly used redshift variable z, as well as by proposing a new method of expansion substituting the usual Taylor approach. Our results confirm the validity of the introduced modifications, as well as yield constraints on the kinematical properties of our universe, affirming the ΛCDM model to be in accordance with observations.
Yet another connection of a quantum phenomenon to large scale scenarios is the theory of the occurrence of a Bose-Einstein condensate in compact objects. We will investigate the impact of the occurrence of a BEC on the properties of objects such as white dwarfs, where conditions allow for the formation of BECs due to a favourable combination of temperature and density. Thus it is of interest to investigate the condensation of bosonic particles under the influence of hard-sphere scattering and gravitational interactions in the framework of a Hartree-Fock theory at finite temperatures. Results can be compared to observations through the computed density profiles and masses of the objects.

We will draw conclusions and ultimately summarize the work presented in the respective project at the end of each part, and comment on its significance and possible further extensions.

Part II.

Dark Energy from the Vacuum Energy of Quantum Fields

2. The Problem of Acceleration

In this part, we will develop a model in order to explain one of the major issues in modern cosmology, i.e. the problem of the accelerated re-expansion of the universe at late times, whose onset we are witnessing at the present time, and whose origin is still to be discovered. There is an abundance of proposals and approaches to the subject, the most famous being the aforementioned ΛCDM model, which features a cosmological constant Λ as the source of the cosmic acceleration. The most natural way to interpret the existence of a cosmological constant is in a quantum field theoretical context as the vacuum fluctuations of quantum fields of elementary particles - but there are major conceptual issues with this notion, as we will discuss in detail in the following. In the present work we will nevertheless strive to find a possibility to identify the vacuum fluctuations of quantum fields as the cosmological constant, despite some apparent obstacles.
In this chapter, we will give an overview of the abundance of models available in the literature to explain dark energy, and then describe the principles of the ansatz interpreting the vacuum energy as the source of cosmic expansion.

2.1. Existing Approaches

Apart from the ΛCDM model, there is a huge range of different proposals, stand-alone models, and generalizations or extensions of the ΛCDM model which aim at explaining the observed accelerated re-expansion in various ways and approaches. They can be roughly categorized into two classes - those that ascribe the cause for the expansion to an effect of space-time geometry, and those who postulate the existence of an unknown and yet undetected substance called *dark energy*. The first class addresses the problem by modifying or developing new or alternative theories of gravity, whereas the second class extends the energy content of the universe by an additional substance, the dark energy. There is a third class of approaches, which however does not acknowledge the observed acceleration as a new phenomenon, but interprets the effect for instance as a consequence of local inhomogeneities [17, 18], i.e. a statistical behavior that leads to the observed behavior. There are also theories which consider the accelerated expansion as a local phenomenon due to

inhomogeneities on small scales, leading to an apparent acceleration of expansion in the local void. Theories of this category lack a deeper physical conundrum - as opposed to the two categories above, which do assume the existence of new physics and the necessity to explain it.

The first class of approaches largely consists of models described by the term *modified gravity* - which comprises any theory of gravitation that takes Einstein's general relativity as a starting point and modifies parts of it in order to incorporate observed effects, thus leading to modified Einstein's field equations. But also new stand-alone models of gravity have been developed in order to account for the accelerated expansion.

The cosmological constant featured in the ΛCDM model would be a candidate of the first category, being incorporated into the theory by a constant positive term on the left hand side of Einstein's equations. However, there are several circumstances which make the seemingly straightforward introduction of a cosmological constant to the Einstein field equations a complicated endeavor facing unexpected problems raising more questions than it answers [19], for example the hierarchy problem which will be elaborated further in the next subsection, or the coincidence problem, i.e. the question why the acceleration of the universe's expansion happens just at the right moment for us to be observable.

In the context of modified gravity, even more issues arise to be answered, like the particular choice of the modification of Einstein, or the degeneracies of models, since many variations of the Einstein-Hilbert action reproduce cosmologies with the same or similar observational consequences. In conventional General Relativity, the field equations are derived from the Einstein-Hilbert action with the Lagrangian density $\mathcal{L} = \mathcal{R}$, which, when varied with respect to the metric $g_{\mu\nu}$, leads to the Einstein field equations without a cosmological constant. As opposed to the original form proposed by Einstein, the subclass of modified gravity dubbed $f(\mathcal{R})$ theories substitute the curvature scalar $\mathcal{R}$ in the integrand by a general function $f(\mathcal{R})$ of it, as for example the one proposed in [20], featuring a function of the curvature scalar which behaves as the Einstein-Hilbert action for small curvature and mimicks a cosmological constant for large curvature. An extensive review about $f(\mathcal{R})$-models is given in [21,22] and references therein. There have also been attempts to include other curvature-related quantities into the gravitational Lagrangian, the earliest proposals of this kind dating back to the seventies, and up to today being a very active field of research. Originating from these attempts, generalizations of Einstein's theory have been found, as e.g. Lovelock gravity [23], the most general theory of gravity using the metric as the variational variable, where the Lagrangian is given by a sum of contractions of the Riemann tensor formulated for a general number of spacetime dimensions $\mathcal{D}$, and yielding Einstein's general relativity in the limit of $\mathcal{D} = 4$. Gauss-Bonnet gravity is a special case of Lovelock gravity with a reduced number of terms in the sum, where the gravitational

Lagrangian consists of a combination of curvature scalar, Ricci tensor and Riemann tensor [24], whereas in conformal gravity the square of the Weyl tensor is used [25]. These are the tensorial generalizations of $f(\mathcal{R})$-theories. Beyond modifications of the gravitational Lagrangian, there are other ways to alter the gravitational field equations, e.g. by changing the principle of variation - such that variation of the action is not, or not exclusively, carried out with respect to the metric, but also other quantities. The so-called Palatini formalism [26] treats the metric and the affine connection Γ^i_{kl} as independent variables and varies the gravitational action with respect to both quantities separately. In another approach dubbed metric-affine gravity the matter Lagrangian is assumed to be dependent on the connection [27]. There have been suggestions to formulate gravity as a gauge theory [28,29], by introducing new gauge fields and covariant derivatives, usually formulated in terms of tetrads instead of a metric. Predictions of such theories agree widely with general relativity in the case of particles without spin, however, differ in the case of particles with nonzero spin, since the introduction of gauge fields results in a spin tensor as well as the commonly known energy-momentum tensor.

In principle, many theories of modified gravity and in particular $f(\mathcal{R})$-theories are able to reproduce the observed effect of accelerated expansion and the desirable cosmologies, with some of the approaches being more successful than others. S of these models rather aim at obtaining the correct phenomenological description of the observed universe, while others are developed in the quest of finding a unification of gravity and the other three fundamental forces of nature.

The second class of approaches to explain the observed acceleration modifies the right-hand side of the Einstein equation by introducing new kinds of substances with appropriate properties and equation of states, whose energy densities contribute to the overall energy content of the universe and thus cause the universe to expand at an accelerating pace. These new substances are generally referred to as dark energy, and have been proposed in various concepts and shapes [30,31]. Its most popular representative is quintessence [32,33], a massive scalar field with a varying equation of state parameter ω, which is determined by a kinetic term and the scalar field's potential in the action. Other proposals in this manner have been phantom energy [34], for which it is possible to have values of the equation of state parameter $\omega < -1$, or k-essence [35,36], short for kinetic quintessence, which has a slightly modified kinetic term for the field. Apart from considering scalar fields and their associated particles, also vector fields have been introduced, which lead e.g. to Scalar-Tensor-Vector gravity [37], featuring the metric and an additional vector field, in addition to promoting three natural constants, the gravitational constant G, the mass of the vector field μ and the coupling strength ω, to scalar fields. Besides explaining the accelerated expansion of the universe, this theory is in accordance to astrophysical observations also on the interstellar

and intergalactic level, i.e. provides an explanation for the existence of dark matter and reproduces the observed matter power spectrum and the cosmic microwave background spectrum. This is not the only theory to aim at explaining both the dark energy and the dark matter problem in one collective theory. Also the Tensor-Vector-Scalar theory [38] claims to unify the dark sector using a similar but distinct combination of scalar, dynamical scalar and vector fields to explain the accelerated expansion of the universe, and in the limit of weak gravity resulting in the MOdified Newtonian Dynamics (MOND) theory [39], proposed to explain the dark matter puzzle. There also exist theories like the so-called dark fluid [40], in which dark energy and dark matter are two phenomena which however originate in one common field and just represent two different manifestations of one theory on different spatial scales.

A third and completely different way to account for the observed acceleration is the argument of cosmic inhomogeneity. In general, on cosmological scales the universe is assumed to be homogeneous and isotropic; however, a local fluctuation of the overall density could lead to a variation in expansion behaviour in a small region around our position in the universe, and be falsely interpreted as a global cosmological effect, when it is in reality just a coincidental local phenomenon. It has been shown that the data can be explained by such a model in which we are assumed to be in the centre of a huge void, and thus see everything else recede from us in an accelerating manner [41]. However, this approach is somewhat unsatisfying in a scientific sense - it relies too much on a statement similar to the anthropic principle, i.e. we exist, therefore chance has put us into a spot with local under-density such that we observe what we observe, without the necessity to introduce new physics. It is not as elegant as if the effect would come out of an underlying, more fundamental theory, but can be shown to work.

2.2. A forgotten approach

A very natural candidate to explain dark energy originating from quantum field theory are the vacuum energy fluctuations of fields present in the universe [42]. This would be an approach which does not belong to either of the aforementioned categories, since it is neither a modification of General Relativity, nor has the necessity to introduce new fields which contribute to the energy density of the universe and give rise to new particles. The vacuum fluctuations of quantum fields, i.e. the nearly instantaneous creation and annihilation of a particle-antiparticle pair in accordance to Heisenberg's uncertainty relation, would have exactly the right behaviour in a cosmological context if interpreted as a perfect fluid, i.e. a constant energy density, similar to a cosmological constant, with a negative pressure driving

the expansion. Unfortunately the predictions for the contributions of quantum fields to the vacuum energy are divergent - or at least very large, depending on the specific calculation. The divergences are illustrated by the concept that in quantum field theory every point in space is pictured as the site of an infinitesimal quantum harmonic oscillator, which gives an infinitely large contribution to the energy of the vacuum in form of the harmonic oscillator ground state energy $\hbar\omega/2$ for every frequency $\omega \in [0, \infty)$. An infinite energy contribution from every point of an infinite space result in an infinite vacuum energy. To justify why the infinite amount of energy is not detectable, or better, why it is still possible to perform reasonable measurements on energies of particles despite this infinity, it is usually argued that in experiments only differences of energies can be detected, which is the basic principle of renormalization, i.e. the subtraction of "unphysical" infinities in calculations. That the vacuum energy of particles is real and not just a mathematical concept can be however proven by measurements of the so-called Casimir effect [43]. Due to resonances of the vacuum in between two metallic plates, a small attractive force is created which moves the plates towards each other. This is taken as the most direct evidence for the existence of vacuum fluctuations. Other indications would be the existence of Hawking radiation, i.e. the detection of one partner of the particle-antiparticle-pair created by a fluctuation, which had the chance to escape annihilation while its partner was sucked into an adjacent black hole [44]. This effect has however not been observed so far. Another conundrum is whether the particle-antiparticle pair during its short lifespan exerts a gravitational force. The expected effect on the expansion of the universe has in principle the correct sign, i.e. a negative pressure, however, since the vacuum energy is supposed to be infinite, and we are only able to detect differences in energies, we shouldn't be able to observe the accelerated expansion as a direct consequence of the fluctuations.

To get rid of those singularities in the vacuum energy, along the lines of renormalization a cutoff at Planck scale can be introduced, with the justification that the commonly accepted field theories for the description of physics at the microscopic scale are only applicable up to Planck scale, and beyond that a new unified theory is needed. A cutoff at Planck scale results in a vacuum energy density of $\rho_\Lambda^{(\mathrm{th})} = 10^{76}\,\mathrm{GeV}^4$. The infinities of the vacuum have thus been cut down to a finite value, which is however too large compared to the dark energy component detected from experiments, which amounts to a value of $\rho_\Lambda^{(\mathrm{obs})} = 10^{-47}\mathrm{GeV}^4$ [31]. The divergence, or at least the large magnitude of the vacuum fluctuations is a notorious weakness of quantum field theories, and the discrepancy of 123 orders of magnitude between the two values is called the *hierarchy problem*. It seems that despite the very promising properties of vacuum energy, it is not possible to explain the accelerated expansion of the universe by these fluctuations. The aim of this chapter is to explain the acceleration of the universe's expansion and solve the hierarchy problem after

all. We shall do this by developing a model able to reproduce the observed dynamics of expansion without any fundamentally new physics being involved, and only employing existing physics interpreted in a new way.

The divergence of the vacuum energy being considered an unphysical property needs to be argued away or eliminated by an appropriate choice renormalization. However, renormalization methods are usually very flexible; the divergences are subtracted or ignored, and the renormalized quantities can in most cases be adjusted easily to conform to experiments, e.g. by an appropriate choice of cutoff. We will instead accept the divergence of the vacuum energy and try to explain the non-zero but finite observed vacuum energy by some kind of mechanism which ensures a physically reasonable value despite the unphysical divergent contributions. A possible candidate for such a mechanism is provided by supersymmetry [45], a theory aiming at cancelling the vacuum energy contributions of fields with each other in order to get rid of the occurring divergences. In supersymmetric theories the Lagrangian obeys certain laws of symmetries between the bosonic and fermionic particles in the model, such that a correspondence between bosonic and fermionic 'superpartners' is established. Using the fact that the vacuum energies of bosons and fermions are of opposite signs, this correspondence can be employed in order to cancel all divergent contributions of particles to the vacuum energy. In maximally supersymmetric models, this balance is exact, whereas in other supersymmetric models the cancellation of contributions happens only partly. However, recent experiments indicate that the predictions of supersymmetric theories might not be in accordance with reality. It seems that the basic minimally supersymmetric models have been ruled out, e.g. by the report of the LHCb collaboration on the decay of B^0 into μ^+ and μ^- [46], which has been predicted correctly by the standard model of particle physics, but is in conflict with the expectations from many of the simpler supersymmetric models. In general the expected experimental confirmation of supersymmetric models has not happened [47]. Besides that, even in maximally supersymmetric models the universe at the present time is supposed to be in the state of broken symmetry, implying a imbalance between bosons and fermions and thus a divergent vacuum energy.

It is however possible to achieve the cancellation of the vacuum energy contributions of fields without the requirements of supersymmetry, only by appropriate choice of number and masses of the bosonic and fermionic fields present. With some fine tuning, the cancellation can be either made exact, or leave room for the observed cosmological constant. The reason for this possibility, and also for the success of supersymmetry, lies in the fact that bosons and fermions have opposite contributions to the vacuum energy. Bosons yield positive and fermions in negative vacuum energy, and thus there is the possibility for mutual cancellation of contributions. This is in analogy to the ground state energy of bosons and fermions in a harmonic oscillator, where $\hbar\omega/2$ is positive for bosons and negative for

fermions. Of course, the overall vacuum energy diverges without applying a renormalization scheme. As we will see later, in the case of the standard model, the fermionic contribution to the vacuum energy dominates, and thus we have to introduce further bosonic particles in order to achieve cancellation of both contributions to the vacuum energy. In order to produce a finite effect of expansion, it is necessary to retain a remainder of the order of the measured value of the cosmological constant $\rho_\Lambda^{(\mathrm{obs})}$. So also in our model it is necessary to introduce new particles - however, these are simply generic bosons as known from the standard model with the same thermal and quantum statistical properties, and not new exotic species of unfamiliar nature.
The contributions of different particles depend on the exact properties of boson or fermion, according to their degrees of freedom (dof). A single fermionic Dirac field ψ produces a vacuum energy that is twice as large and has opposite sign as that of a charged scalar field ϕ,

$$\rho_{\Lambda,\psi} = -2\rho_{\Lambda,\phi}\,, \tag{2.1}$$

or four times as large as the contribution of a neutral scalar field, and so forth. Contributions of vector or tensor bosons give a vacuum energy in the same direction as scalar bosons, but are multiplied by numerical factors according to their degrees of freedom.

This chapter is organized as follows. In Chapter 3 we state some general facts about the functional integral formulation of QFT for bosonic and fermionic fields and their vacuum energy, while in Chapter 4 we elaborate in more detail why the vacuum energy of fields is suitable as a candidate for dark energy, demonstrating the cancellation principle we will employ later. In Chapter 5 the generalisation to curved spacetimes will be done, and it will be shown that the occurring contributions of curvature in the cancellation conditions can help to produce the observed cosmological constant, to the advantage of having less fine-tuning for the masses of the fields present. In Chapter 6 we will provide the results for the curvature terms for a specific choice of metric, apply all the previous derivations and show that it is possible, by appropriate choice of masses and fields together with the curvature contributions, to explain the observed dark energy component of the universe. In Chapter 7 we conclude our work.

3. Vacuum energy of free bosons and fermions

In this chapter we will derive the basic expressions for the vacuum energy, or equivalently, the effective action, of bosonic and fermionic fields. The following definitions and derivations are part of standard quantum field theory, and can be found e.g. in [48]. Starting from the Lagrangian $\mathcal{L}$ for a generic field χ which can be bosonic or fermionic, we can formulate the so-called partition function Z of the system as a path integral over all possible field configurations, defined as

$$Z = \int \mathcal{D}\chi \, \mathcal{D}\bar{\chi} \, \exp\left[iS\right] = \int \mathcal{D}\chi \, \mathcal{D}\bar{\chi} \, \exp\left[i \int d^D x \, \mathcal{L}(\chi, \dot{\chi}, t)\right] . \tag{3.1}$$

In this case, we are assuming χ to be complex, and thus we have to carry out the integral not only over the field itself, but also over its complex conjugate $\bar{\chi}$. Carrying out these integrals requires some integrational methods and tricks, and differs for bosonic and fermionic fields depending on the specific Lagrangian, but usually includes the use of the Gaussian integral formula. The result can be expressed as the determinant of a matrix or function which is called the Greens function G of the system. In the following sections, we will see how exactly the path integral is calculated for particles of bosonic or fermionic nature, not including any interactions between the fields, but just considering free massive particles.
From the partition function, we can define the so-called effective action S_{eff} via

$$Z = e^{iS_{\text{eff}}} . \tag{3.2}$$

The effective action is a quantity introduced in quantum mechanics and quantum field theory to derive equations of motion for the vacuum expectation values (VEVs) of fields. Since all quantum fields are fluctuating, it is not possible to derive the equation of motion for the mean field value (=VEV) from the original action of the problem, since by the fluctuations the action contains an infinite amount of possible field configurations. However, the equation of motion for the VEV is derived from requiring that the effective action of the system be stationary.
We are interested in the effective action as it is the quantity which gives the contributions

of a field to the vacuum energy of a system. It is an energy in analogy to the free energy defined via

$$F = -k_B T \ln Z \,, \tag{3.3}$$

but with opposite sign. Bosons have positive vacuum energy, and thus a negative effective actions, whereas fermions with a negative vacuum energy have positive effective action. The primary interest in the following calculations will thus be to determine the effective action of a system of free particles, for the cases of bosons and fermions, for then we have found also the vacuum energy of the system, which can be directly compared to the cosmological constant that is deduced from experimental data. A cosmological constant Λ appears in the action of the theory as

$$S_\Lambda = -\frac{1}{\kappa}\int d^D x \sqrt{-g}\,\Lambda \,, \tag{3.4}$$

i.e. it has negative action. Calculating the effective actions of the bosons and fermions in the system, we can directly compare those contributions to the cosmological constant, and deduce which modifications of the standard model of particle physics would be necessary to obtain accordance with the cosmic expansion.

3.1. Bosonic fields

Starting with a free complex bosonic field ϕ with mass m_b, we can write the relativistic Lagrangian density as

$$\mathcal{L}_\mathrm{b} = \eta^{\mu\nu}(\partial_\mu\bar{\phi})(\partial_\nu\phi) - m_\mathrm{b}^2\,\bar{\phi}\phi \,, \tag{3.5}$$

where $\eta^{\mu\nu}$ is the Minkowski metric with signature $(+---)$, as defined in the introductory chapter. This leads to the action

$$S_\mathrm{b} = \int d^D x\sqrt{-\eta}\ \left[\eta^{\mu\nu}(\partial_\mu\bar{\phi})(\partial_\nu\phi) - m_\mathrm{b}^2\,\bar{\phi}\phi\right] . \tag{3.6}$$

By partial integration this can be recast as

$$S_\mathrm{b} = -\int d^D x\sqrt{-\eta}\ \bar{\phi}\left(\eta^{\mu\nu}\partial_\mu\partial_\nu + m_\mathrm{b}^2\right)\phi \,. \tag{3.7}$$

In this form, it is possible to read off the inverse Greens function of this system, which is defined as the operator between the two scalar fields in the exponent,

$$G_\mathrm{b}^{-1} := \eta^{\mu\nu}\partial_\mu\partial_\nu + m_\mathrm{b}^2 = \partial^2 + m_\mathrm{b}^2 \tag{3.8}$$

Here, $\partial^2 = \eta^{\mu\nu}\partial_\mu\partial_\nu$ denotes the contraction of two partial derivatives with the Minkowski metric, and $\eta = -1$ is the determinant of the Minkowski metric. The partition function then reads

$$Z_\mathrm{b} = \int \mathcal{D}\bar{\phi}\mathcal{D}\phi\, \exp\left[-i\int d^D x\sqrt{-\eta}\ \bar{\phi}\, G_\mathrm{b}^{-1}\,\phi\right] . \tag{3.9}$$

In order to process the functional integral over $\mathcal{D}\phi$ and $\mathcal{D}\bar{\phi}$ the integration formula for a Gaussian integral is used. It is possible to carry out the integration for arbitrary matrices $\mathbf{M} = G_{\mathrm{b}}^{-1}$ by diagonalising $\mathbf{M} = \mathcal{O}^T \mathbf{G} \mathcal{O}$ and then doing a substitution $y = \mathcal{O}\phi$. A path integral is defined as

$$\int \mathcal{D}\phi = \int \prod_k d\phi_k \equiv \int \prod_k dy_k \,. \tag{3.10}$$

For details, see the review paper in Ref. [49]. The path integral then becomes, for a diagonal matrix $\mathbf{G} = G_{kk}$,

$$\int \prod_{k=1}^{N} dy_k \exp\left[-i \int d^D x \sqrt{-\eta}\, G_{kk}\, y_k^2\right] , \tag{3.11}$$

and can be calculated with the help of the formula for a Gaussian integral to be

$$Z_{\mathrm{b}} = \prod_{k=1}^{N} \sqrt{\frac{2\pi}{G_{kk}}} = \frac{(2\pi)^{N/2}}{\sqrt{\prod_k G_{kk}}} \,. \tag{3.12}$$

Considering that $\mathbf{G}$ is diagonal with the same eigenvalues as those of G_{b}^{-1}, this means that the product of the diagonal elements of $\mathbf{G}$ is equal to the determinant of G_{b}^{-1}, and thus

$$Z_{\mathrm{b}} = \frac{(2\pi)^{N/2}}{\sqrt{\det G_{\mathrm{b}}^{-1}}} \propto \det G_{\mathrm{b}}^{1/2} \,. \tag{3.13}$$

This is the result for a single path integral - in the case of a complex scalar field, we have both integrals over the field and its complex conjugate, and so we end up with

$$Z_{\mathrm{b}} = \det G_{\mathrm{b}} \,. \tag{3.14}$$

Since for an even number of spacetime dimensions D an overall sign in the determinant can be eliminated, the above expression is equivalent to

$$Z_{\mathrm{b}} = \det\left[-G_{\mathrm{b}}^{-1}\right]^{-1} = \det\left[\partial^2 + m_{\mathrm{b}}^2\right]^{-1} \,. \tag{3.15}$$

The effective action is then, as from the definition above, the logarithm of the partition function,

$$S_{\mathrm{eff}}^{(\mathrm{b})} = -i \ln Z = -i \ln \det G_{\mathrm{b}} = i \ln \det\left[\partial^2 + m_{\mathrm{b}}^2\right] \,. \tag{3.16}$$

For a real scalar field, the Lagrangian and the functional integral look slightly different; as mentioned above, the functional integration leads to

$$Z_{\mathrm{b}} = \det G_{\mathrm{b}}^{1/2} \,, \tag{3.17}$$

and thus the effective action for a real scalar field reads

$$S_{\mathrm{eff}}^{(\mathrm{b})} = -i \ln \det G_{\mathrm{b}}^{1/2} = -\frac{i}{2} \ln \det G_{\mathrm{b}} = \frac{i}{2} \ln \det\left[\partial^2 + m_{\mathrm{b}}^2\right] \,. \tag{3.18}$$

3.2. Fermionic fields

For a free complex massive fermionic field ψ, the relativistic Lagrangian density comes from Dirac theory,

$$\mathcal{L}_{\rm f} = \bar{\psi}_i(i\gamma^a_{ij}\partial_a - m_{\rm f}\mathbf{1}_{ab})\psi_j = \bar{\psi}(i\partial\!\!\!/ - m_{\rm f}\mathbf{1})\psi\,, \tag{3.19}$$

where $\partial\!\!\!/ = \gamma^a_{ij}\partial_a$ is the Feynman-slashed derivative operator, and the γ_{ij} are the Dirac γ-matrices in flat spacetime. This Lagrangian leads to the functional integral

$$Z_{\rm f} = \int \mathcal{D}\bar{\psi}\,\mathcal{D}\psi\,\exp\left[i\int d^D x\sqrt{-\eta}\;\bar{\psi}\,G_{\rm f}^{-1}\,\psi\right]. \tag{3.20}$$

with the inverse Greens function, or propagator,

$$G_{\rm f}^{-1} := i\partial\!\!\!/ - m_{\rm f}\mathbf{1}\,. \tag{3.21}$$

For fermions the functional integral is calculated slightly differently, since fermions obey the Pauli principle, which forbids the existence of more than two fermions in the same place. The corresponding governing algebra is a Grassmannian one, i.e. the integral over a Grassmann variable is one, but the integral over the square of a Grassmann variable must vanish, since it is forbidden to have two fermions in the same state. The Gaussian integral over Grassmannian variables $\mathbf{x}$, $\mathbf{y}$ is defined as

$$\int d\mathbf{x}\,d\mathbf{y}\,\exp\left[\mathbf{x}^T\mathbf{A}\mathbf{y}\right] = \det\mathbf{A}\,, \tag{3.22}$$

and thus the partition function for a fermionic field reads (using the same substitution for the field into y as before and diagonalise the inverse Greens function)

$$\begin{aligned} Z_{\rm f} &= \int\prod_k d\bar{\psi}_k\,d\psi_k\,\exp\left[-i\int d^D x\,\sqrt{-\eta}\,\bar{\psi}\,G_{\rm f}^{-1}\,\psi\right] \\ &\propto \det G_{\rm f}^{-1}\,, \end{aligned} \tag{3.23}$$

with the inverse of the Greens function here being

$$G_{\rm f}^{-1} = i\partial\!\!\!/ - m_{\rm f}\mathbf{1}\,. \tag{3.24}$$

This is at first sight quite different to the expression for the bosonic field - not only is it the inverse expression of the bosonic partition function, but also it contains a first order differential operator, and not one of second order, as for the bosons. We can convert the expression for the fermions to a form that is more similar to the bosonic formulation. The inverse Greens function can be rewritten by simply arguing that for fermions described by the Dirac equation the energies are symmetric, and so

$$\det\left[i\partial\!\!\!/ - m_{\rm f}\mathbf{1}\right] = \det\left[-i\partial\!\!\!/ - m_{\rm f}\mathbf{1}\right] = \det\left[+i\partial\!\!\!/ + m_{\rm f}\mathbf{1}\right]\,, \tag{3.25}$$

with the last equality following from the fact that for an even number of spacetime dimensions, an overall sign in the determinant does not matter. So we can write

$$Z_{\mathrm{f}} = \det\left[i\partial\!\!\!/ - m_{\mathrm{f}}\mathbf{1}\right] = \det\left[\sqrt{(i\partial\!\!\!/ - m_{\mathrm{f}}\mathbf{1})(i\partial\!\!\!/ + m_{\mathrm{f}}\mathbf{1})}\right] = \det[\partial^2 + m_{\mathrm{f}}^2\mathbf{1}]^{1/2}\,. \tag{3.26}$$

Consequently, the effective action is

$$S_{\mathrm{eff}}^{(\mathrm{f})} = -i\,\ln Z = -i\ln\det G_{\mathrm{f}} = -i\ln\det[\partial^2 + m_{\mathrm{f}}^2\mathbf{1}]^{1/2} = -\frac{i}{2}\ln\det[\partial^2 + m_{\mathrm{f}}^2\mathbf{1}]\,. \tag{3.27}$$

For a real fermion field, i.e. uncharged spinors like Majorana fermions, the functional integral and thus the effective action again are modified by a factor of 1/2, i.e.

$$Z_{\mathrm{f}} = \det G_{\mathrm{f}}^{-1/2}\,, \tag{3.28}$$

which leads to an effective action for real spinor fields of

$$S_{\mathrm{eff}}^{(\mathrm{f})} = -i\ln\det G_{\mathrm{f}}^{-1/2} = -i\ln\det[\partial^2 + m_{\mathrm{f}}^2\mathbf{1}]^{1/4} = -\frac{i}{4}\ln\det[\partial^2 + m_{\mathrm{f}}^2\mathbf{1}]\,. \tag{3.29}$$

It becomes already clear that it is possible to cast the expressions for the effective action for bosonic and fermionic fields in quite similar shapes due to the advantageous properties of the logarithm. In the following, we will combine the expressions into a general effective action of a system of bosons and fermions.

3.3. Combining bosons and fermions

So far we derived the 1-loop contributions of bosonic and fermionic fields to the effective action, or equivalently to the vacuum energy of the universe, assuming the simplest models of free particles without any interaction terms. We have seen that we can write the partition function as the exponent of an effective action S_{eff}, which in the example of a complex bosonic field reads

$$Z_{\mathrm{b}} = e^{iS_{\mathrm{eff}}} = \det G_{\mathrm{b}} = \det[G_{\mathrm{b}}^{-1}]^{-1}\,, \tag{3.30}$$

By the identity

$$\ln\det\mathbf{A} = \ln\prod_i a_i = \sum_i \ln a_i = \mathrm{Tr}\ln\mathbf{A}\,, \tag{3.31}$$

which uses the fact that the determinant of a matrix $\mathbf{A}$ is given by the product of all eigenvalues a_i to transform the logarithm of the determinant into the trace of the logarithm of the matrix, we can write the effective action for bosons, and thus their vacuum energy, as

$$\begin{aligned} S_{\mathrm{eff}}^{(\mathrm{b})} &= i\ln\det G_{\mathrm{b}}^{-1} = i\ln\det\left[\partial^2 + m_{\mathrm{b}}^2\right] \\ &= i\mathrm{Tr}_{\mathrm{F}}\ln\left[\partial^2 + m_{\mathrm{b}}^2\right]\,. \end{aligned} \tag{3.32}$$

$\mathrm{Tr_F}$ denotes the trace over the D-dimensional functional space of the matrix G_b. Thanks to the property of the logarithm, it is possible to rewrite the logarithm of the determinant of the Greens function as the negative of the logarithm of the determinant of the inverse Greens function, and thus not only avoid the problem of finding the Greens function by inverting G_b^{-1}, but also bring the expressions for the effective actions into similar shapes. In the case of fermions, we have

$$\begin{aligned} S_\mathrm{eff}^{(\mathrm{f})} = -i \ln \det[G_\mathrm{f}^{-1}] &= -\frac{i}{2} \ln \det \left[\not{\partial}^2 + m_\mathrm{f}^2 \mathbf{1}\right] \\ &= -\frac{i}{2} \mathrm{Tr_{F,D}} \ln \left[\not{\partial}^2 + m_\mathrm{f}^2 \mathbf{1}\right] . \end{aligned} \tag{3.33}$$

For the fermions the trace denotes not only the integral over functional space, but also the trace over the Dirac indices μ. This is the same result as for the complex scalar field before, up to a multiplicative factor of $-1/2$, and a contraction of the four-derivative with the gamma matrices, which originates from Dirac theory for spinors. Taking the trace over Dirac space leads to an additional factor of four in the expression:

$$\begin{aligned} S_\mathrm{eff}^{(\mathrm{f})} &= -\frac{i}{2} \mathrm{Tr_{F,D}} \ln \left[\not{\partial}^2 + m_\mathrm{f}^2 \mathbf{1}\right] \\ &= -2i \,\mathrm{Tr_F} \ln \left[\partial^2 + m_\mathrm{f}^2\right] , \end{aligned} \tag{3.34}$$

and thus we end up with the right multiplicative factor - neutral scalar fields have one degree of freedom, complex scalar fields possess two (for charge conjugation), and massive Dirac fermions have four degrees of freedom (two for the charge conjugation and two for the spin orientations). That means the result for the Dirac fermions has to have an additional factor of four with respect to neutral scalar particles and a factor of two for charged scalars, which we have been assuming above, and thus the results are in agreement.
Summarising the results, we can write the partition function of the boson-fermion system as

$$Z = e^{iS_\mathrm{eff}} = \exp\left[-\mathrm{Tr_F} \ln\left(\partial^2 + m_\mathrm{b}^2\right) + 2\,\mathrm{Tr_F} \ln\left(\partial^2 + m_\mathrm{f}^2\right)\right] . \tag{3.35}$$

These calculations are to be modified when considering real scalar fields (uncharged bosons) or Majorana spinors (uncharged fermions, like presumably neutrinos), which will be necessary when calculating the vacuum energy of the standard model. In all cases there will be additional numerical factors to account for the corresponding number of degrees of freedom. A charge implies a factor of two, to consider particle and antiparticle. For a non-zero spin, the different possible spin orientations have to be included as numerical factors as well. This holds for all possible particles species, e.g. also for the vector bosons of the standard model, whose degrees of freedom manifest themselves as different polarisation states $\epsilon^\mu(\nu)$ in the plane wave formulation of the field. For massive bosons with spin 1,

there are two transversal and one longitudinal polarisation mode possible, implying three degrees of freedom, whereas for massless bosons, the longitudinal mode vanishes and two degrees of freedom remain.
Apart from these particularities however, the general rule is that bosons and fermions enter the effective action with opposite signs, bosons having negative and fermions positive effective action. This fact can be employed in order to mutually balance the contributions of bosons and fermions with each other, and to achieve a complete cancellation of divergences and tune possible convergent factors in the effective action.
The following calculations will consider only the first loop diagrams of the effective action, and disregard higher order interactions. To make the model more realistic, further diagrams could be included in the calculations, however, these will be neglected in this work. It is sufficient for the purpose of demonstrating the principle of cancellation to restrict ourselves to the one-loop effective action.

4. Vacuum energy in flat spacetimes

Having established that due to their constant energy density the vacuum fluctuations of quantum fields are the ideal candidate to explain the accelerated expansion of the universe, we know that there is still a small problem preventing us to exploit this fact and identify the vacuum fluctuations as the cause of the expansion: the divergences of these vacuum fluctuations. We have stated that the vacuum energy is originally divergent, or, in the case of introducing a cutoff at Planck scale results in a value of about $\rho_\Lambda^{(\mathrm{th})} \simeq 10^{76}\,\mathrm{GeV}^4$, while the desired cosmological constant that would correctly reproduce the expansion behaviour of the universe is of the order of $\rho_\Lambda^{(\mathrm{obs})} \simeq 10^{-47}\,\mathrm{GeV}^4$.
In this section, we will show some naive estimations of the vacuum energy of a scalar field, and try to peel out the divergences. These considerations are in principle valid also for other types of fields, but as usual it is the easiest to do it for the example of a scalar field. Considering the vacuum energy of a scalar field,

$$S_{\mathrm{eff}} = i\mathrm{Tr}_{\mathrm{F}} \ln\left(\partial^2 + m^2\right) = i \int d^D x \sqrt{-\eta}\, \ln\left(\partial^2 + m^2\right)\,, \tag{4.1}$$

we can transfer the argument of the integral to Fourier space. Dropping the spatial integral for a moment, we aim to calculate the integral

$$\int \frac{d^D p}{(2\pi)^D}\, \ln\left(-p^2 + m^2\right). \tag{4.2}$$

For D spacetime dimensions, we now split the integration into the zero-component and the spatial components, p_0 and p_i, and carry out the integration of the zero-component p_0, to obtain

$$\int \frac{dp_0 d^{D-1}p}{(2\pi)^4}\, \ln\left(-p^2 + m^2\right) = \int \frac{d^{D-1}p}{(2\pi)^3}\, \sqrt{p_i^2 + m^2}\,, \tag{4.3}$$

the p_i^2 in the resulting expression denoting only the spatial components. The square root can be rewritten as $\sqrt{p_i^2 + m^2} = p\,\sqrt{1 + m^2/p^2}$, with p now denoting the norm of p_i, and expanded in the relativistic limit for large momenta p as

$$p\sqrt{1 + \frac{m^2}{p^2}} \simeq p\left[1 + \frac{m^2}{2p^2} - \frac{m^4}{8p^4} + \frac{m^6}{16p^6} - ...\right]. \tag{4.4}$$

That means, the effective action and thus the vacuum energy is proportional to the expression

$$\begin{aligned} S_{\text{eff}} &\propto \int_{p_c}^{\infty} \frac{p^2 \sin\theta \, d\varphi \, d\theta \, dp}{(2\pi)^3} \, p \sqrt{1+\frac{m^2}{p^2}} \\ &= \left[\frac{p^4}{4} + \frac{m^2 \, p^3}{6} - \frac{m^4}{8} \ln p - \frac{m^6}{48 p^2} - ... \right]_{p_c}^{\infty} . \end{aligned} \tag{4.5}$$

This expression diverges in the ultraviolet limit of the momentum for the first three terms; and is moreover dependent on an infrared cutoff parameter p_c. The cutoff p_c has been introduced because the expansion (4.4) is only valid for large momenta, and we are not interested in the behaviour for small momenta. The ultraviolet divergences pose a serious problem since there is no more elegant argumentation for the their renormalisation than the assumption of the invalidity of conventional quantum field theories at scales beyond the Planck scale. The usual way to deal with those infinities is thus to introduce another cutoff [50] in phase space, for example at the Planck scale, and disregard particles with momenta higher than that cutoff, leading to the infamous energy density of $\rho_{\Lambda,\text{th}} \simeq 10^{76}\,\text{GeV}^4$ mentioned before. There are alternative renormalisation methods, such as dimensional regularisation [51], which however all serve the purpose of peeling out the singularities explicitly only to then disregard those terms or eliminate them by appropriate counterterms. The concept we would like to put forward in this work to deal with these divergences is to make the divergent contributions from bosons and fermions cancel exactly, so that only the finite parts of the integral remain, which then determines the vacuum energy. The way to achieve this is by considering the one other quantity occurring in the effective action above, i.e. the mass of the particle. If we would like to cancel the divergences between two particles, and taking into account that bosons and fermions give opposite-sign contributions to the effective action, it is clear that by fine-tuning the masses of the particles in the system accordingly, it is possible to get rid of the divergent parts.

In order to have the first three terms in the above expression for bosons and fermions cancel each other out there are some relations that have to be fulfilled. The total expression for the vacuum energy for i particle species is

$$S_{\text{eff}} \propto \sum_i \left[\frac{\nu_i \, p^4}{4} + \frac{m_i^2 \, p^3}{6} - \frac{m_i^4}{8} \ln p - ... \right] . \tag{4.6}$$

To cancel the first term in the sums, we demand to have the same number of degrees of freedom on the bosonic and fermionic sector of the system, denoted by b and f,

$$\sum_{\text{b}} \nu_{\text{b}} = \sum_{\text{f}} \nu_{\text{f}} . \tag{4.7}$$

To cancel the other two divergent terms in the sum, the masses of the bosons and fermions must obey the relations

$$\begin{aligned} \sum_{\mathrm{b}} m_{\mathrm{b}}^2 &= \sum_{\mathrm{f}} m_{\mathrm{f}}^2 \,, \\ \sum_{\mathrm{b}} m_{\mathrm{b}}^4 &= \sum_{\mathrm{f}} m_{\mathrm{f}}^4 \,. \end{aligned} \tag{4.8}$$

Given the assumption that the masses of bosons and fermions can be chosen to fulfil these relations, this is the basic schedule that has to be obeyed in order to achieve the cancellation of divergences. These simple estimations have shown the principle that we employ. In the following sections, we will calculate the vacuum energy exactly, peel out the divergences with slightly different methods, and try to find the exact cancellation conditions that have to be fulfilled. We expect however that they will be in principle the same as what we obtained from these sketchy considerations.

4.1. Exact calculation of the vacuum energy

Going back to the integral in question,

$$\int \frac{d^D p}{(2\pi)^D} \ln\left(-p^2 + m^2\right) \,, \tag{4.9}$$

we will apply the technique of dimensional regularisation, which means that the integral will be rewritten in terms of Γ-functions as a function of the number of spacetime dimensions D, which will then be set to a natural number plus an infinitesimal part, i.e. $D = 4 - \epsilon$. The resulting expression will be expanded in terms of the small quantity ϵ, and in the end the limit $\epsilon \to 0$ will be taken.

From the above expression, we first carry out a Wick rotation, and then calculate the integral as (see e.g. [52])

$$\int \frac{d^D p}{(2\pi)^D} \ln\left(-p^2 + m^2\right) = -i \frac{\Gamma(-D/2)}{(4\pi)^{D/2}} \frac{1}{(m^2)^{-D/2}}. \tag{4.10}$$

This integral is divergent because the Γ-function diverges for negative even values without any possibility of analytic continuation or such tricks, and for $D = 4$, we have $\Gamma(-2)$ in the numerator. The expression needs to be processed further using dimensional regularisation, i.e. we substitute D by $D = 4 - \epsilon$, which will make it possible to explicitly isolate the infinities in terms which diverge in the limit $\epsilon \to 0$. The result of the integral contains ϵ twice: within the Γ-function, and as power of the mass. It is possible to expand the Γ-function as [53]

$$\Gamma(-n + \epsilon) \simeq \frac{(-1)^n}{n!} \left[\frac{1}{\epsilon} + \psi(n+1) + \frac{\epsilon}{2}\left(\frac{\pi^2}{3} + \psi^2(n+1) - \psi'(n+1)\right)\right] \,, \tag{4.11}$$

where $\psi(n)$ is the Digamma function, and $\psi'(n)$ the Trigamma function. The expansion of the Γ-function then reads

$$\Gamma\left(-2+\frac{\epsilon}{2}\right) \simeq \frac{1}{\epsilon}+1-\frac{\gamma}{2}+\epsilon\left[\frac{\pi^2}{12}+2(1-\gamma)+\frac{\gamma^2}{2}\right]) + \mathcal{O}(\epsilon^2)\,. \tag{4.12}$$

The mass term can be expanded for small ϵ as well,

$$m^{-\epsilon} = \mu^{-\epsilon}\left[\frac{\mu}{m}\right)^{\epsilon} \simeq \mu^{-\epsilon}\left(1+\epsilon\,\ln\frac{\mu}{m}+\mathcal{O}(\epsilon^2)\right]\,, \tag{4.13}$$

where μ is an auxiliary parameter with the dimension of a mass, introduced to make the argument of the logarithm dimensionless. Truncating at linear order in ϵ, we end up with an expression for the effective action as

$$S_{\text{eff}} \simeq -\frac{i\mu^{-\epsilon}}{(4\pi)^2}\,m^4\,\left[\frac{1}{\epsilon}+\ln\frac{\mu}{m}+1-\frac{\gamma}{2}+\mathcal{O}(\epsilon)\right]\,. \tag{4.14}$$

Thus, we see that in order to cancel the divergent terms proportional to $1/\epsilon$, we need to require that the sum over all quartic powers of the masses of the system vanish,

$$\sum_{\text{b}} m_{\text{b}}^4 = \sum_{\text{f}} m_{\text{f}}^4\,, \tag{4.15}$$

which will then ensure the effective energy to be finite. This will also cancel the constant term $1-\gamma/2$ in the effective action. Thus for the convergent part, there is only the term

$$S_{\text{eff,conv}} = -\frac{i\mu^{-\epsilon}}{(4\pi)^2}\,m^4\,\ln\frac{\mu}{m} \tag{4.16}$$

left, which should be tuned to result in the observed cosmological constant by requiring the condition

$$\sum_{\text{b}} m_{\text{b}}^4\,\ln\frac{\mu}{m_{\text{b}}} - \sum_{\text{f}} m_{\text{f}}^4\,\ln\frac{\mu}{m_{\text{f}}} = \rho_\Lambda \tag{4.17}$$

to be fulfilled.

In this argumentation, we ended up with one condition to cancel the divergences, and one to tune the convergent remainder to a specific value ρ_Λ. However, we failed to recover also the condition

$$\sum_{\text{b}} \nu_{\text{b}} = \sum_{\text{f}} \nu_{\text{f}}. \tag{4.18}$$

to balance the degrees of freedom of the particles - a condition that was predicted by the naive estimations of the vacuum energy previously. The reason for this is that within the formalism of dimensional regularisation as applied here the quadratically divergent contributions to the integral are lost due to the application of Veltman's rule [54, 55].

Concretely, an integral like the one in Eq. (4.10) can always be reformulated as an integral over a fraction as

$$\int \frac{d^D p}{(2\pi)^D} \ln\left(-p^2 + m^2\right) = \int \frac{d^D p}{(2\pi)^D} \int dm^2 \, \frac{1}{p^2 + m^2} \,. \tag{4.19}$$

Consider the identity

$$\int \frac{d^D p}{(2\pi)^D} \, \frac{m^2}{p^2 \left(p^2 + m^2\right)} = \int \frac{d^D p}{(2\pi)^D} \left[\frac{1}{p^2} - \frac{1}{p^2 + m^2}\right] . \tag{4.20}$$

By using the formula for Schwinger's proper time integral [56],

$$\frac{i}{(4\pi i s)^{D/2}} \, e^{-i m^2 s} = \int \frac{d^D k}{(2\pi)^D} \, e^{-i s(-k^2 + m^2)} \,, \tag{4.21}$$

and taking into account the integral representation of the Γ-function, we obtain

$$\int \frac{d^D p}{(2\pi)^D} \, \frac{m^2}{p^2 \left(p^2 + m^2\right)} \equiv \int \frac{d^D p}{(2\pi)^D} \, \frac{1}{p^2 + m^2} = \frac{\Gamma(1 - D/2)}{(4\pi)^{D/2}} \, \frac{1}{(m^2)^{-D/2+1}} \,, \tag{4.22}$$

which consequently implies

$$\int \frac{d^D p}{(2\pi)^D} \, \frac{1}{p^2} = 0 \,, \tag{4.23}$$

known as Veltman's formula [52, 54, 55]. That shows that in using the technique of dimensional regularisation, the existence of an additional quadratic pole in the integrand is lost. On the contrary, using the formalism of a cutoff regularisation, the quadratic divergence is obtained correctly with an ultraviolet cutoff at p_Λ:

$$\int_0^{p_\Lambda} \frac{d^D p}{(2\pi)^D} \frac{1}{p^2 + m^2} = -\frac{i}{(4\pi)^2} \left(p_\Lambda^2 - m^2 \ln \frac{p_\Lambda^2}{m^2}\right) . \tag{4.24}$$

In the formalism of a dimensional regularisation, lost quadratic poles as in Eq. (4.23) can be recovered by considering the following reparameterization of the masses:

$$m_i^2 \to m_0^2 + m_i^2 \,, \tag{4.25}$$

where the square of the masses are rewritten as the sum of a constant part m_0^2 and an individually different part m_i^2. m_0^2 is the same for each particle species, and the m_i^2 characterise the differences between the particles. The effective action integral then reads

$$\int \frac{d^D p}{(2\pi)^D} \ln\left(-p^2 + m_0^2 + m_i^2\right) = -i \, \frac{\Gamma(-D/2)}{(4\pi)^{D/2}} \left(m_0^2 + m_i^2\right)^D . \tag{4.26}$$

Doing the same expansions as before, expanding the Gamma function and the mass term, and neglecting terms of linear order in ϵ, we obtain a similar expression as before,

$$S_{\text{eff}} \simeq -\frac{i\mu^{-\epsilon} \left(m_i^4 + 2 m_0^2 \, m_i^2 + m_0^4\right)}{(4\pi)^{2-\epsilon/2}} \left[\frac{1}{\epsilon} + 1 - \frac{\gamma}{2} + \ln \frac{\mu}{\sqrt{m_i^2 + m_0^2}} + \mathcal{O}(\epsilon)\right] . \tag{4.27}$$

We are left with two conditions in order to cancel the divergent parts of the effective action, i.e.

$$\sum_{\mathrm{b}} \left(m_{\mathrm{b}}^4 + 2m_0^2\, m_{\mathrm{b}}^2\right) = \sum_{\mathrm{f}} \left(m_{\mathrm{f}}^4 + 2m_0^2\, m_{\mathrm{f}}^2\right) , \tag{4.28}$$

$$\sum_{\mathrm{b}} \nu_{\mathrm{b}} = \sum_{\mathrm{f}} \nu_{\mathrm{f}} \, . \tag{4.29}$$

The first condition will again cancel the term $1-\gamma/2$ in the effective action as well, whereas the second condition comes from the requirement of cancelling the terms proportional to m_0^4. The term proportional to m_0^4/ϵ in Eq. (4.27) corresponds to the quadratic divergence in Eq. (4.24).
When trying to reproduce the observed cosmological constant with the expression of Eq. (4.27), the following condition has to be fulfilled by the convergent remainder of the effective action in order to achieve the correct value for the convergent part of the vacuum energy,

$$\sum_{\mathrm{b}} \left[\left(m_{\mathrm{b}}^4 + m_0^2 m_{\mathrm{b}}^2 + m_0^4\right) \ln \frac{\mu}{\sqrt{m_{\mathrm{b}}^2 + m_0^2}} \right] - \sum_{\mathrm{f}} \left[\left(m_{\mathrm{f}}^4 + m_0^2 m_{\mathrm{f}}^2 + m_0^4\right) \ln \frac{\mu}{\sqrt{m_{\mathrm{f}}^2 + m_0^2}} \right] = \rho_\Lambda \, , \tag{4.30}$$

which can be rewritten again as

$$\sum_{\mathrm{b}} m_{\mathrm{b}}^4 \ln \frac{\mu}{m_{\mathrm{b}}} - \sum_{\mathrm{f}} m_{\mathrm{f}}^4 \ln \frac{\mu}{m_{\mathrm{f}}} = \rho_\Lambda \, , \tag{4.31}$$

where ρ_Λ is the energy density of the observed cosmological constant that we aim to reproduce with the appropriate choice of masses.
So for the case of flat spacetime, we require conditions (4.28), (4.29) and (4.31) to be fulfilled by the masses of the system. These conditions can be fulfilled by quite a number of different configurations, because there are two equations for an arbitrary number of variables or masses. If we assume the standard model of particle physics to be valid, which encloses four massive bosons and twelve massive fermions, as well as the photons and gluons as massless bosons, it is possible to achieve cancellation of the divergences from (4.28) and tuning of the convergent part with (4.31) by introduction of two new particles. However, we have to consider additionally that their degrees of freedom have to fulfil condition Eq. (4.29). We will not give any explicit solution for these masses here, but content ourselves with the conclusion that in principle it is possible to construct a model with bosonic and fermionic fields, which leads to a cancellation of the divergent contributions to the vacuum energy.

5. Vacuum energy in curved spacetime

We will now proceed to investigate the above calculations in general curved spacetimes. Quantum field theory in curved spacetimes is a well-explored but complicated subject discussed in many papers and books on the subject [48, 57, 58]. Curvature comes into play in several expressions:

- in operators, e.g.
$$\Delta \to \Delta_{\mathrm{LB}} = \frac{1}{\sqrt{-g}}\partial_\mu \sqrt{-g} g^{\mu\nu}\partial_\nu \,, \tag{5.1}$$
where g is the determinant of the metric of the curved spacetime, and LB stands for Laplace-Beltrami,

- in the Dirac γ-matrices,
$$\gamma^\mu = e^\mu_a \gamma^a \,, \tag{5.2}$$
where the e^μ_a are the vierbein fields of the metric of the curved spacetime,

- and as coefficients in the action,
$$S = \int d^D x \sqrt{-g}\, \mathcal{L} \,. \tag{5.3}$$

In general, the Laplacian is not only generalized to the Laplace-Beltrami operator as mentioned above, but also acquires an additional term accounting for the overall curvature of spacetime. A conformally invariant way of writing the generalized Laplace-Beltrami operator is [59]
$$\Delta^{\mathrm{gen}}_{\mathrm{LB}} = \Delta_{\mathrm{LB}} - \frac{1}{4}\frac{D-2}{D-1}R = \Delta_{\mathrm{LB}} - \xi R \,, \tag{5.4}$$
where R is the curvature scalar of spacetime and Δ_{LB} is the aforementioned Laplace-Beltrami operator for a general metric $g^{\mu\nu}$. In total, we have then
$$\Delta^{\mathrm{gen}}_{\mathrm{LB}} = \Delta_{\mathrm{LB}} - \xi R = \frac{1}{\sqrt{-g}}\partial_\mu \sqrt{-g} g^{\mu\nu}\partial_\nu - \xi R \,, \tag{5.5}$$
where $\xi = \frac{1}{6}$ for $D = 4$. It is possible to argue however that the parameter ξ must be zero by considering the case of a quantum mechanical particle moving in curved spacetimes.

It is always possible to find a mapping that describes the motion of a particle in curved spacetime within a local inertial frame with flat local coordinates. In the case of a point particle, this implies that no forces act on the particle except gravity in the description of the local inertial frame. For an extended particle however, tidal forces act on the particle or wave packet in the local inertial frame, and so the quantum mechanical behaviour, i.e. the fluctuations and dispersion of the wave packet, depends on the shape of the wave packet. To take the tidal forces onto an extended object into account, the principle of non-holonomic mapping must be used to find the correct mapping between the curved spacetime and the locally flat inertial frame, and this principle predicts a factor $\xi = 0$ [60]. With $\xi = 0$ the influence of curvature on the vacuum energy is captured by the Laplace-Beltrami operator Δ_{LB} alone.

In the case of small curvature, it is instructive to consider an approximate approach to describe its effects qualitatively. A framework for these investigations is given by the approach brought forward in the 1970s and 1980s by Schwinger, Seeley and de Witt (see [61] and references therein), and further developed in the work of Christensen [62, 63] and Bunch, Parker and Toms [64–66]. More recently, also Vassilevich [67] developed similar analyses under the label of the so-called heat kernel expansion. The basic concept is to write the propagator, i.e. the Greens function of the theory, in terms of an expansion into a power series, with the coefficients of the series being dependent on curvature terms. This expansion is, if truncated, valid for spacetimes with small curvature, and is supposed to reduce to the results for flat spacetimes in the limit of zero curvature. The procedure was developed originally to calculate the energy-momentum tensors of various kinds of fields in curved spacetimes, and served to explicitly identify and eliminate the divergences that occur in the vacuum expectation values of the energy-momentum tensors. The fields are assumed to propagate in a classical curved background spacetime, so gravity is not quantized, and thus we also do not consider any gravitational contribution to the vacuum energy of quantum fields. Gravity enters the theory via a general metric $g_{\mu\nu}$, which will be specified to the example of a Friedmann-Lemaître-Robertson-Walker metric as introduced in Eq. (1.12). In our concrete case, also the assumption of small curvature holds, and so the method and the expansion in terms of curvature is justified.

The theory put forward by the above authors is a method to obtain an expression for the propagator of a theory in terms of an expansion in curvature. It can be used to calculate anything that can be expressed in terms of the Greens function of the system. We are interested in obtaining the effective action of a system of free particles as an expansion in curvature. Thus, we need to bring the effective action in a form containing the Greens function of the respective problem, such that we can then obtain the curvature expansion of the effective action. This will be achieved by differentiation with respect to the mass for

fermions, and differentiating with respect to the squared mass for bosons. We will see later in three specific cases of scalar, spinor and vector particles how this is done.
In general, the expansion of the Greens function in terms of curvature can be carried out according to the following scheme. For the propagator an ansatz is made as an integral over the so-called heat kernel $\langle x, s|x', 0\rangle$ as

$$G(x, x') = -i \int_0^\infty ds \, \langle x, s|x', 0\rangle \, e^{-im^2 s} \, . \tag{5.6}$$

Here s is the so-called proper time, or pseudotime [68], a parameter introduced mathematically as an alternative coordinate, but without a direct physical meaning.
According to [61], the kernel can be written as

$$\langle x, s|x', 0\rangle = \frac{i}{(4\pi i s)^{D/2}} \, \Delta_{VM}(x, x') \, e^{i\sigma(x,x')/2s} \, \Omega(x, x', s) \, , \tag{5.7}$$

where $\Omega(x, x', s)$ is a newly introduced function to be determined, and $\sigma(x, x') = g_{\mu\nu}\sigma^{;\mu}\sigma^{;\nu}$ is the geodesic difference between the points x and x'. $\Delta_{VM}(x, x')$ is the van Vleck-Morette determinant, which is defined as

$$\Delta_{VM}(x, x') = -g^{-1/2}(x) \det\left[-\partial_\mu \partial_\nu \sigma(x, x')\right] g^{-1/2}(x') \, . \tag{5.8}$$

As it will turn out after calculating the yet unknown function $\Omega(x, x', s)$, the Greens function can by this construction be expressed only in terms of the distance along the geodesic connection between the points x and x', and other geometrical quantities related to curvature and derived from the Riemann tensor. Thus the procedure is sometimes also called the covariant geodesic point separation technique.
The determining equation for $\Omega(x, x', s)$ can be obtained by plugging the expansion for the kernel, Eq. (5.7), into the equation for the propagator, which is of the general form

$$\hat{F} \, G(x, x') = -\delta(x, x') \, , \tag{5.9}$$

where the operator $\hat{F}$ describes the system in question, and is the operator which occurs in the equation of motion for the corresponding field. Putting the ansatz for the Greens function in this equation leads to a determining equation for the heat kernel,

$$i\frac{\partial}{\partial s}\langle x, s|x', 0\rangle = \hat{F}\big|_{m=0}\langle x, s|x', 0\rangle \, , \tag{5.10}$$

where now the operator $\hat{F}$ is evaluated for zero mass, $m = 0$. The reason for this is that the mass has been temporarily removed from the procedure by the integral over the proper time, Eq. (5.6). This is also the reason why we exclusively consider massive particles here,

and only later specify what happens to massless particles (the obvious answer of course is that massless particles don't contribute to the vacuum energy since they don't interact with each other, but this will also be found from mathematics later).

From Eq. (5.10), an equation for the function $\Omega(x, x', s)$ can be found, which is determined by the same operator that defines the system, $\hat{F}$. To solve the equation for $\Omega(x, x', s)$ we choose a power series ansatz,

$$\Omega(x, x', s) = \sum_{j=0}^{\infty} (is)^j a_j(x, x') \,, \tag{5.11}$$

where the a_j are determined by the recursion relations which are obtained by plugging this ansatz back into the equation for $\Omega(x, x', s)$:

$$\begin{aligned} \sigma^{;\mu}\, a_{0;\mu} &= 0 \,, \\ \sigma^{;\mu}\, a_{j+1;\mu} + (j+1)\, a_{j+1} &= \Delta^{-1/2}\, \hat{F}\big|_{m=0} \left[\Delta^{1/2} a_j(x, x')\right] \,, \end{aligned} \tag{5.12}$$

with the boundary condition $a_0(x, x') = 1$.

In the coincidence limit $x \to x'$, the van Vleck-Morette determinant becomes the unit matrix, and the geodesic distance $\sigma(x, x')$ between x and x' becomes zero, yielding a rather simple form of the heat kernel,

$$\langle x, s | x, 0 \rangle = \frac{i}{(4\pi i s)^{D/2}} \sum_{j=0}^{\infty} (is)^j a_j(x, x) \,, \tag{5.13}$$

with the $a_j(x, x)$ in the coincidence limit as well. Using the identity [56]

$$\frac{i}{(4\pi i s)^{D/2}}\, e^{-im^2 s} = \int \frac{d^D k}{(2\pi)^D}\, e^{-is(-k^2+m^2)} \,, \tag{5.14}$$

we can write the propagator as

$$\begin{aligned} G(x, x) &= -i \int \frac{d^D k}{(2\pi)^D} \int_0^{\infty} ds \sum_{j=0}^{\infty} (is)^j a_j(x, x)\, e^{-is(-k^2+m^2)} \\ &= -i \int \frac{d^D k}{(2\pi)^D} \int_0^{\infty} ds \sum_{j=0}^{\infty} a_j(x, x) \left(-\frac{\partial}{\partial m^2}\right)^j e^{-is(-k^2+m^2)} \\ &= \int \frac{d^D k}{(2\pi)^D} \sum_{j=0}^{\infty} a_j(x, x) \left(-\frac{\partial}{\partial m^2}\right)^j \left[\frac{1}{-k^2+m^2}\right] . \end{aligned} \tag{5.15}$$

In the following three sections, we will describe in detail how to derive this expansion of the Greens function for the specific cases of scalar bosons, spinor particles and vector bosons, and also address the question of massless particles.

The essential expressions are the expansion of the propagator as given by Eq. (5.15), and the recursion relations which determine the exact form of the coefficients of the expansion, Eqs. (5.12).

5.1. Complex scalar fields

Here we will derive the Seeley-de Witt expansion for the simplest case of a complex scalar field. The effective action reads, with the trace over functional space explicitly stated as an integral over D-dimensional space,

$$\begin{aligned} iS_{\text{eff}}^{(0)} &= -\int d^D x\sqrt{-g}\ \ln\left[\partial^2 + m^2\right] \\ &= -\int d^D x\sqrt{-g}\int dm^2\,\frac{1}{\partial^2+m^2}\,, \end{aligned} \tag{5.16}$$

where the position space propagator is defined as

$$G(x,x') = \frac{1}{\partial^2+m^2}\,. \tag{5.17}$$

In the second line of (5.16) we have carried out the aforementioned differentiation with respect to the squared mass, in order to obtain an expression of the effective action in terms of the propagator. Now we can proceed to calculate the curvature expansion of $G(x,x')$, which will give us the effective action for a free complex scalar field in terms of a curvature expansion.
The propagator is the Greens function of the equation of motion for the scalar field and thus fulfils the equation

$$\left(\partial^2+m^2\right)G(x,x') = -\delta(x,x')\,. \tag{5.18}$$

We define the operator acting on $G(x,x')$ on the left hand side as $\hat{F}$, i.e.

$$\hat{F} = \partial^2 + m^2\,. \tag{5.19}$$

The expansion for the Greens function is carried out according to the recipe outlined in the last section. For a scalar field, the first few coefficients have been calculated from Eqs. (5.12) using Eq. (5.19), resulting in

$$a_0 = 1\,, \tag{5.20a}$$

$$a_1 = \frac{1}{6}R\,, \tag{5.20b}$$

$$a_2 = \frac{1}{30}\Box R + \frac{1}{72}R^2 + \frac{1}{180}\left(R_{\alpha\beta\gamma\delta}R^{\alpha\beta\gamma\delta} - R_{\alpha\beta}R^{\alpha\beta}\right)\,. \tag{5.20c}$$

Filling in the coefficients a_j we have for the Greens function the result

$$G(x,x) = \int\frac{d^Dk}{(2\pi)^D}\left[\frac{a_0}{-k^2+m^2} + \frac{a_1}{(-k^2+m^2)^2} + \frac{2a_2}{(-k^2+m^2)^3} + ...\right], \tag{5.21}$$

and so we obtain for the effective action

$$iS_{\text{eff}}^{(0)} = -\int d^D x\sqrt{-g}\int dm^2 \int \frac{d^D k}{(2\pi)^D}\left[\frac{a_0}{-k^2+m^2} + \frac{a_1}{(-k^2+m^2)^2} + \frac{2a_2}{(-k^2+m^2)^3} + ...\right]. \tag{5.22}$$

Even though $\xi = 0$ this result contains terms proportional to the curvature. What remains to be done is carrying out the integrals over k and m^2. The k-integration has to be calculated using regularization techniques, as it leads, in the four-dimensional case, to divergences.

5.2. Complex spinor fields

The action for a complex spinor field, i.e. a Dirac fermion, denoted by the superscript (1/2), reads

$$S^{(1/2)} = \int d^D x\sqrt{-g}\,\bar{\psi}\,(i\partial\!\!\!/ + m\mathbf{1})\,\psi\,. \tag{5.23}$$

From this, the effective action is calculated as

$$iS_{\text{eff}}^{(1/2)} = \int d^D x\sqrt{-g}\ \text{tr}_{\text{D}} \ln\left[i\partial\!\!\!/ + m\mathbf{1}\right]\,. \tag{5.24}$$

where tr_{D} represents the trace over the Dirac indices of the spinor field. In the case of spinors the effective action is positive since we are dealing with a fermionic field. The position space propagator is defined similarly to before as

$$\mathbf{G}(x,x') = \frac{1}{i\partial\!\!\!/ + m\mathbf{1}}\,, \tag{5.25}$$

fulfilling the equation

$$(i\partial\!\!\!/ + m\mathbf{1})\,\mathbf{G}(x,x') = -\delta(x,x')\,. \tag{5.26}$$

However, to be able to apply the expansion by Schwinger, Seeley and de Witt, we need a quadratic operator, not one proportional to the single derivative operator ∂, as in the case of Dirac spinors. Thus, we use the previously mentioned identity

$$\det\left[i\partial\!\!\!/ - m\mathbf{1}\right] = \det[\partial\!\!\!/^2 + m^2\mathbf{1}]^{1/2}\,, \tag{5.27}$$

and write the effective action for Dirac fermions as

$$iS_{\text{eff}}^{(1/2)} = \frac{1}{2}\int d^D x\sqrt{-g}\ \text{tr}_{\text{D}} \ln\left[\partial\!\!\!/^2 + m^2\mathbf{1}\right]\,, \tag{5.28}$$

now containing a quadratic operator, which is taken into account by the factor of 1/2 in front of the whole expression. Introducing the mass integral as before in the case of the scalar field, the effective action becomes

$$iS_{\text{eff}}^{(1/2)} = \frac{1}{2}\int d^D x\sqrt{-g}\int dm^2\,\text{tr}_{\text{D}}\,\frac{1}{\not\partial^2 + m^2\mathbf{1}}\,, \tag{5.29}$$

where we can carry out the curvature expansion for the Greens function

$$\mathbf{G}(x,x') = \frac{1}{\not\partial^2 + m^2\mathbf{1}}\,. \tag{5.30}$$

The Dirac trace has to be considered after calculating the heat kernel expansion. The Greens function in this case obeys the equation

$$\text{tr}_{\text{D}}\left(\not\partial^2 + m^2\mathbf{1}\right)\mathbf{G}(x,x') = \left(\partial^2 + \frac{1}{4}R - m^2\right)G(x,x') = -\delta(x,x')\,, \tag{5.31}$$

and can be expanded according to the same scheme as before, resulting in

$$\mathbf{G}(x,x) = \int\frac{d^D k}{(2\pi)^D}\sum_{j=0}^{\infty}\mathbf{a}_j(x,x)\left(-\frac{\partial}{\partial m^2}\right)^j\frac{1}{-k^2+m^2}\,, \tag{5.32}$$

with the coefficients for spinor fields as

$$\mathbf{a}_0 = \mathbf{1}\,, \tag{5.33a}$$

$$\mathbf{a}_1 = \frac{1}{12}R\mathbf{1}\,, \tag{5.33b}$$

$$\mathbf{a}_2 = \left(\frac{1}{288}R^2 - \frac{1}{120}\Box R - \frac{1}{180}R_{\alpha\beta}R^{\alpha\beta} + \frac{1}{180}R_{\alpha\beta\gamma\delta}R^{\alpha\beta\gamma\delta}\right)\mathbf{1} - \frac{1}{192}\sigma_{\alpha\beta}\sigma_{\gamma\delta}R^{\alpha\beta\lambda\xi}R^{\gamma\delta}{}_{\lambda\xi}\,, \tag{5.33c}$$

and $\sigma_{\alpha\beta} = \frac{i}{2}\big[\gamma_\alpha,\gamma_\beta\big]_-$ being the commutator of the γ-matrices. The final expression for the effective action thus reads

$$iS_{\text{eff}}^{(1/2)} = \frac{1}{2}\int d^D x\sqrt{-g}\int dm^2\,\text{tr}_{\text{D}}\,\mathbf{G}(x,x)\,, \tag{5.34}$$

with the $\mathbf{G}(x,x')$ given by Eqs. (5.32) and (5.33). What remains to be done is to carry out the trace over the Dirac indices, which will be described in one of the following sections.

5.3. Complex vector fields

The action for a massive charged vector field including a gauge fixing term reads

$$\begin{aligned} S^{(1)} &= \int d^D x\sqrt{-g}\left[-\frac{1}{4}F_{\mu\nu}F^{\mu\nu} - \frac{1}{2\alpha}(\partial_\mu A^\mu)^2 + \frac{1}{2}m^2 A^\nu A_\nu\right] \\ &= \frac{1}{2}\int d^D x\sqrt{-g}\;A_\mu\left[g^{\mu\nu}\left(\partial^2 + m^2\right) - \left(1 - \frac{1}{\alpha}\right)\partial^\mu\partial^\nu\right]A_\nu\,. \end{aligned} \tag{5.35}$$

We include a gauge-fixing term here in order to be able to take the limit of zero mass later on in the computations, which will be necessary to analyse the case of photons and gluons. From Eq. (5.35), the effective action is obtained as

$$iS_{\text{eff}}^{(1)} = -\int d^D x\sqrt{-g}\,\text{tr}_{\text{L}}\,\ln\left(G^{\mu\nu}\right)^{-1}(x,x')\,, \tag{5.36}$$

where tr_{L} denotes the trace over the Lorentz indices, and the position space propagator is defined via the equation

$$\left(G^{\mu\nu}\right)^{-1}(x,x') = g^{\mu\nu}\left(\partial^2 + m^2\right) - \left(1 - \frac{1}{\alpha}\right)\partial^\mu\partial^\nu\,, \tag{5.37}$$

obeying the equation

$$\left[g^{\mu\nu}\left(\partial^2 + m^2\right) - \left(1 - \frac{1}{\alpha}\right)\partial^\mu\partial^\nu\right]G_{\mu\nu}(x,x') = -\delta(x,x')\,. \tag{5.38}$$

We can now introduce the mass integral as usual, considering basic rules of matrix computation and properties of the logarithm function, yielding

$$iS_{\text{eff}}^{(1)} = -\int d^D x\sqrt{-g}\int dm^2\,\text{tr}_{\text{L}}\left[\,g^{\mu\lambda}G_{\lambda\nu}(x,x')\right]\,. \tag{5.39}$$

$G_{\lambda\nu}(x,x')$ can be expanded and calculated with the operator $\hat{F}$ defined by Eq. (5.38), to yield the familiar expression

$$g^{\mu\lambda}G_{\lambda\nu}(x,x') = \int\frac{d^D k}{(2\pi)^D}\sum_{j=0}^{\infty} g^{\mu\lambda}a_{j\lambda\nu}(x,x)\left(-\frac{\partial}{\partial m^2}\right)^j\,\frac{1}{-k^2+m^2}\,. \tag{5.40}$$

Thus the effective action for vector bosons is then given by

$$iS_{\text{eff}}^{(1)} = -\int d^D x\sqrt{-g}\int dm^2\int\frac{d^D k}{(2\pi)^D}\,\text{tr}_{\text{L}}\,g^{\mu\lambda}\left[\frac{a_{0\lambda\nu}}{-k^2+m^2} + \frac{a_{1\lambda\nu}}{(-k^2+m^2)^2} + ...\right]\,, \tag{5.41}$$

and the coefficients in the coincidence limits have been calculated in [63] as

$$a_{0\lambda\nu} = \delta_{\lambda\nu}\,, \tag{5.42a}$$

$$a_{1\lambda\nu} = \frac{1}{6}\left(Rg_{\lambda\nu} - R_{\lambda\nu}\right)\,, \tag{5.42b}$$

$$\begin{aligned} a_{2\lambda\nu} = \Bigg[&-\frac{1}{6}R\,R_{\lambda\nu} - \frac{1}{6}\Box R_{\lambda\nu} + \frac{1}{2}R_{\lambda\alpha}R^{\alpha}_{\ \nu} - \frac{1}{12}R^{\alpha\beta\gamma}_{\ \ \ \ \nu}R_{\alpha\beta\gamma\lambda} \\ &+ \left(\frac{1}{72}R^2 + \frac{1}{30}\Box R - \frac{1}{180}R_{\alpha\beta}R^{\alpha\beta} + \frac{1}{180}R_{\alpha\beta\gamma\delta}R^{\alpha\beta\gamma\delta}\right)g_{\lambda\nu}\Bigg]\,. \end{aligned} \tag{5.42c}$$

These calculations have been obtained using the Feynman gauge, $\alpha = 1$. To completely determine the effective action, it is still necessary to multiply the coefficients of the heat-kernel expansion with the inverse metric $g^{\mu\lambda}$ and then take the trace over the Lorentz indices μ and ν.

5.4. Collecting terms and isolating divergences

To obtain the final expressions for the effective actions, we investigate the obtained expressions limiting the calculations to the first two terms in the expansion of the Greens function, i.e. $j \leq 2$. We have to solve integrals of the form

$$I_\alpha(D) = \int \frac{d^D k}{(2\pi)^D} \frac{1}{(-k^2+m^2)^\alpha}\,, \tag{5.43}$$

for $\alpha = 1, 2, 3$. The result can be expressed in terms of the Gamma function,

$$I_\alpha(D) = \frac{i}{(4\pi)^{D/2}} \frac{\Gamma\left(\alpha - \frac{D}{2}\right)}{\Gamma(\alpha)} \frac{1}{(m^2)^{\alpha - D/2}}\,, \tag{5.44}$$

which for $D = 4$ and with $\alpha = 1, 2$ contains $\Gamma(0)$ and $\Gamma(-1)$, both of which are divergent expressions. The case $\alpha = 3$ contains $\Gamma(1)$, which renders the expression finite, and thus the integral can be calculated by conventional methods. We use dimensional regularization to solve the first two integrals, assuming $D = 4 - \epsilon$ with ϵ taken to zero in the end. In further calculations, we will always carry out the limits $\epsilon \to 0$ if possible and safe. The integrals with $\alpha = 1, 2$ result in

$$I_1(4-\epsilon) = \frac{i}{(4\pi)^{2-\epsilon/2}} \Gamma\left(\frac{\epsilon}{2} - 1\right) m^{2-\epsilon}\,, \tag{5.45}$$

$$I_2(4-\epsilon) = \frac{i}{(4\pi)^{2-\epsilon/2}} \Gamma\left(\frac{\epsilon}{2}\right) m^{-\epsilon}\,. \tag{5.46}$$

whereas the integral for $\alpha = 3$ yields

$$I_3(D) = S_D \int \frac{dk}{(2\pi)^D} \frac{k^{D-1}}{(-k^2+m^2)^3}\,, \tag{5.47}$$

where S_D is the angular integration over the D-dimensional unit sphere. The integral can be carried out for real m via a Wick-rotation $k_E = ik$ and results for $D = 4$ in the expression

$$I_3(4) = \frac{i}{32\pi^2} \frac{1}{m^2}\,. \tag{5.48}$$

Since the results for the integrals with $\alpha = 1, 2$ are divergent in the limit $\epsilon \to 0$, some further calculations have to be carried out in order to single out the divergences in the expressions.

In the case of the scalar field, denoted by superscript (0), and after straightforwardly carrying out the mass integral, the effective action reads

$$S_{\text{eff}}^{(0)} = -\frac{1}{8\pi^2} \int d^{4-\epsilon}x \sqrt{-g} \left[a_0 \Gamma\left(\frac{\epsilon}{2} - 1\right) \frac{m^{4-\epsilon}}{4-\epsilon} + a_1 \Gamma\left(\frac{\epsilon}{2}\right) \frac{m^{2-\epsilon}}{2-\epsilon} + a_2 \ln m - ... \right], \tag{5.49}$$

with the coefficients given by Eq. (5.20). For the Dirac spinor field, denoted by the superscript (1/2), after the mass integral the effective action reads

$$S_{\rm eff}^{(1/2)} = -\frac{1}{32\pi^2}\int d^{4-\epsilon}x\sqrt{-g}\,{\rm tr}_{\rm D}\left[\mathbf{a}_0\,\Gamma\left(\frac{\epsilon}{2}-1\right)\,\frac{m^{4-\epsilon}}{4-\epsilon}+\,\mathbf{a}_1\,\Gamma\left(\frac{\epsilon}{2}\right)\,\frac{m^{2-\epsilon}}{2-\epsilon}+\mathbf{a}_2\,\ln m-...\right], \tag{5.50}$$

where the trace over the Dirac indices of the coefficients of the curvature expansion still needs to be carried out. Doing so, we can define new coefficients $\tilde{a}_i$ as

$$\tilde{a}_0 = 2\,, \tag{5.51a}$$

$$\tilde{a}_1 = \frac{1}{6}R\,, \tag{5.51b}$$

$$\tilde{a}_2 = \frac{1}{144}R^2-\frac{1}{60}\Box R-\frac{1}{90}R_{\alpha\beta}R^{\alpha\beta}+\frac{1}{90}R_{\alpha\beta\gamma\delta}R^{\alpha\beta\gamma\delta}+\frac{1}{96}{\rm tr}_{\rm D}\left[\sigma_{\alpha\beta}\sigma_{\gamma\delta}R^{\alpha\beta\lambda\xi}R^{\gamma\delta}{}_{\lambda\xi}\right], \tag{5.51c}$$

and the effective action in terms of the new coefficients reads then

$$S_{\rm eff}^{(1/2)} = \frac{1}{8\pi^2}\int d^{4-\epsilon}x\sqrt{-g}\left[\tilde{a}_0\,\Gamma\left(\frac{\epsilon}{2}-1\right)\,\frac{m^{4-\epsilon}}{4-\epsilon}+\,\tilde{a}_1\,\Gamma\left(\frac{\epsilon}{2}\right)\,\frac{m^{2-\epsilon}}{2-\epsilon}+\tilde{a}_2\,\ln m-...\right]. \tag{5.52}$$

We see that the coefficient $\tilde{a}_0$ has an overall factor of 2 with respect to a_0 from the expansion for a complex scalar field, which corresponds to the different number of degrees of freedom; moreover, the curvature coefficients are slightly different due to the fermionic nature of the Dirac spinor field.

For vector bosons, denoted by the superscript (1), after the mass integrals we obtain the same expression as for the scalars,

$$\begin{aligned} S_{\rm eff}^{(1)} \;=\; -\frac{1}{8\pi^2}\int d^{4-\epsilon}x\sqrt{-g}\,{\rm tr}_{\rm L}\Big[&g^{\mu\lambda}a_{0\lambda\nu}\,\Gamma\left(\frac{\epsilon}{2}-1\right)\frac{m^{4-\epsilon}}{4-\epsilon} \\ &+g^{\mu\lambda}a_{1\lambda\nu}\,\Gamma\left(\frac{\epsilon}{2}\right)\frac{m^{2-\epsilon}}{2-\epsilon}+g^{\mu\lambda}a_{2\lambda\nu}\,\ln m-...\Big], \end{aligned} \tag{5.53}$$

where the trace over the Lorentz indices has still to be considered.

In order to obtain a reasonable result in the limit $\epsilon\to 0$, we can now expand the Gamma functions as before via Eq. (4.11). Together with an expansion of the mass term for small ϵ we end up with

$$\Gamma\left(\frac{\epsilon}{2}-1\right)\simeq\frac{2}{\epsilon}+\frac{1}{2}-\gamma\,, \tag{5.54}$$

$$\Gamma\left(\frac{\epsilon}{2}\right)\simeq\frac{2}{\epsilon}-\gamma\,,$$

$$m^{-\epsilon}=\mu^{-\epsilon}\left(\frac{\mu}{m}\right)^{\epsilon}\simeq\mu^{-\epsilon}\left(1+\epsilon\ln\frac{\mu}{m}\right), \tag{5.55}$$

where γ is the Euler-Mascheroni constant, and μ the auxiliary parameter already introduced before. In the limit of $\epsilon\to 0$, the factor will go to unity, i.e.

$$\lim_{\epsilon\to 0}\mu^{-\epsilon}=1\,. \tag{5.56}$$

In the following, we will carry out this and other safe limits $\epsilon \to 0$ immediately, like e.g. also those occurring in the denominators of the effective actions.
Plugging these expressions into the effective actions, and omitting all terms $\mathcal{O}(\epsilon)$, we end up with

$$\begin{aligned} S_{\text{eff}} &= -\frac{1}{8\pi^2}\int d^4x\sqrt{-g}\left[\mathfrak{a}_0\,\frac{m^4}{4}\left(\frac{2}{\epsilon}+\frac{1}{2}-\gamma+2\ln\frac{\mu}{m}\right)\right. \\ &\qquad \left.+\mathfrak{a}_1\,\frac{m^2}{2}\left(\frac{2}{\epsilon}-\gamma+2\ln\frac{\mu}{m}\right)+\mathfrak{a}_2\,\ln m+...\right] \end{aligned} \tag{5.57}$$

where

$$\mathfrak{a}_j = \begin{cases} a_j & \text{scalar fields}\,, \\ -\tilde{a}_j & \text{spinor fields}\,, \\ \mathrm{tr_L}\left[g^{\mu\lambda}a_{j\lambda\nu}\right] & \text{vector fields}\,. \end{cases} \tag{5.58}$$

We see that the expressions for bosons and fermions are formally the same, apart from the sign and some differences in the coefficients of the heat kernel expansion. In the next section we will now proceed to apply the obtained results to a specific case of curvature and system of particles.

5.5. Vacuum energy balance

We will now try to set up a concrete example of a system of particles for which we can reach the ultimate goal of obtaining a value of the vacuum energy which is identical to the observationally desired one of $\rho_\Lambda^{(\text{obs})} = 10^{-47}\,\text{GeV}^4$. In the final result for all the vacuum contributions of the fields we have terms in the curvature expansion of the effective action proportional to $\mathfrak{a}_{0,i}\,m^4$, $\mathfrak{a}_{1,i}\,m^2$ and $\mathfrak{a}_{2,i}$, where $\mathfrak{a}$ stands for the coefficients of the ith species, i.e. scalars, spinors or vectors. The first ($j = 0$) and the second ($j = 1$) term in the expansion have dimensionless coefficients with divergent and convergent parts; these have been identified and separated in the calculations of the last section. The third term ($j = 2$) is finite. Our goal now is to make sense of the divergent effective action in cancelling the occurring infinities by appropriate choice of masses like in the case of flat spacetimes.
Omitting the spatial integral and constant numerical coefficients, the effective action for a system with bosonic and fermionic masses can be stated as

$$S_{\text{eff}} \propto \sum_i \left[\mathfrak{a}_{0,i}\,\frac{m_i^4}{4}\left(\frac{2}{\epsilon}+\frac{1}{2}-\gamma+2\ln\frac{\mu}{m_i}\right)+\mathfrak{a}_{1,i}\,\frac{m_i^2}{2}\left(\frac{2}{\epsilon}-\gamma+2\ln\frac{\mu}{m_i}\right)+\mathfrak{a}_{2,i}\,\ln m_i\right], \tag{5.59}$$

where $\mathfrak{a}_{j,i}$ are the corresponding jth coefficients for the ith species. We can now separate the convergent and divergent terms to see more distinctly which are the necessary conditions to cancel the divergences. Rewriting the effective action as

$$\begin{aligned} S_{\text{eff}} \;\propto\; & \left(\frac{2}{\epsilon}+\frac{1}{2}-\gamma\right)\sum_i\left[\mathfrak{a}_{0,i}\,\frac{m_i^4}{4}+a_{1,i}\,\frac{m_i^2}{2}\right]+ \\ & +\sum_i\left[a_{0,i}\,\frac{m_i^4}{2}\ln\frac{\mu}{m_i}+\mathfrak{a}_{1,i}\,m_i^2\left(-\frac{1}{4}+\ln\frac{\mu}{m_i}\right)+\mathfrak{a}_{2,i}\,\ln m_i\right], \end{aligned} \tag{5.60}$$

it becomes obvious that in order to cancel the divergent parts of the effective action we have to require that

$$\sum_i\left[\mathfrak{a}_{0,i}\,\frac{m_i^4}{4}+\mathfrak{a}_{1,i}\,\frac{m_i^2}{2}\right]=0\,, \tag{5.61}$$

with the sum running over all particles of the system. At this point we have to remember that by using dimensional regularization, we have missed one balancing condition, which is obtained by other types of regularization, i.e. the balance of degrees of freedom:

$$\sum_i \nu_i = 0\,. \tag{5.62}$$

In choosing the particles to be introduced to the system in order to eliminate the divergences, we have to consider this relation additionally to eliminate also the quadratic divergences of the effective action, as outlined in Section 4.1. Note that in the balance of the degrees of freedom also massless particles like the photons and gluons contribute.
If these two conditions are fulfilled, the remainder of the effective action will be finite and constitute the contribution of the quantum fluctuations to the vacuum energy driving expansion.
The convergent remainder which will determine the actual magnitude of the expansion, and which should result in the observed value of the cosmological constant Eq. (6.12), is given by the terms

$$\frac{1}{8\pi^2}\sum_i\left[-\mathfrak{a}_{0,i}\,\frac{m_i^4}{2}\ln m_i+\mathfrak{a}_{1,i}\,m_i^2\left(-\frac{1}{4}-\ln m_i\right)+\mathfrak{a}_{2,i}\,\ln m_i\right]=\rho_\Lambda\,. \tag{5.63}$$

The parameter μ does not occur anymore in this equation, since these terms can be eliminated by condition (5.61) after separating the logarithm of the fraction. In our model all the contributions to the free energy are given by the effective action (5.57) with the coefficients Eq. (5.58), and the conditions which have to be fulfilled in order to achieve the correct cosmic expansion are Eqs. (5.61), (5.62) and (5.63). Note that even though the contributions of bosons to the effective action are originally positive and those of fermions negative, in the convergent remainder, which consists of sub-leading order terms, this has

been reversed due to the properties of the logarithm. In the balancing equation to achieve the energy density of the observed cosmological constant, the bosons now enter with positive contributions, and fermions with negative. Since we would like to end up with an overall negative energy density to drive the cosmic accelerated expansion, we need a small fermionic excess in the convergent balancing condition (5.63). As it will turn out, the standard model particle content results in a rather large fermionic excess in all three conditions Eqs. (5.61), (5.62) and (5.63), and thus we need to introduce bosonic particles in order to reduce the convergent remainder of the vacuum energy down to the small observed ρ_Λ.

We will now, after clarifying a minor point on massless particles, proceed to calculate the effective action given by these expressions in the framework of our universe, i.e. with a FLRW-metric and the particles of the standard model, and investigate its compatibility with the values of the cosmological expansion which we hope to achieve by considering the vacuum fluctuations.

5.6. Massless particles

For the case of massless particles, taking the limit $m \to 0$ in expression (5.57) is not straightforward, since there are terms like $m \ln m$ involved. We have to take this limit before carrying out the k-integration, and thus calculate

$$S_{\text{eff}} \propto \int \frac{d^D k}{(2\pi)^D} \left[\frac{\mathfrak{a}_{0,i}}{k^2} + \frac{\mathfrak{a}_{1,i}}{(k^2)^2} + ... \right] , \tag{5.64}$$

i.e. have to solve integrals of the form

$$I_\alpha(D) = \int \frac{d^D k}{(2\pi)^D} \frac{1}{(k^2)^\alpha} , \tag{5.65}$$

which are zero in the formalism of dimensional regularization [52, 54, 55], and lead to quadratic poles in the effective action when using a cutoff regularization, as was argued in Section 4.1. Due to these poles, massless particles need to be considered in the balance of degrees of freedom (5.62), but have no contribution to the mass balances Eqs. (5.61) and (5.63).

6. Application to the current universe

In the previous chapter, we have obtained expressions for the 1-loop contributions to the effective action of a system of bosons and fermions, as an expansion in terms of the curvature of the system. We now proceed to investigate how the accelerated expansion of the universe can be explained from these curvature terms by explicitly calculating them for the case of a specific metric.
We will try to investigate the applicability of the method to the standard model particle content, which comprises, besides the massless photons and gluons, twelve fermions, three vector bosons and as of recently also one scalar boson [69–71]. It will turn out that for the cancellation of the divergences in our system we need to assume the existence of one further boson contributing to the balance, since the divergent part of the effective action calculated for the standard model particles results in a fermionic excess of the vacuum energy. The remaining convergent part is dominated by fermionic contributions as well, and quite some orders of magnitude larger than the required observed energy density ρ_Λ. This requires the introduction of a further bosonic particle in order to nearly achieve the cancellation of that part of the vacuum energy such as to end up with a small negative remainder.
In this chapter we will first calculate the curvature-dependent coefficients of the heat kernel expansion for a specific example of spacetime, and then we will use the obtained results in an attempt to calculate the aforementioned masses of the additional particles necessary to reach the goal of explaining dark energy by the vacuum energy density of quantum fields.

6.1. Calculation of curvature terms for a specific spacetime

We will assume the universe to be Friedmann-Lemaître-Robertson-Walker, employing the Einstein equations in a homogeneous universe without a cosmological constant term, and try to obtain the effect of a cosmological constant by the vacuum energy contributions of fields present in this universe. With the FLRW-metric

$$ds^2 = dt^2 - a(t)^2 \left[dx^2 + dy^2 + dz^2\right] , \tag{6.1}$$

we can calculate the relevant curvature quantities using the formulae for the curvature scalar, Ricci tensor, Riemann curvature tensor and similar quantities occurring in the coefficients of the curvature expansion of the effective action, as introduced in Chapter 1. Having obtained expressions for these basic quantities, we can proceed to calculate the coefficients of the heat kernel expansion, as given by Eqs. (5.20), (5.42) and (5.51). We obtain

$$a_0 = \tilde{a}_0 = 1\,, \tag{6.2a}$$

$$a_1 = \tilde{a}_1 = \frac{[a'(t)^2 + a(t)a''(t)]}{a(t)^2}\,, \tag{6.2b}$$

$$a_2 = \frac{51a'(t)^4 - 20a(t)a'(t)^2a''(t) + 21a(t)^2a''(t)^2 + 6a(t)^3a^{(4)}(t)}{30\,a(t)^4}\,, \tag{6.2c}$$

$$\tilde{a}_2 = \frac{\left[-37 + 5a(t)^2\right]a'(t)^4 + 140a(t)a'(t)^2a''(t) + 6a(t)^2\left[3a''(t)^2 - 2a(t)a^{(4)}(t)\right]}{240\,a(t)^4}\,, \tag{6.2d}$$

$$\mathrm{tr_L}\left[g^{\mu\lambda}a_{0\lambda\nu}\right] = 4\,, \tag{6.2e}$$

$$\mathrm{tr_L}\left[g^{\mu\lambda}a_{1\lambda\nu}\right] = \frac{-\left[1 + 3a(t)^2\right]a'(t)^2 + 2a(t)a''(t)}{a(t)^2}\,, \tag{6.2f}$$

$$\begin{aligned}\mathrm{tr_L}\left[g^{\mu\lambda}a_{2\lambda\nu}\right] = {}& \frac{3a'(t)^4\left[-17 + 41a(t)^2\right] + 10a(t)a'(t)^2a''(t)\left[14 - 15a(t)^2\right]}{30\,a(t)^4} \\ & + \frac{a(t)^2\left\{-2a''(t)^2\left[11 + 12a(t)^2\right] + a(t)a^{(4)}(t)\left[3 + a(t)^2\right]\right\}}{10\,a(t)^4} \\ & - a(t)^2a'(t)a^{(3)}(t)\left[1 + 3a(t)^2\right]\,.\end{aligned} \tag{6.2g}$$

All these expressions involve the scale factor $a(t)$ as the quantity that defines the size of the curvature contributions to the effective action, as well as the derivatives of $a(t)$. In order to be able to express the coefficients in terms of actual numbers, we will utilize several parameters which correspond more or less directly to the derivatives of the scale factor, i.e. the so-called cosmographic series (CS). The first and well-known parameter of this series is the Hubble parameter, given by the first derivative of the scale factor divided by the scale factor itself; further the CS comprises the parameters q_0, j_0 and s_0, corresponding to the higher order derivatives of the scale factor. From the definitions

$$\begin{aligned} H &\equiv \frac{1}{a}\frac{da}{dt}\,, & q &\equiv -\frac{1}{aH^2}\frac{d^2a}{dt^2}\,, \\ j &\equiv \frac{1}{aH^3}\frac{d^3a}{dt^3}\,, & s &\equiv \frac{1}{aH^4}\frac{d^4a}{dt^4}\,, \end{aligned} \tag{6.3}$$

we can obtain the parameters of the CS by evaluating the parameters at present time t_0. The derivatives of the scale factor occurring in the expressions for the curvature expansion

coefficients can be expressed in terms of the cosmographic parameters. A useful tool to question the correctness of the results is dimensional analysis. The scale factor by itself has to be a dimensionless quantity, in order to render the metric dimensionless. It is just a scale, but not a physical length. The usual convention is to fix the scale factor at present time as $a(t_0) = a_0 = 1$. The CS parameters are dimensionless, apart from the Hubble parameter which is dimensionful with $[H] = s^{-1}$. As a consequence, inverting Eqs. (6.3) to express the derivatives of the scale factor in terms of the CS parameters, the n-th derivative of $a(t)$ has dimension s^{-n}.
The problem of extracting the values of the CS parameters from the analysis of current astrophysical data is treated extensively in Part III, resulting in the best fit values [15]

$$\begin{aligned} H_0 &= 74.05\,\mathrm{km/(s\,Mpc)}\,, & q_0 &= -0.663\,, \\ j_0 &= 1\,, & s_0 &= -0.206\,. \end{aligned} \tag{6.4}$$

In terms of the CS, we can restate the coefficients of the effective action as

$$a_0 = \tilde{a}_0 = 1\,, \tag{6.5a}$$

$$a_1 = \tilde{a}_1 = -H_0^2\,(+1 - q_0)\ , \tag{6.5b}$$

$$a_2 = \frac{H_0^4}{30}\left(51 + 20q_0 + 21q_0^2 + 6s_0\right)\ , \tag{6.5c}$$

$$\tilde{a}_2 = \frac{H_0^4}{120}\left(-16 - 70q_0 + 9q_0^2 - 6s_0\right)\ , \tag{6.5d}$$

$$\mathrm{tr_L}\left[g^{\mu\lambda}a_{0\lambda\nu}\right] = 4\,, \tag{6.5e}$$

$$\mathrm{tr_L}\left[g^{\mu\lambda}a_{1\lambda\nu}\right] = -2H_0^2\,(2 + q_0)\ , \tag{6.5f}$$

$$\mathrm{tr_L}\left[g^{\mu\lambda}a_{2\lambda\nu}\right] = \frac{H_0^4}{15}\left(36 + 5q_0 - 69q_0^2 - 60j_0 + 6s_0\right)\ . \tag{6.5g}$$

From the above expressions we see that the coefficients with $j = 0$ are dimensionless, those with $j = 1$ have dimension s^{-2} and those with $j = 2$ have s^{-4}. At first sight this seems odd, however, the different orders of coefficients are paired with different powers of the mass in the vacuum energy expression, as can be seen from Eq. (5.57). Using natural units in which $c = \hbar = 1$, we find that

$$[\mathfrak{a}_{0,i}\,m^4] = [\mathfrak{a}_{1,i}\,m^2] = [\mathfrak{a}_{2,i}] = l_P^{-4}\,, \tag{6.6}$$

i.e. all terms have the dimension of inverse quartic Planck length l_P and are consistent with each other. Together with the integral over four-dimensional spacetime, we end up with a dimensionless effective action, which is necessary since it occurs in the exponent of the partition function.

6.2. Our physical units

For the concrete numerical calculations, we need to find a consistent unit system in which all quantities are formulated, i.e. the masses of the particles, the curvature terms, and also the cosmological constant, in order to be able to compare the vacuum energy of the fields with the measured value of the cosmic expansion in the end. Thus, we choose to express all quantities in terms of GeV, resorting to a natural unit system in which $c = \hbar = 1$. In particle physics, these conventions are common, and masses are generally given in units of GeV. However, as mentioned above, we have different types of terms in our expansion; terms proportional to mass, terms containing combinations of mass and Hubble parameter, and terms with only the Hubble parameter. In order to obtain all terms in units of GeV, we have to convert the Hubble parameter to those units as well.
The Hubble parameter is by definition given in units of s^{-1}, and commonly expressed in units of km/(s Mpc), as indicated in the previous section. However, it can be converted to GeV by expanding the expression with Planck time t_P, and identifying the Planck time as the inverse of the Planck energy, $1/t_P \sim E_P$ (which is true in a unit system where $c = \hbar = 1$). By doing this, we obtain a value of the Hubble parameter today of

$$H_0 \simeq 1.5\,10^{-42} \cdot \mathrm{GeV}\,. \tag{6.7}$$

The last remaining quantity to be expressed in suitable numerical units is the cosmological constant, occurring in the ΛCDM action as

$$S_{\Lambda\mathrm{CDM}} = \int d^D x \sqrt{-g} \left[\frac{1}{2\kappa} (R - 2\Lambda) + \mathcal{L}_M \right] , \tag{6.8}$$

with $\kappa = 8\pi G$ in our unit system. The corresponding energy density is ρ_Λ, defined as

$$\rho_\Lambda = \Lambda/\kappa\,. \tag{6.9}$$

From observations, the value of this energy density can be inferred to be given by (see e.g. [31])

$$\rho_\Lambda^{(\mathrm{obs})} \simeq 10^{-122}\,\rho_P \simeq 10^{-47}\,\mathrm{GeV}^4\,, \tag{6.10}$$

where $\rho_P \equiv m_P^4$ is the Planck density. This number can be easily confirmed using the Friedmann equations and assuming that today the universe is approximately dominated by the cosmological constant; i.e.

$$\Lambda \simeq H_0^2\,. \tag{6.11}$$

Then the observed energy density originating from the cosmological constant is

$$\rho_\Lambda^{(\mathrm{obs})} = \frac{\Lambda}{8\pi G} \simeq \frac{H_0^2\,E_P^2}{8\pi} \simeq 10^{-47}\mathrm{GeV}^4\,. \tag{6.12}$$

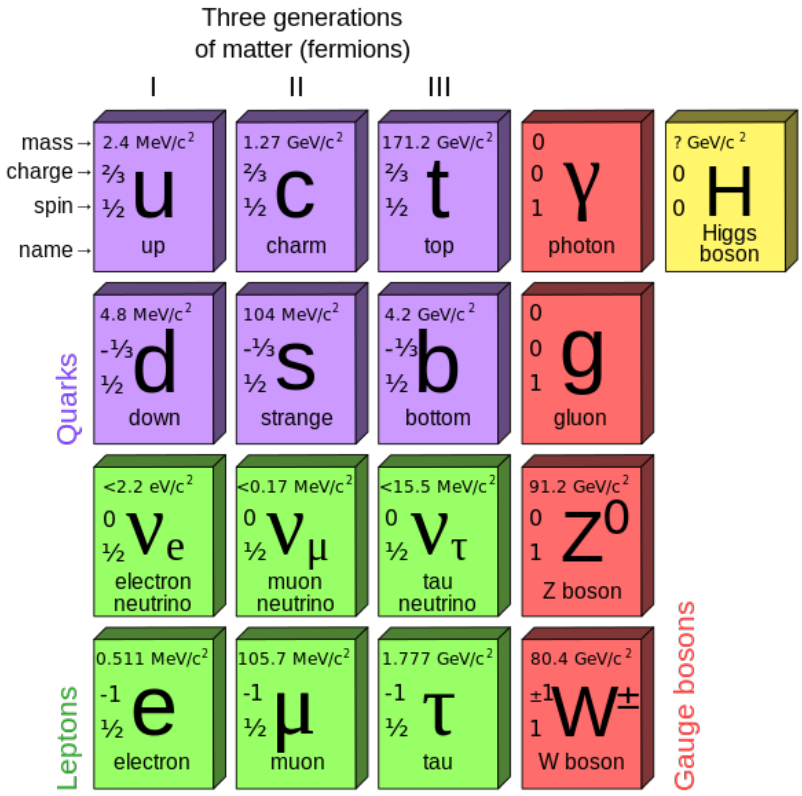

Figure 6.1.: Standard Model of particle physics [72].

This is the order of magnitude we need to reproduce in the balance of masses, i.e. which should remain after cancelling the divergences. Now that the unit system is established and it is clear how to insert the different quantities into the balance, we can proceed to the numerical calculations of the masses.

6.3. Standard model particles

The standard model of particle physics [71] as known of today comprises 16 massive particles, of which there are four bosons, one scalar and three vector, and twelve fermions, all spinors, as can be seen from Fig. 6.1. A list of particles and their masses, including the massless photon and gluons can be found in Tab. 6.1.

We have two expressions to evaluate: one is the condition for the cancellation of divergences, given by Eq. (5.61), which must be fulfilled to render the vacuum energy a finite quantity; and the convergent remainder, given by Eq. (5.63), which has to be tuned to result in the value of the energy density of the observed cosmological constant. Moreover, the balance of degrees of freedom (5.62) has to be considered in the choice of the new

Spin	name	mass	deg. of freed.
0	H	125.3 GeV	1
1/2	u, $\bar{u}$	2.4 MeV	4
	d, $\bar{d}$	4.8 MeV	4
	c, $\bar{c}$	1.27 GeV	4
	s, $\bar{s}$	104 MeV	4
	t, $\bar{t}$	171.2 GeV	4
	b, $\bar{b}$	4.2 GeV	4
	e^-, e^+	0.511 MeV	4
	μ^-, μ^+	105.7 MeV	4
	τ^-, τ^+	1.777 GeV	4
	ν_e, $\bar{\nu_e}$	< 2.2 eV	2
	ν_μ, $\bar{\nu_\mu}$	< 0.17 MeV	2
	ν_τ, $\bar{\nu_\tau}$	< 15.5 MeV	2
1	γ	0	2
	$8\,g$	0	$8 \cdot 2$
	Z^0	91.2 GeV	3
	W^+, W^-	80.4 GeV	$2 \cdot 3$

Note. Masses in units where $c = \hbar = 1$.

Table 6.1.: Standard Model of particle physics [72].

particles postulated.

As already indicated before, the above mentioned particle content leads to an excess of fermions in all three balancing conditions. It is thus clear that we need to introduce two new bosonic particles in order to be able to tune the vacuum energy to the required level. Considering the balance of the degrees of freedom in order to infer which types of particles are required to fulfil this condition, from the standard model we have 42 fermionic degrees of freedom opposing 28 on the bosonic side. The difference of 14 degrees of freedom must be achieved by the two new bosons. Ten of the fourteen degrees of freedom could be ascribed to a spin 2 particle with a $U(1)$ type of charge, whereas the remaining four degrees of freedom have to originate from the second boson, which could be a spin 1 particle with a more complicated type of charge, similar to the charges of the $U(1) \times SU(2)$ group in electroweak theory. It is likely however that the charges we are referring to are none of the charges known in the standard model, since if so, the new particles would interact via established mechanisms with the standard model particles, and could have possibly been found in experiments. This will become more clear after determining the exact values of their masses, since then we can predict if and which experiments could detect or should have detected the two new particles.

We now have to calculate the masses of the two new particles from the conditions (5.61) and (5.63) in order to achieve the correct value of the cosmic expansion,

$$\sum_i \left[\mathfrak{a}_{0,i} \frac{m_i^4}{4} + \mathfrak{a}_{1,i} \frac{m_i^2}{2} \right] = 0 \,, \tag{6.13a}$$

$$\sum_i \frac{1}{8\pi^2} \left[-\mathfrak{a}_{0,i} \frac{m_i^4}{2} \ln m_i + \mathfrak{a}_{1,i}\, m_i^2 \left(-\frac{1}{4} - \ln m_i \right) + \mathfrak{a}_{2,i} \ln m_i \right] = \rho_\Lambda \,. \tag{6.13b}$$

One more simplification can be taken into account here due to the consideration of curvature in this problem. From the calculation of the curvature coefficients $\mathfrak{a}_i$ we know that the higher-order terms, i.e. $\mathfrak{a}_{1,i}$, $\mathfrak{a}_{2,i}$ etc. go with the Hubble parameter as H_0^2, H_0^4, etc. Recalling that the Hubble parameter is of the order of 10^{-42} GeV in the units we use, and the masses maximally of the order 10^{11} GeV, we see that for achieving an energy density of $\rho_\Lambda \simeq 10^{-47}\mathrm{GeV}^4$, we can safely neglect the terms proportional to $\mathfrak{a}_{1,i}$ and $\mathfrak{a}_{2,i}$ and further orders in the convergent part of the balance. That simplifies the above conditions to

$$\sum_i \left[\mathfrak{a}_{0,i} \frac{m_i^4}{4} + \mathfrak{a}_{1,i} \frac{m_i^2}{2} \right] = 0 \,, \tag{6.14a}$$

$$-\sum_i \frac{1}{8\pi^2}\, \mathfrak{a}_{0,i} \frac{m_i^4}{2} \ln m_i = \rho_\Lambda \,. \tag{6.14b}$$

For two additional bosonic particles this can be easily solved and leads to the masses of

the two bosons, here denoted by X and Y, as

$$\begin{aligned} m_X &= 168.9\,\mathrm{GeV}\,, \\ m_Y &= 67.7\,\mathrm{GeV}\,. \end{aligned} \tag{6.15}$$

With those two additional particles in the standard model, we can construct the cancellation of the divergent parts of the vacuum energy, and at the same time achieve a value of the remaining convergent parts to be of the right order of magnitude to explain the currently observed energy density that drives the cosmic expansion.

Judging from the computed values of the new bosons, none of them lies within the reach of current particle detectors. Since there is no evidence so far for any particle with those masses, we have to assume that the bosons do not interact with any of the known standard model particles via any of the common interactions. In this case, they could only be detected indirectly through their interaction with other particles. In order to evaluate the possibility of their existence and calculate their signature in standard model particle interactions, it would be necessary to assume more about their nature and properties. Given the multitude of different extensions of the standard model of cosmology and particle physics, there are surely possible candidates which fit the properties of the bosons predicted here. We will however content ourselves with the calculated value of their mass and leave further speculations on their nature to future works.

7. Conclusions and Outlook

In this chapter we have calculated the vacuum energy contributions of non-interacting bosonic and fermionic particles in flat and curved spacetime in order to explain the existence of a constant vacuum energy density driving the accelerated expansion of the universe. Vacuum energy from zero-point fluctuations of particles are perfectly suited for the purpose since they possess the desired properties of a constant energy density in space and a negative equation of state when interpreted as a cosmic fluid. However, as is well-known and was outlined in the introduction, the energy of the vacuum fluctuations of any elementary particle is infinite, since there is an infinite energy contribution from the fluctuations of every point in space. We have quantitatively formulated this infinity by choosing the method of dimensional regularization, a mathematical technique modifying the number of spacetime dimensions from $D = 4$ to $D = 4 - \epsilon$ in order to be able to formally calculate the vacuum energy integrals. In this way, it is possible to identify the divergences as poles in ϵ, a quantity which has to be taken to zero, and separate the divergences from a physically relevant convergent part.

We have obtained conditions for the case of flat spacetime, Eqs. (4.15), (4.17) and (4.18), and curved spacetime, Eqs. (5.61), (5.62) and (5.63), which - when fulfilled - lead to a cancellation of the divergent contributions to the vacuum energy, and tune the convergent part exactly to the value of the observed cosmological constant, driving the expansion of the universe. The results for the case of non-zero spacetime curvature have been obtained by carrying out an expansion of the Greens function of the system in terms of a power series, with the coefficients depending on curvature-related quantities, the so-called heat kernel expansion. These coefficients have then been evaluated for the case of a Friedmann-Lemaître-Robertson-Walker metric with a scale factor $a(t)$, using current cosmographic parameters obtained from the investigation of observational data on supernovae.

We then proceeded to investigate the standard model of particle physics in the context of curved spacetimes, i.e. we calculated the divergent and convergent parts of the vacuum energy in order to evaluate whether bosonic or fermionic contributions dominate the balancing conditions. In the case of the standard model, there is a imbalance in favour of the fermionic part, so in order to even out the vacuum energy contributions, new bosonic particles are required. Following the argument of cancelling out the divergent contributions

by exact cancellation of bosonic and fermionic energy, we then analysed how such a balance could be achieved. It turns out that with the introduction of two additional bosonic particles, one with a mass of 168.9 GeV and a second of about 67.7 GeV, it is possible to exactly cancel the divergent contributions of the vacuum energy, and obtain the desired value of the cosmological constant to reproduce the observed expansion of the universe.
With these results, we have achieved what we set out to do, i.e. explaining the fact of the accelerated expansion of the universe as a consequence of the vacuum energy of particles in the universe. We have acknowledged the existence of divergences in the vacuum energy, and have dealt with them not in the conventional way by renormalizing the theory, but by exact cancellation of divergent contributions with different signs from bosonic and fermionic species. This principle has been proven to work, but at the same time it undoubtedly involves a lot of fine-tuning. In a sense, we have transformed the hierarchy problem to a fine-tuning problem by demanding the existence of two new particles which have not been observed yet and exactly fit the requirements for the purpose of balancing the vacuum energy. The masses of these two particles have to be tuned to a very high precision in order to achieve the balance, otherwise the cancellation is not successful and the physical result can not be obtained. However, it has been shown that vacuum energy and the pure presence of particles can give rise to an observationally significant effect, which does not necessarily require a completely or also just partly new theory at its basis, as other approaches in this context do. In this model, the two newly introduced particles are commonly baryonic as the rest of the standard model particles, presumably with the equation of state of dust. The main achievement of the present model is that it works without assuming exotic matter leading to negative energy densities. It simply features two further bosonic particles, which due to their high mass or new types of charge have not been detected yet. These particles could be candidates for dark matter [73–75]. The resulting masses computed in the present work applied to the problem of dark matter would support the theory of weakly interacting massive particles (WIMPs) as dark matter candidates.
We would like to make one more comment on an implication of dark matter calculations [74, 75] referring to the fractal structure of space obtained in these simulations. If indeed the assumption of homogeneous and isotropic spacetime is wrong, the presence of inhomogeneities has to be taken into account and the ansatz of a FLRW-metric has to be modified correspondingly. Fluctuations of (mainly dark) matter would lead to a constant term in the Friedmann equations [76–78], much like a cosmological constant requires. In nearly all areas of physics, fluctuations are modelled to be Gaussian - this would however not lead to the correct magnitude of the effect, and would not suffice to explain dark energy. Taking into account non-Gaussian perturbations however, and considering all fluctuations

up to a cutoff of the current size of the universe, the resulting contribution to the Friedmann equation would likely lead to an appropriate effect [79]. Thus, changing the basic assumption of a homogeneous and isotropic universe changes significantly the preferable approach to the subject; in this work however, we have contented ourselves with the simple presumption of a Friedmann universe.

Besides the uncomfortable feature of fine-tuning, it is clear that this model is not particularly realistic concerning particle interactions either. We have assumed non-interacting particles, i.e. no forces between particles and no compound particles. This is of course not corresponding to particle physical reality, quite on the contrary - the standard model of particle physics features a rich variety of interactions between elementary particles. Interaction terms occur in the effective action and thus have influence on the convergent part of the vacuum energy, and so including interactions into the balance would change the second balancing condition completely. The principle of balancing would remain to be valid, however, the outcome for the masses would be possibly different. It is to be assumed however that these higher order contributions have much lower probabilities, and so would not alter the result significantly. Besides, this work should be understood rather as a demonstration of the functionality of a concept. Further investigations could include the complete standard model with particle interactions and compute the effect of the interaction terms on the convergent balance. It is clear that the order of magnitude of the outcoming masses would still lie within a similar range around the values of the highest masses of particles known today, and it would lead to more realistic predictions as to which particles should be expected in future high energy particle experiments.

Part III.

Dark Energy from an Observational Point of View

8. Principles of Cosmography

In this part, we will approach the issue of dark energy as introduced in the first part from an experimental point of view. The evidence gathered by several renowned experimental groups [5, 6] has lead to the consolidated opinion in the physical community that the universe is expanding at an accelerated pace [7–9]. In this chapter we aim at quantitatively describing the kinematical effect of the accelerated expansion of the universe, without specifying a particular model to explain its cause. As mentioned and described in detail in Part II, there is an abundance of ideas trying to model the effect or investigate its origins. A general overview of the matter is given in [80–82], with a particular emphasis on the experimental contributions coming from observations.

The currently most accepted model incorporating most of modern cosmology's observed features is the concordance model of cosmology, the ΛCDM paradigm [83], describing the universe today as a mixture of three substances, i.e. common baryonic matter, dark matter and a cosmological constant [84] to represent dark energy. For a more detailed description of these components, we refer to the thorough introduction in Part I and Part II. As successful as the ΛCDM model is in its general description of the universe, there are some inexplicable features of the observed universe, which cannot be explained [30]. Even though dark matter and dark energy are incorporated in the model as seemingly well-known components, in fact neither their nature nor their origin are satisfactorily constrained and still subject of speculation. Besides, ΛCDM is plagued by the hierarchy problem, which is treated extensively in Part II, and the coincidence problem [85, 86], i.e. the fact that the onset of the accelerated expansion of the universe is happening right at the current time. Despite the lack of explanations for these points, ΛCDM is considered as the most successful candidate to describe the observable universe, and assumed to be the limiting case of a more fundamental paradigm, which is still to be uncovered. In search for this more fundamental theory, there has been an abundance of propositions (see Part II), and it becomes increasingly difficult to retain an overview of all existing approaches, or discriminate fairly between them and evaluate their validity and quality. This has lead to the development of a branch of cosmology termed cosmography, i.e. a specific methodology of data analysis which aims at extracting quantitative statements on the properties of the universe without assuming an underlying paradigm or model to be true. With a minimum

set of assumptions, we describe the expansion of the universe by a FLRW-metric with a scale factor $a(t)$,

$$ds^2 = c^2dt^2 - a(t)^2\left(\frac{dr^2}{1-kr^2} + \sin^2\theta d\phi^2 + d\theta^2\right), \tag{8.1}$$

where k describes the curvature of the universe and we chose a spherically symmetric spatial part of the metric. The basics of cosmography can be found in [12, 13, 87–91] and in [14]. In this part, we investigate the concept of cosmography and critically question all its assumptions and principles. We find sufficient room for refinement, and suggest two modifications of conventional cosmographic theory, which we apply to data in order to support our claims of improvement. In Section 8.1, we will first introduce the basic scheme of cosmography, and derive several cosmological implications and quantities. We then proceed to pointing out its drawbacks in Chapter 9, and suggest two alterations, one being the introduction of alternative redshift variables in order to parameterize the scale factor, and the other one substituting the use of Taylor expansions in cosmography by the less well-known concept of Padé approximants. In Chapter 10, we present the statistical analyses carried out with the modified cosmographical methods, comparing them with existing procedures in cosmography, and interpreting our cosmological results in the light of the analyses of experimental groups [10, 11]. In Chapter 11, we conclude this part and its findings.

8.1. Conventional methodology

Since cosmological tests are usually based on the assumption that the model to be tested is the correct one, it appears evident that a model-independent way of characterizing cosmological models is necessary in order to honestly compare and evaluate different paradigms. Hence, in this paper, we are interested to find kinematical quantities which allow us to understand the validity of a given model only judging by some basic assumptions, without using model-dependent hypotheses. In other words, we are looking for a procedure allowing us to predict the free parameters of a certain model with a minimum of assumptions. Cosmography provides us with such a procedure; it tries to infer the kinematical quantities of a given model, making only the minimal dynamical assumptions that the geometry and symmetries of the FLRW metric hold and that the scale factor can be expanded into a Taylor series around the present time. In this way the standard Hubble law becomes a Taylor series valid for small times or redshifts. Analogously it is possible to expand the relation of pressure and density in a similar manner. Following the work of [13], we can

write down a Taylor series expansion of the scale factor as

$$\begin{aligned} a(t) &= a_0 \left[1 + \frac{da}{dt}\Big|_{t_0} (t-t_0) + \frac{1}{2!}\frac{d^2a}{dt^2}\Big|_{t_0} (t-t_0)^2 + \frac{1}{3!}\frac{d^3a}{dt^3}\Big|_{t_0} (t-t_0)^3 \right. \\ &+ \left. \frac{1}{4!}\frac{d^4a}{dt^4}\Big|_{t_0} (t-t_0)^4 + \frac{1}{5!}\frac{d^5a}{dt^5}\Big|_{t_0} (t-t_0)^5 + \frac{1}{6!}\frac{d^6a}{dt^6}\Big|_{t_0} (t-t_0)^6 + \mathcal{O}\left((t-t_0)^7\right) \right], \end{aligned} \tag{8.2}$$

where $\Delta t = t - t_0$ is the difference of an arbitrary time t to current time t_0, and $a_0 = a(t_0)$. Adapting the conventionally accepted choice $a_0 = 1$, this leads to

$$\begin{aligned} a(t) &= 1 - \frac{\dot{a}}{a}\Big|_{t_0} \Delta t + \frac{1}{2!}\frac{\ddot{a}}{a}\Big|_{t_0} \Delta t^2 - \frac{1}{3!}\frac{a^{(3)}}{a}\Big|_{t_0} \Delta t^3 + \frac{1}{4!}\frac{a^{(4)}}{a}\Big|_{t_0} \Delta t^4 \\ &\quad - \frac{1}{5!}\frac{a^{(5)}}{a}\Big|_{t_0} \Delta t^5 + \frac{1}{6!}\frac{a^{(6)}}{a}\Big|_{t_0} \Delta t^6 + \mathcal{O}\left(\Delta t^7\right) , \end{aligned} \tag{8.3}$$

where the dot indicates derivative with respect to time.
From this expansion of the scale factor, several parameters describing the kinematics of the universe can be defined corresponding to the respective order of expansion or derivative of the scale factor,

$$\begin{aligned} H(t) &\equiv \frac{1}{a}\frac{da}{dt} , & q(t) &\equiv -\frac{1}{aH^2}\frac{d^2a}{dt^2} , \\ j(t) &\equiv \frac{1}{aH^3}\frac{d^3a}{dt^3} , & s(t) &\equiv \frac{1}{aH^4}\frac{d^4a}{dt^4} , \\ l(t) &\equiv \frac{1}{aH^5}\frac{d^5a}{dt^5} , & m(t) &\equiv \frac{1}{aH^6}\frac{d^6a}{dt^6} . \end{aligned} \tag{8.4}$$

The parameters are termed Hubble, acceleration, jerk, snap, crackle and pop, respectively. Evaluated at the current time t_0, the parameters form the so-called cosmographic series (CS), and values for them can be extracted from fits of observational data. The parameters of the CS have distinct physical meaning. The Hubble parameter describes the change in scale factor, whereas the acceleration parameter gives its curvature. A negative q_0 indicates that the universe is accelerating. The jerk parameter in turn gives information about the change of q_0. A positive j_0 implies that in the past there has been a change in the acceleration behaviour, i.e. that there has been a transition from a decelerating to an accelerating expansion of the universe [92, 93].
By calculating the derivatives of the Hubble parameter and substituting the derivatives of the scale factor by the CS, we can derive the mutual dependence between the parameters

as

$$\begin{aligned} q &= -\frac{\dot{H}}{H^2} - 1\,, \\ j &= \frac{\ddot{H}}{H^3} - 3q - 2\,, \\ s &= \frac{H^{(3)}}{H^4} + 4j + 3q^2 + 12q + 6\,, \\ l &= \frac{H^{(4)}}{H^5} - 10jq - 20j - 30q^2 - 60q + 5s - 24\,, \\ m &= \frac{H^{(5)}}{H^6} + 10j^2 + 120jq + 120j + 6l + 30q^3 + 270q^2 - 15qs + 360q - 30s + 120\,. \end{aligned} \tag{8.5}$$

All these definitions and expressions parameterize the evolution of the universe with respect to time. Since the cosmological redshift z is a variable that can be used equivalently to time, all of the above can be formulated in terms of redshift instead of time. In order to transform the expansion of the scale factor and the parameters into functions of z, a simple transformation law is necessary, provided by

$$\frac{\partial}{\partial t} = -(1+z)\,H\,\frac{\partial}{\partial z}\,. \tag{8.6}$$

With this conversion, in principle the expressions of the CS in terms of the redshift can be calculated straightforwardly by simply substituting the multiple time derivatives of the Hubble parameter in the expressions for the CS by the derivatives with respect to the redshifts.

Using the definitions (8.4), we can then write for the scale factor

$$\begin{aligned} a(t) &= 1 - H_0\Delta t - \frac{q_0}{2!}H_0^2\Delta t^2 - \frac{j_0}{3!}H_0^3\Delta t^3 + \frac{s_0}{4!}H_0^4\Delta t^4 \\ &\qquad - \frac{l_0}{5!}H_0^5\Delta t^5 + \frac{m_0}{6!}H_0^6\Delta t^6 + \mathcal{O}\left(\Delta t^7\right)\,. \end{aligned} \tag{8.7}$$

For further calculations, we define

$$x := H_0\Delta t + \frac{q_0}{2!}H_0^2\Delta t^2 + \frac{j_0}{3!}H_0^3\Delta t^3 - \frac{s_0}{4!}H_0^4\Delta t^4 + \frac{l_0}{5!}H_0^5\Delta t^5 - \frac{m_0}{6!}H_0^6\Delta t^6\,, \tag{8.8}$$

such that the scale factor reads

$$a(t) \simeq 1 - x\,, \tag{8.9}$$

assuming that the series is truncated after the sixth order term.

We would like to obtain numerical values of the CS parameters by fitting observational data. Conventionally data from the observations of the luminosity of type Ia supernovae as a function of their redshift are used. Specifically, the difference of apparent and absolute luminosity of a supernova event, the so-called distance modulus,

$$\mu_D = \mu_{\text{apparent}} - \mu_{\text{absolute}}\,, \tag{8.10}$$

is used in analyses. The absolute magnitude is the absolute brightness of an object or event at the source of its origin, whereas the apparent magnitude is its brightness as perceived by an observer on earth, diminished by the distance the object has from the observer. Observations usually give the data of the distance modulus versus redshift. In fitting procedures, it is however more common to use the luminosity distance, defined via its connection to the distance modulus,

$$\mu_D = 25 + \frac{5}{\ln 10} \ln\left(\frac{d_L}{1\,\mathrm{Mpc}}\right) . \tag{8.11}$$

The luminosity distance can alternatively be defined via the relation of the luminosity L of an object or event and its flux F [14]. The flux is defined as

$$F = \frac{L}{4\pi d^2} , \tag{8.12}$$

being simply given by the absolute luminosity divided by the area of a spherical surface of radius d around the object or event. The distance d can be expressed in terms of the scale factor $a(t)$ and the coordinate or comoving distance r_0 as

$$d = r_0\, a(t_0) . \tag{8.13}$$

The comoving distance is a possibility to define the distance from an object or an event to an observer assuming that both are moving with the Hubble flow of expansion. It is given by the physical time t scaled by $a(t)$, and multiplied by a factor of c, and thus measures the distance that a photon emitted at a position $r = r_0$ at time t_1 travels until it reaches the observer at $r = 0$ at present time t_0. It can be written in terms of the conformal time η as

$$r_0 = c\,\eta = c \int_{t_1}^{t_0} \frac{dt}{a(t)} . \tag{8.14}$$

At large distances, the expression for the flux needs some further modifications though. We need to account for the damping of the energy $h\nu$ of the photons by a factor of $(1+z)$, as well as the diminution of the photon rate arriving at the observer for the same amount (see e.g. [14]). Thus, the flux reads

$$F = \frac{L}{4\pi d_L^2} = \frac{L}{4\pi r_0^2\, a(t_0)^2\, (1+z)^2} , \tag{8.15}$$

from which the luminosity distance d_L can be determined as

$$d_L = r_0\, a(t_0)\, (1+z) = r_0\, a_0\, (1+z) . \tag{8.16}$$

Even though the luminosity distance d_L being the main object of interest for fitting purposes, in the light of the cosmographic principle of striving for model independence alternative fitting functions, e.g. different notions of cosmological distances, should be considered. There are four other definitions of distance, namely the photon flux distance d_F, the photon count distance d_P, the deceleration distance d_Q and the angular diameter distance d_A,

$$d_F = \frac{d_L}{(1+z)^{1/2}}\,, \tag{8.17a}$$

$$d_P = \frac{d_L}{(1+z)}\,, \tag{8.17b}$$

$$d_Q = \frac{d_L}{(1+z)^{3/2}}\,, \tag{8.17c}$$

$$d_A = \frac{d_L}{(1+z)^2}\,. \tag{8.17d}$$

The photon flux distance d_F is in contrast to the luminosity distance d_L not calculated from the energy flux in the detector, but from the photon flux, which is usually easier to measure in experiments. The photon count distance d_P in turn is based on the total number of photons arriving at the detector as opposed to the photon rate or flux. The acceleration distance d_Q has been introduced in [12] in analogy to the photon flux distance and the photon count distance, without any immediate physical meaning, but featuring a very simple and practical dependence on the acceleration parameter q_0. Finally, the angular diameter distance d_A was defined in [14] as the ratio of the physical size of the object at the time of light emission and its angular diameter observed today. These four additional distances can be used in fitting procedures instead of the luminosity distance.
Using the redshit relation

$$1 + z = \frac{a_0}{a(t)} = \frac{1}{a(t)}\,, \tag{8.18}$$

we can express the different distance notions as

$$d_L = r_0\,\frac{1}{a(t)}\,, \tag{8.19a}$$

$$d_F = r_0\,\frac{1}{\sqrt{a(t)}}\,, \tag{8.19b}$$

$$d_P = r_0\,, \tag{8.19c}$$

$$d_Q = r_0\,\sqrt{a(t)}\,, \tag{8.19d}$$

$$d_A = r_0\,a(t)\,. \tag{8.19e}$$

In order to obtain these notions of distance in terms of the redshift, we insert the expansion of the scale factor $a(t) \simeq 1 - x$ from above into the distances and expand for small x. The

distances thus read

$$d_L \simeq r_0 \left[1 - x + x^2 - x^3 + x^4 + x^5 + x^6 + \mathcal{O}\left(x^7\right)\right] , \tag{8.20a}$$

$$d_F \simeq r_0 \left[1 + \frac{x}{2} + \frac{3x^2}{8} + \frac{5x^3}{16} + \frac{35x^4}{128} + \frac{63x^5}{256} + \frac{231x^6}{1024} + \mathcal{O}\left(x^7\right)\right] , \tag{8.20b}$$

$$d_P = r_0 , \tag{8.20c}$$

$$d_Q \simeq r_0 \left[1 - \frac{x}{2} - \frac{x^2}{8} - \frac{x^3}{16} - \frac{5x^4}{128} - \frac{7x^5}{256} - \frac{21x^6}{1024} - \mathcal{O}\left(x^7\right)\right] , \tag{8.20d}$$

$$d_A \simeq r_0 \left(1 - x\right) . \tag{8.20e}$$

To completely determine the expansion of the distances in terms of the redshift, now we only need to calculate r_0 defined by Eq. (8.14). We can calculate this quantity by inserting the expansion of $a(t)$ into Eq. (8.14) and integrating every term in the sum separately. Pulling out a factor of H_0, we arrive at the result

$$\begin{aligned} r_0 \;=\; & \frac{c}{H_0}\left[H_0\Delta t + \frac{1}{2}H_0^2\Delta t^2 + H_0^3\Delta t^3\left(\frac{q_0}{6} + \frac{1}{3}\right) + H_0^4\Delta t^4\left(\frac{j_0}{24} + \frac{q_0}{4} + \frac{1}{4}\right)\right. \\ & + H_0^5\Delta t^5\left(\frac{1}{5} + \frac{j_0}{15} + \frac{3q_0}{10} + \frac{q_0^2}{20} - \frac{s_0}{120}\right) \\ & \left. + H_0^6\Delta t^6\left(\frac{1}{6} + \frac{j_0}{12} + \frac{l_0}{720} + \frac{q_0}{3} + \frac{j_0 q_0}{36} + \frac{q_0^2}{8} - \frac{s_0}{72}\right)\right] . \end{aligned} \tag{8.21}$$

Joining together Eqs. (8.20a) and (8.21) and inserting Eq. (8.8), we obtain lengthy expressions for the cosmological distances in terms of power series in $H_0\Delta t$. To finally be able to have the distances as functions of the redshifts, we need the connection of $H_0\Delta t$ to the redshift. Using Eq. (8.18) and expanding the scale factor again, we can easily express the redshift in terms of $H_0\Delta t$, and inverting the relation yields the expression for $H_0\Delta t$ as a function of z. Thus we obtain the different notions of distances as functions of the redshift. The results for the distances as functions of the redshift z can be found in Appendix A 1 of [15].

8.2. Distance modulus in terms of redshift

As mentioned before, the distance modulus μ_D is defined in terms of the luminosity distance as

$$\mu_D = 25 + \frac{5}{\ln 10}\ln\left(\frac{d_L}{1\,\mathrm{Mpc}}\right) . \tag{8.22}$$

In terms of the other distances, we have

$$\begin{aligned}\mu_D &= 25 + \frac{5}{\ln 10}\ln\left(\frac{d_F\sqrt{1+z}}{1\,\mathrm{Mpc}}\right) = 25 + \frac{5}{\ln 10}\ln\left(\frac{d_P(1+z)}{1\,\mathrm{Mpc}}\right) = \\ &= 25 + \frac{5}{\ln 10}\ln\left(\frac{d_Q(1+z)^{3/2}}{1\,\mathrm{Mpc}}\right) = 25 + \frac{5}{\ln 10}\ln\left(\frac{d_A(1+z)^2}{1\,\mathrm{Mpc}}\right).\end{aligned} \tag{8.23}$$

Since the distance modulus is defined in terms of the luminosity distance, there is only one unique Taylor-expanded expression for it, which will be calculated from d_L. In order to obtain a Taylor-expanded form of μ_D, we are looking for an expression of the form

$$\mu_D = 25 + \frac{5}{\ln 10}\left[\ln\left(\frac{d_H}{1\,\mathrm{Mpc}}\right) + \ln z + \alpha\, z + \beta\, z^2 + \gamma\, z^3 + ...\right]. \tag{8.24}$$

Due to the logarithmic dependence of the distance modulus on d_L besides the polynomial contribution there is a term proportional to $\ln z$ in the expansion. The dependence of the coefficients $\alpha, \beta\,\gamma$ on the CS is given by

$$\begin{aligned}\alpha &= \frac{1}{2} - \frac{q_0}{2}, \\ \beta &= -\frac{7}{24} - \frac{j_0}{6} + \frac{5q_0}{12} + \frac{3q_0^2}{8}, \\ \gamma &= \frac{5}{24} + \frac{7j_0}{24} - \frac{3q_0}{8} + \frac{j_0 q_0}{3} - \frac{2q_0^2}{3} - \frac{5q_0^3}{12} + \frac{s_0}{24}.\end{aligned} \tag{8.25}$$

8.3. Alternative cosmographic parameters

Cosmology can be formulated within a thermodynamic approach using the concept of fluids moving in a specific spacetime. As described in Chapter 2, the dynamics of the universe depend on the properties of the energy and matter present, and it is possible to express the kinematic evolution by certain thermodynamic parameters, like the equation of state parameter ω. An expression for the EoS is naturally associated to each cosmological fluid, and is determined by the thermodynamical properties of the fluid in question. Most current cosmological models feature several fluid components in the universe, like e.g. radiation with an EoS parameter $\omega = 1/3$, matter or dust with $\omega \simeq 0$, and dark energy, the so far unknown and undetected substance driving the accelerated expansion of the universe, with $\omega = -1$. Only involving basic assumptions as a FLRW-metric and a homogeneous and isotropic universe, we recall that the scale factor evolves in time as

$$a(t) \propto t^{\frac{2}{3(1+\omega)}}. \tag{8.26}$$

Thus, reconstructing the expansion history of the universe can be done via determining the correct EoS during different phases of expansion. Many physical mechanisms are hidden in

the EoS parameter ω. Following the principles of cosmography however, we cannot assume an EoS of the universe beforehand, because we do not want to specify any particular cosmological model to rely on. The overall EoS of the Universe is determined by a mixture of fluids with respective EoS parameters summing up to $\omega = \sum_i P_i / \sum_i \rho_i$, with the index i labelling the different fluids the universe contains. To evaluate ω, the total pressure $P = \sum_i P_i$ and the total density $\rho = \sum_i \rho_i$ have to be known. However, even without knowing the correct EoS of the universe explicitly, we can still apply the procedures of cosmography and expand the pressure in terms of the cosmic time or redshifts into a power series as

$$P = \sum_{k=0}^{\infty} \frac{1}{k!} \frac{d^k P}{dt^k}\Big|_{t_0} (t - t_0)^k = \sum_{k=0}^{\infty} \frac{1}{k!} \frac{d^k P}{dz^k}\Big|_0 z^k \,, \tag{8.27}$$

This defines a set of coefficients, i.e. the derivatives of the pressure, which can be related to the CS by employing the Friedmann equation

$$H^2 = \frac{1}{3}\rho \tag{8.28}$$

and the continuity equation

$$\frac{d\rho}{dt} + 3H(P + \rho) = 0 \,. \tag{8.29}$$

Here, we have used the convention $8\pi G_N = c = 1$ for brevity.
Using these expressions, we can explicitly state the dependence of the total pressure of the universe and its derivatives $d^k P/dt^k$ in terms of the CS as

$$P = \frac{1}{3} H^2 \left(2q - 1\right) \,, \tag{8.30a}$$

$$\frac{dP}{dt} = \frac{2}{3} H^3 \left(1 - j\right) \,, \tag{8.30b}$$

$$\frac{d^2 P}{dt^2} = \frac{2}{3} H^4 \left(j - 3q - s - 3\right) \,, \tag{8.30c}$$

$$\frac{d^3 P}{dt^3} = \frac{2}{3} H^5 \Big[\left(2s + j - l + q\left(21 - j\right) + 6q^2 + 12\right] \,, \tag{8.30d}$$

$$\frac{d^4 P}{dt^4} = \frac{2}{3} H^6 \Big[j^2 + 3l - m - 144q - 81q^2 - 6q^3 - 12j\left(2 + q\right) - 3s - 3q\, s - 60\Big] \,. \tag{8.30e}$$

With the previously introduced conversion rules (9.12), we can transform the above derivatives to derivatives with respect to the redshift.
Not only the pressure and its derivatives can be given in terms of the CS, but also the overall equation of state parameter of the universe and its derivatives. Dividing the pressure Eq. (8.30a) by the density given by Eq. (8.28), we find the equation of state parameter of the universe as

$$\frac{P}{\rho} = \omega = \frac{2q - 1}{3} \,. \tag{8.31}$$

Taking the derivative with respect to the redshift, we can obtain the first derivative of the EoS parameter,

$$\omega' = \frac{d\omega}{dz} = \frac{2}{3}\frac{(j - q - 2q^2)}{1+z}\,. \tag{8.32}$$

From these results, it is now possible to express the CS parameters as functions of this newly defined parameter set $\{\omega, P_1, P_2, P_3, P_4\}$, where $P_k = d^k P/dz^k$. By fitting observational data of luminosity distance with the fitting functions formulated in terms of the EoS parameter set, it is possible to directly obtain numerical constraints on the EoS parameter set. The constraints on ω and the derivatives of the pressure can then be tested on a specific model of the universe by comparing to the obtained fitting values. The coefficients $d^k P/dz^k$ as functions of the CS are given in Appendix C of [15]. The required fitting functions for the numerical analyses can easily be obtained by using these relations in the luminosity distance. The explicit expression for d_L in terms of the EoS parameters is reported in Appendix D of [15].

9. Issues with Cosmography and possible remedies

Even though cosmography is emphasizing on a clean, model-independent and as neutral as possible approach to data analysis, drawbacks or limitations to the procedures involved are inevitable. Obviously, since the basic principle lies in the Taylor-expansion of quantities with respect to time, the approach is of limited accuracy, since necessarily there is a maximum order up to which the analysis can be carried out. One disadvantage thus lies in the fact that we can only include a finite amount of terms in the calculations of the fitting functions. Of course it is always possible to calculate and include even higher orders into the analyses; however, this comes at the cost of increased inaccuracy of the fitting results, since higher orders imply the inclusion of more and more fitting parameters. Every additional order of expansion introduces yet another CS parameter to be determined from the fitting analysis, leading to an even higher-dimensional parameter space and thus to a broadening of the posterior distributions. Inclusion of higher-order terms can improve the accuracy, but at a certain point it becomes rather disadvantageous since it is not possible anymore to constrain the resulting values well.

Besides, Taylor expansions are an approximation of an exact function at and in the vicinity of a specific point, whose accuracy decreases with increasing distance of the point of expansion. The convergence range of power series expansions is limited, and beyond that regime expansions of physical quantities like the luminosity distance are not supposed to converge. This is problematic in particular when using high redshift data. The latest observational data on type Ia supernovae goes up to redshifts of $z \in [0, 1.414]$, i.e. might exceed the convergence regime of the Taylor expansions used in the construction of the fitting functions. The most straightforward remedy for this problem is to limit the analysed data to the convergence regime of the expansion and simply ignore higher redshift data in cosmographic analyses. This is however not only a reduction of accuracy since we use less data points and thus decrease the statistics, but also equals a waste of information, and it would on the contrary be desirable to find a way to enable the inclusion of high redshift data to cosmographic analyses, not only from high redshift supernovae, but also from other energy sources as e.g. gamma ray bursts, which have been observed for redshifts as high

as $z = 8$.

In order to alleviate these weaknesses of cosmography there are several options based on different approaches. One possibility is to mathematically transform the available data in such a way that the convergence of the Taylor series is preserved. In order to do so, the redshift z itself can be redefined in a different form, with the hope that the convergence of the Taylor series is given in the resulting range of data formulated in terms of the new redshift. A second, but completely different approach to the above problems of cosmography tries to tackle the problem at its root, and introduces the concept of Padé approximants to replace the Taylor expansion method. Padé approximations base on a different functional dependence on parameters and have better convergence properties than Taylor series. Thus using them as the basis of the expansion of physical quantities around the current values might improve the goodness of the cosmographic analysis.

These two attempts to improve cosmography will be described in detail in the two following sections.

9.1. Alternative redshifts

As described above, one possibility to improve the cosmographic analysis is by introducing new notions of redshift, which would yield a higher convergence of the Taylor series. Concretely this can be achieved by variables which compress the available data to a smaller interval of redshifts. One such option was introduced in the literature in the past [13] as

$$y_1 = \frac{z}{z+1} = x\,, \tag{9.1}$$

where for the second equality we have used the previously introduced definition of the redshift $z = a_0/a(t) - 1 = x/(1-x)$. Equivalently, it is possible to give the conventional redshift z as function of y_1 by

$$z = \frac{y_1}{1-y_1}\,. \tag{9.2}$$

This new redshift has better convergence at the two relevant limits of past and future universe; for the past, we obtain

$$z \in [0,\infty) \quad \Rightarrow \quad y_1 \in [0,1]\,, \tag{9.3}$$

while in the future,

$$z \in [-1,0] \quad \Rightarrow \quad y_1 \in [-\infty,0]\,. \tag{9.4}$$

Besides redshift y_1, three further options have been introduced [15],

$$y_2 = \arctan\left(\frac{z}{z+1}\right), \tag{9.5a}$$

$$y_3 = \frac{z}{1+z^2}, \tag{9.5b}$$

$$y_4 = \arctan z\,. \tag{9.5c}$$

which in the limits of past and future universe behave like

$$z \in [0,\infty) \quad \Rightarrow \quad y_2 \in \left[0,\frac{\pi}{4}\right], \quad y_3 \in [0,0], \quad y_4 \in \left[0,\frac{\pi}{2}\right], \tag{9.6a}$$

$$z \in [-1,0] \quad \Rightarrow \quad y_2 \in \left[\frac{\pi}{2},0\right], \quad y_3 \in \left[-\frac{1}{2},0\right], \quad y_4 \in \left[-\frac{\pi}{4},0\right]. \tag{9.6b}$$

For the current time t_0, where $z = 0$, the new redshifts result in the values

$$z = 0 \quad \Rightarrow \quad y_2 = 0\,, \quad y_3 = 0\,, \quad y_4 = 0\,. \tag{9.7}$$

We adopted the arctan in the parameterizations of y_2 and y_4 because of its asymptotic approach to a constant value for large arguments. It behaves smoothly and is suited to give well-defined limits at $z \to \infty$. On the contrary, y_1 and y_3 are polynomials in z, but might still happen to give better convergence properties than z.
By using

$$z = \frac{a_0}{a(t)} - 1 = \frac{x}{1-x}\,, \tag{9.8}$$

and consequently the dependence of the new redshifts y_i on $a(t)$ and in turn on $H_0\Delta t$, we can derive the functional dependence of $y_i\,(H_0\Delta t)$. Inverting these relations gives the $H_0\Delta t(y_i)$, and in analogy to before we can thus calculate the cosmological distances in terms of the alternative redshifts y_i, with the results being given in Appendices A 2 – A 5 of [15].

The new redshift parameterizations have been introduced with the aim of avoiding divergences in the Taylor expansions of the distances for large z. Thus, we can now ask whether they will live up to these expectations and turn out to be suitable for constraining the CS. The answer can be partly predicted by comparing the supernova data of the luminosity distance to the curves obtained with the different redshift parameterizations z and y_i, as shown in Fig. 9.1.

The (binned) original data, i.e. luminosity distance over redshift z, is given by the red curve, extending up to redshifts of $z = 1.414$. The other curves give the luminosity distance data plotted versus the other redshifts. All of the alternative redshift definitions lead to a reduction of the redshift interval, where the redshift y_4, given by the black curve, is bound by $y_4 < 1$, and the others obey the even smaller bound $y_i \lesssim 0.5$, with $i = 1,2,3$. The

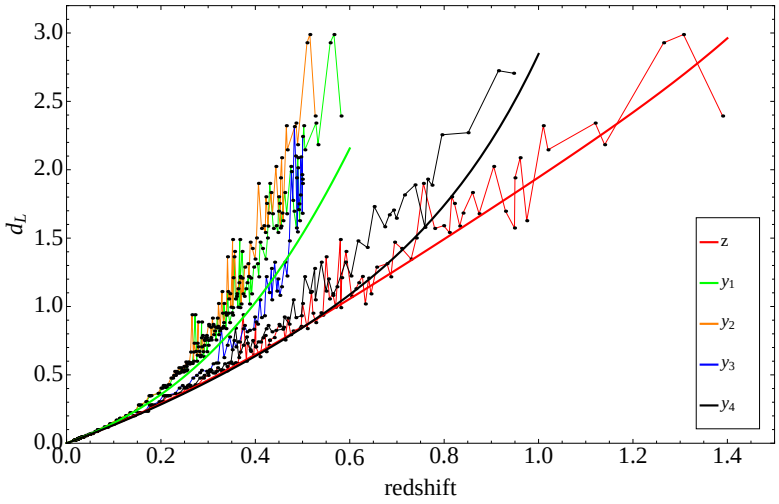

Figure 9.1.: Luminosity distance in Mpc, over different redshifts z (red), y_1 (green), y_2 (orange), y_3 (blue) and y_4 (black).

original aim was thus achieved - compressing the redshift variables to a regime where the convergence of a Taylor expansion is more likely to be given. We should however consider possible drawbacks of the contractions as well.

As can be seen in Fig. 9.1, the luminosity distance curves over redshift are slightly flexed, becoming steeper towards higher redshifts. All newly introduced redshifts y_1, y_2, y_3 and y_4 lead to steeper curves than z, with redshift y_3 behaving the most extreme, bending nearly vertically at redshifts $y_3 \sim 0.5$, the region of $z \in [0, 1.414]$ thus being reduced to a much smaller interval $y_3 \in [0, 0.5]$. It is to expect that with extreme bends in the fitting data, the fitting process will become more difficult, since the fitting function has to follow highly abrupt jumps instead of a smooth evolution. Moreover, as the curve trends become more extreme, a suppression of lower redshifts to the advantage of higher ones can occur, since an abundance of data for low redshifts is compressed to a smaller regime and the important features, i.e. the bends, are encoded in the higher redshift region. We therefore conclude that y_3 would be a good parameterization of the redshift if all or most of the cosmological data was in the regime $z \gg 1$; but since the original data mainly lie in the very low z region, we presume that the parameterization y_3 has more drawbacks than merits. This conjecture is also backed by the fitting results, which confirm that y_3 does not work well in the application to SNeIa data. Another disadvantage of y_3 is that it does not have a

uniquely defined inverse function. For these reasons, we decide to discard it in the numerical analysis. Through similar arguments, we disregard the second-worst redshift y_2 as well, contenting ourselves with the previously introduced y_1 and the new suggestions, y_4. We expect the latter to perform better than y_1, since the curve is less flexed, but still compresses the regime of redshifts to the interval $y_4 \in [0, 1]$.
Summing up the above explanations, in order to construct a viable new redshift parametrization, the following conditions must be satisfied:

1. The luminosity distance curve should compress the redshift data to the interval $z < 1$.
2. The luminosity distance curve should not exhibit sudden flexes or bend too steeply.
3. The curve should be one-to-one invertible.

Thus, the rest of the analysis including further calculations and fittings is carried out for the redshifts z, y_1 and y_4, and disregarding y_2 and y_3. The corresponding expressions for the distance modulus μ_D are given as before by

$$\mu_D = 25 + \frac{5}{\ln 10}\left[\ln\left(\frac{d_H}{1\,\mathrm{Mpc}}\right) + \ln y_i + \alpha\, y_i + \beta\, y_i^2 + \gamma\, y_i^3 + ...\right], \tag{9.9}$$

where now for redshift y_1 the coefficients are

$$\begin{aligned} \alpha &= \frac{3}{2} - \frac{q_0}{2}, \\ \beta &= \frac{17}{24} - \frac{j_0}{6} - \frac{q_0}{12} + \frac{3q_0^2}{8}, \\ \gamma &= \frac{11}{24} - \frac{j_0}{24} - \frac{q_0}{24} + \frac{j_0 q_0}{3} + \frac{q_0^2}{12} - \frac{5q_0^3}{12} + \frac{s_0}{24}, \end{aligned} \tag{9.10}$$

and for redshift y_4

$$\begin{aligned} \alpha &= \frac{1}{2} - \frac{q_0}{2}, \\ \beta &= \frac{1}{24} - \frac{j_0}{6} + \frac{5q_0}{12} + \frac{3q_0^2}{8}, \\ \gamma &= \frac{3}{8} + \frac{7j_0}{24} - \frac{13q_0}{24} + \frac{j_0 q_0}{3} - \frac{2q_0^2}{3} - \frac{5q_0^3}{12} + \frac{s_0}{24}. \end{aligned} \tag{9.11}$$

The corresponding expressions for the pressure and its derivatives in terms of the new redshift variables can be found in Appendix C of [15]. Ultimately, we mention that also for the new redshift parameterizations, a conversion from time to redshift derivative is possible. The complete set of transformation rules is given by

$$\frac{\partial}{\partial t} = -(1 + y_1)\, H\, \frac{\partial}{\partial y_1} = -\cos y_4\, (\cos y_4 + \sin y_4)\, H\, \frac{\partial}{\partial y_4}. \tag{9.12}$$

One way of dealing with convergence problems in cosmography is thus provided by new redshift parameterizations, which will be put to the test in Section 10.1, where we compare fits for the Taylor-expanded forms of the luminosity distance in terms of the CS parameters. First however, we will introduce alternative ways to approach the convergence problem.

9.2. Padé approximants

Cosmography is aiming at analyzing data under as few basic assumptions as possible, to extract statements that are independent of the validity of a specific model of cosmology. To carry this thought further, it is of course also possible to question even the small number of basic principles cosmography does rely on. Here we would like to point out an alternative method to carry out the expansion around the present time, not in terms of a Taylor expansion, but with the concept of Padé approximants (PAs) [94–98]. For a generic function $f(x)$, the Padé approximant of order (m, n) is given by

$$P_{mn}(x) = \frac{a_0 + a_1 x + a_2 x^2 + ... + a_M x^m}{1 + b_1 x + b_2 x^2 + ... + b_n x^n} \,. \tag{9.13}$$

It is an alternative way to approximate functions for small variations around a fixed point. We will now apply this approach to the fitting functions in cosmography, and express the luminosity distance d_L as a function of the redshift z instead of in terms of a conventional Taylor series for small z around $z = 0$ as

$$d_L = \alpha z + \beta z^2 + \gamma z^3 + ... \,, \tag{9.14}$$

where $\alpha, \beta, \gamma...$ are dependent on the parameters of the CS, but in terms of a $(1, 2)$ Padé approximant as

$$d_{L,\text{Padé}} = \frac{a_0 + a_1 z}{1 + b_1 z + b_2 z^2} \,. \tag{9.15}$$

Also here the coefficients a_i, b_i depend on the parameters of the CS. The choice of $m = 1$ and $n = 2$ is an arbitrary one, and since we do not want to assume anything about the asymptotic behaviour of the universe, different choices of (m, n) might work differently well. However, since Padé expansions are in general known to have a more stable convergence behaviour, we hope for better results even for a random form of the expansion.
The correspondence between the two functional forms can be calculated from demanding that the two different expressions for d_L and their derivatives be equal at the point $z = 0$ around which the functions are expanded. In order to have an equal number of parameters in the functional form, we choose $a_0 = 0$. In general, the correspondence between $\{\alpha, \beta, \gamma\}$

and $\{a_1, b_1, b_2\}$ can then be given by

$$a_1 = \alpha\,, \tag{9.16a}$$

$$b_1 = -\frac{\beta}{\alpha}\,, \tag{9.16b}$$

$$b_2 = \frac{\beta^2 - \alpha\gamma}{\alpha^2}\,. \tag{9.16c}$$

For the luminosity distance as a function of the redshift z, as computed in Section 8.1, here given only up to third order,

$$d_L = \frac{c}{H_0}\left[z + \left(\frac{1}{2} - \frac{q_0}{2}\right) z^2 + \left(-\frac{1}{6} - \frac{j_0}{6} + \frac{q_0}{6} + \frac{q_0^2}{2}\right) z^3 + ...\right], \tag{9.17}$$

we obtain the following form of a Padé approximant of order $(1, 2)$,

$$d_{\mathrm{L,Padé}} = \frac{12 d_H z}{12 + 6(q_0 - 1)z + (5 + 2j_0 - 8q_0 - 3q_0^2)z^2}\,, \tag{9.18}$$

i.e. the coefficients are

$$a_1 = d_H\,, \tag{9.19a}$$

$$b_1 = \frac{1}{2}(q_0 - 1)\,, \tag{9.19b}$$

$$b_2 = \frac{1}{12}(5 + 2j_0 - 8q_0 - 3q_0^2)\,. \tag{9.19c}$$

In contrast to the previous section, in the Padé approach we will limit ourselves to the conventional redshift z, in order to be able to separately investigate the impact of the Padé treatment on the fitting behaviour in comparison to Taylor expansions.

While the above form of the Padé expanded luminosity distance on first sight doesn't look better or worse than the Taylor expression, some considerations show that there are advantages as well as drawbacks to the idea. The obvious disadvantage of using the Padé expansion is that it is an approximation of an approximation. The conventional Taylor approach to cosmography is based on expanding the scale factor $a(t)$ into a Taylor series around the present time, and defines the coefficients in the expansion as the parameters of the CS. Thus, any procedure using the CS as the fitting parameters implicitly employs Taylor expansions. In our above derivation of Padé approximants, we find a correspondence between a Taylor series and a Padé expansion, expressing also the Padé form in terms of the parameters of the CS, and so the result is a double approximation. Avoiding this would only be possible in adopting alternative parameter sets defined via a Padé expansion from the very beginning, i.e. starting with a Padé approximant already for the scale factor $a(t)$. The cosmographic parameters defined from such an expansion however

would not have such intuitive and physically reasonable interpretations as the derivatives of the scale factor provide. We therefore discard this possibility, and accept the adoption of Taylor-expanded parameters in a Padé type expansion.
However, there are other arguments to be stated in favor of Padé approximations, concerning properties which are able to overcome severe restrictions of the Taylor treatment intrinsic to the expansion process and crucial to the applicability of basic cosmography as defined in the literature. The concept of Taylor expansions is by definition limited to its regime of convergence, which depends on the exact form of the series. Depending on the series in question, the convergence radius can be quite small. The convergence properties of Padé expressions however are much better, which will be shown in more detail in one of the next subsections, where we explicitly derive the convergence radii for both Taylor and Padé approximations of the luminosity distance. It is here that Padé shows definite advantages over a Taylor approach, since fitting procedures in cosmography makes use of supernovae data with redshifts up to $z = 1.414$, and it is desirable to extend data sets to even higher redshift sources. Strictly speaking, we will see that applying Taylor approximations of fitting functions to conventional supernova data is not allowed, since the convergence radius is exceeded. Thus we carried out calculations of the luminosity distance and also the distance modulus within the Padé treatment and performed fits obtaining numerical results for the CS, in order to support the above claim that a fit with a Taylor expansion always falls short of the quality achieved with a Padé expansion.
By the above mentioned method, we can now calculate the Padé-expanded version of the distance modulus as well, which results in a very involved expression of the general form

$$\mu_{\mathrm{D,Padé}} = \frac{5}{\ln 10}\left[\ln z + \frac{\mathcal{A}}{\mathcal{B}}\right] , \tag{9.20}$$

where

$$\mathcal{A} = a_0 + a_1 z \,, \tag{9.21a}$$

$$\mathcal{B} = b_0 + b_1 z + b_2 z^2 \,, \tag{9.21b}$$

and

$$a_0 = -24\left[5\ln 10 + \ln\left(\frac{d_{\mathcal{H}}}{1\text{Mpc}}\right)\right]\left[q_0^2\left(-6+45\ln 10\right) + 2q_0\left(6+25\ln 10\right)\right. \tag{9.22a}$$
$$\left. -6-35\ln 10-20j_0\ln 10+\left(9q_0^2+10q_0-4j_0-7\right)\ln\left(\frac{d_{\mathcal{H}}}{1\text{Mpc}}\right)\right],$$

$$a_1 = 24\left(q_0-1\right)\left[-3-35\ln 10-20j_0\ln 10+q_0^2\left(-3+45\ln 10\right)\right. \tag{9.22b}$$
$$\left. +q_0\left(6+50\ln 10\right)+\left(9q_0^2+10q_0-4j_0-7\right)\ln\left(\frac{d_{\mathcal{H}}}{1\text{Mpc}}\right)\right],$$

$$b_0 = 24\left(4j_0-9q_0^2-10q_0+7\right)\ln\left(\frac{d_{\mathcal{H}}}{1\text{Mpc}}\right)+480j_0\ln 10+144q_0^2 \tag{9.22c}$$
$$-1080q_0^2\ln 10-288q_0-1200q_0\ln 10+144+840\ln 10\,,$$

$$b_1 = -12\left(4j_0+17\right)q_0+48j_0+108q_0^3+12q_0^2+84\,, \tag{9.22d}$$

$$b_2 = 16j_0^2-2\left(36j_0+13\right)q_0^2-20\left(4j_0+7\right)q_0+56j_0+81q_0^4+180q_0^3+49\,. \tag{9.22e}$$

9.2.1. Convergence radii of Taylor and Padé series

We will now proceed to calculate the convergence radii of both the Taylor and Padé expanded luminosity distance, and for simplicity restrict ourselves to expansions of second order in z and order $(1,1)$, respectively. The inclusion of higher orders may refine the results, but should not considerably change the conclusions derived from them.
The Taylor expression for d_L up to second order reads

$$d_L = d_H\left[z+\left(\frac{1}{2}-\frac{q_0}{2}\right)z^2\right]. \tag{9.23}$$

Using the ratio criterion to calculate the convergence radius can be achieved for a general power series

$$\sum_{n=1}^{\infty}a_n x^n = a_1x+a_2x^2+... \tag{9.24}$$

to first order, by computing

$$\mathcal{R}_{\text{Taylor}} \simeq \left|\frac{a_2}{a_1}\right|, \tag{9.25}$$

result, for the above example of the luminosity distance Eq. (9.23) and disregarding the factor of d_H in

$$\mathcal{R}_{\text{Taylor}} \simeq \frac{1-q_0}{2}\,. \tag{9.26}$$

For an expected range of the acceleration parameter of $q_0 \sim [-0.6,-0.4]$, this results in numerical values for the convergence radius of $\mathcal{R}_{\text{Taylor}} \sim [0.7, 0.8]$, i.e. a convergence regime

smaller than unity.

Equivalently we consider the corresponding Padé expansion of d_L of order (1,1),

$$d_{L,\text{Padé}} = d_H \frac{\mathcal{A}z}{\mathcal{B}+\mathcal{C}z}\,, \tag{9.27}$$

where

$$\mathcal{A} = 1\,, \tag{9.28a}$$

$$\mathcal{B} = 1\,, \tag{9.28b}$$

$$\mathcal{C} = \frac{1}{2}(q_0 - 1)\,. \tag{9.28c}$$

Demanding that the luminosity distance thus formulated remains positive leads to the condition

$$q_0 > -1\,, \tag{9.29}$$

which gives a natural bound on the acceleration parameter q_0 without having referred to any observational data. This condition excludes theoretically a pure de Sitter universe, and is consistent with current values of q_0 found from the analyses of experimental data.

Employing the definition of the geometrical series for a generic variable $x < 1$,

$$\sum_{n=0}^{\infty} x^n \equiv \frac{1}{1-x}\,, \tag{9.30}$$

and reformulating the luminosity distance in a slightly different way,

$$d_{L,\text{Padé}} = \frac{2}{q_0 - 1}\Big[1 - \frac{2}{2 + (q_0-1)z}\Big]\,, \tag{9.31}$$

d_L can be restated in terms of a geometrical series as

$$d_{L,\text{Padé}} = \frac{2}{q_0 - 1}\left[1 - \sum_{n=0}^{\infty} \frac{z^n}{\left(\frac{2}{1-q_0}\right)^n}\right]\,. \tag{9.32}$$

The series, and thus the luminosity distance, converges if the redshift is bound by

$$z < \frac{2}{1-q_0}\,. \tag{9.33}$$

The convergence radius of the Padé series is thus given by

$$\mathcal{R}_{\text{Padé}} = \frac{2}{1-q_0}\,, \tag{9.34}$$

which for the usual range of the acceleration parameter $q_0 \sim [-0.6, -0.4]$ yields values of $\mathcal{R}_{\text{Padé}} \sim [1.2, 1.5]$. We thus see that the Padé treatment allows for significantly larger convergence regimes as compared to the Taylor approach.

In Section 10.2 we will explicitly calculate both $\mathcal{R}_{\text{Taylor}}$ and $\mathcal{R}_{\text{Padé}}$ for the obtained fitting results for q_0.

10. Numerical analyses

In this chapter, we will present the results for the numerical fitting procedures we have carried out with the derived fitting functions. Corresponding to the respective publications we have divided the chapter in two parts. Section 10.1 will comprise the fitting analyses employing the three different redshifts z, y_1 and y_4 introduced in Section 9.1 for fits of the luminosity distance formulated in terms of the CS and EoS parameter sets. From this part we will thus obtain constraints on the CS and the equation of state of the universe, and be able to compare the performance of the different redshifts [15].
In Section 10.2 we will dedicate our attention to the theory of Padé approximants introduced in Section 9.2 and compare the numerical results for fits of the distance modulus μ_D carried out with Taylor and Padé treatment [16].
Since these results have been published separately about a year apart, we have been using two different data sets due to updates in observational data. The details are described in the respective sections.
We determine the best fit values on the CS by maximizing the likelihood function

$$\mathcal{L} \propto \exp(-\chi^2/2)\,, \tag{10.1}$$

which corresponds to minimizing the chi-square function

$$\chi^2 = \sum_k \frac{(d_k^{\mathrm{th}} - d_k^{\mathrm{obs}})^2}{\sigma_k^2}\,. \tag{10.2}$$

Here, the d_k^{th} are the theoretically predicted values of the fitting function, i.e. the values of the luminosity distance or the distance modulus, respectively, for a certain redshift, whereas the d_k^{obs} are the observed data points for that redshift. The σ_k are the error bars of the measurement, provided by the experimental observations as well.

10.1. Taylor fits for CS and EoS

For the first part of the fitting, we used the data of type Ia SNe of the union 2 compilation of the supernova cosmology project (SCP) [99], comprising 557 measurements of the distance modulus of supernova events. From the relation of the distance modulus with the luminosity

distance (8.11), we obtained the experimental values of the luminosity distance, to be used with the fitting function d_L in terms of CS and EoS parameters. Moreover, we adopted also the results of the Hubble Space Telescope (HST) for the luminosities of 600 Cepheides, giving a Gaussian prior of $H_0 = 74.0 \pm 3.6\,\mathrm{km/s/Mpc}$ on the current Hubble parameter [100], and the measurements of the Hubble parameter $H(z)$ determined by twelve different redshifts between $z = 0.1$ to $z = 1.75$ [101]. In our analysis, we carried out fits using only the union 2 results with the prior from the HST, denoted as set 1, as well as fits including the union 2 data, the prior of the HST and the $H(z)$ measurements, denoted as set 2 of observations.

The focus of the analyses in this section lies in testing the newly introduced redshift y_4 for its suitability in cosmography, and comparing the results and their quality to the ones obtained with the conventional redshift z and the alternative y_1. Further, since we extended the CS up to sixth order, we want to examine to what extent this worsens the numerical accuracy as compared to previous investigations. Finally we want to extract predictions for the CS and EoS parameter sets in order to determine whether the concordance model ΛCDM is in agreement with the bounds given by cosmography. To this end, we will use the constraints on the EoS parameter and the pressure derivatives to draw some comparisons with alternative models.

In the fitting procedure, we used different sets of the CS with different maximum order of parameters, namely

$$\begin{aligned} \mathcal{A} &= \{H_0, q_0, j_0, s_0\}\,, \\ \mathcal{B} &= \{H_0, q_0, j_0, s_0, l_0\}\,, \\ \mathcal{C} &= \{H_0, q_0, j_0, s_0, l_0, m_0\}\,. \end{aligned} \tag{10.3}$$

Since set $\mathcal{B}$ and $\mathcal{C}$ contain more fitting parameters, we expect slower convergence, and possibly less pronounced posterior distributions, since the accuracy of fitting will not be as high as in set $\mathcal{A}$ containing only four fitting parameters.

Since the different observations are not correlated, the chi-square function in this case is given by the sum of the chi-square functions of each data set,

$$\chi^2 = \chi^2_{\text{union 2}} + \chi^2_{\text{HST}} + \chi^2_{H(z)} \tag{10.4}$$

Minimization of the likelihood was carried out using the publicly available code CosmoMC [102], which contains an implementation of a Markov Chain Monte Carlo simulation. Analyses were done for the three different sets of parameter space, for the three redshifts z, y_1 and y_4, and for two sets of observations, union 2 + HST, and union 2 + HST + $H(z)$, resulting in 18 different numerical fits. Parameter space was limited by flat

priors to the intervals $-6 < q_0 < 6$, $-20 < j_0 < 20$, $-200 < s_0 < 200$, $-500 < l_0 < 500$, and $-3000 < m_0 < 3000$.
Tables 10.1, 10.2, and 10.3 contain the best fits and the respective 1σ-likelihoods for the three redshifts z, y_1 and y_4 respectively. In Fig. 10.1 the 1-dimensional marginalized posterior distributions are compared for each parameter and redshift. While the conventional redshift z seems to yield the best results, we can also infer that the highest order CS parameters l_0 and m_0 are not well-constrained for the redshift y_1, whereas the newly introduced y_4 obtains reasonably good results as well. This result can be confirmed also from the numerical values shown in the tables, where $N.C.$ indicates not sufficiently narrow posterior distributions for extracting a specific numerical value. In order to investigate the impact of the inclusion of higher order parameters of the CS into the analysis, we show the posterior distributions for the three parameter sets $\mathcal{A}$, $\mathcal{B}$ and $\mathcal{C}$ for the first four CS parameters in Fig. 10.2. Dispersions are significantly broadened with the inclusion of l_0, but remain stable when extending the analysis with m_0. Fig. 10.3 finally presents all contours and marginalized distributions for the redshift y_4 and the parameter set $\mathcal{C}$.

We now proceed to the numerical analyses involving the EoS parameter set introduced in the last chapter. By using the expressions for the EoS parameter and the pressure derivatives to formulate the luminosity distance, we can directly constrain the EoS parameter set $\mathcal{D} = \{\omega, P_1, P_2, P_3, P_4\}$ at current time from numerical fits. In principle, we could also proceed differently by using the results obtained for the CS in expressions (8.30a)-(8.30e) and (8.31) to calculate the EoS parameter and the pressure derivatives. However, in this case we would have to consider error propagation through the context of CS and EoS parameters. In order to reduce the numerical errors in the analysis, we thus directly fit the luminosity data with functions in terms of parameter set $\mathcal{D}$, and thus straightforwardly obtain bounds on the EoS parameter and the thermodynamic state of the universe.
The results are presented in Tab. 10.4, with the corresponding marginalized posterior distributions in Fig. 10.4. Also here we can confirm that the newly introduced redshift y_4 shows advantages over the redshift y_1, while redshift z continues to be a good fitting parameter. The results for the EoS parameter ω lie in the regime $\omega \in [-0.7439, -0.7141]$, which confirms that the universe is currently assumed to be in a transition between a matter-dominated phase with $\omega = 0$, and an accelerated expansion with $\omega = -1$. The pressure derivatives are all compatible with the value zero, however with quite large error bars, so a definite statement about the variation of pressure is not quite justified.

10.1.1. Comparison with models

Judging from the fitting results for the EoS parameter set, up to now the ΛCDM model with a constant negative cosmological constant as the cause for accelerated expansion has not been refuted. Even though the error bars on the results for the pressure derivatives are quite large, they are compatible with zero. However, due to degeneracies between models it is still possible that other models fit the numerical results just as well. For comparison we will investigate the predictions for ΛCDM as well as for a more general model with a varying dark energy term. The Hubble parameter for ΛCDM is given by

$$H = H_0\sqrt{\Omega_m(1+z)^3 + 1 - \Omega_m}\,, \tag{10.5}$$

where Ω_m is the normalized density of baryonic and dark matter, and the density of dark energy is given by $\Omega_\Lambda = 1 - \Omega_m$, assuming that the universe contains exclusively those two fluids. The Hubble parameter can be used to express the CS parameters in terms of Ω_m as

$$q_0 = -1 + \frac{3}{2}\Omega_m\,, \tag{10.6a}$$

$$j_0 = 1\,, \tag{10.6b}$$

$$s_0 = 1 - \frac{9}{2}\Omega_m\,, \tag{10.6c}$$

$$l_0 = 1 + 3\Omega_m - \frac{27}{2}\Omega_m^2\,, \tag{10.6d}$$

$$m_0 = 1 - \frac{27}{2}\Omega_m^2 - 81\Omega_m^2 - \frac{81}{2}\Omega_m^3\,. \tag{10.6e}$$

Using these expressions, the luminosity distance can be formulated only in terms of Ω_m and the Hubble parameter H_0, and then be constrained by the fitting procedure. The values thus obtained for Ω_m and H_0, and in the further course for the CS, are found in Tab. 10.5. Comparing to the values obtained for the CS in the previous fits, we confirm that all results from the ΛCDM are compatible with our model-independent constraints within the 1σ error limits.

To compare the ΛCDM with a more general model with a varying dark energy term, described by

$$H = H_0\sqrt{\Omega_m(1+z)^3 + G(z)}\,, \tag{10.7}$$

we express $G(z)$ and its derivatives at the current time as functions of the CS for all three redshifts used in the previous analyses. The results can be found in Appendix E of [15]. Using the numerically obtained values for the CS and the value for the matter density $\Omega_m = 0.274^{+0.015}_{-0.015}$ from the WMAP collaboration [10], we calculated the values of $G(z)$ and its derivatives at the current time, shown in Tab. 10.6. These values can be compared to any

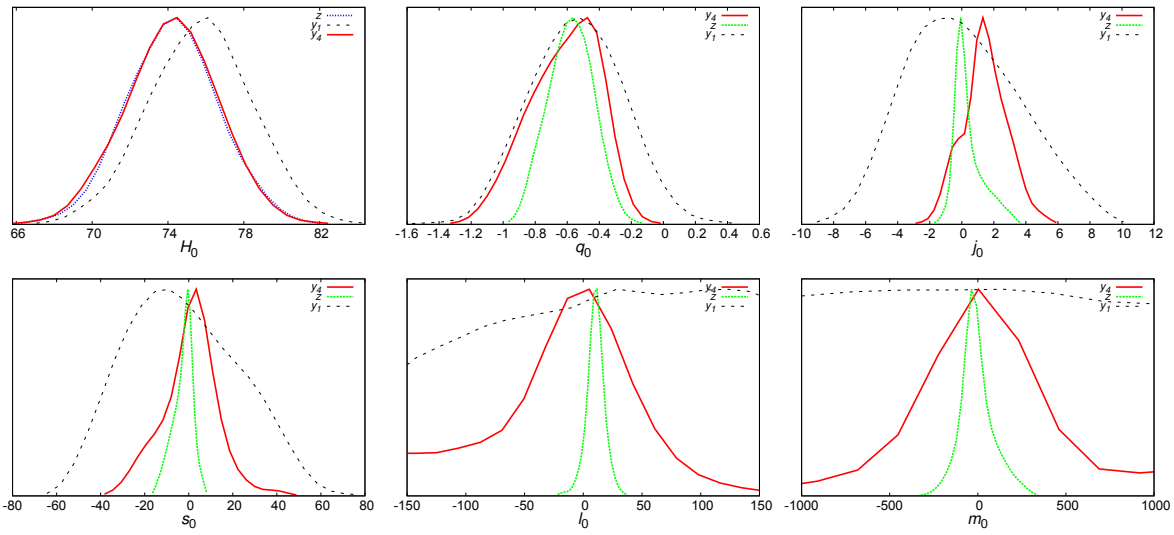

Figure 10.1.: 1-dimensional marginalized posteriors for the complete CS (parameter set $\mathcal{C}$), using set 2 of observations (union 2 + HST + $H(z)$). Dotted (green) line is redshift z, dashed (black) line is y_1 and solid (red) line is y_4.

dark energy model with the above form by computing the function $G(z)$ and its derivatives at the current time. ΛCDM implies $G_0 = G(z = 0) = 1 - \Omega_m$, which using the WMAP-value for the matter density results in $G_0 = 0.726^{+0.015}_{-0.015}$. Expressing the matter density in terms of q_0 we can obtain the current value of the function $G(z)$ as $G(0) = (1 - 2q_0)/3$. Consulting Tab. 10.6, we conclude that the value for $G(0)$ obtained using the WMAP result for the matter density is compatible with the cosmographic constraints on the current value of $G(z = 0)$ obtained with the best fit values for q_0, for the three redshifts from the fits using the combined data of union 2 + HST + $H(z)$.

Table 10.1.: Table of best fits and their likelihoods (1σ) for redshift z, for the three sets of parameters $\mathcal{A}$, $\mathcal{B}$ and $\mathcal{C}$. Set 1 of observations is union 2 + HST. Set 2 of observations is union 2 + HST + $H(z)$.

Parameter	$\mathcal{A}$, Set 1	$\mathcal{A}$, Set 2	$\mathcal{B}$, Set 1	$\mathcal{B}$, Set 2	$\mathcal{C}$, Set 1	$\mathcal{C}$, Set 2
	$\chi^2_{min} = 530.1$	545.6	530.1	544.5	530.0	544.3
H_0	$74.35^{+7.39}_{-7.50}$	$74.22^{+5.23}_{-5.08}$	$73.77^{+8.36}_{-7.35}$	$74.20^{+5.01}_{-5.49}$	$73.72^{+8.47}_{-7.12}$	$73.65^{+5.92}_{-5.35}$
q_0	$-0.7085^{+0.6074}_{-0.5952}$	$-0.6149^{+0.2716}_{-0.2238}$	$-0.6250^{+0.5580}_{-0.4953}$	$-0.6361^{+0.3720}_{-0.3645}$	$-0.6208^{+0.4849}_{-0.6773}$	$-0.5856^{+0.3884}_{-0.3445}$
j_0	$1.605^{+6.738}_{-4.481}$	$1.030^{+0.722}_{-1.001}$	$0.392^{+4.585}_{-4.511}$	$0.994^{+1.904}_{-2.665}$	$-1.083^{+8.359}_{-2.218}$	$-0.117^{+3.621}_{-1.257}$
s_0	$2.53^{+60.61}_{-10.45}$	$0.16^{+1.45}_{-1.03}$	$-5.59^{+33.74}_{-34.55}$	$-1.47^{+4.20}_{-10.72}$	$-25.52^{+65.60}_{-10.90}$	$-7.71^{+14.77}_{-7.83}$
l_0	—	—	$-3.50^{+196.09}_{-89.19}$	$4.47^{+41.53}_{-8.47}$	*N.C.*	$8.55^{+23.39}_{-27.86}$
m_0	—	—	—	—	*N.C.*	$71.93^{+382.17}_{-315.76}$

Notes.

a. H_0 is given in Km/s/Mpc.

b. *N.C.* means the results are not conclusive. The data do not constrain the parameters sufficiently.

Table 10.2.: Table of best fits and their likelihoods (1σ) for redshift y_1, for the three sets of parameters $\mathcal{A}$, $\mathcal{B}$ and $\mathcal{C}$. Set 1 of observations is union 2 + HST. Set 2 of observations is union 2 + HST + $H(z)$.

Parameter	$\mathcal{A}$ Set 1	$\mathcal{A}$ Set 2	$\mathcal{B}$ Set 1	$\mathcal{B}$ Set 2	$\mathcal{C}$ Set 1	$\mathcal{C}$ Set 2
	$\chi^2_{min} = 530.1$	550.1	529.9	544.5	530.0	545.1
H_0	$74.05^{+7.90}_{-7.19}$	$75.25^{+4.72}_{-4.87}$	$73.68^{+7.77}_{-6.94}$	$73.30^{+5.59}_{-5.22}$	$73.91^{+7.60}_{-6.97}$	$74.49^{+5.07}_{-5.59}$
q_0	$-0.6633^{+0.5753}_{-0.6580}$	$-0.4106^{+0.2919}_{-0.5774}$	$-0.0004^{+0.2513}_{-1.6617}$	$-0.2652^{+0.5071}_{-0.7977}$	$-0.5360^{+0.8468}_{-0.8965}$	$-0.4624^{+0.5804}_{-0.8391}$
j_0	$1.268^{+6.986}_{-4.273}$	$-7.746^{+15.526}_{-2.252}$	$-13.695^{+30.901}_{-1.703}$	$-7.959^{+13.529}_{-5.228}$	$-1.646^{+11.637}_{-8.345}$	$-1.862^{+11.021}_{-5.397}$
s_0	$1.21^{+61.24}_{-9.24}$	$-88.91^{+57.62}_{-11.08}$	$-180.95^{+331.75}_{-18.93}$	$-112.63^{+156.60}_{-82.53}$	$-30.97^{+90.96}_{-43.47}$	$-16.95^{+73.68}_{-38.79}$
l_0	—	—	*N.C.*	*N.C.*	*N.C.*	*N.C.*
m_0	—	—	—	—	*N.C.*	*N.C.*

Notes.
a. H_0 is given in Km/s/Mpc.
b. *N.C.* means the results are not conclusive. The data do not constrain the parameters sufficiently.

Table 10.3.: Table of best fits and their likelihoods (1σ) for redshift y_4, for the three sets of parameters $\mathcal{A}$, $\mathcal{B}$ and $\mathcal{C}$. Set 1 of observations is union 2 + HST. Set 2 of observations is union 2 + HST + $H(z)$.

Parameter	$\mathcal{A}$ Set 1	$\mathcal{A}$ Set 2	$\mathcal{B}$ Set 1	$\mathcal{B}$ Set 2	$\mathcal{C}$ Set 1	$\mathcal{C}$ Set 2
	$\chi^2_{min} = 530.3$	544.8	529.7	544.6	529.9	544.5
H_0	$74.55^{+7.54}_{-7.53}$	$73.71^{+5.29}_{-5.24}$	$73.95^{+7.99}_{-7.22}$	$73.43^{+6.05}_{-5.74}$	$74.12^{+8.27}_{-7.78}$	$73.27^{+6.86}_{-5.91}$
q_0	$-0.7492^{+0.5899}_{-0.6228}$	$-0.6504^{+0.4275}_{-0.3303}$	$-0.4611^{+0.5422}_{-0.6710}$	$-0.7230^{+0.5851}_{-0.4585}$	$-0.4842^{+2.7126}_{-0.9280}$	$-0.7284^{+0.6062}_{-0.4838}$
j_0	$2.558^{+7.441}_{-8.913}$	$1.342^{+1.391}_{-1.780}$	$-3.381^{+10.613}_{-2.149}$	$2.017^{+3.149}_{-3.022}$	$-1.940^{+8.041}_{-2.148}$	$2.148^{+3.414}_{-4.036}$
s_0	$9.85^{+74.69}_{-26.69}$	$3.151^{+3.920}_{-1.771}$	$-37.67^{+89.51}_{-60.10}$	$5.278^{+13.076}_{-14.732}$	$-13.48^{+71.65}_{-31.28}$	$2.179^{+42.126}_{-35.919}$
l_0	—	—	*N.C.*	$-0.13^{+96.75}_{-65.87}$	*N.C.*	$-11.60^{+193.88}_{-187.96}$
m_0	—	—	—	—	*N.C.*	$70.9^{+2497.8}_{-2254.5}$

Notes.

a. H_0 is given in Km/s/Mpc.

b. *N.C.* means the results are not conclusive. The data do not constrain the parameters sufficiently.

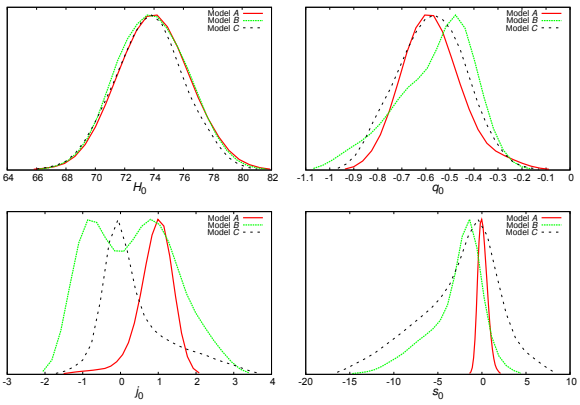

Figure 10.2.: 1-dimensional marginalized posteriors for H_0, q_0, j_0 and s_0, using set 2 of observations (union 2 + HST + $H(z)$). Solid (red) line is parameter set $\mathcal{A}$, dotted (green) line is parameter set $\mathcal{B}$ and dashed (black) line is parameter set $\mathcal{C}$.

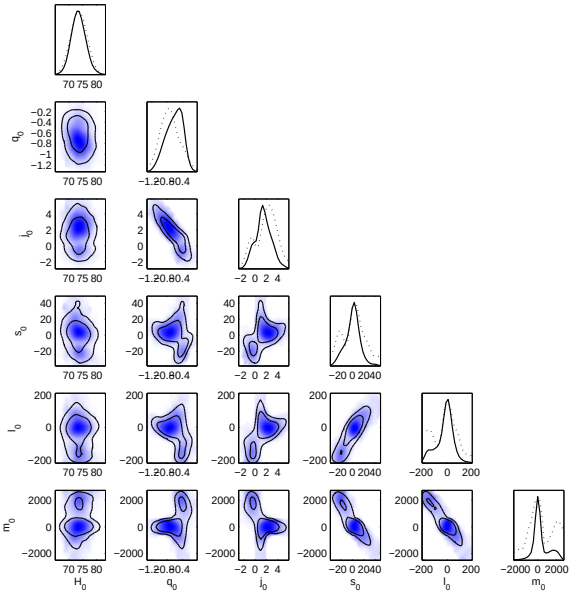

Figure 10.3.: Marginalized posterior constraints for redshift y_4 and parameter set $\mathcal{C}$, using set 2 of observations (union 2 + HST + $H(z)$). The shaded region and the dotted lines show the likelihoods of the samples.

Table 10.4.: Table of mean values of the posteriors and their likelihoods (1σ) for the three redshifts, using set 2 of observations being union 2 + HST + $H(z)$, evaluated at $t = t_0$. $P_1(z)$, $P_1(y_1)$, $P_1(y_4)$, $P_2(z)$, $P_2(y_4)$ and $P_3(z)$ are in units of $10^4\, c^2/\kappa$, $P_2(y_1)$ and $P_4(y_4)$ in units of $10^5\, c^2/\kappa$, $P_3(y_4)$ and $P_4(z)$ in units of $10^6\, c^2/\kappa$, $P_3(y_1)$ in units of $10^7\, c^2/\kappa$, and $P_4(y_1)$ in units of $10^8\, c^2/\kappa$.

Parameter	Redshift z	Redshift y_1	Redshift y_4
H_0	$74.23^{+2.31}_{-2.36}$	$74.20^{+2.37}_{-2.36}$	$75.70^{+2.68}_{-2.66}$
ω_0	$-0.7174^{+0.0922}_{-0.0964}$	$-0.7439^{+0.3085}_{-0.3222}$	$-0.7315^{+0.1193}_{-0.1373}$
$P_1(0)$	$-0.209^{+0.347}_{-0.261}$	$-0.991^{+2.393}_{-2.213}$	$-0.228^{+0.506}_{-0.528}$
$P_2(0)$	$0.988^{+2.012}_{-1.539}$	$-0.134^{+1.623}_{-1.729}$	$-0.246^{+4.133}_{-3.927}$
$P_3(0)$	$0.630^{+4.010}_{-4.932}$	$0.205^{+0.294}_{-0.257}$	$0.217^{+0.625}_{-0.400}$
$P_4(0)$	$-0.107^{+0.099}_{-0.170}$	$-0.150^{+0.209}_{-0.187}$	$-0.289^{+4.690}_{-6.112}$

Notes.
a. H_0 is given in Km/s/Mpc.

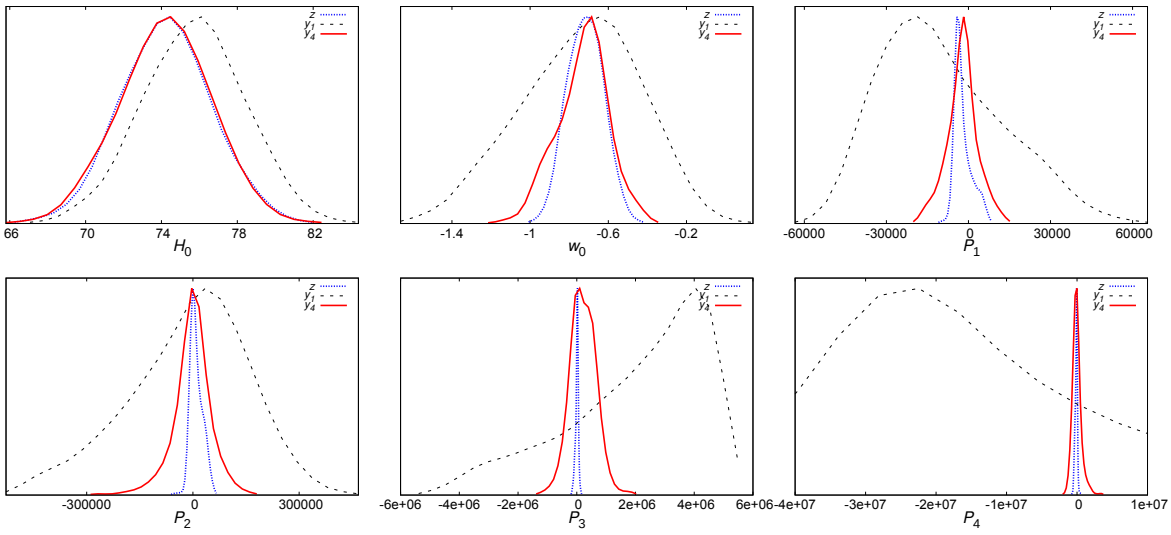

Figure 10.4.: 1-dimensional marginalized posteriors for the complete set of parameters of the EoS analysis, using set 2 of observations (union 2 + HST + $H(z)$). Dotted (blue) lines are used for z, dashed (black) lines for y_1, and solid (red) lines are for redshift y_4.

Table 10.5.: Table of best fits and their likelihoods (1σ) for the estimated (top panel) and derived (lower panel) parameters for the ΛCDM model, using set 2 of observations (union 2 + HST + $H(z)$).

Parameter	Redshift z
$\Omega_m h^2$	$0.1447^{+0.0181}_{-0.0174}$
H_0	$74.05^{+7.90}_{-7.19}$
q_0	$-0.6633^{+0.5753}_{-0.6580}$
j_0	1
s_0	$-0.2061^{+0.1772}_{-0.2015}$
l_0	$2.774^{+0.485}_{-0.382}$
m_0	$-8.827^{+2.263}_{-2.941}$

Notes.
H_0 is given in Km/s/Mpc. Here h is defined through the relation $H_0 = 100\,h$km/s/Mpc.

Table 10.6.: Table of derived values and their likelihoods (1σ) for the derivatives of $G(y_i)$ for the three redshifts z, y_1, y_4, evaluated at $t = t_0$, using set $\mathcal{C}$ of parameters and set 2 of observations (union 2 + HST + $H(z)$).

Parameter	Redshift z	Redshift y_1	Redshift y_4
$G(0)$	$0.724^{+0.26}_{-0.23}$	$0.642^{+0.56}_{-0.39}$	$0.819^{+0.32}_{-0.40}$
$G_1(0)$	$0.007^{+1.30}_{-1.23}$	$0.250^{+1.57}_{-1.87}$	$-0.279^{+1.60}_{-1.44}$
$G_2(0)$	$-2.220^{+4.61}_{-3.33}$	$-4.710^{+9.13}_{-8.80}$	$1.738^{+4.89}_{-4.94}$
$G_3(0)$	$13.650^{+8.04}_{-5.80}$	$0.7476^{+55.73}_{-49.34}$	$-3.430^{+13.34}_{-12.43}$
$G_4(0)$	$-17.240^{+35.27}_{-31.89}$	*N.C.*	$-16.291^{+50.88}_{-47.6}$
$G_5(0)$	$-129.740^{+174.29}_{-130.39}$	*N.C.*	$-8.745^{+332.41}_{-323.68}$

Notes.
a. *N.C.* means the results are not conclusive. The data do not constrain the parameters sufficiently.

10.2. Padé fits

In the following we will present the results obtained for the fitting with Padé expressions. In this part the updated union 2.1 compilation of the SCP [80] was used, comprising 580 measurements of type Ia supernovae events. In these analyses, we have used the distance modulus μ_D as the fitting function, and thus employed all expressions for μ_D derived in Section 9.2 within the Padé approach. The best fit values were obtained as previously by minimizing the chi-square function or equivalently maximizing the likelihood, but using a Metropolis algorithm [103–105] implemented in a Monte Carlo simulation. The investigated parameter space was limited by $0.4 < h < 0.9$, $-1.5 < q_0 < 0$ and $-2 < j_0 < 2$, where h is defined via $H_0 = 100\,h\,\mathrm{km/(s\,Mpc)}$. For most of the fits we used data from the complete redshift regime of the union 2.1 compilation, $z \in [0, 1.414]$, except for one fit carried out in a restricted sample with redshifts of $z \in [0, 0.36]$.

As in the previous section, we imposed different priors on the fitting procedures in order to further constrain the parameter space. For H_0, we used two different priors, one being $H_0 = 67.11\,\mathrm{km/(s\,Mpc)}$ obtained by the Planck collaboration [11], and the second being obtained by a restricted fit of a part of the union 2.1 compilation, i.e. only using data with redshifts $z < 0.36$, with the fitting function

$$d_L \simeq \frac{1}{H_0}\, z\,, \tag{10.8}$$

i.e. a first order expression of the luminosity distance for which Taylor and Padé treatment coincide. This results in a value of $H_0 = 69.96^{+1.12}_{-1.16}\,\mathrm{km/(s\,Mpc)}$, which provides a second prior on the Hubble parameter.

Besides these priors on H_0, we imposed constraints on q_0 as well assuming the validity of the ΛCDM model. With a Hubble parameter given by Eq. (10.5), and using the value extracted from observations by the Planck mission for the matter density, $\Omega_m = 0.3175$, the parameter q_0 can be given by

$$q_0 = -1 + \frac{3}{2}\Omega_m = -0.5132\,. \tag{10.9}$$

We carried out seven numerical fits, differing from each other by treatment or priors imposed. Without any priors, fit (1) was done using the Taylor approach, fit (2) features the Padé-parameterized fitting function, and fit (3) is the same as (2) but for the restricted redshift range $z \in [0, 0.36]$. Further, in fit (4) we presumed the Planck prior on H_0, in fit (5) the Planck prior on q_0, and in fit (6) both of those priors simultaneously. In fit (7) finally, we imposed the fit from the first-order expansion of d_L. The results for the parameters as well as the respective p-values of the fit can be found in Tab. 10.7. The p-value is a statistical quantity to infer the goodness of fit and supposed to be close to

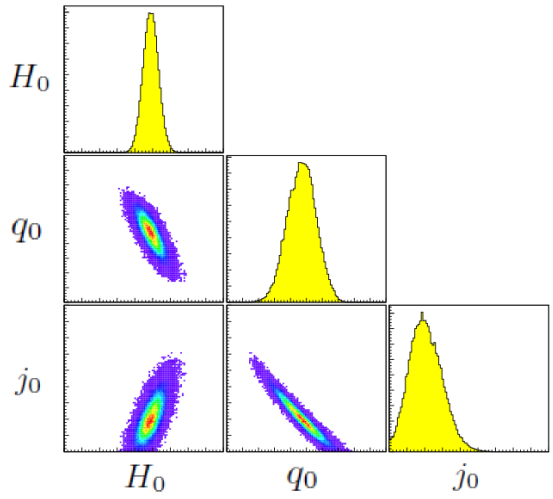

Figure 10.5.: (color online) Contour plots and posterior distributions for H_0, q_0 and j_0, for a fit with Taylor parametrization and without any priors imposed.

unity. It represents the probability for the outcome of the fit to be obtained assuming the null hypothesis to be true, which discards any mutual context a priori between the fitting parameters [106]. The contour plots and marginalized posterior distributions of these fits can be found in Figures 10.5-10.10.

The differences in priors assumed in these analyses is mirrored in the outcomes for the fitting parameters. From fits (1) and (2) without any priors, comparisons can be drawn between the Taylor and Padé treatment. The result from the Padé approximants leads to a slightly higher Hubble parameter, as well as a larger acceleration of the universe and a much larger jerk parameter. The Taylor results for q_0 and j_0 are closer to the predictions of the ΛCDM model, but as the Padé treatment with a Hubble parameter significantly larger than obtained from ΛCDM. The p-values of (1) and (2) are similar, with a slight advantage for the Padé treatment. The p-value for fit (3) is even closer to unity, which is ascribed to the higher statistical accuracy due to the limited redshift range. Its outcomes support the results of fit (2), with a Hubble parameter in between the values of (1) and (2), but with q_0 and j_0 being very close to the results of (2). The comparison of those three fits seems to indicate the validity and confirm the virtues of the Padé approach, only slightly dependent on the range of redshifts used. The imposition of priors in fits (4) and (5) leads to surprisingly disastrous results, with the predicted values for q_0 and j_0 far outside the expected range in fit (4), and a negative result for j_0 also in fit (5). A negative j_0 refutes the assumption of changes in the cosmological history, a rather consolidated feature in most cosmological theories, whereas the predicted q_0 in fit (4) is a lot smaller than usually

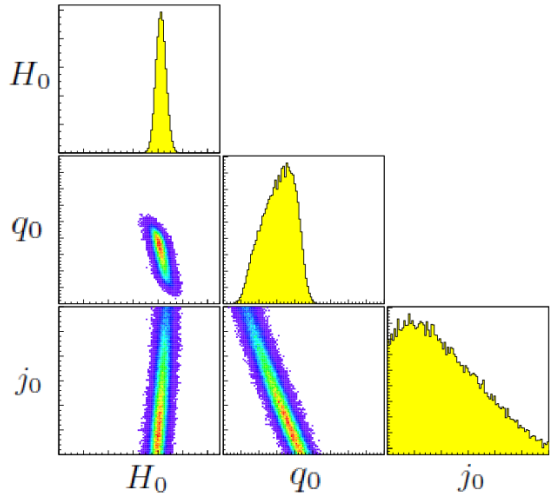

Figure 10.6.: (color online) Contour plots and posterior distributions for H_0, q_0 and j_0, for a fit with Padé parametrization and without any priors imposed.

expected. Correspondingly, the p-values are lower than in the first three fits, in fit (4) even as low as 0.242. Only in fit (6), with the imposition of both priors on H_0 and q_0, the result for j_0 is positive, and quite much larger than unity, which seems to confirm the high j_0-values obtained by the Padé treatment in fits (2) and (3). The p-value of fit (6) is the smallest in the whole analysis, but this is more likely due to an obvious correlation of the parameters due to the priors used. Fit (7) finally has the highest p-value, identically with fit (2), and yields quite expected values for q_0 and j_0, q_0 being slightly less negative than predicted by fits (2) and (3), and j_0 nearly equal to unity, which is very close to the ΛCDM result.

In summary, considering all results and their respective p-values and significance, it seems that the value of the Hubble parameter is slightly higher than claimed in the analyses of the Planck collaboration, supported by the good outcomes of fits (2), (3) and (7), as well as the poor results in fits (4) and (5). The acceleration parameter obtained in our analyses is close to the result of Planck, whereas the jerk parameter is negative, but predicted to be significantly larger than the ΛCDM value.

10.2.1. Implications for the convergence radii

From the expressions for the convergence radii of the Padé expansions as calculated in Section 9.2, and using the obtained fitting results for q_0, we computed the values for the convergence radii of Taylor and Padé treatment, shown in Tab. 10.8. For the Padé treatment, all values are greater than one, i.e. the convergence of the Padé approach always

Table 10.7.: Table of best fits and their likelihoods (1σ) for the parameters $\mathcal{H}_0$, q_0 and j_0.

fit	fit (1)	fit (2)	fit (3)	fit (4)	fit (5)	fit (6)	fit (7)
p-value	0.690	0.694	0.811	0.242	0.689	0.019	0.694
$\mathcal{H}_0$	$69.90^{+0.438}_{-0.433}$	$70.25^{+0.410}_{-0.403}$	$70.090^{+0.460}_{-0.450}$	67.11	$69.77^{+0.288}_{-0.290}$	67.11	$69.96^{+1.12}_{-1.16}$
q_0	$-0.528^{+0.092}_{-0.088}$	$-0.683^{+0.084}_{-0.105}$	$-0.658^{+0.098}_{-0.098}$	$-0.069^{+0.051}_{-0.055}$	-0.513	-0.513	$-0.561^{+0.055}_{-0.042}$
j_0	$0.506^{+0.489}_{-0.428}$	$2.044^{+1.002}_{-0.705}$	$2.412^{+1.065}_{-0.978}$	$-0.955^{+0.228}_{-0.175}$	$-0.785^{+0.220}_{-0.208}$	$2.227^{+0.245}_{-0.237}$	$0.999^{+0.346}_{-0.468}$

Note. $\mathcal{H}_0$ is given in Km/(s Mpc).

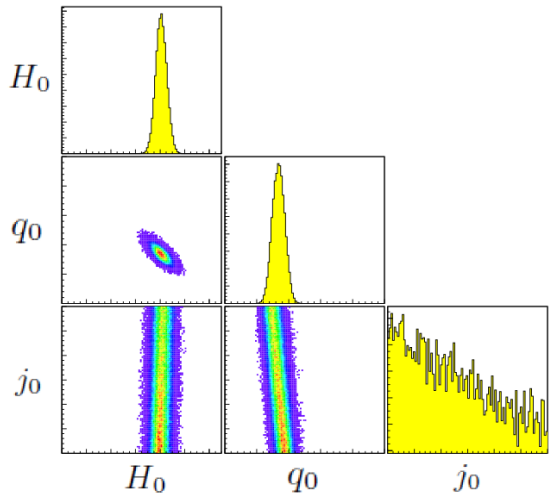

Figure 10.7.: (color online) Contour plots and posterior distributions for H_0, q_0 and j_0, for a fit with Padé parametrization and without any priors imposed, for the short redshift range.

extends to a larger regime than the one of the Taylor formalism, which varies in the range $\mathcal{R}_{\text{Taylor}} \in [0.535, 0.829]$. Nearly all of the results for $\mathcal{R}_{\text{Padé}}$ cover the whole range $z \in [0.015, 1.414]$ of supernova data provided by the supernova cosmology project, and thus using the complete sample for the Padé analysis is justified in the Padé approach. The result from fit (4) was non-conclusive, which is due to the fact that condition (9.29) on q_0 wasn't met for this fit. However, fit (4) in general has lead to some dubious results, and thus its results are not very trustworthy.

10.2.2. Implications for the EoS parameter

As introduced in Section 8.3, physical quantities related to thermodynamics and the equation of state of the universe cannot only be used directly as fitting parameters as we elaborated in the previous section, but can be computed from fitting results for the CS. We will thus proceed to compute results for the EoS parameter ω and its first derivative with respect to the redshift, as given by Eqs. (8.31) and (8.32), from the above obtained best fit values for the CS, in particular for q_0 and j_0. Evaluated at the present time, ω and ω' are expressed as

$$\omega_0 = \frac{2q_0 - 1}{3}\,, \tag{10.10a}$$
$$\omega_0' = \frac{2}{3}\left(j_0 - q_0 - 2q_0^2\right)\,.$$

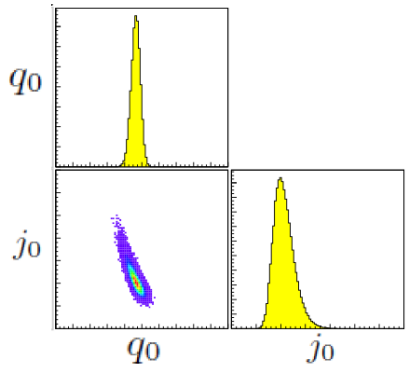

Figure 10.8.: (color online) Contour plots and posterior distributions for H_0, q_0 and j_0, for a fit with Padé parametrization and with a prior on $\mathcal{H}_0$ from the Planck results.

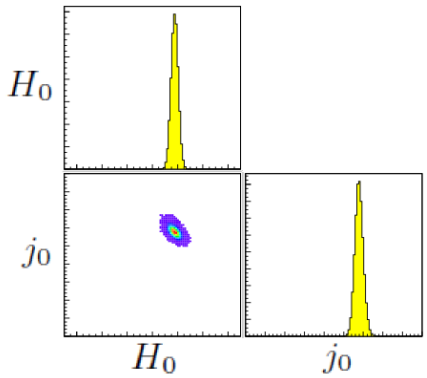

Figure 10.9.: (color online) Contour plots and posterior distributions for H_0, q_0 and j_0, for a fit with Padé parametrization and with a prior on q_0 from the Planck results.

Tab. 10.8 shows the corresponding values for the seven fits carried out in this part of the work. All fits except fit (4) yielded expected results, with the EoS parameter in the range $\omega_0 \in [-0.789, -0.675]$. The values from fit (5) and (6) being the least negative, fits (2) and (3) resulted in larger absolute values. Cosmography thus predicts a slightly more negative EoS of the universe, and thus a higher amount of dark energy present than the ΛCDM model, which purports

$$\omega_0 = -1 + \Omega_m \,. \tag{10.11}$$

With a value of $\Omega_m = 0.314 \pm 0.02$ from the Planck collaboration [11] this leads to an EoS parameter constrained in the range $\omega_0 \in [-0.688, -0.684]$. The first derivative of the EoS parameter, indicating changes in the EoS, is clearly positive in all fits except (4) and (5), which corresponds to an evolution of ω towards less negative values in the past, i.e. towards more negative values in the future, and thus confirms the ongoing transition from

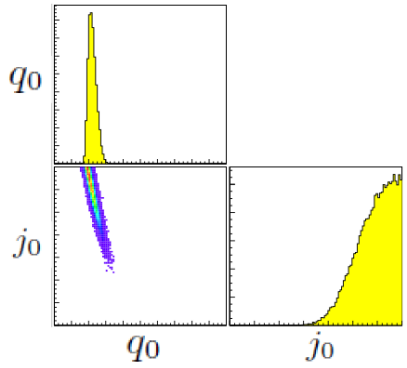

Figure 10.10.: (color online) Contour plots and posterior distributions for H_0, q_0 and j_0, for a fit with Padé parametrization and with a prior on $\mathcal{H}_0$ from the first order fit of the luminosity distance.

a matter- to a dark energy-dominated universe. For ω', the ΛCDM model predicts

$$\omega_0' = 3\,(1 - \Omega_m)\,\Omega_m\,, \tag{10.12}$$

resulting in the range $\omega_0' \in [0.644, 0.648]$, which is nearly in all cases in accordance with our results.

Table 10.8.: Table of convergence radii for the Padé expansion of the luminosity distance, as well as the EoS parameter ω_0 and its first derivative ω_0' at current time, for diverse results of q_0 and j_0 obtained.

fit	q_0	j_0	$\mathcal{R}_{\text{Padé}}$	$\mathcal{R}_{\text{Taylor}}$	ω_0	ω_0'
fit (1)	$-0.528^{+0.092}_{-0.088}$	$0.506^{+0.489}_{-0.428}$	$1.309\ ^{+0.079}_{-0.075}$	$0.764^{+0.046}_{-0.044}$	$-0.685^{+0.061}_{-0.059}$	$0.317^{+0.333}_{-0.293}$
fit (2)	$-0.683^{+0.084}_{-0.105}$	$2.044^{+1.002}_{-0.705}$	$1.188^{+0.059}_{-0.074}$	$0.842^{+0.042}_{-0.052}$	$-0.789^{+0.056}_{-0.07}$	$1.196^{+0.675}_{-0.485}$
fit (3)	$-0.658^{+0.098}_{-0.098}$	$2.412^{+1.065}_{-0.978}$	$1.206^{+0.071}_{-0.071}$	$0.829^{+0.049}_{-0.049}$	$-0.772^{+0.065}_{-0.065}$	$1.469^{+0.718}_{-0.661}$
fit (4)	$-0.069^{+0.051}_{-0.055}$	$-0.955^{+0.228}_{-0.175}$	$1.870^{+0.089}_{-0.096}$	$0.535^{+0.025}_{-0.027}$	$-0.380^{+0.034}_{-0.036}$	$-0.597^{+0.154}_{-0.12}$
fit (5)	-0.513	$-0.785^{+0.220}_{-0.208}$	1.322	0.757	-0.675	$-0.532^{+0.147}_{-0.138}$
fit (6)	-0.513	$2.227^{+0.245}_{-0.237}$	1.322	0.757	-0.675	$1.476^{+0.164}_{-0.158}$
fit (7)	$-0.561^{+0.055}_{-0.042}$	$0.999^{+0.346}_{-0.468}$	$1.281^{+0.045}_{-0.034}$	$0.780^{+0.027}_{-0.021}$	$-0.707^{+0.037}_{-0.028}$	$0.620^{+0.235}_{-0.314}$

11. Conclusions and Outlook

We have dedicated this part to an experiment-based approach to the issue of dark energy and presented a thorough analysis of observational astrophysical data to the purpose of obtaining information on the kinematics of the universe. In particular, we have tried to extract the late time accelerating behaviour of the universe in order to infer the required framework that a theory of dark energy, like the model presented in Part II, has to fulfill. To do so, we have made use of cosmography, an approach to data analysis which aims for a maximally neutral treatment of data, with a minimum set of assumptions involved. Solely characterizing the kinematical evolution of the universe by a FLRW-universe described by a scale factor $a(t)$ and employing the mathematical concept of Taylor expansions with respect to the cosmological redshift, cosmography defines a set of cosmological parameters termed the cosmographic series, determining the dynamics of expansion. Even though cosmography is a very successful method for model-independent data analysis, it has some weaknesses connected to the convergence of the expansions involved. We proposed two possibilities of improvement of the convergence problem - the first suggesting a reparameterization of all quantities and expansions in terms of alternative redshift variables, the second substituting the method of Taylor expansions by the concept of Padé approximants instead. Through statistical fitting analyses, we found constraints on the cosmographic parameters and thus inferred the necessary requirements on any fundamental model for the evolution of the universe. Besides the kinematical parameters of the CS, we also derived the expressions for thermodynamic quantities like the equation of state parameter and the pressure of the universe in terms of the CS, and set up an alternative parameter set employing those thermodynamic quantities, which were then determined by fitting procedures as well. We thus obtained information on the thermodynamic state of the universe by derivation from the results obtained from the CS as well as by direct fits. In a first part of the numerical analyses we compare the fitting outcomes for the different notions of redshift introduced, whereas in a second set of fits we investigate the validity of Padé approximants in cosmography in contrast to the conventional Taylor approach.
We find that both new notions of redshift and substitution of the Taylor treatment by Padé improves the quality and convergence behaviour of cosmographic analyses, and are viable modifications of the conventional approach. On the cosmological aspect of the outcomes,

our results are in accordance with the standard ΛCDM model of cosmology, and allow for the possibility of a cosmological constant as the origin of the accelerated expansion of the universe. Unfortunately, it is not possible to alleviate the problem of degeneracy between models with our analyses, since the models give too similar predictions, and only based on the parameters obtained in our fits it is not possible to deduce more differentiated statements to discriminate between models. Hence, also models with a varying dark energy term instead of a cosmological constant cannot be excluded yet; however, a cosmological constant remains a very good candidate for dark energy, and so the work of this part supports the model developed in Part II.

Part IV.

Bose-Einstein condensates in Compact Objects

12. Bose-Einstein condensates in Astrophysics

In the last part of this thesis we will turn our attention to another quantum phenomenon in the context of large scale physics, i.e. the possible occurrence of a Bose-Einstein condensate (BEC) in compact objects in astrophysics.
Laboratory experiments on cold gases have first confirmed [107, 108] the existence of a particular state of matter occurring for bosonic particles when cooled down to very low temperatures in low-density environments. Originating from Bose's re-derivation of Planck's law of black body radiation [109], Einstein predicted the phenomenon employing a new statistics for the distributions of bosons in an ensemble, describing a synchronization of the wave functions of all particles in the system [110]. Velocity-distribution data from experiments [111] show a macroscopic occupation of the ground state, thus demonstrating the existence of a quantum phenomenon with impacts on large scales.
Even though the effect is known from laboratory physics, it can be considered in completely different circumstances as well, as for example in compact objects in astrophysics. Generally a BEC is created when the temperature in a system falls below the critical temperature

$$T_{\text{crit}} = \left[\frac{n}{\zeta(3/2)}\right]^{2/3} \frac{2\pi\hbar^2}{m k_B}\,, \tag{12.1}$$

corresponding to the point where the thermal de Broglie wavelength equals the average interparticle distance, and the wave functions of individual particles overlap and synchronize. Rather surprisingly, considering the typical temperatures and densities in astrophysical scenarios extracted from observations, condition (12.1) seems to be met in most cases of compact objects, as shown in Tab. 12.1, where typical temperatures and corresponding critical temperatures derived from typical densities in different scenarios are compared. A possible example for BECs in compact objects in astrophysics are boson stars - either as an abstract concept of a bosonic field in a spherically symmetric metric [112], or as the concrete case of a white dwarf consisting of bosonic particles. Helium white dwarfs are an obvious candidate [113, 114], even though due to the ongoing fusion processes inside the star the abundance of objects solely made up of helium is presumably small. A white

Table 12.1.: Estimates for the typical temperatures and critical temperatures derived from typical densities in different compact objects.

scenario	n [m^{-3}]	T_{crit} [K]	T_{typ} [K]
^{4}He white dwarf	10^{35}	10^5	$10^4 - 10^7$
neutron star (core)	10^{44}	10^{11}	$10^{10} \rightarrow 10^6$
neutron star (crust)	10^{36}	10^6	10^6

dwarf predominantly consisting of ^{4}He atoms could be however a suitable candidate to be described by such a theory. Moreover, the possible existence of BECs in neutron stars has been considered as well [115].

Even though neutrons are fermions, neutron stars are potential example candidates for a theory of astrophysical BECs, as we will argue in the following. Neutron stars have been considered firstly by Tolman [116] as well as Oppenheimer and Volkoff [117]. They investigated a fluid of self-gravitating neutrons, for which the equation of state is determined by Fermi statistics, in general relativity embedded in a spherically symmetric metric, and searched for stable equilibrium configurations of the system. In the scenario assumed by Tolman, Oppenheimer and Volkoff, the gravitational collapse of a cloud of neutrons is counterbalanced by the degeneracy pressure of the neutrons as a consequence of the Pauli exclusion principle. The maximum stable mass of such a system was found to be about $0.7\,M_\odot$. On the contrary, observations [118] have found neutron stars with masses up to a value of $2\,M_\odot$, which exceeds the limit given by Refs. [116, 117]. Hence, there has been an abundance of proposals and models [119] to explain the observed masses of neutron stars, suggesting the existence of other states or types of matter in the core of the objects, reaching from strange baryons over heavy mesons like kaons or pions to quark matter, while the crust of neutron stars is usually assumed to consist of neutrons and electrons [120]. A general consensus exists over the fact that neutrons in a neutron star should be in a superfluid phase [121], i.e. the particles are bound in Cooper pairs and can be treated as composite bosons with an effective mass of $m = 2m_n$. Estimations of typical temperatures and densities show that the existence of a Bose-Einstein condensate is possible in the inner core regions of a neutron star as well as in the outer crust, characterized by different temperatures and densities. A microscopically exact way of treating such a system is the theory of a BCS-BEC-crossover [122, 123], i.e. a transition from the quantum state of superfluidity (BCS phase) to a Bose-Einstein condensate. The phenomenon has been observed in the laboratory [124] before, and has recently also been applied to the case of neutron matter inside stars [125].

In contrast to that, theories of white dwarfs are more uniform since they are built around the occurrence of fusion processes in the center of a star. The particles in the system are assumed to be ionized, and, depending on the mass of the object, at different stages of the fusion process. In so-called main sequence stars, predominantly made up by hydrogen, temperatures are high enough to enable the fusion of hydrogen to helium. Once the hydrogen content is exhausted, the lack of nuclear reactions in the core causes the star to collapse, leading to an increase in density and temperature, which can reignite hydrogen fusion in a shell around the helium core. This leads to a rise in temperature and luminosity, causing the outer layers of the star to cool and expand. Stars in this stage are called red giants, since their emission is typically shifted to the red end of the visible spectrum. Depending on the total initial mass of the system, temperatures can be high enough, exceeding $10^8\,\mathrm{K}$, which leads to further fusion of helium to carbon or oxygen via the triple alpha process [126]. Once the fusion processes have ceased, eventually the red giant will lose its outer layers forming planetary nebulae, while the core remains and is then termed a white dwarf. White dwarfs are thus the final stage of a certain class of stars after all fusion processes have stopped, and stable configurations are the result of a balance between gravitational and electron degeneracy pressure. The atoms are assumed to be ionized and surrounded by a sea of electrons, whose quantum degeneracy supports the star against gravitational collapse.

For initial masses of about $0.5\,M_\odot$, temperatures are too low for helium fusion, and thus the remainder white dwarf predominantly consists of helium. However, the time span to reach this final stage is presumably longer than the current age of the universe, so the existence of helium white dwarfs is commonly ascribed to the occurrence of white dwarfs in binary systems, where the mass loss of the white dwarf due to the companion prevents helium burning and leads to the creation of helium-dominated remainders [127]. Since it is assumed that about a third of stars are part of a binary system [128], the occurrence of helium-dominated white dwarfs is plausible, and has been proven by observations [129,130]. For these scenarios, an upper bound on the mass of the object can be given by the Chandrasekhar limit. It is derived from three simple equations: the definition of the gravitational potential, the spatial variation of pressure in hydrostatics, and an equation of state in the form of a context of pressure and density of the system [131]. The gravitational potential Φ is given by

$$g = \frac{G_N M(r)}{r^2} = -\frac{d\Phi}{dr}\,, \tag{12.2}$$

where g is the acceleration, G_N is Newton's constant and $M(r)$ is the mass of the system enclosed in a sphere of radius r. In turn, in a static fluid with density ρ the hydrostatic

pressure p is solely determined by the weight of the fluid above a certain point, given by

$$dp = -g\,\rho\,dr\,. \tag{12.3}$$

Combining these two equations leads to the following relation between pressure and gravitational potential:

$$dp = \rho\,d\Phi\,. \tag{12.4}$$

Furthermore, the Poisson equation relates the gravitational potential to the density as

$$\nabla^2\Phi = -4\pi G_N\,\rho\,. \tag{12.5}$$

At last, we use a polytropic ansatz for the equation of state of the fluid,

$$p = \kappa\,\rho^\gamma\,, \tag{12.6}$$

where $\gamma = 1 + 1/n$ defines the polytropic index n, and κ represents a suitable constant of proportionality. Combining these expressions, we obtain a differential equation determining the gravitational potential,

$$\frac{1}{r}\frac{d^2}{dr^2}\Big[r\,\Phi\Big] = -\alpha^2\Phi^n\,, \tag{12.7}$$

where $\alpha^2 = 4\pi G_N/[(n+1)\kappa]^n$. The density ρ can directly be obtained from the result for the gravitational potential by the relation

$$\rho = \left[\frac{\Phi}{(n+1)\kappa}\right]^n\,. \tag{12.8}$$

From this context, we can transform Eq. (12.7) into a differential equation for the density ρ, which reads

$$\frac{1}{r}\frac{d^2}{dr^2}\Big[r\,\rho^{1/n}\Big] = -\frac{4\pi G_N}{(n+1)\kappa}\,\rho\,. \tag{12.9}$$

Eq. (12.7) has straightforward solutions e.g. for $n = 0, 1$, but requires the method of quadratures for other values. The calculations in those cases are outlined in Ref. [131], and lead to the following criterion for the mass of the configuration:

$$\left(\frac{G_N M}{M'}\right)^{n-1}\left(\frac{R'}{R}\right)^{n-3} = \frac{1}{\alpha^2}\,. \tag{12.10}$$

Here M' and R' are constants related to the solution for Φ, and can be given for specific values of n. The first calculations of the mass M for a system of self-gravitating, non-relativistic and non-interacting fermions were done by Stoner [132] and Anderson [133] using the above derivations and a polytropic equation of state for the electrons with $n = 2/3$. Chandrasekhar [134] pointed out the limited range of applicability of a non-relativistic

equation of state, and obtained his well-known mass limit for white dwarfs using a polytrope equation of state with $n = 3$. The above expression for the mass then yields

$$M_{\max} = M' \frac{\sqrt{3\pi}}{2} \frac{M_P^3}{m^2}, \tag{12.11}$$

where $M_P = \sqrt{\hbar c/G_N}$ is the Planck mass, $M' \simeq 2.015$ for $n = 3$, and m is the molecular weight of the particles constituting the system. For the case of hydrogen, $m = 2m_H$, which leads to a mass limit of $1.4\,M_\odot$, where $M_\odot \simeq 1.98 \cdot 10^{30}\,\mathrm{kg}$ denotes the solar mass. For the case of monatomic helium, the maximum mass is $M_{\max,\mathrm{He}} \simeq 1.001\,M_\odot$.

In the present work, we focus on helium white dwarfs as the main application of our theory, using a very simplified picture however, considering a system of bosons subject to hard-shell contact scattering and gravitational interaction amongst each other. We disregard the ionization of the atoms, which would require the inclusion of Coulomb interactions between the particles, and neglect the electron Fermi fluid coexisting with the bosons. The energy required to ionize helium amounts to 24.58 eV per electron, i.e. for the complete ionization of helium temperatures of about $10^5\,\mathrm{K}$ are necessary. Considering the typical temperatures in white dwarfs as shown in Tab. 12.1, it is clear that the helium in white dwarfs is mostly present in ionized form, except for a small region in the outermost layer, where the temperature drops significantly. Our model is thus a rather crude picture of the situation inside a white dwarf, and has large potential for improvements. However, the fact that results predict quite realistic and reasonable scenarios validate this theory as a qualitative basis of a more complete scenario.

A similar situation has been considered in Ref. [135], where systems of self-gravitating bosonic (and fermionic) particles have been considered. For the case of Newtonian gravity, these investigations have resulted in unstable configurations, which could be stabilized only by the inclusion of general relativistic effects. In contrast to our model however, the bosons in Ref. [135] are assumed to be free, and only subject to gravitational interactions, i.e. no contact interaction has been included. The hard shell scattering will be employed in our case to stabilize the system against gravitational collapse, since even for zero temperatures with vanishing thermal pressure and in the case of Newtonian gravity, the contact interaction provides the necessary pressure to counterbalance gravity.

A system of bosons in a Bose-Einstein condensed phase with contact and gravitational interactions for the case of zero temperatures has been treated in Ref. [115] and applied to the example of superfluid neutron stars. A generalization to a BEC at finite temperatures was recently worked out in Ref. [136], but then however applied to the example of a dark matter BEC in a FLRW universe. The theory of Bose-Einstein condensation for the case of bosonic dark matter was also considered by other authors, see Refs. [137–139]. Due to

the widely unknown nature and properties of dark matter, it is however a rather speculative field, and the effects of the presence of a Bose-Einstein condensate of dark matter particles in contrast to thermal phase dark matter are difficult to detect, most likely only by the gravitational lensing behaviour of dark matter halos. However, the environmental conditions in dark matter halos are supposed to be suitable for the existence of a BEC of dark matter particles, assuming that dark matter is bosonic [140].
The scenario of a BEC at finite temperatures has never been extended to the example of compact objects, so this work represents the first attempt in this direction. In Section 12.1 we will first review the zero-temperature case as presented in Ref. [115], and then in Section 12.2 outline the contents of the following chapters containing our own work, including a motivation for the specific choice of treatment.

12.1. Zero-temperature case

A BEC subject to contact and gravitational interaction has been formulated in Ref. [115] via a Schrödinger-type equation for the bosonic field operator $\hat{\Psi}(\mathbf{x},t)$ representing bosons with mass m. The resulting Heisenberg equation of motion reads

$$i\hbar\frac{\partial}{\partial t}\hat{\Psi}(\mathbf{x},t) = \left[-\frac{\hbar}{2m}\Delta + g\left|\hat{\Psi}(\mathbf{x},t)\right|^2 - \int d^3x' \frac{G_N m^2}{|\mathbf{x}-\mathbf{x}'|}\left|\hat{\Psi}(\mathbf{x},t)\right|^2\right]\hat{\Psi}(\mathbf{x},t)\,, \tag{12.12}$$

where $g = 4\pi\hbar^2 a/m$ denotes the strength of the repulsive contact interaction, a scattering term describing two-body interactions between the particles, and a is the s-wave scattering length of the bosons in the system characterizing the scattering process. To implement the presence of a condensate as well as of thermal and quantum fluctuations, the field operator can be split into a mean-field condensate and fluctuations. For the zero-temperature case and weak enough interparticle interactions, we will not consider any fluctuations, but simply work with a mean-field condensate, represented by the wave function

$$\Psi(\mathbf{x},t) = \langle\hat{\Psi}(\mathbf{x},t)\rangle\,. \tag{12.13}$$

The Heisenberg equation (12.12) then reduces to the Gross-Pitaevskii (GP) equation,

$$i\hbar\frac{\partial}{\partial t}\Psi(\mathbf{x},t) = \left[-\frac{\hbar}{2m}\Delta + g\left|\Psi(\mathbf{x},t)\right|^2 + \Phi(\mathbf{x},t)\right]\Psi(\mathbf{x},t)\,, \tag{12.14}$$

where we have defined the Newtonian gravitational potential $\Phi(\mathbf{x},t)$ as

$$\Phi(\mathbf{x},t) = -\int d^3x' \frac{G_N m^2}{|\mathbf{x}-\mathbf{x}'|}\left|\Psi(\mathbf{x}',t)\right|^2\,. \tag{12.15}$$

Assuming a Madelung representation of the condensate wave function, i.e. using an ansatz featuring an amplitude and a phase,

$$\Psi(\mathbf{x},t) = \sqrt{n_{\mathbf{0}}(\mathbf{x},t)}\; e^{iS(\mathbf{x},t)}\,, \tag{12.16}$$

we can identify the density of the condensate as

$$n_{\mathbf{0}}(\mathbf{x},t) = |\Psi(\mathbf{x},t)|^2\ . \tag{12.17}$$

With (12.16), we can split the Gross-Pitaevskii equation (12.14) into two equations by setting its real and imaginary part to zero separately, resulting in two coupled hydrodynamic equations, i.e. the continuity equation for the density $n_{\mathbf{0}}$ and the Euler equation for the velocity field $\mathbf{v} = \hbar\,\nabla S/m$,

$$\frac{\partial n_{\mathbf{0}}}{\partial t} + \nabla\cdot(n_{\mathbf{0}}\,\mathbf{v}) = 0\,, \tag{12.18a}$$

$$m\,n_{\mathbf{0}}\left[\frac{d\mathbf{v}}{dt} + (\mathbf{v}\cdot\nabla)\,\mathbf{v}\right] = -g\,n_{\mathbf{0}}\,\nabla n_{\mathbf{0}} - m\,n_{\mathbf{0}}\,\nabla\Phi - \nabla\cdot\sigma^{Q}_{ij}\,. \tag{12.18b}$$

The last term in the Euler equation contains the so-called quantum stress tensor

$$\sigma^{Q}_{ij} = \frac{\hbar^2}{4m}\,n_{\mathbf{0}}\,\nabla_i\nabla_j \ln n_{\mathbf{0}}\,, \tag{12.19}$$

representing a quantum contribution originating in the Laplacian term in the Gross-Pitaevskii equation. Commonly the Thomas-Fermi approximation is adapted, in which the kinetic term for the condensate is neglected. Thus, the quantum stress tensor can be dropped in the further course of the calculations. Also all other time dependences and time-dependent terms will be neglected from here on, since we want to consider static configurations only.

By comparison of Eq. (12.18b) with the general form of the Euler equation of a fluid, we can identify the first term on the RHS as the gradient of the pressure p,

$$\nabla p = g\,n_{\mathbf{0}}\,\nabla n_{\mathbf{0}}\,. \tag{12.20}$$

The pressure is then given by

$$p = \frac{g}{2}\,n_{\mathbf{0}}^2\,. \tag{12.21}$$

The pressure of the condensate is non-zero even for zero temperatures, which is a direct consequence of the presence of the contact interaction. Setting the contact interaction strength $g = 0$, we see that the pressure vanishes for zero temperature, as should be the case for a free Bose gas [135, 141].

We can define the mass density of the system as

$$\rho = m\,n_{\mathbf{0}}\,, \tag{12.22}$$

which leads to the equation of state,

$$p = \frac{g}{2m^2}\,\rho^2\,. \tag{12.23}$$

This is a polytropic equation of state as introduced before in Eq. (12.6) with the polytropic index $n = 1$ and $\kappa = 2\pi\hbar^2 a/m^3$.
Neglecting all time dependent terms in Eq. (12.18b) leads to

$$\nabla p = -\rho\,\nabla\Phi\,. \tag{12.24}$$

Combining Eqs. (12.23), (12.24) and (12.5) results in the so-called Lane-Emden equation, a second-order differential equation for the mass density of the condensate ρ as a function of the radial coordinate r, which is equivalent to Eq. (12.9). Even though our initial point was the quantum mechanical GP equation, we ultimately end up with the same three classical concepts that already Stoner, Anderson and Chandrasekhar were employing: the definition of the gravitational potential, the hydrostatic pressure in a fluid and an equation of state. For $n = 1$ the system can be solved analytically, and we can derive the corresponding mass limit straightforwardly. With the substitutions $\theta = (\rho/\rho_c)^{1/n}$, where ρ_c is the central condensate density and n the polytropic index of the equation of state, and $\xi = r\sqrt{4\pi G_N/\left[\kappa(n+1)\rho_c^{-1+1/n}\right]}$, Eq. (12.9) can be brought into the form

$$\frac{1}{\xi^2}\frac{d}{d\xi}\left(\xi^2\,\frac{d\theta}{d\xi}\right) = -\theta^n\,. \tag{12.25}$$

The exact solution to this equation for $n = 1$ is easily found as

$$\theta\,(\xi) = \frac{\sin\xi}{\xi}\,, \tag{12.26}$$

which gives the radius R_0 of the star by the condition $\theta\,(R_0) = 0$, i.e. $R_0 = \pi$, yielding

$$R_0 = \pi\sqrt{\frac{\hbar^2 a}{G_N m^3}}\,, \tag{12.27}$$

the condensate radius, which has been obtained in real units by using the definitions of κ and n. The mass of the object can then be obtained by integrating the density profile up to that point,

$$M = \frac{4}{\pi}\,R_0^3\,\rho_c = 4\pi^2\left(\frac{\hbar^2 a}{G_N m^3}\right)^{3/2}\rho_c\,, \tag{12.28}$$

where the condensate density at the center of the star ρ_c is yet undetermined. These results have been obtained in Ref. [115] and evaluated for the example of neutron stars. Note that for the previously derived case of $n = 3$, the mass limit was independent on the central

density, as can be inferred from Eq. (12.10). If however the dependence on the radius does not drop out of the expression, a dependence on the central density is inevitable. With a polytropic index $n = 1$, the maximum mass of the configuration thus depends on the central density. We will have to invoke alternative criteria to determine a limit on the central density, which will then yield a maximum mass. In Ref. [115] a limit on the central density was obtained by demanding that the adiabatic speed of sound in the fluid at the center of the star be bound by the speed of light. We will employ this criterion in our derivations as well, as elaborated further in Chapter 16.

We would like to note that the results for the equation of state can be used in more general versions of the theory, i.e. when extending the treatment to general relativistic settings. Perfect fluids can be described in Einstein's theory of General Relativity by an energy-momentum tensor $T^{\mu\nu}$ defined as

$$T^{\mu\nu} = \left(\rho + \frac{p}{c^2}\right) u^\mu u^\nu + p g^{\mu\nu} \,, \tag{12.29}$$

where ρ and p are the density and pressure of the fluid, respectively, and u^μ is the velocity vector field of the fluid. The stress-energy tensor enters the field equations on the right-hand side:

$$G^{\mu\nu} = \frac{8\pi G_N}{c^4} T^{\mu\nu} \,. \tag{12.30}$$

Together with the assumption of a spherically symmetric geometry, in general formulated as

$$ds^2 = e^{\nu(r)} c^2 dt^2 - \frac{dr^2}{1 - \frac{2G_N M(r)}{c^2 r}} - r^2 d\Omega^2 \,, \tag{12.31}$$

and the constraint on the metric function $\nu(r)$ obtained from the Einstein equations,

$$\frac{d\nu(r)}{dr} = -\left[\frac{2}{P(r) + \rho(r)c^2}\right] \frac{dP(r)}{dr} \,, \tag{12.32}$$

we obtain the Tolman-Oppenheimer-Volkoff equation [116, 117]

$$\frac{dP(r)}{dr} = -\frac{G_N \left[\rho(r) + \frac{P(r)}{c^2}\right] \left[\frac{4\pi P(r) r^3}{c^2} + M(r)\right]}{r^2 \left[1 - \frac{2G_N M(r)}{rc^2}\right]} \,. \tag{12.33}$$

Eq. (12.33) together with an equation of state $p = p(\rho)$ as e.g. given by (12.23), and the mass conservation equation

$$\frac{dM(r)}{dr} = 4\pi \rho(r)\, r^2 \tag{12.34}$$

completely determines the system. In this way, the equation of state extracted from the above procedure can be used in the context of general relativity as well. This has been done for the zero-temperature condensate in Ref. [115] in addition to the Newtonian case.

Alternatively, the equation of state might serve as an input parameter in astrophysical simulations on the subject which do not consider the physics inside the star from first principles but approach the issue on a more phenomenological level.

12.2. Finite-temperature case applied to Helium white dwarfs

In the work presented in this part of the thesis, we will take a generalized approach to the same issue, aiming at deriving a theory of a Bose-Einstein condensate subject to repulsive contact interactions and attractive gravitational interactions for the case of finite temperatures. This has been done in the framework of the Heisenberg equation in Ref. [136], where the field operator is split into a mean field contribution and a fluctuating term, i.e. $\hat{\Psi}(\mathbf{x},t) = \langle\hat{\Psi}(\mathbf{x},t)\rangle + \hat{\psi}(\mathbf{x},t)$. However, the authors solely calculated the equation of state of condensate and thermal density, and applied it to the example of dark matter, deriving the resulting expansion behaviour of the universe in a cosmological scenario. In our case, we will investigate the behaviour of a self-gravitating Bose-Einstein condensate in compact objects, compute the density profiles of a BEC star at finite temperatures and derive locally relevant quantities, which can then be compared to astrophysical observations.
To do so, we first need to determine the appropriate treatment for the scenario in question. One aspect to be reflected upon is the gravitational framework of the theory, i.e. the choice between Newtonian gravity and general relativity. Estimating the typical size scales of the system and comparing them to their corresponding Schwarzschild radii

$$r_S = \frac{2G_N M}{c^2} \tag{12.35}$$

shows whether the general relativistic regime is reached or Newtonian gravity suffices in the description of the gravitational interactions. Furthermore, we need to consider the typical velocities of particles in the system to be able to distinguish between non-relativistic and relativistic dispersion relations. From the typical temperatures in compact objects we can estimate the typical particle velocities from

$$v = \sqrt{\frac{2k_B T}{m}}\,, \tag{12.36}$$

and a comparison with the speed of light will determine the appropriate treatment. For $v << c$, we can resort to a non-relativistic quantum-mechanical treatment with a Schrödinger-type equation as outlined above, whereas for $v \sim c$, it would be necessary to formulate the theory in terms of a relativistic generalization described by a Klein-Gordon equation.

Table 12.2.: Estimates for the ratio of in different compact objects.

scenario	r_{typ}/r_S	v/c
^{4}He white dwarf	10^3	10^{-3}
neutron star (core)	2.7	10^{-1}
neutron star (crust)	2.7	10^{-3}

The ratios of typical radii to Schwarzschild radii and typical particle velocities to speed of light have been worked out for several examples in [142] and are shown in Tab. 12.2. We see that the case of ^{4}He white dwarfs is non-relativistic in both regards, i.e. Newtonian gravity and a non-relativistic energy dispersion provides a suitable description of the system. We will thus treat the system in the framework of a Hartree-Fock theory, and set up self-consistency governing equations for the densities of the BEC and the thermal cloud of excited atoms outside the condensate. We will start from a general Hamiltonian and derive the governing Hartree-Fock equations for the wave functions of the particles in the ground state and in the thermally excited states in Chapter 13. Still for the general case of a Hamiltonian with unspecified interactions $U(\mathbf{x}, \mathbf{x}')$ we will consider the semi-classical limit of the theory and derive the equations for the macroscopic densities of condensate and thermal excitations in Chapter 14. In Chapter 15 we will evaluate the previously obtained expressions for the case of contact and gravitational interactions, and derive the final equations which have to be solved for the densities. We will show the numerical solution of the system of equations in Chapter 16, and then derive astrophysical consequences and quantities like the total mass of the system, size scales and the equation of state of matter inside the star. We will investigate the physical viability of the system and obtain a similar criterion for the maximally possible masses as the Chandrasekhar limit. In Chapter 17 ultimately, we will comment on the significance of our work in the astrophysical context and conclude the part with a concise outlook.

13. Hartree-Fock theory for bosons

In this chapter, we will introduce the basis for our computations and derive the Hartree-Fock theory at finite temperatures for a generic system of bosons, employing the formalism of the grand-canonical ensemble and its definition of the free energy. By means of a variational principle we will then derive the governing equations of the system, i.e. a set of coupled equations of motion for the wave functions of both condensate and thermal fluctuations.

13.1. Free energy

The Hartree-Fock theory for bosons [143] starts from defining the second-quantized Hamiltonian operator,

$$\hat{\mathcal{H}} = \int d^3x\, \hat{\Psi}^\dagger(\mathbf{x}) \left[h(\mathbf{x}) - \mu + \frac{1}{2} \int d^3x'\, \hat{\Psi}^\dagger(\mathbf{x}') U(\mathbf{x}, \mathbf{x}') \hat{\Psi}(\mathbf{x}') \right] \hat{\Psi}(\mathbf{x}) \,, \tag{13.1}$$

where the first-quantized Hamiltonian operator $h(\mathbf{x})$ is defined as the kinetic term plus an external potential,

$$h(\mathbf{x}) = -\frac{\hbar^2}{2m}\Delta + V(\mathbf{x}) \,, \tag{13.2}$$

and the interaction term $U(\mathbf{x}, \mathbf{x}')$ will be specified later to the interactions present in our system. In this expression, the field operators $\hat{\Psi}^\dagger$ and $\hat{\Psi}$ obey the usual commutator relations for bosonic particles,

$$\left[\hat{\Psi}^\dagger(\mathbf{x}), \hat{\Psi}^\dagger(\mathbf{x}') \right] = \left[\hat{\Psi}(\mathbf{x}), \hat{\Psi}(\mathbf{x}') \right] = 0 \,, \tag{13.3a}$$

$$\left[\hat{\Psi}(\mathbf{x}), \hat{\Psi}^\dagger(\mathbf{x}') \right] = \delta(\mathbf{x} - \mathbf{x}') \,. \tag{13.3b}$$

The grand-canonical formalism defines the partition function Z as

$$Z = e^{-\beta F} = \mathrm{Tr} \left[e^{-\beta \hat{\mathcal{H}}} \right] \,, \tag{13.4}$$

where F is the free energy of the system, $\beta = 1/k_\mathrm{B}T$ is the inverse temperature and the trace in the expression has to be taken over all states of the Fock space.
We now derive the equations that govern the state of the field operators. To this purpose, we introduce a for now unknown one-particle basis $\Psi_\mathbf{n}(\mathbf{x})$ characterized by discrete quantum

numbers $\mathbf{n}$, and write the field operator as an expansion with respect to these functions $\Psi_{\mathbf{n}}(\mathbf{x})$ as

$$\hat{\Psi}(\mathbf{x}) = \sum_{\mathbf{n}} \hat{a}_{\mathbf{n}} \Psi_{\mathbf{n}}(\mathbf{x}) \,, \tag{13.5}$$

$$\hat{\Psi}^{\dagger}(\mathbf{x}) = \sum_{\mathbf{n}} \hat{a}^{\dagger}_{\mathbf{n}} \Psi^{*}_{\mathbf{n}}(\mathbf{x}) \,. \tag{13.6}$$

The expansion coefficients $\hat{a}^{\dagger}_{\mathbf{n}}$ and $\hat{a}_{\mathbf{n}}$ represent the creation and annihilation operators of a particle with the quantum number $\mathbf{n}$, and they obey similar commutator relations as the field operators $\hat{\Psi}^{\dagger}$ and $\hat{\Psi}$ above. The one-particle basis is chosen to be orthonormal and thus

$$\int d^3x \, \Psi^{*}_{\mathbf{n}}(\mathbf{x}) \Psi_{\mathbf{n}'}(\mathbf{x}) = \delta_{\mathbf{n},\mathbf{n}'} \,, \tag{13.7}$$

$$\sum_{\mathbf{n}} \Psi^{*}_{\mathbf{n}}(\mathbf{x}) \Psi_{\mathbf{n}}(\mathbf{x}') = \delta(\mathbf{x} - \mathbf{x}') \tag{13.8}$$

hold. We can then write the Hamiltonian operator (13.1) in terms of these creation and annihilation operators as

$$\hat{\mathcal{H}} = \sum_{\mathbf{n}} \sum_{\mathbf{n}'} E_{\mathbf{n},\mathbf{n}'} \, \hat{a}^{\dagger}_{\mathbf{n}} \hat{a}_{\mathbf{n}'} + \frac{1}{2} \sum_{\mathbf{n}} \sum_{\mathbf{m}} \sum_{\mathbf{m}'} \sum_{\mathbf{n}'} U_{\mathbf{n},\mathbf{m},\mathbf{m}',\mathbf{n}'} \, \hat{a}^{\dagger}_{\mathbf{n}} \hat{a}^{\dagger}_{\mathbf{m}} \hat{a}_{\mathbf{m}'} \hat{a}_{\mathbf{n}'} \,, \tag{13.9}$$

where

$$E_{\mathbf{n},\mathbf{n}'} = \int d^3x \, \Psi^{*}_{\mathbf{n}}(\mathbf{x}) \left[h(\mathbf{x}) - \mu \right] \Psi_{\mathbf{n}'}(\mathbf{x}) \,, \tag{13.10}$$

$$U_{\mathbf{n},\mathbf{m},\mathbf{m}',\mathbf{n}'} = \int d^3x \int d^3x' \, \Psi^{*}_{\mathbf{n}}(\mathbf{x}) \Psi^{*}_{\mathbf{m}}(\mathbf{x}') \, U(\mathbf{x},\mathbf{x}') \, \Psi_{\mathbf{m}'}(\mathbf{x}') \Psi_{\mathbf{n}'}(\mathbf{x}) \,. \tag{13.11}$$

To treat the system further, we suppose the existence of an effective Hamiltonian $\hat{\mathcal{H}}_{\text{eff}}$ describing the system as effectively non-interacting with one-particle energies $\epsilon_{\mathbf{n}}$, i.e.

$$\hat{\mathcal{H}}_{\text{eff}} = \sum_{\mathbf{n}} \left(\epsilon_{\mathbf{n}} - \mu \right) \hat{a}^{\dagger}_{\mathbf{n}} \hat{a}_{\mathbf{n}} \,. \tag{13.12}$$

Thus, the system is formulated in terms of an unknown one-particle basis $\Psi_{\mathbf{n}}(\mathbf{x})$ with unknown one-particle energies $\epsilon_{\mathbf{n}}$. These quantities have been artificially introduced, which means that in the end the result should not depend on them. Inspired by variational perturbation theory [48, 51], we now express the real Hamiltonian in terms of the effective Hamiltonian and an additional parameter η as

$$\hat{\mathcal{H}}(\eta) = \hat{\mathcal{H}}_{\text{eff}} + \eta \left(\hat{\mathcal{H}} - \hat{\mathcal{H}}_{\text{eff}} \right) \,. \tag{13.13}$$

If $\hat{\mathcal{H}}_{\text{eff}}$ is a good approximation for the real Hamiltonian $\hat{\mathcal{H}}$, then the second term is small, and the grand-canonical partition function can be expanded into a Taylor series with respect

to the difference of the two Hamiltonians. In the end, we have to set $\eta = 1$ in order to obtain a valid identity in Eq. (13.13).
Using relation (13.13), the partition function (13.4) can be written as

$$Z(\eta) = \mathrm{Tr}\left\{ e^{-\beta\left[\hat{\mathcal{H}}_{\mathrm{eff}} + \eta\left(\hat{\mathcal{H}} - \hat{\mathcal{H}}_{\mathrm{eff}}\right)\right]} \right\} . \tag{13.14}$$

Expanding this expression into a Taylor series with respect to the assumed smallness of $\hat{\mathcal{H}} - \hat{\mathcal{H}}_{\mathrm{eff}}$ leads to

$$\begin{aligned} Z(\eta) &= \mathrm{Tr}\left[e^{-\beta\hat{\mathcal{H}}_{\mathrm{eff}}}\right] + (-\beta\eta)\ \mathrm{Tr}\left[\left(\hat{\mathcal{H}} - \hat{\mathcal{H}}_{\mathrm{eff}}\right) e^{-\beta\hat{\mathcal{H}}_{\mathrm{eff}}}\right] \\ &\quad + \frac{1}{2}\left(-\beta\eta\right)^2\ \mathrm{Tr}\left[\left(\hat{\mathcal{H}} - \hat{\mathcal{H}}_{\mathrm{eff}}\right)^2 e^{-\beta\hat{\mathcal{H}}_{\mathrm{eff}}}\right] + \dots . \end{aligned} \tag{13.15}$$

After defining the notions of the effective partition function

$$Z_{\mathrm{eff}} = \mathrm{Tr}\left[e^{-\beta\hat{\mathcal{H}}_{\mathrm{eff}}}\right] \tag{13.16}$$

and the effective expectation value of an operator $\hat{X}$ as

$$\langle \hat{X} \rangle_{\mathrm{eff}} = \frac{1}{Z_{\mathrm{eff}}} \mathrm{Tr}\left[\hat{X}\, e^{-\beta\hat{\mathcal{H}}_{\mathrm{eff}}}\right] , \tag{13.17}$$

we can rewrite the expansion of the partition function as

$$Z(\eta) = Z_{\mathrm{eff}}\ \left[1 + (-\beta\eta)\,\langle\left(\hat{\mathcal{H}} - \hat{\mathcal{H}}_{\mathrm{eff}}\right)\rangle_{\mathrm{eff}} + \frac{1}{2}\left(-\beta\eta\right)^2 \langle\left(\hat{\mathcal{H}} - \hat{\mathcal{H}}_{\mathrm{eff}}\right)^2\rangle_{\mathrm{eff}} + \dots\right] . \tag{13.18}$$

This is an expansion in terms of the moments, i.e. for the n^{th} order in the expansion the n^{th} power of the effective expectation value of $\left(\hat{\mathcal{H}} - \hat{\mathcal{H}}_{\mathrm{eff}}\right)$ appears. The free energy

$$F(\eta) = -\frac{1}{\beta} \ln Z(\eta) \tag{13.19}$$

can then be written as

$$F(\eta) = F_{\mathrm{eff}} - \frac{1}{\beta} \ln\left\{1 - \beta\eta\,\langle\left(\hat{\mathcal{H}} - \hat{\mathcal{H}}_{\mathrm{eff}}\right)\rangle_{\mathrm{eff}} + \frac{1}{2}\,\beta^2\eta^2 \langle\left(\hat{\mathcal{H}} - \hat{\mathcal{H}}_{\mathrm{eff}}\right)^2\rangle_{\mathrm{eff}} + \dots\right\} , \tag{13.20}$$

with the effective free energy defined as

$$F_{\mathrm{eff}} = -\frac{1}{\beta} \ln Z_{\mathrm{eff}} . \tag{13.21}$$

We can then employ the Taylor expansion of the logarithm,

$$\ln(1 + z) = z - \frac{1}{2}\, z^2 + \dots \tag{13.22}$$

to expand the free energy into a series as

$$F(\eta) = F_{\text{eff}} + \eta \left\langle \left(\hat{\mathcal{H}} - \hat{\mathcal{H}}_{\text{eff}} \right) \right\rangle_{\text{eff}} - \frac{1}{2} \beta \eta^2 \left[\left\langle \left(\hat{\mathcal{H}} - \hat{\mathcal{H}}_{\text{eff}} \right)^2 \right\rangle_{\text{eff}} - \left\langle \left(\hat{\mathcal{H}} - \hat{\mathcal{H}}_{\text{eff}} \right) \right\rangle_{\text{eff}}^2 \right] + \dots . \quad (13.23)$$

This expression is now an expansion using the so-called cumulants, i.e. the n^{th} order of the expansion contains the n^{th} power of the effective expectation value of $\left(\hat{\mathcal{H}} - \hat{\mathcal{H}}_{\text{eff}} \right)$ and the effective expectation value of the n^{th} power of $\left(\hat{\mathcal{H}} - \hat{\mathcal{H}}_{\text{eff}} \right)$. For the further course of the calculations, we will approximate the expression of the free energy by cutting off the series after the first-order term. In order to obtain the original free energy, we have to set $\eta = 1$, which leads to

$$F^{(1)}(1) = F_{\text{eff}} + \left\langle \left(\hat{\mathcal{H}} - \hat{\mathcal{H}}_{\text{eff}} \right) \right\rangle_{\text{eff}} . \quad (13.24)$$

As the unknown one-particle basis $\Psi_{\mathbf{n}}(\mathbf{x})$ and energies $\epsilon_{\mathbf{n}}$ have been introduced artificially into the analysis, the result for the free energy should not depend on them. This is however only true for the exact expressions for F, and doesn't hold for the approximated form that we will use in the further analysis. That means $F^{(1)}(1)$ does indeed depend on the one-particle basis and energies, but this dependence is unphysical and undesired. For this reason, we have to demand that the dependence of $F^{(1)}(1)$ on these quantities be as small as possible - which mathematically corresponds to an extremization, i.e. we require that

$$\frac{\delta F^{(1)}(1)}{\delta \Psi^*_{\mathbf{n}}(\mathbf{x})} = 0 = \frac{\delta F^{(1)}(1)}{\delta \Psi_{\mathbf{n}}(\mathbf{x})} , \qquad \frac{\partial F^{(1)}(1)}{\partial \epsilon_{\mathbf{n}}} = 0 . \quad (13.25)$$

This is the principle of minimal sensitivity, which was firstly introduced in Ref. [144]. We can further evaluate the free energy $F^{(1)}(1)$ by inserting the original and effective Hamiltonians and taking the effective expectation value of the occurring operators, to result in

$$\begin{aligned} F^{(1)}(1) \;=\; & F_{\text{eff}} + \sum_{\mathbf{n}} \sum_{\mathbf{n}'} \left[E_{\mathbf{n},\mathbf{n}'} - (\epsilon_{\mathbf{n}} - \mu)\, \delta_{\mathbf{n},\mathbf{n}'} \right] \langle \hat{a}^\dagger_{\mathbf{n}} \hat{a}_{\mathbf{n}'} \rangle_{\text{eff}} \\ & + \frac{1}{2} \sum_{\mathbf{n}} \sum_{\mathbf{m}} \sum_{\mathbf{m}'} \sum_{\mathbf{n}'} U_{\mathbf{n},\mathbf{m},\mathbf{m}',\mathbf{n}'} \langle \hat{a}^\dagger_{\mathbf{n}} \hat{a}^\dagger_{\mathbf{m}} \hat{a}_{\mathbf{m}'} \hat{a}_{\mathbf{n}'} \rangle_{\text{eff}} . \end{aligned} \quad (13.26)$$

We now process the effective expectation values further by applying the Wick rule [145]. For the four-point correlation function in the interaction term, this leads to the decomposition into products of two-point correlation functions as

$$\langle \hat{a}^\dagger_{\mathbf{n}} \hat{a}^\dagger_{\mathbf{m}} \hat{a}_{\mathbf{m}'} \hat{a}_{\mathbf{n}'} \rangle_{\text{eff}} = \left(\delta_{\mathbf{n},\mathbf{n}'} \delta_{\mathbf{m},\mathbf{m}'} + \delta_{\mathbf{n},\mathbf{m}'} \delta_{\mathbf{m},\mathbf{n}'} \right) \langle \hat{a}^\dagger_{\mathbf{n}} \hat{a}_{\mathbf{n}} \rangle_{\text{eff}} \langle \hat{a}^\dagger_{\mathbf{m}} \hat{a}_{\mathbf{m}} \rangle_{\text{eff}} . \quad (13.27)$$

From the investigation of the effective free energy, we can deduce a concrete expression for the two-point function that we are now left with. The effective free energy reads

$$F_{\text{eff}} = -\frac{1}{\beta} \ln \text{Tr} \left[e^{-\beta \sum_{\mathbf{n}} (\epsilon_{\mathbf{n}} - \mu)\, \hat{a}^\dagger_{\mathbf{n}} \hat{a}_{\mathbf{n}}} \right] , \quad (13.28)$$

which can be processed using the definition of the geometric series to

$$F_{\text{eff}} = \frac{1}{\beta} \sum_{\mathbf{n}} \ln \left[1 - e^{-\beta(\epsilon_{\mathbf{n}} - \mu)} \right] . \tag{13.29}$$

Differentiating both versions (13.28), (13.29) of F_{eff} with respect to the energies $\epsilon_{\mathbf{n}}$ leads to an identity for the expectation value of the two-point function,

$$\langle \hat{a}^\dagger_{\mathbf{n}} \hat{a}_{\mathbf{n}} \rangle_{\text{eff}} = \frac{1}{e^{\beta(\epsilon_{\mathbf{n}} - \mu)} - 1} , \tag{13.30}$$

i.e. the Bose-Einstein distribution function.
We now introduce by hand the macroscopic occupation of the ground state, which is the predominant attribute of Bose-Einstein-condensation, by setting

$$\hat{a}^\dagger_{\mathbf{0}} \simeq \hat{a}_{\mathbf{0}} \simeq \sqrt{N_{\mathbf{0}}} = \psi , \tag{13.31}$$

with $N_{\mathbf{0}}$ being the total number of particles in the ground state, i.e. with quantum number $\mathbf{n} = \mathbf{0}$. We will now split all the terms into the $\mathbf{n} = \mathbf{0}$ and the $\mathbf{n} \neq \mathbf{0}$ contributions, and introduce a condensate wave function as

$$\Psi(\mathbf{x}) = \psi \, \Psi_{\mathbf{0}}(\mathbf{x}), \quad \Psi^*(\mathbf{x}) = \psi \, \Psi^*_{\mathbf{0}}(\mathbf{x}) . \tag{13.32}$$

This wave function has the normalization

$$\int d^3x \, \Psi^*(\mathbf{x}) \Psi(\mathbf{x}) = \psi^2 \int d^3x \, \Psi^*_{\mathbf{0}}(\mathbf{x}) \Psi_{\mathbf{0}}(\mathbf{x}) = \psi^2 = N_{\mathbf{0}} . \tag{13.33}$$

Under consideration of the small detail that the four-point correlation function as processed in Eq. (13.27) by the Wick rule, has to be modified for the condensate as

$$\langle \hat{a}^\dagger_{\mathbf{0}} \hat{a}^\dagger_{\mathbf{0}} \hat{a}_{\mathbf{0}} \hat{a}_{\mathbf{0}} \rangle_{\text{eff}} = \psi^4 , \tag{13.34}$$

and inserting the normalization

$$1 = \int d^3x \, \Psi^*_{\mathbf{n}}(\mathbf{x}) \Psi_{\mathbf{n}}(\mathbf{x}) \tag{13.35}$$

into the effective free energy, we have as a result

$$\begin{aligned} F^{(1)}(1) \;=\; & F_{\text{eff}} + \left[E_{\mathbf{0},\mathbf{0}} - (\epsilon_{\mathbf{0}} - \mu) \int d^3x \, \Psi^*_{\mathbf{0}}(\mathbf{x}) \Psi_{\mathbf{0}}(\mathbf{x}) \right] \psi^2 \\ & + \sum_{\mathbf{n} \neq \mathbf{0}} \left[E_{\mathbf{n},\mathbf{n}} - (\epsilon_{\mathbf{n}} - \mu) \int d^3x \, \Psi^*_{\mathbf{n}}(\mathbf{x}) \Psi_{\mathbf{n}}(\mathbf{x}) \right] \langle \hat{a}^\dagger_{\mathbf{n}} \hat{a}_{\mathbf{n}} \rangle_{\text{eff}} \\ & + \frac{1}{2} U_{\mathbf{0},\mathbf{0},\mathbf{0},\mathbf{0}} \, \psi^4 + \sum_{\mathbf{n} \neq \mathbf{0}} \left(U_{\mathbf{n},\mathbf{0},\mathbf{0},\mathbf{n}} + U_{\mathbf{n},\mathbf{0},\mathbf{n},\mathbf{0}} \right) \psi^2 \langle \hat{a}^\dagger_{\mathbf{n}} \hat{a}_{\mathbf{n}} \rangle_{\text{eff}} \\ & + \frac{1}{2} \sum_{\mathbf{n} \neq \mathbf{0}} \sum_{\mathbf{m} \neq \mathbf{0}} \left(U_{\mathbf{n},\mathbf{m},\mathbf{m},\mathbf{n}} + U_{\mathbf{n},\mathbf{m},\mathbf{n},\mathbf{m}} \right) \langle \hat{a}^\dagger_{\mathbf{n}} \hat{a}_{\mathbf{n}} \rangle_{\text{eff}} \langle \hat{a}^\dagger_{\mathbf{m}} \hat{a}_{\mathbf{m}} \rangle_{\text{eff}} , \end{aligned} \tag{13.36}$$

where $F_{\rm eff}$ now consists of the two terms

$$F_{\rm eff} = (\epsilon_{\mathbf{0}} - \mu)\,\psi^2 + \frac{1}{\beta}\sum_{\mathbf{n}\neq\mathbf{0}} \ln\left[1 - e^{-\beta(\epsilon_{\rm n}-\mu)}\right] . \tag{13.37}$$

Introducing the expressions for $E_{\mathbf{n},\mathbf{n}'}$ and $U_{\mathbf{n},\mathbf{m},\mathbf{m}',\mathbf{n}'}$ as defined in Eq. (13.10) and (13.11), we can now write the total free energy, which will in the following be denoted shortly by F, as

$$\begin{aligned} F \;=\; & F_{\rm eff} + \int d^3x\, \Psi^*(\mathbf{x})\,[h(\mathbf{x}) - \mu]\,\Psi(\mathbf{x}) - (\epsilon_{\mathbf{0}} - \mu)\int d^3x\, \Psi^*(\mathbf{x})\Psi(\mathbf{x}) \\ & + \sum_{\mathbf{n}\neq\mathbf{0}} \left\{ \int d^3x\, \Psi^*_{\mathbf{n}}(\mathbf{x})\,[h(\mathbf{x}) - \mu]\,\Psi_{\mathbf{n}}(\mathbf{x}) - (\epsilon_{\mathbf{n}} - \mu)\int d^3x\, \Psi^*_{\mathbf{n}}(\mathbf{x})\Psi_{\mathbf{n}}(\mathbf{x}) \right\} \langle \hat{a}^+_{\mathbf{n}}\hat{a}_{\mathbf{n}}\rangle_{\rm eff} \\ & + \frac{1}{2}\int d^3x d^3x'\, \Psi^*(\mathbf{x})\Psi^*(\mathbf{x}')\,U(\mathbf{x},\mathbf{x}')\,\Psi(\mathbf{x}')\Psi(\mathbf{x}) \\ & + \sum_{\mathbf{n}\neq\mathbf{0}} \int d^3x d^3x'\, \Psi^*_{\mathbf{n}}(\mathbf{x})\Psi^*(\mathbf{x}')\,U(\mathbf{x},\mathbf{x}') \left[\Psi(\mathbf{x}')\Psi_{\mathbf{n}}(\mathbf{x}) + \Psi_{\mathbf{n}}(\mathbf{x}')\Psi(\mathbf{x})\right] \langle \hat{a}^+_{\mathbf{n}}\hat{a}_{\mathbf{n}}\rangle_{\rm eff} \\ & + \frac{1}{2}\sum_{\mathbf{n}\neq\mathbf{0}}\sum_{\mathbf{m}\neq\mathbf{0}} \int d^3x d^3x' \Big[\Psi^*_{\mathbf{n}}(\mathbf{x})\Psi^*_{\mathbf{m}}(\mathbf{x}')\,U(\mathbf{x},\mathbf{x}')\,\Psi_{\mathbf{m}}(\mathbf{x}')\Psi_{\mathbf{n}}(\mathbf{x}) \\ & \qquad + \Psi^*_{\mathbf{n}}(\mathbf{x})\Psi^*_{\mathbf{m}}(\mathbf{x}')\,U(\mathbf{x},\mathbf{x}')\,\Psi_{\mathbf{n}}(\mathbf{x}')\Psi_{\mathbf{m}}(\mathbf{x})\Big] \langle \hat{a}^+_{\mathbf{n}}\hat{a}_{\mathbf{n}}\rangle_{\rm eff}\, \langle \hat{a}^+_{\mathbf{m}}\hat{a}_{\mathbf{m}}\rangle_{\rm eff} . \end{aligned} \tag{13.38}$$

In this theory, the condensate wave function encodes the behaviour of the particles in the condensate, i.e. a majority of particles in the system for low enough temperatures, while the wave functions with $\mathbf{n} \neq \mathbf{0}$ describe the thermal fluctuations on top of the condensate with increasing quantum numbers $\mathbf{n}$.

13.2. Equations of Motion

The Hartree-Fock equations of motion can be obtained by varying the free energy (13.38) with respect to the condensate and thermal wave functions $\Psi^*(\mathbf{x})$ and $\Psi^*_{\mathbf{n}}(\mathbf{x})$; furthermore we have the particle number equation from the derivation of F with respect to the chemical potential. These equations read

$$\frac{\delta F}{\delta\Psi^*(\mathbf{x})} = \frac{\delta F}{\delta\Psi^*_{\mathbf{n}}(\mathbf{x})} = 0\,, \quad \frac{\partial F}{\partial\epsilon_{\mathbf{n}}} = 0\,, \quad -\frac{\partial F}{\partial\mu} = N\,, \tag{13.39}$$

with the densities of condensate and thermal fluctuations defined as

$$n_{\mathbf{0}}(\mathbf{x}) = |\Psi(\mathbf{x})|^2\,, \quad n_{\rm th}(\mathbf{x},\mathbf{x}') = \sum_{\mathbf{n}\neq\mathbf{0}} \frac{\Psi^*_{\mathbf{n}}(\mathbf{x})\,\Psi_{\mathbf{n}}(\mathbf{x}')}{e^{\beta(\epsilon_{\mathbf{n}}-\mu)} - 1}\,. \tag{13.40}$$

For equal arguments of the thermal density, we will use the abbreviation

$$n_{\rm th}(\mathbf{x},\mathbf{x}) \to n_{\rm th}(\mathbf{x})\,. \tag{13.41}$$

Now we will derive the Hartree-Fock equations and the derivative of the free energy with respect to the energies $\epsilon_{\mathbf{n}}$ and the chemical potential.

- The variation of the free energy with respect to the condensate wave function leads to the equation

$$\frac{\delta F}{\delta \Psi^*(\mathbf{x})} = \left[h(\mathbf{x}) - \mu\right] \Psi(\mathbf{x}) + \int d^3\mathbf{x}'\, U(\mathbf{x},\mathbf{x}') \Big\{ \left[n_{\mathbf{0}}(\mathbf{x}') + n_{\rm th}(\mathbf{x}')\right] \Psi(\mathbf{x}) + n_{\rm th}(\mathbf{x}',\mathbf{x}) \Psi(\mathbf{x}') \Big\} = 0\,. \tag{13.42}$$

- The variation of F with respect to the thermal wave functions leads to the equation

$$\frac{\delta F}{\delta \Psi^*_{\mathbf{n}}(\mathbf{x})} = \left[h(\mathbf{x}) - \epsilon_{\mathbf{n}}\right] \Psi_{\mathbf{n}}(\mathbf{x}) + \int d^3\mathbf{x}'\, U(\mathbf{x},\mathbf{x}') \Big\{ \left[n_{\mathbf{0}}(\mathbf{x}') + n_{\rm th}(\mathbf{x}')\right] \Psi_{\mathbf{n}}(\mathbf{x}) + \left[\Psi^*(\mathbf{x}')\Psi(\mathbf{x}) + n_{\rm th}(\mathbf{x}',\mathbf{x})\right] \Psi_{\mathbf{n}}(\mathbf{x}') \Big\} = 0\,. \tag{13.43}$$

In these two equations, the first, local part of the interaction are referred to as Hartree terms, or direct interaction terms, whereas the second, bilocal parts are the Fock terms, or exchange interaction terms.

- The derivation of the free energy with respect to the energies $\epsilon_{\mathbf{n}}$ leads to the already known identity (13.30) for the expectation value of the two-point correlation function of the creator and annihilator operators,

$$\frac{\partial F}{\partial \epsilon_{\mathbf{n}}} = \langle \hat{a}^\dagger_{\mathbf{n}} \hat{a}_{\mathbf{n}} \rangle_{\rm eff} - \frac{1}{e^{\beta(\epsilon_{\rm n} - \mu)} - 1} = 0\,. \tag{13.44}$$

- Finally, the negative derivative of the free energy with respect to the chemical potential recovers correctly the total number of particles in the system,

$$-\frac{\partial F}{\partial \mu} = \int d^3\mathbf{x}\, \left[n_{\mathbf{0}}(\mathbf{x}) + n_{\rm th}(\mathbf{x})\right] = N\,. \tag{13.45}$$

In order to solve these Hartree-Fock equations, we will consider the semi-classical approximation in the subsequent chapter.

14. Semi-classical Hartree-Fock theory

In this section we will consider the free energy functional given by Eq. (13.38), and try to find the physical state of the system by identifying its minimum. Instead of using the wave functions of condensate and thermal fluctuations, we will pursue a different approach here and define the densities of condensate and thermal cloud in the semi-classical limit as the basic variables instead. Let us thus first take the semi-classical limit of the free energy, introducing both condensate and thermal density instead of the wave functions, and then check whether it is possible to derive the correct Hartree-Fock equations by variation of the semi-classical free energy with respect to the densities. We will introduce this method in this chapter for a general case with an external potential $V(\mathbf{x})$ and an interaction $U(\mathbf{x}, \mathbf{x}')$, and then investigate the special case of a star with contact and gravitational interaction in the next chapter.

In the semi-classical approximation we use plane waves as an ansatz for the thermal wave functions, i.e. $\Psi_{\mathbf{n}}(\mathbf{x}) \to \Psi_{\mathbf{k}}(\mathbf{x}) = e^{i\mathbf{k}\mathbf{x}}$, so the discrete energies $\epsilon_{\mathbf{n}}$ become the local dispersions $\epsilon_{\mathbf{k}}(\mathbf{x})$, as well as the Thomas-Fermi approximation for the condensate, which means neglecting the Laplace term for the condensate wave functions. In addition, the sums over $\mathbf{n}$ are replaced by integrals in $\mathbf{k}$-space, which changes the thermal density in (13.40) to

$$n_{\rm th}(\mathbf{x}) = \int \frac{d^3k}{(2\pi)^3} \, \frac{1}{e^{\beta[\epsilon_{\mathbf{k}}(\mathbf{x})-\mu]} - 1} =: \int \frac{d^3k}{(2\pi)^3} \, n_{\rm th}(\mathbf{x}, \mathbf{k}) \, . \tag{14.1}$$

Here we have defined the thermal Wigner quasiprobability $n_{\rm th}(\mathbf{x}, \mathbf{k})$, which will become the variational parameter instead of the thermal density itself.

Arguing that the free energy is an extensive quantity, one can introduce a spatial integral d^3x into the first term of Eq. (13.38). Applying all the prescriptions above, the semi-classical free energy $F_{\rm SC}$ then reads

$$\begin{aligned} F_{\rm SC} \;=\; & \frac{1}{\beta} \int d^3x \int \frac{d^3k}{(2\pi)^3} \, \ln\left\{1 - e^{-\beta[\epsilon_{\mathbf{k}}(\mathbf{x})-\mu]}\right\} + \int d^3x \, \left[V(\mathbf{x}) - \mu\right] n_{\mathbf{0}}(\mathbf{x}) \\ & + \int d^3x \int \frac{d^3k}{(2\pi)^3} \, \left[\frac{\hbar^2\mathbf{k}^2}{2m} + V(\mathbf{x}) - \epsilon_{\mathbf{k}}(\mathbf{x})\right] n_{\rm th}(\mathbf{x}, \mathbf{k}) \\ & + \int d^3x d^3x' \, U(\mathbf{x}, \mathbf{x}') \left[\frac{1}{2} \, n_{\mathbf{0}}(\mathbf{x}) \, n_{\mathbf{0}}(\mathbf{x}') + n_{\mathbf{0}}(\mathbf{x}') \, n_{\rm th}(\mathbf{x}) \right. \\ & \left. + \sqrt{n_{\mathbf{0}}(\mathbf{x}') n_{\mathbf{0}}(\mathbf{x})} \, n_{\rm th}(\mathbf{x}, \mathbf{x}') + \frac{1}{2} \, n_{\rm th}(\mathbf{x}) \, n_{\rm th}(\mathbf{x}') + \frac{1}{2} n_{\rm th}(\mathbf{x}, \mathbf{x}') \, n_{\rm th}(\mathbf{x}', \mathbf{x})\right] . \end{aligned} \tag{14.2}$$

14.1. Semi-classical Hartree-Fock equations

Let us derive the semi-classical Hartree-Fock equations by variation of $F_{\rm SC}$ with respect to the densities and the chemical potential.

- The variation of $F_{\rm SC}$ with respect to the condensate density $n_{\mathbf{0}}(\mathbf{x})$ yields

$$\begin{aligned}\frac{\delta F_{\rm SC}}{\delta n_{\mathbf{0}}(\mathbf{x})} &= V(\mathbf{x}) - \mu + \int d^3x'\, U(\mathbf{x},\mathbf{x}') \Big[n_{\mathbf{0}}(\mathbf{x}') + n_{\rm th}(\mathbf{x}') \Big] \\ &\quad + \frac{1}{2} \int d^3x'\, U(\mathbf{x},\mathbf{x}') \sqrt{\frac{n_{\mathbf{0}}(\mathbf{x}')}{n_{\mathbf{0}}(\mathbf{x})}} \Big[n_{\rm th}(\mathbf{x}',\mathbf{x}) + n_{\rm th}(\mathbf{x},\mathbf{x}') \Big] . \end{aligned} \tag{14.3}$$

  Considering a multiplication with the wave function $\Psi(\mathbf{x}) \equiv \sqrt{n_{\mathbf{0}}(\mathbf{x})}$, this correctly corresponds to the Hartree-Fock equation for the condensate (13.42) in the Thomas-Fermi-approximation.

- The variation of $F_{\rm SC}$ with respect to the thermal quasiprobability $n_{\rm th}(\mathbf{x},\mathbf{k})$ requires some more thoughts, as we first have to define the Wigner quasiprobability function for the bilocal thermal density. Generalizing the notion (14.1) straightforwardly for different arguments $\mathbf{x},\mathbf{x}'$, we get from (13.40)

$$n_{\rm th}(\mathbf{x},\mathbf{x}') \to n_{\rm th}(\mathbf{R},\mathbf{s}) = \int \frac{d^3k}{(2\pi)^3} \frac{e^{-i\mathbf{k}\mathbf{s}}}{e^{\beta[\epsilon_{\mathbf{k}}(\mathbf{R})-\mu]}-1} =: \int \frac{d^3k}{(2\pi)^3}\, e^{-i\mathbf{k}\mathbf{s}}\, n_{\rm th}(\mathbf{R},\mathbf{s},\mathbf{k}) , \tag{14.4}$$

  where we have adapted the center-of-mass coordinate $\mathbf{R} = (\mathbf{x}+\mathbf{x}')/2$ and the relative coordinate $\mathbf{s} = \mathbf{x}-\mathbf{x}'$ instead of $\mathbf{x}$ and $\mathbf{x}'$. This general definition is in accordance with the definition (14.1) for the local expression of the thermal density, since in the case $\mathbf{x} = \mathbf{x}'$ we have

$$n_{\rm th}(\mathbf{x},\mathbf{x}) \equiv n_{\rm th}(\mathbf{R},\mathbf{s}=\mathbf{0}) = \int \frac{d^3k}{(2\pi)^3} \frac{1}{e^{\beta[\epsilon_{\mathbf{k}}(\mathbf{R})-\mu]}-1} = \int \frac{d^3k}{(2\pi)^3}\, n_{\rm th}(\mathbf{R},\mathbf{k}) , \tag{14.5}$$

  which is identical with the Wigner quasiprobability defined in Eq. (14.1). The semi-

classical free energy (14.2) can be rewritten in terms of $\mathbf{R}$ and $\mathbf{s}$ as

$$\begin{aligned} F_{\rm SC} &= \frac{1}{\beta}\int d^3R \int \frac{d^3k}{(2\pi)^3}\,\ln\left\{1-e^{-\beta[\epsilon_{\mathbf{k}}(\mathbf{R})-\mu]}\right\} + \int d^3R\,[V(\mathbf{R})-\mu]\,n_{\mathbf{0}}(\mathbf{R}) \\ &+ \frac{1}{2}\int d^3Rd^3s\,U(\mathbf{s})\,n_{\mathbf{0}}\left(\mathbf{R}+\frac{\mathbf{s}}{2}\right)\,n_{\mathbf{0}}\left(\mathbf{R}-\frac{\mathbf{s}}{2}\right) \\ &+ \int d^3R \int \frac{d^3k}{(2\pi)^3}\,\left[\frac{\hbar^2\mathbf{k}^2}{2m}+V(\mathbf{R})-\epsilon_{\mathbf{k}}(\mathbf{R})\right] n_{\rm th}(\mathbf{R},\mathbf{k}) \\ &+ \int d^3Rd^3s \int \frac{d^3k}{(2\pi)^3}\,U(\mathbf{s})\left[n_{\mathbf{0}}\left(\mathbf{R}-\frac{\mathbf{s}}{2}\right)\,n_{\rm th}\left(\mathbf{R}+\frac{\mathbf{s}}{2}\right)\right. \\ &\qquad \left. +\sqrt{n_{\mathbf{0}}\left(\mathbf{R}+\frac{\mathbf{s}}{2}\right)n_{\mathbf{0}}\left(\mathbf{R}-\frac{\mathbf{s}}{2}\right)}\,n_{\rm th}(\mathbf{R},\mathbf{k})\,e^{-i\mathbf{ks}}\right] \\ &+ \frac{1}{2}\int d^3Rd^3s \int \frac{d^3kd^3k'}{(2\pi)^6}\,U(\mathbf{s})\left[n_{\rm th}\left(\mathbf{R}+\frac{\mathbf{s}}{2},\mathbf{k}\right)\,n_{\rm th}\left(\mathbf{R}-\frac{\mathbf{s}}{2},\mathbf{k}'\right)\right. \\ &\qquad \left. +e^{-i\mathbf{s}(\mathbf{k}-\mathbf{k}')}\,n_{\rm th}(\mathbf{R},\mathbf{k})\,n_{\rm th}(\mathbf{R},\mathbf{k}')\right]. \end{aligned} \tag{14.6}$$

The total variation of the free energy with respect to $n_{\rm th}(\mathbf{R},\mathbf{k})$ then reads

$$\begin{aligned} \frac{\delta F_{\rm SC}}{\delta n_{\rm th}(\mathbf{R},\mathbf{k})} &= \frac{\hbar^2\mathbf{k}^2}{2m}+V(\mathbf{R})-\epsilon_{\mathbf{k}}(\mathbf{R})+\int d^3s\,U(\mathbf{s})\,n_{\mathbf{0}}\left(\mathbf{R}-\frac{\mathbf{s}}{2}\right) \\ &+ \int d^3s\,U(\mathbf{s})\,e^{-i\mathbf{ks}}\sqrt{n_{\mathbf{0}}\left(\mathbf{R}+\frac{\mathbf{s}}{2}\right)n_{\mathbf{0}}\left(\mathbf{R}-\frac{\mathbf{s}}{2}\right)} \\ &+ \int d^3s \int \frac{d^3k'}{(2\pi)^3}\,U(\mathbf{s})\left[n_{\rm th}\left(\mathbf{R}-\frac{\mathbf{s}}{2},\mathbf{k}'\right)\right. \\ &\qquad \left. +e^{-i\mathbf{s}(\mathbf{k}-\mathbf{k}')}\,n_{\rm th}\left(\mathbf{R}+\frac{\mathbf{s}}{2},\mathbf{k}\right)\right] = 0\,. \end{aligned} \tag{14.7}$$

This yields the local dispersion of the thermal fluctuations in terms of $\mathbf{R}$ and $\mathbf{s}$ as

$$\begin{aligned} \epsilon_{\mathbf{k}}(\mathbf{R}) &= \frac{\hbar^2\mathbf{k}^2}{2m}+V(\mathbf{R})+\int d^3s\,U(\mathbf{s})\,n_{\mathbf{0}}\left(\mathbf{R}-\frac{\mathbf{s}}{2}\right) \\ &+ \int d^3s\,U(\mathbf{s})\,e^{-i\mathbf{ks}}\sqrt{n_{\mathbf{0}}\left(\mathbf{R}+\frac{\mathbf{s}}{2}\right)n_{\mathbf{0}}\left(\mathbf{R}-\frac{\mathbf{s}}{2}\right)} \\ &+ \int d^3s \int \frac{d^3k'}{(2\pi)^3}\,U(\mathbf{s})\left[n_{\rm th}\left(\mathbf{R}-\frac{\mathbf{s}}{2},\mathbf{k}'\right)+e^{-i\mathbf{s}(\mathbf{k}-\mathbf{k}')}\,n_{\rm th}\left(\mathbf{R}+\frac{\mathbf{s}}{2},\mathbf{k}\right)\right]. \end{aligned} \tag{14.8}$$

In terms of $\mathbf{x}$ and $\mathbf{x}'$ these local dispersions read

$$\begin{aligned} \epsilon_{\mathbf{k}}(\mathbf{x}) &= \frac{\hbar^2\mathbf{k}^2}{2m}+V(\mathbf{x})+\int d^3x'\,U(\mathbf{x},\mathbf{x}')\,n_{\mathbf{0}}(\mathbf{x}') \\ &+ \int d^3x'\,U(\mathbf{x},\mathbf{x}')\,e^{-i\mathbf{k}(\mathbf{x}-\mathbf{x}')}\sqrt{n_{\mathbf{0}}(\mathbf{x})\,n_{\mathbf{0}}(\mathbf{x}')} \\ &+ \int d^3x' \int \frac{d^3k'}{(2\pi)^3}\,U(\mathbf{x},\mathbf{x}')\left[n_{\rm th}(\mathbf{x}',\mathbf{k}')+e^{-i(\mathbf{x}-\mathbf{x}')(\mathbf{k}-\mathbf{k}')}\,n_{\rm th}(\mathbf{x},\mathbf{k}')\right]. \end{aligned} \tag{14.9}$$

- The derivation of $F_{\rm SC}$ with respect to the energies $\epsilon_{\mathbf{k}}(\mathbf{x})$ yields

$$\frac{\delta F_{\rm SC}}{\delta \epsilon_{\mathbf{k}}(\mathbf{x})} = \int d^3x' \int \frac{d^3k'}{(2\pi)^3} \left\{ \frac{1}{e^{\beta[\epsilon_{\mathbf{k}'}(\mathbf{x}')-\mu]}-1} - n_{\rm th}(\mathbf{x}',\mathbf{k}') \right\} \frac{\delta \epsilon_{\mathbf{k}'}(\mathbf{x}')}{\delta \epsilon_{\mathbf{k}}(\mathbf{x})} = 0\,, \qquad (14.10)$$

  which simply reconfirms the form of the function $n_{\rm th}(\mathbf{x},\mathbf{k})$ as introduced in Eq. (14.1).

- The derivation of $F_{\rm SC}$ with respect to the chemical potential μ

$$-\frac{\partial F_{\rm SC}}{\partial \mu} = \int d^3x \int \frac{d^3k}{(2\pi)^3} \frac{1}{e^{\beta[\epsilon_{\mathbf{k}}(\mathbf{x})-\mu]}-1} + N_{\mathbf{0}} \qquad (14.11)$$

  leads as expected again to the particle number equation,

$$\int d^3x \; [n_{\mathbf{0}}(\mathbf{x}) + n_{\rm th}(\mathbf{x})] = N\,. \qquad (14.12)$$

The fact that we obtained consistent equations from the variation of the semi-classical free energy with respect to the condensate and thermal density shows that the semi-classical limit was carried out correctly and conserves the physical properties of the system.

15. Contact and gravitational interaction

In this chapter we specify the Hartree-Fock theory to an interaction consisting of repulsive contact interaction and attractive gravitational interaction, described by

$$U(\mathbf{x}-\mathbf{x}') = g\,\delta(\mathbf{x}-\mathbf{x}') - \frac{G_N m}{|\mathbf{x}-\mathbf{x}'|}\,. \tag{15.1}$$

We also set the external potential to zero, i.e. $V(\mathbf{x}) = 0$.

15.1. Hartree-Fock theory

The free energy functional (13.38) for the case of this interaction becomes a rather lengthy expression. Using the definition of the densities of condensate and thermal fluctuations from (13.40) wherever possible, we obtain

$$\begin{aligned} F \;=\; & \frac{1}{\beta}\sum_{\mathbf{n}\neq\mathbf{0}} \ln\left[1-e^{-\beta(\epsilon_{\mathbf{n}}-\mu)}\right] + \int d^3x\,\Psi^*(\mathbf{x})\,h(\mathbf{x})\,\Psi(\mathbf{x}) - \mu\int d^3x\,n_{\mathbf{0}}(\mathbf{x}) \\ & + \sum_{\mathbf{n}\neq\mathbf{0}}\int d^3x\,\Psi^*_{\mathbf{n}}(\mathbf{x})\left[h(\mathbf{x})-\epsilon_{\mathbf{n}}\right]\Psi_{\mathbf{n}}(\mathbf{x})\langle\hat{a}^+_{\mathbf{n}}\hat{a}_{\mathbf{n}}\rangle_{\rm eff} \\ & + g\int d^3x\,\left[\frac{1}{2}\,n^2_{\mathbf{0}}(\mathbf{x}) + 2\,n_{\mathbf{0}}(\mathbf{x})n_{\rm th}(\mathbf{x}) + n^2_{\rm th}(\mathbf{x})\right] \\ & - \int d^3x d^3x'\,\frac{G_N m^2}{|\mathbf{x}-\mathbf{x}'|}\left[\frac{1}{2}\,n_{\mathbf{0}}(\mathbf{x})\,n_{\mathbf{0}}(\mathbf{x}') + n_{\mathbf{0}}(\mathbf{x}')\,n_{\rm th}(\mathbf{x})\right. \\ & \left. + \sqrt{n_{\mathbf{0}}(\mathbf{x}')n_{\mathbf{0}}(\mathbf{x})}\,n_{\rm th}(\mathbf{x},\mathbf{x}') + \frac{1}{2}\,n_{\rm th}(\mathbf{x})\,n_{\rm th}(\mathbf{x}') + \frac{1}{2}\,n_{\rm th}(\mathbf{x},\mathbf{x}')\,n_{\rm th}(\mathbf{x}',\mathbf{x})\right]. \end{aligned} \tag{15.2}$$

Here we have used the identification

$$\Psi^*(\mathbf{x}')\Psi(\mathbf{x}) \equiv \sqrt{n_{\mathbf{0}}(\mathbf{x}')n_{\mathbf{0}}(\mathbf{x})} \tag{15.3}$$

by assuming that the condensate wave function $\Psi(\mathbf{x})$ just contains a global phase, which is justified for a stationary superfluid with vanishing velocity. Furthermore, we can reexpress

the two Hartree-Fock equations (13.42) and (13.43) as

$$[h(\mathbf{x})-\mu]\,\Psi(\mathbf{x})+g\,[n_{\mathbf{0}}(\mathbf{x})+2n_{\rm th}(\mathbf{x})]\,\Psi(\mathbf{x}) \tag{15.4}$$
$$-\int d^3\mathbf{x}'\,\frac{G_N m^2}{|\mathbf{x}-\mathbf{x}'|}\Big\{\,[n_{\mathbf{0}}(\mathbf{x}')+n_{\rm th}(\mathbf{x}')]\,\Psi(\mathbf{x})+n_{\rm th}(\mathbf{x}',\mathbf{x})\Psi(\mathbf{x}')\Big\}=0\,,$$

and

$$0 \;=\; [h(\mathbf{x})-\epsilon_{\mathbf{n}}]\,\Psi_{\mathbf{n}}(\mathbf{x})+g\,[2n_{\mathbf{0}}(\mathbf{x})+2n_{\rm th}(\mathbf{x})]\,\Psi_{\mathbf{n}}(\mathbf{x}) \tag{15.5}$$
$$-\int d^3\mathbf{x}'\,\frac{G_N m^2}{|\mathbf{x}-\mathbf{x}'|}\Big\{\,[n_{\mathbf{0}}(\mathbf{x}')+n_{\rm th}(\mathbf{x}')]\,\Psi_{\mathbf{n}}(\mathbf{x})+\Big[\sqrt{n_{\mathbf{0}}(\mathbf{x}')n_{\mathbf{0}}(\mathbf{x})}+n_{\rm th}(\mathbf{x}',\mathbf{x})\Big]\,\Psi_{\mathbf{n}}(\mathbf{x}')\Big\}\,,$$

respectively. The first parts of each equation are familiar from a system of particles in an external trap considering only contact interaction between the particles, as is the case for most BEC experiments in the lab. With the gravitational interaction the situation becomes a little less convenient due to its nonlocality. In particular, the Fock terms of the gravitational interaction pose a problem since they contain the bilocal form of the densities, i.e. $n_{\rm th}(\mathbf{x}',\mathbf{x})$ and $\sqrt{n_{\mathbf{0}}(\mathbf{x}')n_{\mathbf{0}}(\mathbf{x})}$.

15.2. Semi-classical Hartree-Fock theory

The semi-classical free energy (14.2) specified for the case of contact and gravitational interaction and without an external potential reads

$$\begin{aligned}F_{\rm SC} \;=\;& \frac{1}{\beta}\int d^3x\int\frac{d^3k}{(2\pi)^3}\,\ln\left\{1-e^{-\beta[\epsilon_{\mathbf{k}}(\mathbf{x})-\mu]}\right\}-\mu\int d^3x\,n_{\mathbf{0}}(\mathbf{x})\\
&+\int d^3x\int\frac{d^3k}{(2\pi)^3}\left[\frac{\hbar^2\mathbf{k}^2}{2m}-\epsilon_{\mathbf{k}}(\mathbf{x})\right]n_{\rm th}(\mathbf{x},\mathbf{k})\\
&+g\int d^3x\left[\frac{1}{2}n_{\mathbf{0}}^2(\mathbf{x})+2n_{\mathbf{0}}(\mathbf{x})\,n_{\rm th}(\mathbf{x})+n_{\rm th}^2(\mathbf{x})\right]\\
&-\int d^3x d^3x'\,\frac{G_N m^2}{|\mathbf{x}-\mathbf{x}'|}\left[\frac{1}{2}\,n_{\mathbf{0}}(\mathbf{x})\,n_{\mathbf{0}}(\mathbf{x}')+n_{\mathbf{0}}(\mathbf{x}')\,n_{\rm th}(\mathbf{x})\right.\\
&\left.+\sqrt{n_{\mathbf{0}}(\mathbf{x}')n_{\mathbf{0}}(\mathbf{x})}\,n_{\rm th}(\mathbf{x},\mathbf{x}')+\frac{1}{2}\,n_{\rm th}(\mathbf{x},\mathbf{x})\,n_{\rm th}(\mathbf{x}')+\frac{1}{2}n_{\rm th}(\mathbf{x},\mathbf{x}')\,n_{\rm th}(\mathbf{x}',\mathbf{x})\right].\end{aligned} \tag{15.6}$$

Then the first Hartree-Fock equation (14.3) obtained from the variation of the semi-classical free energy with respect to the condensate density becomes

$$\frac{\delta F_{\rm SC}}{\delta n_{\mathbf{0}}(\mathbf{x})} \;=\; -\mu+g\,[n_{\mathbf{0}}(\mathbf{x})+2\,n_{\rm th}(\mathbf{x})] \tag{15.7}$$
$$-\int d^3x'\,\frac{G_N m^2}{|\mathbf{x}-\mathbf{x}'|}\left\{n_{\mathbf{0}}(\mathbf{x}')+n_{\rm th}(\mathbf{x}')+\frac{1}{2}\sqrt{\frac{n_{\mathbf{0}}(\mathbf{x}')}{n_{\mathbf{0}}(\mathbf{x})}}\left[n_{\rm th}(\mathbf{x}',\mathbf{x})+n_{\rm th}(\mathbf{x},\mathbf{x}')\right]\right\},$$

and the variation of $F_{\rm SC}$ with respect to the thermal density,

$$\frac{\delta F_{\rm SC}}{\delta n_{\rm th}(\mathbf{x})} = 0\,, \tag{15.8}$$

gives the dispersions $\epsilon_{\mathbf{k}}(\mathbf{x})$ of the thermal wave functions in analogy to (14.9),

$$\begin{aligned}\epsilon_{\mathbf{k}}(\mathbf{x}) \;=\; & \frac{\hbar^2\mathbf{k}^2}{2m} + 2g\left[n_{\mathbf{0}}(\mathbf{x}) + n_{\rm th}(\mathbf{x})\right] - \int d^3x'\,\frac{G_N m^2}{|\mathbf{x}-\mathbf{x}'|}\left[n_{\mathbf{0}}(\mathbf{x}') + n_{\rm th}(\mathbf{x}')\right] \\ & - \int d^3x'\,\frac{G_N m^2}{|\mathbf{x}-\mathbf{x}'|}\,e^{-i\mathbf{k}(\mathbf{x}-\mathbf{x}')}\left[\sqrt{n_{\mathbf{0}}\,(\mathbf{x})\,n_{\mathbf{0}}\,(\mathbf{x}')} + \int \frac{d^3k'}{(2\pi)^3}\,e^{i\mathbf{k}'(\mathbf{x}-\mathbf{x}')}\,n_{\rm th}(\mathbf{x},\mathbf{k}')\right].\end{aligned} \tag{15.9}$$

Differentiation of $F_{\rm SC}$ with respect to the chemical potential as usual yields the total number of particles as according to (14.11).

In the following, we will simply discard the bilocal Fock terms of the gravitational interaction, i.e., we carry out a Hartree-approximation for the gravitational part of the system. For the contact interaction, we will keep both Hartree and Fock terms. This leads to the new equation for the condensate density,

$$-\mu + g\,\left[n_{\mathbf{0}}(\mathbf{x}) + 2\,n_{\rm th}(\mathbf{x})\right] - \int d^3x'\,\frac{G_N m^2}{|\mathbf{x}-\mathbf{x}'|}\left[n_{\mathbf{0}}(\mathbf{x}') + n_{\rm th}(\mathbf{x}')\right] = 0\,, \tag{15.10}$$

and new thermal energies $\epsilon_{\mathbf{k}}(\mathbf{x})$,

$$\epsilon_{\mathbf{k}}(\mathbf{x}) = \frac{\hbar^2\mathbf{k}^2}{2m} + 2g\left[n_{\mathbf{0}}(\mathbf{x}) + n_{\rm th}(\mathbf{x})\right] - \int d^3x'\,\frac{G_N m^2}{|\mathbf{x}-\mathbf{x}'|}\left[n_{\mathbf{0}}(\mathbf{x}') + n_{\rm th}(\mathbf{x}')\right]. \tag{15.11}$$

With the form of the thermal energies as given by Eq. (15.11), the logarithmic term in the free energy (15.6) can be further processed by substituting $\epsilon = \hbar^2\mathbf{k}^2/(2m)$ and using the series representation of the logarithm,

$$\ln\left(1 - e^{-x}\right) = -\sum_{\nu=1}^{\infty}\frac{e^{-\nu x}}{\nu}\,. \tag{15.12}$$

Thus, the first term of the free energy yields the integral

$$\int \frac{d^3k}{(2\pi)^3}\,\ln\left\{1 - e^{-\beta[\epsilon_{\mathbf{k}}(\mathbf{x})-\mu]}\right\} = -\frac{1}{\sqrt{2}\pi^2}\left(\frac{m}{\hbar^2}\right)^{3/2}\int_0^\infty d\epsilon\,\epsilon^{1/2}\sum_{\nu=1}^{\infty}\frac{1}{\nu}\,e^{-\beta\nu\,(\epsilon+\alpha)}\,, \tag{15.13}$$

where

$$\alpha(\mathbf{x}) = 2g\left[n_{\mathbf{0}}(\mathbf{x}) + n_{\rm th}(\mathbf{x})\right] + \Phi(\mathbf{x}) - \mu\,. \tag{15.14}$$

Here, we have introduced for brevity the gravitational potential

$$\Phi(\mathbf{x}) = -\int d^3x'\,\frac{G_N m^2}{|\mathbf{x}-\mathbf{x}'|}\left[n_{\mathbf{0}}(\mathbf{x}') + n_{\rm th}(\mathbf{x}')\right]. \tag{15.15}$$

The integral over ϵ in Eq. (15.13) can be solved with the help of a standard integral [146], resulting in

$$\int_0^\infty d\epsilon\, \epsilon^{1/2} \sum_{\nu=1}^{\infty} \frac{1}{\nu}\, e^{-\beta\nu\,(\epsilon+\alpha)} = \sum_{\nu=1}^{\infty} \frac{1}{\nu^{5/2}} e^{-\beta\,\alpha}\,, \tag{15.16}$$

which can be identified as the series representation of the polylogarithmic function,

$$\zeta_a(z) = \sum_{\nu=1}^{\infty} \frac{z^\nu}{\nu^a}\,. \tag{15.17}$$

The free energy reads then

$$\begin{aligned} F_{\rm SC} \;=\; & -\frac{1}{\beta\lambda^3} \int d^3x\, \zeta_{5/2}\left(e^{-\beta\,\alpha(\mathbf{x})}\right) - \mu \int d^3x\, n_{\mathbf{0}}(\mathbf{x}) \\ & + \int d^3x \int \frac{d^3k}{(2\pi)^3} \left[\frac{\hbar^2\mathbf{k}^2}{2m} - \epsilon_{\mathbf{k}}(\mathbf{x})\right] n_{\rm th}(\mathbf{x},\mathbf{k}) \\ & + g \int d^3x \left[\frac{1}{2} n_{\mathbf{0}}^2(\mathbf{x}) + 2 n_{\mathbf{0}}(\mathbf{x})\, n_{\rm th}(\mathbf{x}) + n_{\rm th}^2(\mathbf{x})\right] \\ & - \int d^3x d^3x' \, \frac{G_N m^2}{|\mathbf{x}-\mathbf{x}'|} \left[\frac{1}{2}\, n_{\mathbf{0}}(\mathbf{x})\, n_{\mathbf{0}}(\mathbf{x}') + n_{\mathbf{0}}(\mathbf{x}')\, n_{\rm th}(\mathbf{x}) \right. \\ & \left. + n_{\mathbf{0}}(\mathbf{x})\, n_{\rm th}(\mathbf{x}') + n_{\rm th}(\mathbf{x})\, n_{\rm th}(\mathbf{x}')\right]. \end{aligned} \tag{15.18}$$

Differentiation of (15.18) with respect to the chemical potential μ yields (14.11) with the thermal density

$$n_{\rm th}(\mathbf{x}) = \frac{1}{\lambda^3}\, \zeta_{3/2}\left(e^{-\beta\,\alpha(\mathbf{x})}\right)\,, \tag{15.19}$$

where $\lambda = (2\pi\beta\hbar^2/m)^{1/2}$ is the thermal de Broglie wavelength

15.3. Introduction of spherical coordinates

Before we proceed to process the derived expressions, we will simplify the equations by assuming spherical symmetry which justifies to introduce spherical coordinates. Thus, both condensate and thermal density are assumed to be spherically symmetric:

$$n_{\mathbf{0}}(\mathbf{x}) = n_{\mathbf{0}}(r)\,, \quad n_{\rm th}(\mathbf{x}) = n_{\rm th}(r)\,. \tag{15.20}$$

Furthermore, we will reformulate the gravitational potential (15.15) in terms of a multipole expansion in spherical coordinates. Separating the areas of $r \le r'$ and $r \ge r'$, we can express the $1/r$-term occurring in the gravitational potential (15.15) with a general function

$f(\mathbf{x}) \equiv f(r)$ as

$$\int d^3x' \, \frac{1}{|\mathbf{x}-\mathbf{x}'|} \, f(\mathbf{x}') = \sum_{l=0}^{\infty} \sum_{m=-l}^{l} \frac{4\pi}{2l+1} \, Y_{lm}(\Omega) \times \int_0^{\pi} \int_0^{2\pi} d\Omega' \, Y_{lm}^*(\Omega') \left[\int_0^r dr' \, \frac{r'^{l+2}}{r^{l+1}} \, f(r') + \int_r^{\infty} dr' \, \frac{r^l}{r'^{l-1}} f(r') \right] . \tag{15.21}$$

We can now apply these substitutions to the Hartree-Fock equations, recalling some of the mathematical properties of the spherical harmonics as the addition theorem,

$$\sum_{m=-l}^{l} Y_{lm}^*(\Omega) \, Y_{lm}(\Omega') = \frac{2l+1}{4\pi} \, , \tag{15.22}$$

the normalization condition,

$$\int d\Omega \, Y_{lm}^*(\Omega) \, Y_{l'm'}(\Omega) = \delta_{ll'} \delta_{mm'} \, , \tag{15.23}$$

and the fact that $Y_{00}(\Omega) = 1/\sqrt{4\pi}$. Using these, we can write the first Hartree-Fock equation (15.10) as

$$-\mu + g \left[n_{\mathbf{0}}(r) + 2 n_{\mathrm{th}}(r) \right] + \Phi(r) = 0 \, , \tag{15.24}$$

where we have introduced the gravitational potential $\Phi(r)$ in spherical coordinates,

$$\Phi(r) = -4\pi G_N m^2 \left\{ \frac{1}{r} \int_0^r dr' \, r'^2 \left[n_{\mathbf{0}}(r') + n_{\mathrm{th}}(r') \right] + \int_r^{\infty} dr' \, r' \left[n_{\mathbf{0}}(r') + n_{\mathrm{th}}(r') \right] \right\} . \tag{15.25}$$

For the thermal density, introducing spherical coordinates is also straightforward, leading to

$$n_{\mathrm{th}}(r) = \frac{1}{\lambda^3} \, \zeta_{3/2} \left[e^{-\beta \left(2g \left[n_{\mathbf{0}}(r) + n_{\mathrm{th}}(r) \right] + \Phi(r) - \mu \right)} \right] . \tag{15.26}$$

This result for the thermal density is a general result valid for the thermal density everywhere in the system. The argument of the exponent contains an expression which depends on the radial coordinate. For our system, we expect two regimes: the inner zone, where the condensate density is nonzero and coexists with the thermal density, and the outer regime, where the condensate vanishes, but a thermal phase continues to exist. The boundary between those two regions is given by the Thomas-Fermi radius, i.e. the point where the condensate density vanishes,

$$n_{\mathbf{0}}(R_0) = 0 \, . \tag{15.27}$$

Therefore, we have to consider two different versions of the thermal density for the inner and outer regime, which will be denoted by subscripts 1 and 2, respectively. The condensate

exists solely in the inner region, and is zero outside the Thomas-Fermi radius.
In the following two sections, we will treat the two regimes in more detail and further process the equations for the condensate and the thermal densities analytically up to a point, where we then have to resort to iterative or numerical methods to continue, which will then be presented in Chapter 16.

15.4. Inner regime

In the inner regime, we can employ the first Hartree-Fock equation (15.24) to simplify the argument of the exponent in the thermal density and obtain

$$n_{\mathrm{th},1}(r) = \frac{1}{\lambda^3}\,\zeta_{3/2}\Big[e^{-\beta g\, n_{\mathbf{0}}(r)}\Big]\,. \tag{15.28}$$

Having specified this solution for the thermal density in the inner regime, we can now consider the first Hartree-Fock equation,

$$-\mu + g\, n_{\mathbf{0}}(r) + 2g\, n_{\mathrm{th},1}(r) + \Phi(r) = 0\,, \tag{15.29}$$

in order to obtain a solution for the condensate density, and subsequently calculate the thermal density in the inner region via (15.28). The first Hartree-Fock equation (15.29) can be further processed by multiplying the equation by r and differentiating twice with respect to r to get rid of the integrals in the gravitational interactions. For the differentiation of the integrals with the radial coordinate r in the integral limits, we make use of the formula

$$\frac{\partial}{\partial x}\int_a^x f(x,y)\,dy = \int_a^x \frac{\partial f(x,y)}{\partial x}\,dy + f(x,x)\,. \tag{15.30}$$

Thus, the integral equation (15.29) becomes a purely differential equation

$$\frac{\partial^2}{\partial r^2}\left\{r\left[n_{\mathbf{0}}(r) + 2n_{\mathrm{th},1}(r)\right]\right\} = -\frac{4\pi\, G_N m^2}{g}\, r\left[n_{\mathbf{0}}(r) + n_{\mathrm{th},1}(r)\right]. \tag{15.31}$$

This equation only depends on the condensate density, since the thermal density can be expressed as a function of condensate density via (15.28). Defining the inverse length scale

$$\sigma = \sqrt{\frac{4\pi\, G_N m^2}{g}}\,, \tag{15.32}$$

which determines the typical size scales of the system, and substituting

$$\varphi(r) = n_{\mathbf{0}}(r) + 2\, n_{\mathrm{th},1}(r)\,, \tag{15.33}$$

we can restate the equation as a simple differential equation for $\varphi(r)$,

$$\frac{\partial^2}{\partial r^2}\Big[r\,\varphi(r)\Big] + \sigma^2\, r\,\varphi(r) =: f(r)\,, \tag{15.34}$$

where

$$f(r) = \sigma^2\, r\, n_{\mathrm{th},1}(r) \tag{15.35}$$

defines the inhomogeneous part of the differential equation.
The most general solution for the homogeneous equation is

$$\varphi_{\mathrm{h}}(r) = \frac{A\,\sin(\sigma r)}{r} + \frac{B\,\cos(\sigma r)}{r}\,, \tag{15.36}$$

where A and B are integrational constants which need to be fixed by boundary conditions. Demanding that the condensate density has to remain finite for all r, and considering that

$$\lim_{r\to 0}\frac{\cos(\sigma r)}{r} \to \infty\,, \tag{15.37}$$

we can constrain the general solution for $\varphi_{\mathrm{h}}(r)$ in setting $B = 0$. The homogeneous solution for the differential equation (15.34) thus reads

$$\varphi_{\mathrm{h}}(r) = \frac{A\,\sin(\sigma r)}{r}\,. \tag{15.38}$$

For the particular solution we use the ansatz

$$\varphi_{\mathrm{p}}(r) = \frac{u_1(r)\sin(\sigma r)}{r} + \frac{u_2(r)\cos(\sigma r)}{r}\,. \tag{15.39}$$

The yet unknown functions $u_1(r)$ and $u_2(r)$ are then determined by the equations

$$\begin{aligned} \frac{\partial u_1(r)}{\partial r} &= \frac{1}{\sigma}\cos(\sigma r)\, f(r)\,, \\ \frac{\partial u_2(r)}{\partial r} &= -\frac{1}{\sigma}\sin(\sigma r)\, f(r)\,. \end{aligned} \tag{15.40}$$

We can write down the solutions for $u_1(r)$ and $u_2(r)$ explicitly in form of integrals over the inhomogeneity $f(r)$ as

$$\begin{aligned} u_1(r) &= \frac{1}{\sigma}\int_0^r dr'\,\cos\left(\sigma r'\right) f(r')\,, \\ u_2(r) &= -\frac{1}{\sigma}\int_0^r dr'\,\sin\left(\sigma r'\right) f(r')\,. \end{aligned} \tag{15.41}$$

The particular solution (15.39) then can be computed as

$$\varphi_{\mathrm{p}}(r) = \frac{1}{\sigma r}\int_0^r dr'\, f(r')\,\sin\left[\sigma(r-r')\right]. \tag{15.42}$$

The total solution for $\varphi(r)$ is the sum of the homogeneous and the particular term,

$$\varphi(r) = \varphi_{\rm h}(r) + \varphi_{\rm p}(r)\,, \tag{15.43}$$

and yields

$$\varphi(r) = \frac{A\,\sin(\sigma r)}{r} + \frac{\sigma}{r}\int\limits_0^r dr'\,r'\,\sin\left[\sigma(r-r')\right]\,n_{\rm th,1}(r')\,. \tag{15.44}$$

Considering (15.33) and the dependence of the thermal density on the condensate given by Eq. (15.28), from (15.44) we obtain an integral equation for the condensate,

$$\begin{aligned} n_{\mathbf{0}}(r) \;\;=\;\; & \frac{A\,\sin(\sigma r)}{r} - \frac{2}{\lambda^3}\,\zeta_{3/2}\Big[e^{-\beta g\,n_{\mathbf{0}}(r)}\Big] \\ & + \frac{\sigma}{\lambda^3 r}\int\limits_0^r dr'\,r'\,\sin\left[\sigma(r-r')\right]\,\zeta_{3/2}\Big[e^{-\beta g\,n_{\mathbf{0}}(r')}\Big]\,. \end{aligned} \tag{15.45}$$

This equation contains the condensate density itself as well as integrals over the condensate density within the argument of the polylog function. We will elaborate in more detail in Chapter 16 how to solve this equation for the condensate density employing an iterative approach. The thermal density can then be obtained from the result for $n_{\mathbf{0}}(r)$ using Eq. (15.28).

In the limit of zero temperatures, the thermal fluctuations are zero, and the condensate density is exactly determined from (15.45) as

$$n_{\mathbf{0}}(r) = A\,\frac{\sin(\sigma r)}{r}\,. \tag{15.46}$$

In this case, the constant A can be determined by calculating the total number of particles in the system,

$$N = 4\pi\int\limits_0^{R_0} dr\,r^2\,n_{\mathbf{0}}(r)\,, \tag{15.47}$$

yielding

$$A(T=0) = \frac{N}{4\pi^2}\,. \tag{15.48}$$

For zero temperature, it is also possible to analytically determine the Thomas-Fermi radius R_0,

$$\frac{N}{4\pi^2}\,\frac{\sin(\sigma R_0)}{R_0} = 0 \quad\Longrightarrow\quad R_0 = \frac{\pi}{\sigma}\,. \tag{15.49}$$

Considering the definition of σ in Eq. (15.32), the result (12.27) is recovered. For non-zero temperatures, the Thomas-Fermi radius will differ from this value, since the condensate obtains corrections due to the thermal fluctuations.

The significance of A can be inferred by considering Eq. (15.45) at the center of the star. Denoting the integral term in (15.45) as $I(r)$, in the limit $r \to 0$ the equation reduces to

$$n_{\mathbf{0}}(0) = \sigma\, A - \frac{2}{\lambda^3}\,\zeta_{3/2}\Big[e^{-\beta g\, n_{\mathbf{0}}(0)}\Big] + \frac{\sigma}{\lambda^3}\lim_{r\to 0}\left[\frac{1}{r} I(r)\right] . \tag{15.50}$$

Writing $I(r)$ as a Taylor series and then carrying out the limit, we obtain

$$\lim_{r\to 0}\left[\frac{1}{r} I(r)\right] = 0\,, \tag{15.51}$$

and thus A is given by

$$A = \frac{1}{\sigma}\left\{ n_{\mathbf{0}}(0) + \frac{2}{\lambda^3}\,\zeta_{3/2}\Big[e^{-\beta g\, n_{\mathbf{0}}(0)}\Big]\right\} . \tag{15.52}$$

Considering the definition of the thermal density in the inner regime, Eq. (15.28), this is equivalent to

$$A = \frac{1}{\sigma}\left[n_{\mathbf{0}}(0) + 2\, n_{\mathrm{th},1}(0)\right] . \tag{15.53}$$

Thus, A is connected to both the condensate and thermal densities at the center of the star.

15.5. Outer regime

In the outer regime, the thermal density (15.26) can be specified further considering the fact that $n_{\mathbf{0}}(r) = 0$. The thermal density then reads

$$n_{\mathrm{th},2}(r) = \frac{1}{\lambda^3}\,\zeta_{3/2}\left[e^{-\beta\left(2g\, n_{\mathrm{th},2}(r) + \Phi(r) - \mu\right)}\right] , \tag{15.54}$$

where the gravitational potential (15.25) is evaluated for $r > R_0$ as

$$\Phi(r) = -4\pi G_N m^2 \left\{ \frac{1}{r}\int_0^{R_0} dr'\, r'^2 \Big[n_{\mathbf{0}}(r') + n_{\mathrm{th},1}(r')\Big] + \frac{1}{r}\int_r^{r} dr'\, r'^2 n_{\mathrm{th},2}(r') + \int_{R_0}^{\infty} dr'\, r' n_{\mathrm{th},2}(r')\right\} . \tag{15.55}$$

Note that $\Phi(r)$ still contains the condensate density in the first term, since the presence of the condensate in the inner regime gravitationally influences the thermal density in the outer region. However, this dependence can be notationally simplified introducing

$$\begin{aligned} N_{\mathbf{0}} &= 4\pi \int_0^{R_0} dr\, r^2\, n_{\mathbf{0}}(r)\,, \\ N_{\mathrm{th},1} &= 4\pi \int_0^{R_0} dr\, r^2\, n_{\mathrm{th},1}(r)\,. \end{aligned} \tag{15.56}$$

The gravitational potential in the outer region then reads

$$\Phi(r) = -\frac{G_N m^2 \left(N_{\mathbf{0}} + N_{\mathrm{th},1}\right)}{r} - 4\pi G_N m^2 \left[\frac{1}{r}\int\limits_{R_0}^{r} dr'\, r'^2 n_{\mathrm{th},2}(r') + \int\limits_{r}^{\infty} dr'\, r' n_{\mathrm{th},2}(r')\right]. \quad (15.57)$$

The determining equation (15.54) to solve in order to obtain $n_{\mathrm{th},2}(r)$ is rather involved due to the polylogarithmic function and the occurrence of the thermal density as the argument of the integral in the gravitational potential (15.57). In order to solve the equation, we will carry out some substitutions to transform the integral equation to a differential one. First, we integrate expression (15.54),

$$4\pi \left[\frac{1}{r}\int\limits_{R_0}^{r} dr'\, r'^2\, n_{\mathrm{th},2}(r') + \int\limits_{r}^{\infty} dr'\, r'\, n_{\mathrm{th},2}(r')\right] = \quad (15.58)$$
$$\frac{4\pi}{\lambda^3}\left\{\frac{1}{r}\int\limits_{R_0}^{r} dr'\, r'^2\, \zeta_{3/2}\left[z(r')\right] + \int\limits_{r}^{\infty} dr'\, r'\, \zeta_{3/2}\left[z(r')\right]\right\},$$

where

$$z(r) = e^{-\beta\left[2g\, n_{\mathrm{th},2}(r) + \Phi(r) - \mu\right]}. \quad (15.59)$$

Since Eq. (15.54) is only valid for the region outside of the Thomas-Fermi radius, the spatial integral is restricted to the regime $r \in [R_0, \infty]$, $\theta \in [0, \pi]$ and $\varphi \in [0, 2\pi]$.
Substituting this expression with a function $h(r)$, defined by

$$h(r) := \left[\frac{1}{r}\int\limits_{R_0}^{r} dr'\, r'^2\, n_{\mathrm{th},2}(r') + \int\limits_{r}^{\infty} dr'\, r'\, n_{\mathrm{th},2}(r')\right], \quad (15.60)$$

Eq. (15.58) then reads

$$h(r) = \frac{1}{\lambda^3}\left\{\frac{1}{r}\int\limits_{R_0}^{r} dr'\, r'^2\, \zeta_{3/2}\left[z(r')\right] + \int\limits_{r}^{\infty} dr'\, r'\, \zeta_{3/2}\left[z(r')\right]\right\}, \quad (15.61)$$

where

$$z(r) = \mathrm{Exp}\left\{-\beta\left[-\frac{2g}{r}\frac{d^2}{dr^2}\left[r\, h(r)\right] - \frac{G_N m^2 \left(N_{\mathbf{0}} + N_{\mathrm{th},1}\right)}{r} - 4\pi G_N m^2\, h(r) - \mu\right]\right\}. \quad (15.62)$$

The thermal density can be obtained by multiplying $h(r)$ with r and differentiating twice, i.e.

$$n_{\mathrm{th},2}(r) = -\frac{1}{r}\frac{d^2}{dr^2}\left[r\, h(r)\right]. \quad (15.63)$$

We also have to insert an expression for the chemical potential into the equation. It is obtained by evaluating the first Hartree-Fock equation (15.29) at the Thomas-Fermi radius as

$$\mu = 2g\, n_{\mathrm{th},1}(R_0) + \Phi(R_0)\,, \tag{15.64}$$

which yields with (15.28), (15.57) and (15.60)

$$\mu = \frac{2g}{\lambda^3}\,\zeta_{3/2}(1) - \frac{G_N m^2\,(N_{\mathbf{0}} + N_{\mathrm{th},1})}{R_0} - 4\pi G_N m^2\, h(R_0)\,.$$

By multiplying Eq. (15.61) with r and differentiating twice with respect to r we end up with a differential equation for $h(r)$,

$$\frac{d^2}{dr^2}\Big[r\, h(r)\Big] = -\frac{r}{\lambda^3}\,\zeta_{3/2}\left[z(r)\right]\,, \tag{15.65}$$

with the argument of the exponent as

$$\begin{aligned} z(r) \;=\; \mathrm{Exp}\Big\{ -\beta\Big[-\frac{2g}{r}\,\frac{d^2}{dr^2}\left[r\, h(r)\right] - 4\pi G_N m^2\left[h(r) - h(R_0)\right] \\ -\frac{2g}{\lambda^3}\,\zeta_{3/2}(1) - G_N m^2\,(N_{\mathbf{0}} + N_{\mathrm{th},1})\left(\frac{1}{r} - \frac{1}{R_0}\right)\Big]\Big\}\,. \end{aligned} \tag{15.66}$$

For convenience we will carry out another substitution, i.e.

$$H(r) = h(r) - h(R_0)\,. \tag{15.67}$$

This eliminates the unknown $h(R_0)$-term in the exponent, while (15.63) leads to

$$n_{\mathrm{th},2}(r) = -\frac{1}{r}\,\frac{d^2}{dr^2}\Big[r\, H(r)\Big]\,. \tag{15.68}$$

The final differential equation for $H(r)$ thus reads

$$\begin{aligned} \frac{d^2}{dr^2}\Big[r\, H(r)\Big] \;=\; -\frac{r}{\lambda^3}\,\zeta_{3/2}\Bigg(\mathrm{Exp}\Big\{ -\beta\Big[-\frac{2g}{r}\,\frac{d^2}{dr^2}\left[r\, H(r)\right] - 4\pi G_N m^2 H(r) \\ -\frac{2g}{\lambda^3}\,\zeta_{3/2}(1) - G_N m^2\,(N_{\mathbf{0}} + N_{\mathrm{th},1})\left(\frac{1}{r} - \frac{1}{R_0}\right)\Big]\Big\}\Bigg)\,. \end{aligned} \tag{15.69}$$

In order to solve it in the outer regime for $r > R_0$, we have to specify appropriate boundary conditions. From the definition of $H(r)$ in (15.67), we deduce the condition

$$H(R_0) = 0\,. \tag{15.70}$$

Furthermore, we have to demand that the thermal densities of inner and outer regime be equal at the Thomas-Fermi radius, i.e.

$$n_{\mathrm{th},1}(R_0) = n_{\mathrm{th},2}(R_0)\,. \tag{15.71}$$

From the context (15.68) of $n_{\mathrm{th},2}(r)$ with $H(r)$ as well as (15.28), we end up with the second boundary condition

$$\frac{1}{\lambda^3}\zeta_{3/2}(1) = -H''(R_0) - \frac{2}{R_0}H'(R_0)\,. \tag{15.72}$$

Solving (15.69) with the boundary conditions (15.70) and (15.72) thus determines the thermal density (15.68) in the outer region.

16. Numerical solution

We will now proceed to describe the exact procedure to solve the coupled equations for the two densities as outlined in the previous chapter. We distinguish two regimes, the condensate area, $0 \leq r \leq R_0$, and the outer area, $r > R_0$, where the condensate density $n_{\mathbf{0}}(r)$ is zero. The thermal density $n_{\mathrm{th}}(r)$ is nonzero in both regimes. We have to solve the algebraic equation (15.45) for the condensate density in the inner regime, which will then give the thermal density in the inner regime via (15.28); whereas for the outer regime we have to solve Eq. (15.69) with the boundary conditions (15.70) and (15.72) to obtain the thermal density in the outer regime via (15.68). Note that in the whole procedure we do not need to specify the chemical potential μ since we have managed to eliminate or substitute it wherever it occurred. The only input parameter to our system is the constant A, connected to the central densities of condensate and thermal cloud according to (15.53), which ultimately determines the total number of particles in the system. In the following, we will introduce dimensionless quantities to simplify the numerical treatment of the equations.

16.1. Dimensionless variables

In order to cleanly carry out the numerical calculations, we will rewrite all expressions using dimensionless quantities according to

$$r \longrightarrow \rho = \sigma r\,, \tag{16.1a}$$

$$T \longrightarrow \theta = \frac{T}{T_{\mathrm{ch}}}\,, \tag{16.1b}$$

$$n \longrightarrow \tilde{n} = n\,\lambda_{\mathrm{ch}}^3 = n\,\frac{g}{k_B T_{\mathrm{ch}}}\,, \tag{16.1c}$$

$$\epsilon \longrightarrow \tilde{\epsilon} = \frac{\epsilon}{k_B T_{\mathrm{ch}}}\,, \tag{16.1d}$$

where n stands for a particle number density and ϵ for an energy. Any other quantity, when expressed with a tilde, as e.g. $\tilde{\mu}$, $\tilde{\Phi}$, denotes the corresponding dimensionless quantity. The

newly introduced constants are

$$\sigma = \sqrt{\frac{4\pi\, G_N m^2}{g}}\,, \quad T_{\rm ch} = \frac{\hbar^2 \pi}{2a^2 m k_B}\,, \text{ and } \lambda_{\rm ch} = \sqrt{\frac{2\pi\hbar^2}{m k_B T_{\rm ch}}} = 2a\,. \tag{16.2}$$

Here $T_{\rm ch}$ is a characteristic temperature for the system in question, and $\lambda_{\rm ch}$ denotes the corresponding de Broglie wavelength. The inverse length scale σ has been introduced before and determines the typical size scale of the system in question. In Section 16.4 we will elaborate on the concrete values of all parameters used in the computations.

16.2. Inner regime

For the inner regime, we first express the integral equation (15.45) in terms of dimensionless quantities, resulting in

$$\tilde{n}_{\mathbf{0}}(\rho) = \frac{\tilde{A}\,\sin\rho}{\rho} - 2\,\theta^{3/2}\,\zeta_{3/2}\Big[e^{-\tilde{n}_{\mathbf{0}}(\rho)/\theta}\Big] + \frac{\theta^{3/2}}{\rho}\int_0^\rho d\rho'\,\rho'\,\sin(\rho-\rho')\,\zeta_{3/2}\Big[e^{-\tilde{n}_{\mathbf{0}}(\rho')/\theta}\Big]\,. \tag{16.3}$$

The thermal density in the inner region (15.28) is given by

$$\tilde{n}_{\rm th,1}(\rho) = \theta^{3/2}\,\zeta_{3/2}\Big[e^{-\tilde{n}_{\mathbf{0}}(\rho)/\theta}\Big]\,. \tag{16.4}$$

We will resort to an iterative procedure to solve Eq. (16.3) for $\tilde{n}_{\mathbf{0}}(\rho)$. Using the zero temperature result (15.46) as the zeroth order of the iterative solution for the condensate, i.e.

$$n_{\mathbf{0}}^{(0)}(r) = \tilde{A}\,\frac{\sin\rho}{\rho}\,, \tag{16.5}$$

we can obtain the $(i+1)$th order of the iteration from the ith order via

$$\tilde{n}_{\mathbf{0}}^{(i+1)}(\rho) = \frac{\tilde{A}\,\sin\rho}{\rho} - 2\,\theta^{3/2}\,\zeta_{3/2}\Big[e^{-\tilde{n}_{\mathbf{0}}^{(i)}(\rho)/\theta}\Big] + \frac{\theta^{3/2}}{\rho}\int_0^\rho d\rho'\,\rho'\,\sin(\rho-\rho')\,\zeta_{3/2}\Big[e^{-\tilde{n}_{\mathbf{0}}^{(i)}(\rho')/\theta}\Big]\,. \tag{16.6}$$

Iterations will be carried out up to the point where the solution converges, i.e. the $(i+1)$th result does not significantly differ from the ith anymore. The thermal density will then be obtained via Eq. (16.4) using the final convergent result for the condensate density from the iterative procedure. In Section 16.4 we will describe the particular details of the numerical solution and comment on the values of the parameters θ and $\tilde{A}$ used in the simulations.

16.3. Outer regime

In the outer region the dimensionless form of Eq. (15.69) reads

$$\frac{\partial^2}{\partial\rho^2}\left[\rho\,\tilde{H}(\rho)\right] = -\theta^{3/2}\,\rho\,\zeta_{3/2}\Bigg(\mathrm{Exp}\Bigg\{-\frac{1}{\theta}\Bigg[-\frac{2}{\rho}\,\frac{\partial^2}{\partial\rho^2}\left[\rho\,\tilde{H}(\rho)\right]-4\pi\,\tilde{H}(\rho) \\ -2\theta^{3/2}\,\zeta_{3/2}(1)-(N_{\mathbf{0}}+N_{\mathrm{th},1})\left(\frac{1}{\rho}-\frac{1}{\rho_0}\right)\Bigg]\Bigg\}\Bigg)\,, \tag{16.7}$$

while the boundary conditions (15.70) and (15.72) are transformed to

$$\begin{aligned}\tilde{H}(\rho_0) &= 0\,, \\ \theta^{3/2}\zeta_{3/2}(1) &= -\tilde{H}''(\rho_0)-\frac{2}{\rho_0}\tilde{H}'(\rho_0)\,.\end{aligned} \tag{16.8}$$

The solution of Eq. (16.7) has been carried out with a manually programmed forward Runge-Kutta method, solving for $\tilde{H}(\rho)$ and then taking the second derivative to obtain the thermal density via

$$\tilde{n}_{\mathrm{th},2}(\rho) = -\frac{1}{\rho}\,\frac{\partial^2}{\partial\rho^2}\left[\rho\,\tilde{H}(\rho)\right], \tag{16.9}$$

in the range of parameters as used for the solution in the inner regime. For the solution in the outer regime, results from the inner region were used as input parameters, i.e. the particle numbers $N_{\mathbf{0}}$ and $N_{\mathrm{th},1}$ according to (15.56), as well as the Thomas-Fermi radius R_0 from (15.27). Apart from these values, however, no additional external input is necessary in the outer regime, and thus the complete solution of the system in both the inner and outer region is determined only by specifying the parameter $\tilde{A}$.

16.4. Simulation details and results

For the calculation of a solution to the above equations, we have to decide upon a specific application of our theory. As already outlined in the introduction, several types of compact objects are eligible candidates for the occurrence of a BEC. For the case of our framework, we have established that helium white dwarfs are a suitable choice to apply our calculations to, and thus we have to adjust the simulation parameters to the conditions within these objects. We will resort to observational information to fix the appropriate range of parameters in order to be in accordance with physically realistic scenarios.

The Chandrasekhar limit (12.11) suggests the existence of white dwarfs with masses up to about one solar mass, whereas helium white dwarfs with masses as low as $0.18M_\odot$ have been observed [129]. Assuming the white dwarf to consist of ^{4}He atoms with a mass of $m_{\mathrm{He}} \simeq 4\mathrm{u}$, where u is the atomic mass unit, we deduce that a white dwarf contains between $5\cdot10^{55}$ and $1.5\cdot10^{56}$ ^{4}He particles. The parameter that controls the total number

of particles in our Hartree-Fock theory is $\tilde{A}$, connected to the central density of the star. We have to tune the value of $\tilde{A}$ in order obtain a specific number of particles. Considering the typical masses of helium white dwarfs and the mass of one ^{4}He atom, we carried out the simulation for a total number of particles of $N_{\mathrm{tot}} = 10^{56}$.

A microscopic parameter to be determined is the contact interaction strength g, which in turn depends on the s-wave scattering length a of the ^{4}He particles inside the star. As a rough estimate for a, we will use the average volume which is to be expected for each particle in the star. According to Ref. [147] typical radii of white dwarfs of about the earth's radius, $6 \cdot 10^3$ km, and a total number of particles of 10^{56}, each particle can move within a volume of radius 10^{-12} m.

As for the range of temperatures, we have to consider that in realistic astrophysical environments the temperature is not uniform, but varies spatially within the star, the outer regions of a star being cooler and the core hotter. In the theory developed here we do not assume a spatial variation of the temperature, and thus the results are only valid to a limited extent. The uniform temperature approximation might however not be too inappropriate. In general, according to Ref. [148], the temperatures in the cores of white dwarfs are assumed to be of the order of 10^7 K, but in a thin surface layer, which makes up about 1% of the star, the temperature presumably drops to values of about 10^4 K. In our simulations, we covered a range of temperatures between 10^7 K and $2 \cdot 10^8$ K, which exceeds the expected temperatures in white dwarfs. The reason for choosing such high temperatures lies in the results themselves: we found the thermal fluctuations negligible for temperatures below 10^7 K, implying that in that range the zero-temperature treatment is sufficient. The upper limit of the temperature range denotes the maximum temperature to which the theory can be applied - for higher temperatures than 10^8 K, the fusion of helium to heavier elements is possible [126] and thus the theory ceases to be valid.

For the outlined values of the parameter, the inverse length scale σ is computed from (15.32) as

$$\sigma \simeq 1.6 \cdot 10^{-5}\,\mathrm{m}^{-1}\,. \tag{16.10}$$

This leads to a Thomas-Fermi radius at zero temperature (15.49) of

$$R_0 \simeq 196.346\,\mathrm{km}\,. \tag{16.11}$$

The typical size scales to be expected from our Hartree-Fock theory lie thus in the region of 200 km. With those parameters we can iterate Eq. (16.6) until convergence to obtain a solution for the condensate density and subsequently employ Eq. (16.4) to calculate the thermal density in the inner regime. Using the boundary conditions (16.8) at ρ_0 and quantities like $N_{\mathbf{0}}$ and $N_{\mathrm{th},1}$ extracted from the inner solution, we then continue to solve Eq. (16.7) for

T [K]	0	$2.5 \cdot 10^7$	$5 \cdot 10^7$	$7.5 \cdot 10^7$	10^8	$1.5 \cdot 10^8$
ρ_c [10^{10}g/cm^3]	4.44	4.29	4.28	4.15	4.13	4
R_0 [km]	196.314	195.986	195.327	194.997	194.334	191.326
R_{th} [km]	–	196.611	196.577	197.497	197.772	200.076
T_{crit} – %	–	0.979	0.946	0.9	0.852	0.604

Table 16.1.: Summary of simulated data: central condensate density ρ_c, Thomas-Fermi radius R_0, total radius of the star R_{th} and the percentage value of the Thomas-Fermi radius for which the temperature lies below the critical temperature.

$\tilde{H}(\rho)$ and obtain the thermal density in the outer regime from Eq. (16.9). In Fig. 16.1 we show the solutions for both of the densities for a range of temperatures and for $N_{\text{tot}} = 10^{56}$. The condensate is given by the black curve, whereas the thermal density is plotted in red.

In Fig. 16.2 we further show a close-up of the density profiles for the highest considered temperature $T = 2 \cdot 10^8$K, where we can distinguish in more detail the two curves and their behavior. We see that the condensate falls off very abruptly directly before the Thomas-Fermi radius, and thus the thermal density jumps equally suddenly. In the outer region, the thermal density decreases slightly more smoothly.

For all simulations, the central density ρ_c, the Thomas-Fermi radius and the thermal radius are shown in Tab. 16.1. The thermal radius denotes the border of the star, i.e. the point where the thermal density in the outer regime has fallen off to zero. We renounce from providing the values for $\tilde{A}$ for each respective simulation since the central density ρ_c is an equivalent quantity.

It is of use to comment further on the issue of the critical temperature and the transition point between the condensate phase and a purely thermal state of the matter. The critical temperature T_{crit} depends on the (number) density n of the condensate according to (12.1). From our system of equations, we will obtain the densities of condensate and thermal cloud as a function of the radius. Thus T_{crit} varies within the star as a function of r as well, and we can calculate its value for each point inside the star. It is clear that with decreasing density, the critical temperature will drop, and thus at the border of the star the critical temperature will be much lower than in the core. Since we assume a uniform temperature throughout the star, at some point towards the outer regions of the star the critical temperature will be exceeded, and thus the condensate breaks down. As already mentioned before however, the temperature of matter in the star is supposed to drop significantly in a thin layer on the surface of the star, which makes out about 1% of the total volume. Thus, in principle we have to limit the simulations to the region of temperatures for which the critical temperature

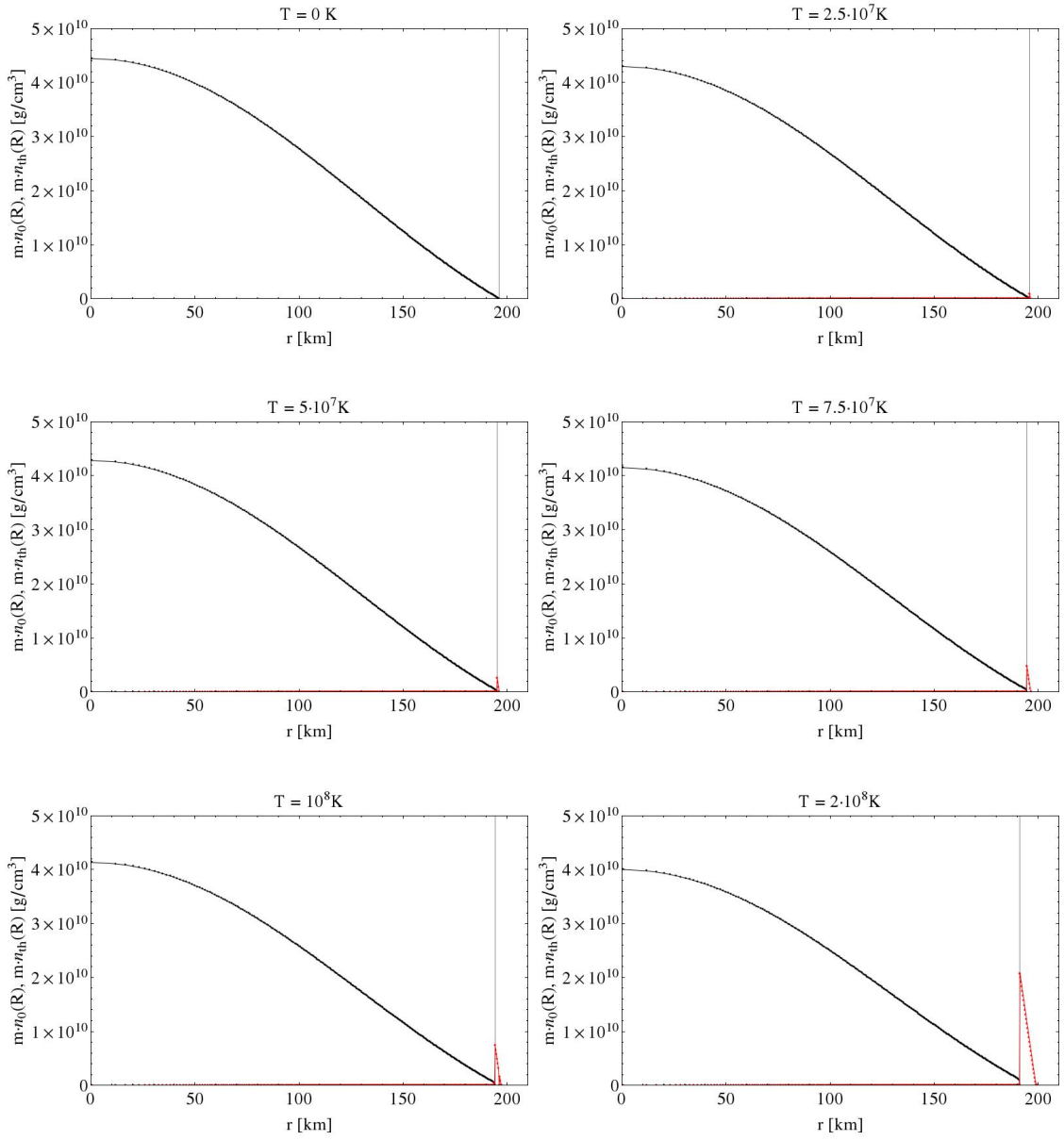

Figure 16.1.: Radial profiles of condensate (black) and thermal density (red) with increasing temperature for $N_{\mathrm{tot}} = 10^{56}$.

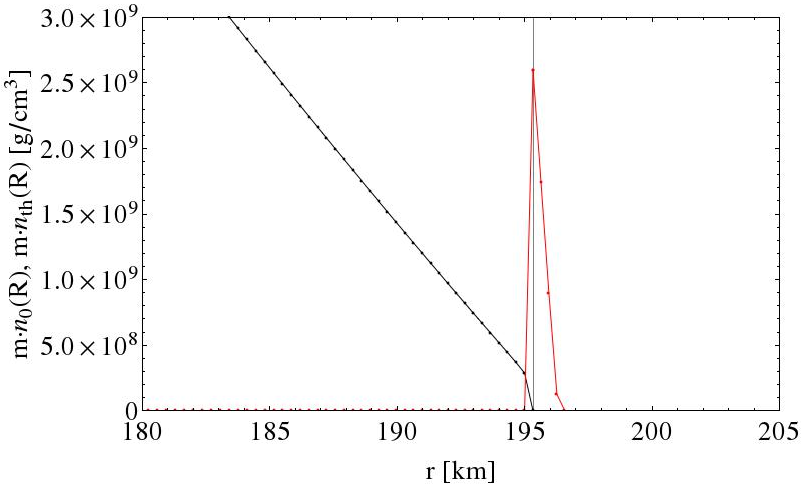

Figure 16.2.: Close-up on the radial profiles of condensate (black) and thermal density (red) for the case of $T = 2 \cdot 10^8$K and $N_{\text{tot}} = 10^{56}$.

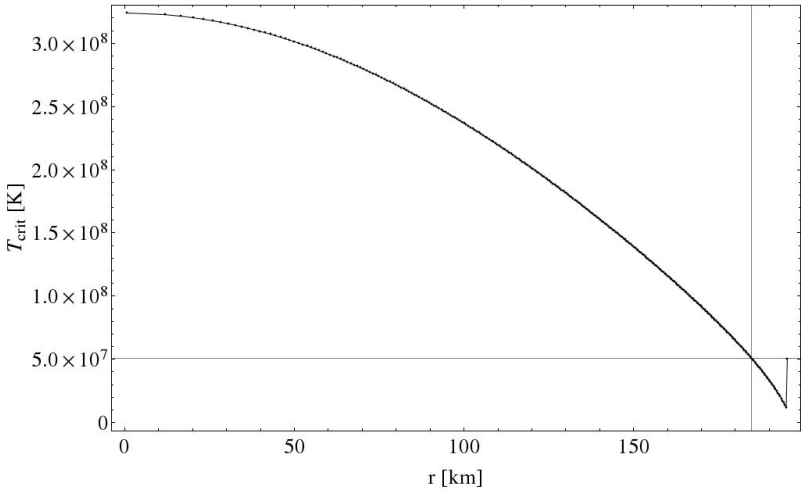

Figure 16.3.: Critical temperature (12.1) as a function of r, compared to the temperature of $5{\cdot}10^7$ K (horizontal line) fixed for this simulation. The condensate would break down at the intersection of the two curves (vertical line), which corresponds to $r = 0.946\, R_0$.

is not exceeded for the inner 99% of the volume of the star, or equivalently for a sphere with $0.996\,R_{\rm th}$ of the total radius. Fig. 16.3 shows a plot of the variation of $T_{\rm crit}$ inside the star for the example of $T = 5 \cdot 10^7$K. We see in this example that the critical temperature drops below the simulated temperature at around $0.946\,R_{\rm th}$, i.e. earlier than in the allowed range of $0.996\,R_{\rm th}$ where the temperature drop occurs. This is the case for all the simulations carried out, as can be seen from Tab. 16.1, where we give the percentage values of the condensate radius at which the condensate breaks down.
We note further that the above used definition of the critical temperature is valid only for an ideal homogeneous Bose gas, whereas interactions between the particles shifts the critical temperature. For the example of contact interaction, the shift of $T_{\rm crit}$ is negative, i.e. leads to a decrease of the critical temperature [149, 150]. Therefore, due to the opposite sign of the interaction, it is to be expected that gravity will lead to an increase. However, we do not elaborate on this point further, but content ourselves with using the non-interacting critical temperature given by Eq. (12.1).

16.5. Astrophysical implications

We will now proceed to extract results from the above calculations which are of astrophysical relevance, i.e., macroscopic and observable quantities.

16.5.1. Mass and density plots

The total mass of the star is given by

$$M = 4\pi\, m \int_0^{R_{\rm th}} dr\, r^2 \left[n_{\mathbf{0}}(r) + n_{\rm th}(r) \right], \tag{16.12}$$

obtained via the numerical integration of the density profiles and multiplication with the mass of a ^{4}He particle. Our simulations were carried out for $N_{\rm tot} = 10^{56}$, and thus the obtained mass is $M \simeq 0.2\,M_\odot$. It is unfortunately not possible to define the total mass directly through a simulation parameter, since the total number of particles is not an input parameter to the solution. Instead we are specifying $\tilde{A}$ which is equivalent to the central densities of condensate and thermal cloud. We can obtain density profiles and thus objects with arbitrarily high mass by modifying $\tilde{A}$.
As previously derived, for zero temperature the context of mass and central condensate density is given by (12.28), which describes a linear dependence of the mass M on the central density ρ_c. For finite temperatures this relation should be modified since the particles outside the condensate phase obey Boltzmann statistics and thus lead to a comparatively

lower central density of the condensate at constant mass, as can be seen from the simulations. However, at the same time the star's radius increases, and so two effects act against each other. Presumably the maximum mass will overall increase, since the decrease in central density is very small, and the thermal radius grows more rapidly with increasing temperatures. Unfortunately, we cannot obtain an upper limit on the mass from our calculations since the simulations can be carried out for an arbitrary number of particles. We therefore resort to two other methods to obtain a limitation of the mass, one being the Schwarzschild limit of gravitational collapse, and the other being a bound for the speed of sound.

The Schwarzschild limit requires the object to be larger than its Schwarzschild radius, i.e.,

$$R_{\mathrm{th}} \gtrsim r_S = \frac{2G_N M}{c^2}\,. \tag{16.13}$$

For the simulation with $N_{\mathrm{tot}} = 10^{56}$ particles, i.e. a mass of $M \simeq 0.2 M_\odot$, the Schwarzschild radius is $r_S \simeq 0.6\,\mathrm{km}$, which is well below the obtained thermal radii of the configurations. Thus, we will consult the second criterion, demanding the adiabatic speed of sound c_S inside the object to be smaller than the speed of light. The detailed derivations of the equation of state of both condensate and thermal fluctuations and the speed of sound derived from it will be presented in Section 16.5.3, and a maximum mass will be derived in Section 16.5.4. First, however, we will investigate the obtained size scales of the system.

16.5.2. Size scales

Besides the masses, another quantity of interest is the size of the system. We show the condensate radius R_0 and the total radius R_{th} of the star in Figs. 16.4 and 16.5 as a function of temperature. The dots give the numerical results obtained in the simulations, and the curves show the best fit of the numerical data. For both condensate and thermal radius, the general form

$$R(T) = R_0 + a_1\, T^{a_2} \tag{16.14}$$

was used for the fit, where $R_0 = \pi/\sigma = 196.346\,\mathrm{km}$ is the Thomas-Fermi radius for zero temperatures. For the condensate radius, the best fit results are

$$a_1 = -4.9 \cdot 10^{-10}\,, \quad a_2 = 1.206\,, \tag{16.15}$$

whereas for the thermal radius we obtained

$$a_1 = 7.7 \cdot 10^{-13}\,, \quad a_2 = 1.528\,. \tag{16.16}$$

Both exponents are close to the value 1.5, which can be ascribed to the leading dependence of any occurring quantities on the temperature to the power of 3/2. The deviation is most

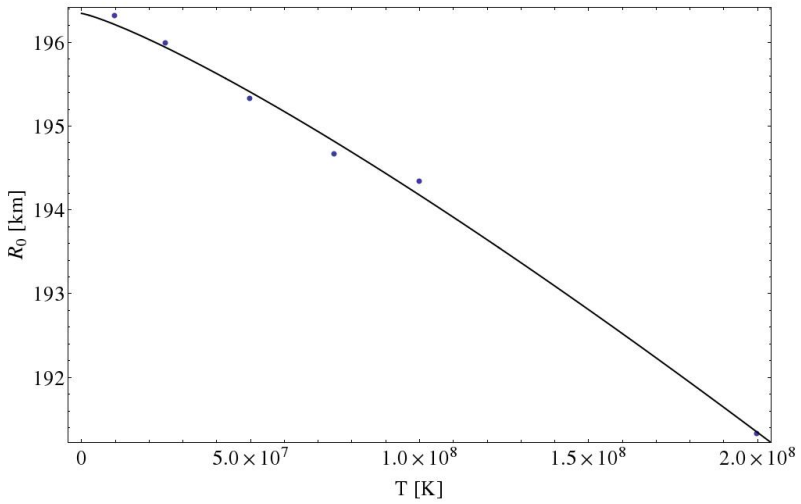

Figure 16.4.: Dependence of the Thomas-Fermi radius R_0 on temperature T: results from the simulations (dots) and numerical fit (solid) as given by Eqs. (16.14) and (16.15).

likely coming from the argument of the polylogarithmic function, which contains a further dependence on the temperature. We see that the condensate radius is decreasing with rising temperatures, whereas the thermal cloud expands and increases the overall radius of the star. In both cases however, the changes are rather subtle, which can be inferred from the respective smallness of a_1.

16.5.3. Equation of state and speed of sound criterion

The adiabatic speed of sound of a fluid is given by the thermodynamic expression

$$c_S^2 = \left.\frac{\partial p}{\partial \rho}\right|_T . \tag{16.17}$$

In physically viable systems, c_S is bound by the speed of light, i.e.

$$c_S \leq c\,. \tag{16.18}$$

In order to determine the speed of sound, we have to calculate the equation of state of the system, i.e. the characteristic relation of pressure and density, $p = p(\rho)$. Since in our system two different phases of matter coexist, we can define an equation of state for each of them independently. In the case of thermal fluctuations, in addition we have to consider the two different regimes inside and outside of the Thomas-Fermi radius. Thus we have to

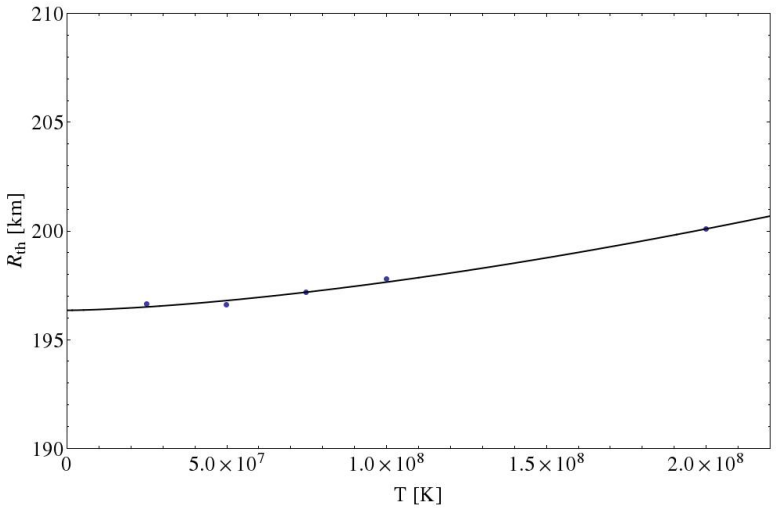

Figure 16.5.: Dependence of the Thomas-Fermi radius $R_{\rm th}$ on temperature T: results from the simulations (dots) and numerical fit (solid) as given by Eqs. (16.14) and (16.16).

distinguish three phases of matter with different equations of state.
To derive the equation of state of the condensate, we will start from the Heisenberg equation (12.12). The existence of thermal fluctuations in addition to the condensate is considered by splitting the field operator into a mean field contribution and a small perturbation,

$$\hat{\Psi}(\mathbf{x},t) = \langle\hat{\Psi}(\mathbf{x},t)\rangle + \hat{\psi}(\mathbf{x},t)\,. \tag{16.19}$$

As before, the average value of the field operator $\hat{\Psi}(\mathbf{x},t)$ equals the condensate wavefunction $\Psi(\mathbf{x},t)$, i.e.

$$\langle\hat{\Psi}(\mathbf{x},t)\rangle = \Psi(\mathbf{x},t)\,, \tag{16.20}$$

whereas the mean value of the fluctuation operator is zero,

$$\langle\hat{\psi}(\mathbf{x},t)\rangle = 0\,. \tag{16.21}$$

Plugging (16.19) into Eq. (12.12), we obtain diverse terms containing different orders of the fluctuations. We will neglect two of those terms, namely the so-called anomalous (off-diagonal) density, $n_{\rm an} = \langle\hat{\psi}(\mathbf{x},t)\hat{\psi}(\mathbf{x},t)\rangle$, and the three-field correlation function $n_3 = \langle\hat{\psi}^\dagger(\mathbf{x},t)\hat{\psi}(\mathbf{x},t)\hat{\psi}(\mathbf{x},t)\rangle$ (see Ref. [136] and references therein). Thus, the Gross-Pitaevskii equation then reads

$$i\hbar\frac{\partial}{\partial t}\Psi(\mathbf{x},t) = \left[-\frac{\hbar^2}{2m}\Delta + g\,|\Psi(\mathbf{x},t)|^2 + 2gn_{\rm th}(\mathbf{x},t) + \Phi(\mathbf{x},t)\right]\Psi(\mathbf{x},t)\,, \tag{16.22}$$

where the density of the thermal fluctuations in this formalism is defined as

$$n_{\rm th}(\mathbf{x},t) = \langle \hat{\psi}^\dagger(\mathbf{x},t)\,\hat{\psi}(\mathbf{x},t)\rangle\,. \tag{16.23}$$

Again, by using the Madelung representation (12.16) for the condensate wave function, the GP equation can be transformed into two hydrodynamic equations. The gradient of the pressure of the condensate can then be identified from the analogy with the hydrodynamic Euler equation (12.18b). For nonzero temperatures, this equation reads

$$m\,n_{\mathbf{0}}\left[\frac{d\mathbf{v}}{dt} + (\mathbf{v}\cdot\nabla)\,\mathbf{v}\right] = -n_{\mathbf{0}}\,\nabla\left[g\;(n_{\mathbf{0}} + 2n_{\rm th})\right] - m\,n_{\mathbf{0}}\,\nabla\Phi - \nabla\cdot\sigma_Q\,, \tag{16.24}$$

and so the gradient of the condensate pressure is read off as

$$\nabla p_{\mathbf{0}} = n_{\mathbf{0}}\,\nabla\left[g\,(n_{\mathbf{0}} + 2n_{\rm th})\right]\,. \tag{16.25}$$

Subsequently we can calculate the pressure of the condensate by integration of Eq. (16.25). Partially integrating the relation (16.25) leads to the well-known polytropic equation of state for the pure condensate and a correction term proportional to a polylogarithm of order 5/2, as well as a term containing both condensate and thermal fluctuations, and a constant,

$$p_{\mathbf{0}} = \frac{g}{2m^2}\,\rho_{\mathbf{0}}^2 + \frac{2}{\beta\lambda^3}\,\zeta_{5/2}\big[e^{-\frac{\beta g}{m}\rho_{\mathbf{0}}}\big] + \frac{2g}{m^2\,\lambda^3}\,\rho_{\mathbf{0}}\,\zeta_{3/2}\big[e^{-\frac{\beta g}{m}\rho_{\mathbf{0}}}\big] - \frac{2}{\beta\lambda^3}\,\zeta_{5/2}(1)\,, \tag{16.26}$$

where now

$$\rho_{\mathbf{0}} = m\,n_{\mathbf{0}}\,. \tag{16.27}$$

Eq. (16.26) is the equation of state for the condensate with corrections from the thermal density. For $\rho_{\mathbf{0}} = 0$, the pressure correctly vanishes. Fig. 16.6 shows the condensate pressure given as a function of the condensate density for the example of $T = 5\cdot 10^7$K and $N_{\rm tot} = 10^{56}$. As we can see from the close-up of the condensate equation of state in Fig. 16.7, the pressure becomes negative for small densities. This is a consequence of the Thomas-Fermi approximation for the condensate: at the border of the star, where the condensate density is small, the quantum pressure of the condensate, represented by the term $\nabla\cdot\sigma_Q$ in Eq. (16.24), becomes important. However, we have neglected this term in the Thomas-Fermi approximation. For the small densities at the border of the star, the quantum pressure would thus correct the unphysical negative pressures obtained in (16.26). Besides the exact form of the condensate pressure (16.26), denoted by the dots, and the zero-temperature limit (dashed), Fig. 16.7 contains a fit (solid), carried out with the general polytropic ansatz

$$p_{\mathbf{0}} = \frac{g}{2m^2}\,\rho_{\mathbf{0}}^2 + b_1\,\rho_{\mathbf{0}}^{b_2}\,. \tag{16.28}$$

The best fit for the parameters b_1 and b_2 resulted in the values

$$b_1 = -1.7 \cdot 10^{17}\,, \qquad b_2 = 0.1588\,. \tag{16.29}$$

The parameterv b_2 in the exponent leads to the polytropic index

$$n_2 = -1.1889\,, \tag{16.30}$$

which implies that the polytropic form with $n = 1$ for the condensate at $T = 0$ is modified at finite temperatures to obtain another polytropic component with negative index n_2. This component is due to the presence of the thermal density. Negative polytropic indices denote metastable states of matter, which can occur in highly energetic processes and environments in astrophysics [151]. Since the thermal cloud makes up only a very small fraction of the total number of particles however, and moreover negative pressures only occur for very small densities of the order of $10^8\,\mathrm{g/cm^3}$, as at the border of the star, it is assumed that the negative polytrope component does not endanger the stability of the system as a whole. We have calculated the percentage of the Thomas-Fermi radius for which the pressure becomes negative, which happens at the density $\rho_{\mathbf{0}} \simeq 5.089 \cdot 10^8 \mathrm{g/cm^3}$. For the example of $T = 5{\cdot}10^7\,\mathrm{K}$ this happens at $r = 194.003\,\mathrm{km}$, which corresponds to $0.993\,R_0$.

For the thermal cloud, the pressure can be obtained from its definition

$$p_{\mathrm{th}}(r) = \int \frac{d^3k}{(2\pi)^3} \frac{\hbar^2\mathbf{k}^2/2m}{e^{\beta[\epsilon_{\mathbf{k}}(r)-\mu]}-1}\,, \tag{16.31}$$

which leads to a polylogarithmic function, similar to the thermal density, but with an index 5/2:

$$p_{\mathrm{th}}(r) = \frac{1}{\beta\lambda^3}\,\zeta_{5/2}\left[e^{-\beta(2g\,[n_{\mathbf{0}}(r)+n_{\mathrm{th}}(r)]+\Phi(r)-\mu)}\right]\,. \tag{16.32}$$

For the two regimes, we can express the pressure as

$$p_{\mathrm{th},1}(r) = \frac{1}{\beta\lambda^3}\,\zeta_{5/2}\left[e^{-\beta g n_{\mathbf{0}}(r)}\right]\,, \tag{16.33}$$

$$p_{\mathrm{th},2}(r) = \frac{1}{\beta\lambda^3}\,\zeta_{5/2}\left[e^{-\beta\left(2g\,n_{\mathrm{th},2}(r)+\Phi(r)-\mu\right)}\right]\,. \tag{16.34}$$

The results can be obtained in analogy to the solution for the thermal density in the respective regimes. For thermal fluctuations, the results (16.33) and (16.34) are exactly what is to be expected for a thermal gas of bosons, and confirm the vanishing pressure of free bosons for zero temperatures as found in Ref. [135], where an equation of state for systems of self-gravitating bosons and fermions has been investigated.

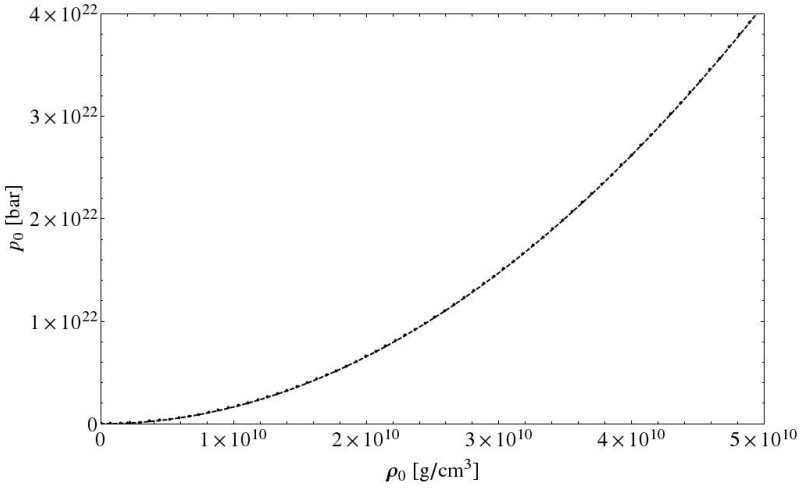

Figure 16.6.: Equation of state of the condensate for the example of $T = 5 \cdot 10^7$K and $N_{\text{tot}} = 10^{56}$, as obtained from the exact formulation (dots) and the equation of state for the zero-temperature limit (dashed). The curves are so close that they cannot be distinguished in this plot.

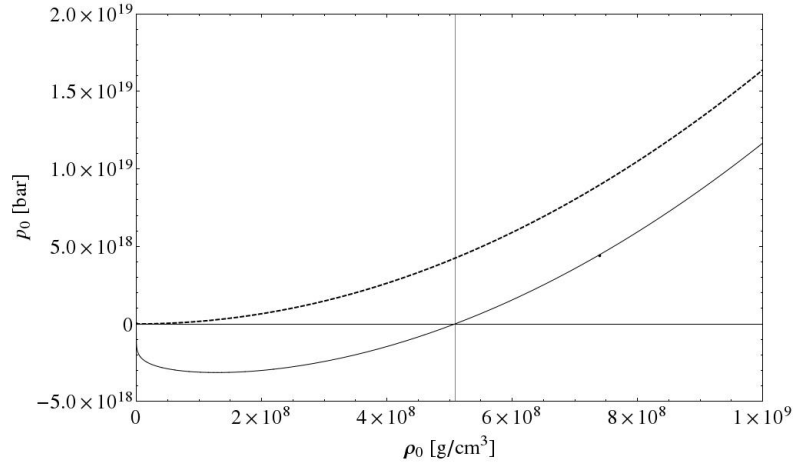

Figure 16.7.: Equation of state of the condensate, as obtained from the exact formulation (dots), a numerical fit (solid) as given by Eqs. (16.28) and (16.29) and the equation of state for the zero-temperature limit (dashed), in a close-up for small densities. The vertical line represents the density $\rho_{\mathbf{0}} \simeq 5.089 \cdot 10^8 \text{g/cm}^3$ for which the pressure becomes negative.

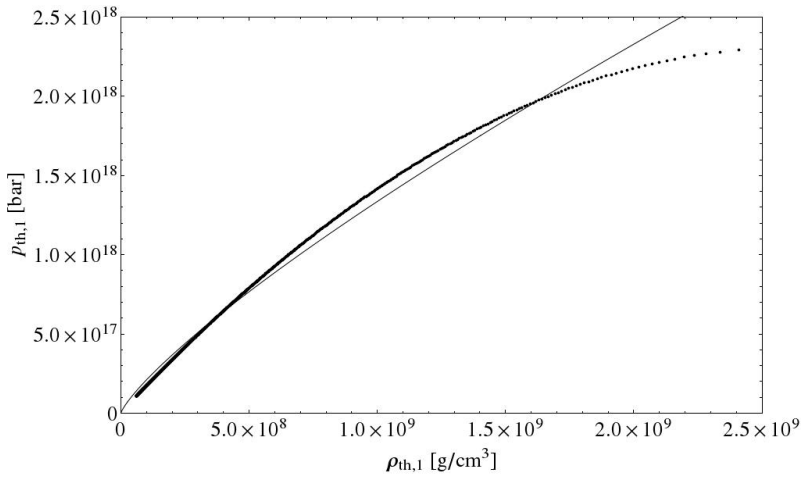

Figure 16.8.: Equation of state of the thermal density in the inner regime, as obtained from the exact formulation (dots) and a numerical fit (solid) as given by Eqs. (16.35) and (16.36).

Since in the inner regime, both thermal density and pressure are given as an analytic function of the condensate density, we can plot the equation of state directly from Eq. (16.33), shown in Fig. 16.8 (dots). Carrying out a fit of the curve of the general form

$$p_{\mathrm{th},1} = c_1 \, \rho_{\mathrm{th},1}^{c_2} \,, \tag{16.35}$$

we find the best fit values for the parameters as

$$c_1 = 8.2 \cdot 10^{10} \,, \quad c_2 = 0.801 \,. \tag{16.36}$$

The value of the exponent c_2 corresponds to a polytropic index $n = -5.033$, again a negative value denoting a metastable state.
For the equation of state in the outer regime, the pressure can in principle be calculated by Eq. (16.34), in analogy to the solution for the thermal density in the outer region. However, since the solution in the outer regime falls off very quickly, and as a result, the thermal pressure is only given for a very small range of density, it is not possible to obtain a meaningful curve for the corresponding equation of state.

16.5.4. Maximum mass

Ultimately, we can proceed to derive a maximum mass for the system by employing the upper limit on the speed of sound as outlined before. We will consider the speed of sound

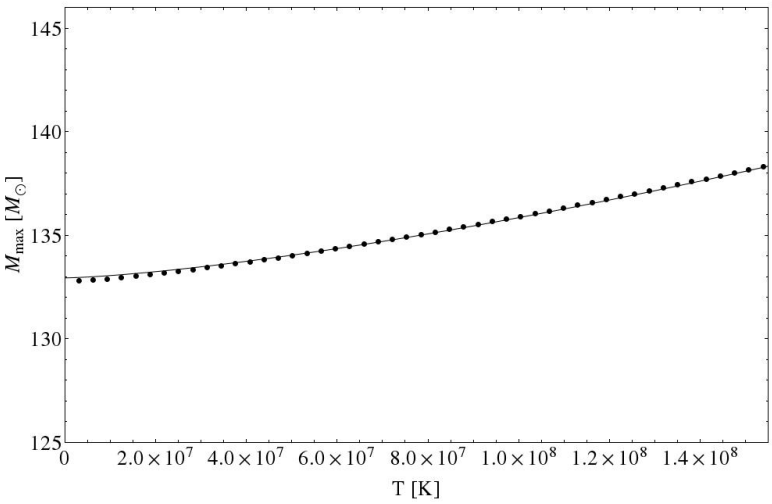

Figure 16.9.: Maximum mass as a function of temperature, as inferred from the limits given by the speed of sound criterion: numerical results (dots) and a fit (solid) as given by Eqs. (16.40) and (16.41).

in the center of the configuration, and calculate c_S by derivation of $p_{\mathbf{0}}$ given by Eq. (16.26) with respect to $\rho_{\mathbf{0}}$, neglecting the pressure of the thermal cloud at the center of the star. As a result, we obtain the condition

$$c_S^2 = \frac{\partial p_{\mathbf{0}}}{\partial \rho_{\mathbf{0}}} = \frac{g}{m^2}\,\rho_{\mathbf{0}} - \frac{2\beta g^2}{m^2\lambda^3}\,\rho_{\mathbf{0}}\,\zeta_{1/2}\left[e^{-\frac{\beta g}{m}\rho_{\mathbf{0}}}\right] \leq c^2\,. \tag{16.37}$$

This criterion can be directly tested for all simulations by inserting the condensate density at the center of the star. It turns out that all simulated cases obey this relation, and the speed of sound does not exceed the speed of light in any of the computed cases. We can now further use this relation to obtain a dependence of the maximum mass on the temperature.

Considering the limiting case of $c_S = c$ in Eq. (16.37), we can calculate the maximum central condensate density $\rho_c^{(\max)}$ in dependence of the temperature. Together with the temperature-dependent result for the thermal radius $R_{\rm th}(T)$ obtained from the numerical solutions, we can then approximately calculate the maximum mass of the configuration by adapting the result (12.28) for non-zero temperatures,

$$M^{(\max)}(T) = \frac{4}{\pi}\,R_{\rm th}^3(T)\,\rho_c^{(\max)}(T)\,. \tag{16.38}$$

The thermal radius of the system can be obtained from the numerical results interpolated with the fitting function given by (16.14) and (16.16). The resulting curve for the maximum allowed masses is shown in Fig. 16.9.

The zero-temperature limit corresponds to the value predicted in Section 12.1,

$$M_{\max}(0) = 4\pi^2 \left(\frac{\hbar^2 a}{G_N m^3}\right)^{3/2} \rho_c \simeq 132.94\, M_\odot\,. \tag{16.39}$$

The qualitative temperature dependence of $M_{\max}$ can be inferred again from a fit of the curve with a general fitting function

$$M_{\max}(T) = M_{\max}(0) + d_1\, T^{d_2}\,, \tag{16.40}$$

resulting in the best fit values

$$d_1 = 1.58 \cdot 10^{-11}\,, \quad d_2 = 1.408\,. \tag{16.41}$$

We obtain a small, but distinct dependence on the temperature to the power of 3/2.
The values computed for the maximum masses of the system are rather high, two orders of magnitude larger than the mass limit predicted by Chandrasekhar for an $n = 3$ polytrope in Eq. (12.11). The discrepancy is due to the different properties of matter with a polytropic index $n = 1$.

17. Conclusions and Outlook

The work in this last part of this dissertation investigated the occurrence of a Bose-Einstein condensate phase in compact astrophysical objects, which, after careful consideration of the typical environments in some examples of compact objects, is a viable possibility and thus validates the efforts spent to study such a system and compute observable quantities that can be compared to observations. The problem in question was treated within the framework of a Hartree-Fock theory, starting from a Hamiltonian including contact and gravitational interactions between the particles. Self-consistency equations determining the wave functions of condensate and thermal fluctuations were obtained from the variation of the free energy of the system. In analogy to these derivations, the semi-classical limit of both the free energy and the Hartree-Fock equations was formulated, describing the system in terms of the densities of condensate and thermal fluctuations. The resulting equations were processed further up to a certain point, before the solution for both the profiles of condensate and thermal density as a function of the radial distance from the center of the star was obtained by iterative and numerical procedures. Integrating out the obtained densities leads to the total mass of the system, which was calculated in the last part along with other quantities, where astrophysical consequences were elaborated.

The theory contains several simplifications introduced in order to make the system more treatable. Some of them were mathematically motivated, whereas others have been general physical assumptions within our model from the beginning. We considered a phenomenon mainly known from ultracold quantum gases in laboratory scenarios and applied the established mathematical treatment to a rather unusual field of application, namely the large scales of astrophysics. It is therefore to be expected that simplifications and idealizations are necessary in order to obtain results.

On the mathematical side, we have carried out a Hartree-approximation for the gravitational part of the interactions in order to avoid having to deal with the bilocal Fock terms occurring in the expressions. This approximation is a priori not justified, but was however necessary to further proceed with the calculations.

As already mentioned in the introductory chapter, this work considers a star consisting of helium particles only, i.e. a very idealized system of identical particles, assuming that the existence of other elements like hydrogen or carbon and oxygen is negligible. The

calculations have thus been carried out up to a maximum temperature of about 10^8 K, the onset of fusion processes of helium to heavier nuclei. The theory is strictly limited to low temperatures, where by definition the particles in the thermal phase are few and the condensate dominates. The necessity to develop a more complete theory featuring a smoother description of the high-temperature transition region between condensate and thermal state of the system, incorporating the breakdown of the condensate as a phase transition, is however obvious. A further assumption of the theory is a spatially constant temperature throughout the star. In realistic physical situations, this is unlikely to hold, since towards the surface of the star the temperature decreases. This is closely connected to the issue of breakdown of the condensate towards the outer layers of the star, which is inevitable without the inclusion of temperature variation. A spatial gradient of temperature would provide the possibility for the conservation of condensate even in these outer regimes, if the temperature would fall steeply enough in the outermost 1% of the star.
Furthermore, we neglect the ionization of the helium particles and thus also disregard the presence of a sea of electrons. Thus, in more realistic scenarios, Coulomb interactions between the ions and the existence of a Fermi fluid of electrons should be included. In such a system, the gravitational pressure is mainly balanced by the electron degeneracy pressure, and the situation can be well described by the phenomenological theory developed by Chandrasekhar, as presented in Chapter 12 - a very different approach. Having obtained our results, we can now compare the predictions for white dwarfs from Refs. [134, 147] to our outcomes. In particular, we have obtained much higher maximum masses for our configurations than in Chandrasekhar's approach, with a difference of two orders of magnitude. This is due to the difference in the polytropic index, i.e. the fact that bosons can exist in much denser states than fermions. This is mirrored in the central density of the compact object as well, which in our case lies in the region of $10^{10}\,\mathrm{g/cm^3}$, three orders of magnitude higher than the central densities in Chandrasekhar's approach [134]. Equivalently, the size scales of the stars obtained in our calculations are about one order of magnitude smaller, i.e. instead of the usual radii of white dwarfs of the order of the earth's radius, we obtained objects with radii only around 200 km. In short, our model results in smaller, denser and heavier white dwarfs than conventionally assumed, which is attributed to the very different state of matter we have been considering in this work.
In this context, we would like to comment on the possibility of rotation. It is presumed that most of the compact objects in the universe rotate, since an evolution of a completely static system is highly unlikely in an initially hot and violent universe. Rotation of BECs in laboratory environments have been shown to exhibit new phenomena like the formation of vortices of normal phase matter inside the BEC [152], growing with increasing temperature until the breakdown of condensate at the transition to the thermal phase. The existence of

a vortex in a Bose star, or, more realistically, a grid of vortices, should be assumed, which grow in width and finally cause a transition to a normal phase Bose star with an increase in temperature. The inclusion of rotation is expected to lead to a destabilization of the system due to the presence of tidal forces, and thus should lead to a smaller maximum mass. Considering this, the developed theory has already led to reasonable results. However, of course there is a large number of possibilities to generalize and extend the present work.

Bibliography

[1] A. Einstein. Die Grundlagen der allgemeinen Relativitätstheorie. *Ann. d. Phys.*, 49:769–822, 1916.

[2] H. Kleinert. *Multivalued Fields in Condensed Matter, Electromagnetism, and Gravitation,* Chapter 11, p. 337, Eq. (11.128), `http://klnrt.de/b11`. World Scientific, 2008.

[3] S. Weinberg. *Gravitation and cosmology: principles and applications of the general theory of relativity.* Wiley, 1972.

[4] A. Friedmann. Über die Krümmung des Raumes. *Zeitschr. f. Phys.*, 10:377–385, 1922.

[5] A. G. Riess et al. (High-z Supernova Search Team). Observational evidence from supernovae for an accelerating universe and a cosmological constant. *Astron. J.*, 116:1009, 1998.

[6] S. Perlmutter et al. (Supernova Cosmology Project). Measurements of Omega and Lambda from 42 high redshift supernovae. *Astrophys. J.*, 517:565–586, 1999.

[7] P. M. Garnavich et al. Supernova limits on the cosmic equation of state. *Astrophys. J.*, 509:74, 1998.

[8] S. M. Carroll. Why is the universe accelerating? *AIP Conf. Proc.*, 743:16–32, 2005.

[9] M. Tegmark et al. Cosmological constraints from the SDSS luminous red galaxies. *Phys. Rev. D*, 74:123507, 2006.

[10] E. Komatsu et al. (WMAP Collaboration). Seven-year Wilkinson Microwave Anisotropy Probe (WMAP) observations: Cosmological interpretation. *Astrophys. J. Suppl.*, 192:18, 2011.

[11] P. A. R. Ade et al. (Planck collaboration). Planck 2013 results. XVI. Cosmological parameters. arXiv:1303.5076 [astro-ph.CO], 2013.

[12] M. Visser. Cosmography: Cosmology without the Einstein equations. *Gen. Rel. Grav.*, 37:1541–1548, 2005.

[13] C. Cattoen and M. Visser. Cosmographic Hubble fits to the supernova data. *Phys. Rev. D*, 78:063501, 2008.

[14] S. Weinberg. *Cosmology*. Oxford University Press, 2008.

[15] A. Aviles, C. Gruber, O. Luongo, and H. Quevedo. Cosmography and constraints on the equation of state of the universe in various parametrizations. *Phys. Rev. D*, 86:123516, 2012.

[16] C. Gruber and O. Luongo. Cosmographic analysis of the equation of state of the universe through Padé approximations. arXiv:1309.3215 [gr-qc], accepted for publication in Phys. Rev. D, 2013.

[17] H. Kleinert. Is dark matter made entirely of the gravitational field? *Phys. Scripta*, T 151:14081, `http://klnrt.de/395`, 2012.

[18] K. Huang. Dark energy and dark matter in a superfluid universe. arXiv:1309.5707 [gr-qc], 2013.

[19] T. Padmanabhan. Dark energy and gravity. *Gen. Rel. Grav.*, 40:529–564, 2008.

[20] H. Kleinert and H.-J. Schmidt. Cosmology with curvature-saturated gravitational Lagrangian. *Gen. Rel. Grav.*, 35:1295, `http://klnrt.de/311`, 2002.

[21] T. P. Sotiriou and V. Faraoni. f(R) theories of gravity. *Rev. Mod. Phys.*, 82:451–497, 2010.

[22] R. Durrer and R. Maartens. Dark energy and dark gravity. *Gen. Rel. Grav.*, 40:301, 2008.

[23] D. Lovelock. The Einstein tensor and its generalizations. *J. Math. Phys.*, 12:498, 1971.

[24] K. S. Stelle. Classical gravity with higher derivatives. *Gen. Rel. Grav.*, 9:353–371, 1978.

[25] P. D. Mannheim. Alternatives to dark matter and dark energy. *Prog. Part. Nucl. Phys.*, 56:340–445, 2006.

[26] A. Palatini. Deduzione invariantiva delle equazioni gravitazionali dal principio di Hamilton. *Rend. Circ. Mat. Palermo*, 43:203, 1919.

[27] V. Vitagliano, T. P. Sotiriou, and S. Liberati. The dynamics of metric-affine gravity. *Ann. d. Phys.*, 326:1259–1273, 2011.

[28] R Utiyama. Invariant theoretical interpretation of interaction. *Phys. Rev.*, 101:1597, 1956.

[29] A. Lasenby, C. Doran, and S. Gull. Gravity, gauge theories and geometric algebra. *Phil. Trans. Roy. Soc. Lond. A*, 356:487, 1998.

[30] P. J. E. Peebles and B. Ratra. The cosmological constant and dark energy. *Rev. Mod. Phys.*, 75:559–606, 2003.

[31] E. J. Copeland, M. Sami, and S. Tsujikawa. Dynamics of dark energy. *Int. J. Mod. Phys. D*, 15:1753–1936, 2006.

[32] C. Wetterich. Cosmology and the fate of dilatation symmetry. *Nucl. Phys. B*, 302:668–696, 1988.

[33] I. Zlatev, L. Wang, and P. J. Steinhardt. Quintessence, cosmic coincidence, and the cosmological constant. *Phys. Rev. Lett.*, 82:896–899, 1999.

[34] R. R. Caldwell. A phantom menace? Cosmological consequences of a dark energy component with super-negative equation of state. *Phys. Lett. B*, 545:23–29, 2002.

[35] C. Armenderiaz-Picon, T. Damour, and V. Mukhanov. k-inflation. *Phys. Lett. B*, 458:209–218, 1999.

[36] C. Armenderiaz-Picon, V. Mukhanov, and P. J. Steinhardt. Dynamical solution to the problem of a small cosmological constant and late-time cosmic acceleration. *Phys. Rev. Lett.*, 85:4438–4441, 2000.

[37] J. W. Moffat. Scalar-tensor-vector gravity theory. *JCAP*, 3:004, 2006.

[38] J. D. Bekenstein. Relativistic gravitation theory for the MOND paradigm. *Phys. Rev. D*, 70:083509, 2004.

[39] M. Milgrom. A modification of the Newtonian dynamics as a possible alternative to the hidden mass hypothesis. *Astrophys. J.*, 270:365–370, 1983.

[40] A. Halle, H. Zhao, and B. Li. A nonuniform dark energy fluid: Perturbation equations. *Astrophys. J. Supp.*, 177:1, 2008.

[41] F. C. Carvalho, J. S. Alcaniz, J. A. S. Lima, and R. Silva. Scalar-field-dominated cosmology with a transient accelerating phase. *Phys. Rev. Lett.*, 97:081301, 2006.

[42] A. D. Sakharov. Vacuum quantum fluctuations in curved space and the theory of gravitation. *Sov. Phys. Dokl.*, 12:1040, 1968. reprinted in Gen. Rel. Grav. 32, 365-367, 2000.

[43] H. B. G. Casimir and D. Polder. The influence of retardation on the London-van der Waals forces. *Phys. Rev.*, 73:360, 1948.

[44] S. W. Hawking. Black hole explosions. *Nature*, 248:30–31, 1974.

[45] S. P. Martin. A Supersymmetry primer. arXiv:9709356 [hep-ph], 1997.

[46] R. Aaij et al. (LHCb Collaboration). First evidence for the decay $b_s^0 \to \mu_+\mu_-$. *Phys. Rev. Lett.*, 110:021801, 2013.

[47] M. Shifman. Reflections and impressionistic portrait at the conference "Frontiers beyond the standard model". arXiv:1211.0004 [physics.pop-ph], 2012.

[48] H. Kleinert. *Path Integrals in Quantum Mechanics, Statistics, Polymer Physics, and Financial Markets,* `http://klnrt.de/b5`. World Scientific, 2009.

[49] H. Kleinert. Collective quantum fields. *Fortschr. Physik*, 26:565–571, `http://klnrt.de/55`, 1978.

[50] N. Bilic, S. Domazet, and B. Guberina. Vacuum fluctuations of the supersymmetric field in curved background. *Phys. Lett. B*, 707:221, 2012.

[51] H. Kleinert and V. Schulte-Frohlinde. *Critical Properties of ϕ^4 Theories,* `http://klnrt.de/b8`. World Scientific, 2001.

[52] See Ref. [51], Chapter 8, p. 107, Eq. (8.27).

[53] See Ref. [51], Chapter 8, p. 128, Eq. (8D.24).

[54] G. Leibbrandt. Introduction to the technique of dimensional regularization. *Rev. Mod. Phys.*, 74:849, 1975.

[55] M. J. G. Veltman. The infrared - ultraviolet connection. *Acta Phys. Polon. B*, 12:437, 1981.

[56] See Ref. [51], Chapter 8, p. 106, Eq. (8.20).

[57] N. D. Birrell and P. C. W. Davies. *Quantum Fields in Curved Space.* Cambridge University Press, 1984.

[58] L. E. Parker and D. J. Toms. *Quantum Field Theory in Curved Spacetime*. Cambridge University Press, 2009.

[59] See Ref. [48], Chapter 13, p. 973, Eq. (13.245).

[60] See Ref. [48], Chapter 10.3.2, Chapter 11.5.

[61] B. de Witt. *Dynamical Theory of Groups and Fields*. Gordon and Breach, 1965.

[62] S. M. Christensen. Vacuum expectation value of the stress tensor in an arbitrary curved background: The covariant point-separation method. *Phys. Rev. D*, 14:2490–2501, 1976.

[63] S. M. Christensen. Regularization, renormalization, and covariant geodesic point separation. *Phys. Rev. D*, 17:946–963, 1978.

[64] T. S. Bunch and L. Parker. Feynman propagator in curved spacetime: A momentum-space representation. *Phys. Rev. D*, 20:2499–2510, 1979.

[65] L. Parker and D. J. Toms. New form for the coincidence limit of the Feynman propagator, or heat kernel, in curved spacetime. *Phys. Rev. D*, 31:953–956, 1985.

[66] L. Parker and D. J. Toms. Explicit curvature dependence of coupling constants. *Phys. Rev. D*, 31:2424–2438, 1985.

[67] D. V. Vassilevich. Heat kernel expansion: User's manual. *Phys. Rep.*, 338:279, 2003.

[68] See Ref. [48], Chapter 12, p. 932, Eq. (12.25).

[69] G. Aad et al. (ATLAS Collaboration). Observation of a new particle in the search for the standard model Higgs boson with the ATLAS detector at the LHC. *Phys. Lett. B*, 719:1–29, 2012.

[70] S. Chatrchyan et al. (CMS Collaboration). Observation of a new boson at a mass of 125 GeV with the CMS experiment at the LHC. *Phys. Lett. B*, 719:30–61, 2012.

[71] W. N. Cottingham and D. A. Greenwood. *An Introduction to the Standard Model of Particle Physics*. Cambridge University Press, 1998.

[72] `http://en.wikipedia.org/wiki/File:Standard_Model_of_Elementary_Particles.svg` .

[73] V. Trimble. Existence and nature of dark matter in the universe. *Ann. Rev. Astron. Astrophys.*, 25:425–472, 1987.

[74] V. Springel et al. Simulations of the formation, evolution and clustering of galaxies and quasars. *Nature*, 435:629–636, 2005.

[75] J. Einasto, I. Suhhonenko, and G. Hütsi. Towards understanding the structure of voids in the cosmic web. *Astron. & Astrophys.*, 534:A128, 2011.

[76] T. Buchert, M. Kerscher, and C. Sicka. Back reaction of inhomogeneities on the expansion: The evolution of cosmological parameters. *Phys. Rev. D*, 62:043525, 2000.

[77] M. Kerscher, T. Buchert, and T. Futamase. On the abundance of collapsed objects. *Astrophys. J.*, 558:L79–L82, 2001.

[78] T. Buchert. Dark energy from structure - a status report. *Gen. Rel. Grav.*, 40:467–527, 2008.

[79] H. Kleinert. `http://klnrt.de/talks/CastTaiw.ppt`; `http://klnrt.de/403`; `http://klnrt.de/406`; `http://klnrt.de//399/399-TAIPEH.pdf`.

[80] N. Suzuki et al. (Supernova Cosmology Project). The Hubble Space Telescope cluster supernova survey: V. Improving the dark energy constraints above $z > 1$ and building an early-type-hosted supernova sample. *Astrophys. J.*, 746:85, 2012.

[81] K. Bamba, S. Capozziello, S. Nojiri, and S. D. Odintsov. Dark energy cosmology: The equivalent description via different theoretical models and cosmography tests. *Astrophys. Space Sci.*, 342:155–228, 2012.

[82] M. Li, X.-D. Li, S. Wang, and Y. Wang. Dark energy. *Commun. Theor. Phys.*, 56:525, 2011.

[83] J. L. Cervantes-Cota and G. Smoot. Cosmology today - a brief review. *AIP Conf. Proc.*, 1396:28–52, 2011.

[84] J. Martin. Everything you always wanted to know about the cosmological constant problem (but were afraid to ask). *Compt. Rend. Phys.*, 13:566, 2012.

[85] N. Arkani-Hamed, L. J. Hall, C. Kolda, and H. Murayama. A new perspective on cosmic coincidence problems. *Phys. Rev. Lett.*, 85:4434, 2000.

[86] M. Kunz. The phenomenological approach to modeling the dark energy. *Compt. Rend. Phys.*, 13:539–565, 2012.

[87] R. R. Caldwell and M. Kamionkowski. Expansion, geometry, and gravity. *JCAP*, 9:009, 2004.

[88] M. Visser. Jerk, snap and the cosmological equation of state. *Class. Quant. Grav.*, 21:2603–2615, 2004.

[89] S. Capozziello, R. Lazkoz, and V. Salzano. Comprehensive cosmographic analysis by Markov chain method. *Phys. Rev. D*, 84:124061, 2011.

[90] C. Cattoen and M. Visser. Cosmography: Extracting the Hubble series from the supernova data. arXiv:0703122 [gr-qc], 2007.

[91] C. Cattoen and M. Visser. The Hubble series: Convergence properties and redshift variables. *Class. Quant. Grav.*, 24:5985, 2007.

[92] E. R. Harrison. Observational tests in cosmology. *Nature*, 260:591, 1976.

[93] P. T. Landsberg. Q in cosmology. *Nature*, 263:217, 1976.

[94] H. Padé. Sur la représentation approchée d'une fonction par des fractions rationelles. *Ann. Sci. Ecole Norm. Sup.*, 9:1–93, 1892.

[95] S. G. Krantz and H. R. Parks. *A primer of real analytic functions.* Birkhäuser, 1992.

[96] A. R. Liddle, P. Parsons, and J. D. Barrow. Formalising the slow-roll approximation in inflation. *Phys.Rev. D*, 50:7222, 1994.

[97] V. Nestoridis. Universal Padé approximants with respect to the chordal metric. *J. of Contemp. Math. Anal.*, 47:168–181, 2012.

[98] M. Della Morte, B. Jager, A. Juttner, and H. Wittig. Towards a precise lattice determination of the leading hadronic contribution to $(g-2)_\mu$. *JHEP*, 1203:055, 2012.

[99] R. Amanullah et al. (Supernova Cosmology Project). Spectra and light curves of six type ia supernovae at $0.511 < z < 1.12$ and the union2 compilation. *Astrophys. J.*, 716:712–738, 2010.

[100] A. G. Riess et al. A redetermination of the Hubble constant with the Hubble Space Telescope from a differential distance ladder. *Astrophys. J.*, 699:539–563, 2009.

[101] D. Stern, R. Jimenez, L. Verde, M. Kamionkowski, and S. A. Stanford. Cosmic chronometers: constraining the equation of state of dark energy. i: H(z) measurements. *JCAP*, 2:008, 2010.

[102] A. Lewis and S. Bridle. Cosmological parameters from CMB and other data: A Monte-Carlo approach. *Phys. Rev. D*, 66:103511, 2002.

[103] N. Metropolis, A. W. Rosenbluth, M. N. Rosenbluth, A. H. Teller, and E. Teller. Equation of state calculations by fast computing machines. *J. Chem. Phys.*, 21:1087, 1953.

[104] H. Haario, E. Saksman, and J. Tamminen. Adaptive proposal distribution for random walk Metropolis algorithm. *Comput. Stat.*, 14:375–395, 1999.

[105] S. Brooks, A. Gelman, G. Jones, and X.-L. Meng. *Handbook of Markov chain Monte Carlo*. Chapman and Hall/CRC, 2011.

[106] L. Verde. Statistical methods in cosmology. *Lect. Not. Phys.*, 800:147–177, 2010.

[107] M. H. Anderson, J. R. Ensher, M. R. Matthews, C. E. Wieman, and E. A. Cornell. Observation of Bose–Einstein condensation in a dilute atomic vapor. *Science*, 269:198–201, 1995.

[108] K. B. Davis, M.-O. Mewes, M. R. Andrews, M. J. Van Druten, D. S. Durfee, D. M. Kurn, and W. Ketterle. Bose-Einstein condensation in a gas of sodium atoms. *Phys. Rev. Lett.*, 75:3969–3973, 1995.

[109] S. N. Bose. Plancks Gesetz und Lichtquantenhypothese (Planck's law and light quantum hypothesis). *Zeitschr. f. Phys.*, 26:178–181, 1924.

[110] A. Einstein. Quantentheorie des einatomigen idealen Gases. *Sitz.ber. Preuss. Akad. Wiss.*, 1:3–14, 1925.

[111] `http://patapsco.nist.gov/imagegallery/details.cfm?imageid=193` .

[112] B. Kleihaus, J. Kunz, and S. Schneider. Stable phases of Boson stars. *Phys. Rev. D*, 85:024045, 2012.

[113] O. G. Benvenuto and M. A. Vito. On the occurrence and detectability of Bose-Einstein condensation in Helium white dwarfs. *JCAP*, 2:033, 2011.

[114] N. Nag and S. Chakrabarty. Can a very low-luminosity and cold white dwarf be a self-gravitating Bose condensed system? arXiv:0008477 [astro-ph], 2000.

[115] P. H. Chavanis and T. Harko. Bose-Einstein condensate general relativistic stars. *Phys. Rev. D*, 86:064011, 2012.

[116] R. C. Tolman. Static solutions of Einstein's field equations for spheres of fluid. *Phys. Rev.*, 55:364–373, 1939.

[117] J. R. Oppenheimer and G. M. Volkoff. On massive neutron cores. *Phys. Rev.*, 55:374–381, 1939.

[118] P. B. Demorest, T. Pennucci, S. M. Ransom, M. S. E. Roberts, and J. W. T. Hessels. A two-solar-mass neutron star measured using Shapiro delay. *Nature*, 467:1081–1083, 2010.

[119] P. Haensel, A. Y. Potekhin, and D. G. Yakovlev. *Neutron Stars 1: Equation of State and Structure*. Springer, 2007.

[120] R. Belvedere, D. Pugliese, J. A. Rueda, R. Ruffini, and S.-S. Xue. Neutron star equilibrium configurations within a fully relativistic theory with strong, weak, electromagnetic, and gravitational interactions. *Nucl. Phys. A*, 883:1–24, 2012.

[121] D. Page, M. Prakash, J. M. Lattimer, and A. W. Steiner. Rapid cooling of the neutron star in Cassiopeia A triggered by neutron superfluidity in dense matter. *Phys. Rev. Lett.*, 106:081101, 2011.

[122] C. A. R. Sa de Melo, M. Randeria, and J. R. Engelbrecht. Crossover from BCS to Bose superconductivity: Transition temperature and time-dependent Ginzburg-Landau theory. *Phys. Rev. Lett.*, 71:3202, 1993.

[123] J. R. Engelbrecht, M. Randeria, and C. A. R. Sa de Melo. BCS to Bose crossover: Broken-symmetry state. *Phys. Rev. B*, 55:15153, 1997.

[124] M. Greiner, C. A. Regal, and D. S. Jin. Emergence of a molecular Bose-Einstein condensate from a Fermi gas. *Nature*, 426:537, 2003.

[125] L. Salasnich. Fermionic condensation in ultracold atoms, nuclear matter and neutron stars. *22nd International Laser Physics Workshop Proc.*, arXiv:1308.0922 [cond-mat.quant-gas], 2013.

[126] E. E. Salpeter. Nuclear reactions in stars without hydrogen. *Astrophys. J.*, 115:326–328, 1952.

[127] G. Laughlin, P. Bodenheimer, and F. C. Adams. The end of the main sequence. *Astrophys. J.*, 482:420, 1997.

[128] C. J. Lada. Stellar multiplicity and the IMF: Most stars are single. *Astrophys. J.*, 640:L63–L66, 2006.

[129] J. Liebert, P. Bergeron, D. Eisenstein, H. C. Harris, S. J. Kleinman, A. Nitta, and J. Krzesinski. A Helium white dwarf of extremely low mass. *Astrophys. J.*, 606:L147–L149, 2004.

[130] D. J. Eisenstein et al. A catalog of spectroscopically confirmed white dwarfs from the Sloan Digital Sky Survey data release 4. *Astrophys. J. Supp.*, 167:40–58, 2006.

[131] A. Eddington. *The Internal Constitution of the Stars*. Cambridge University Press, 1930.

[132] E. C. Stoner. The limiting density of white dwarf stars. *Phil. Mag. (7th series)*, 7:63–70, 1929.

[133] W. Anderson. Über die Grenzdichte der Materie und der Energie. *Zeitschr. f. Phys.*, 56:851–856, 1929.

[134] S. Chandrasekhar. The maximum mass of ideal white dwarfs. *Astrophys. J.*, 74:81–82, 1931.

[135] R. Ruffini and S. Bonazzola. Systems of self-gravitating particles in general relativity and the concept of an equation of state. *Phys. Rev.*, 187:1767–1783, 1969.

[136] T. Harko and G. Mocanu. Cosmological evolution of finite temperature Bose-Einstein condensate dark matter. *Phys. Rev. D*, 85:084012, 2012.

[137] P. H. Chavanis. BEC dark matter, Zeldovich approximation, and generalized Burgers equation. *Phys. Rev. D*, 84:063518, 2011.

[138] T. Harko. Cosmological dynamics of dark matter Bose-Einstein condensation. *Phys. Rev. D*, 83:123515, 2011.

[139] X. Y. Li, T. Harko, and K. S. Cheng. Condensate dark matter stars. *JCAP*, 6:001, 2012.

[140] T. Matos and A. Suarez. Bose-Einstein condensate dark matter phase transition from U(1) symmetry breaking. *Europhys. Lett.*, 96:56005, 2011.

[141] L. D. Landau and E. M. Lifshitz. *Statistical Physics*. Elsevier, 3rd edition, 1980.

[142] C. Gruber and A. Pelster. Bose-Einstein condensates in compact astrophysical objects. *Proc. Int. Symp. on Synergetics, Ed. A. Pelster and G. Wunner, Springer (to be published)*, 2013.

[143] P. Oehberg and S. Stenholm. A Hartree-Fock study of a Bose-condensed gas. *J. Phys. B: At. Mol. Opt. Phys.*, 30:2749, 1997.

[144] P.M. Stevenson. Optimized perturbation theory. *Phys. Rev. D*, 23:2916–2944, 1981.

[145] G. C. Wick. The evaluation of the collision matrix. *Phys. Rev.*, 80:268–272, 1950.

[146] I. S. Gradshteyn and I. M. Ryzhik. *Table of integrals, series and products,* Eq. (3.361). Academic Press Inc., 1965.

[147] S. Chandrasekhar. The highly collapsed configurations of a stellar mass (Second paper). *MNRAS*, 95:207–225, 1935.

[148] M. L. Kutner. *Astronomy: A physical perspective.* Cambridge University Press, 2003.

[149] H. Kleiner. Five-loop critical temperature shift in weakly interacting homogeneous Bose-Einstein condensate. *Mod. Phys. Lett. B*, 17:1011, 2003.

[150] B. Kastening. Bose-Einstein condensation temperature of a homogeneous weakly interacting Bose gas in variational perturbation theory through six loops. *Phys. Rev. A*, 68:061601, 2003.

[151] G. P. Horedt. *Polytropes: Applications In Astrophysics And Related Fields.* Springer, 2004.

[152] A. L. Fetter. Rotating trapped Bose-Einstein condensates. *Rev. Mod. Phys.*, 81:647–691, 2009.

Publications

Some ideas and figures have appeared previously in the following publications:

[1] A. Aviles, C. Gruber, O. Luongo, H. Quevedo. Cosmography and constraints on the equation of state of the Universe in various parametrizations. *Phys. Rev. D*, 86:123516, 2012. arXiv:1204.2007 [astro-ph.CO].

[2] A. Aviles, C. Gruber, O. Luongo, H. Quevedo. Constraints from Cosmography in various parameterizations. *Proc. 13th Marcel Grossmann Meeting*, Stockholm, Sweden. World Scientific, 2012. arXiv:1301.4044 [astro-ph.CO].

[3] C. Gruber, A. Pelster. Bose-Einstein condensates in astrophysical compact objects. *Proc. Int. Symp. on Self-Organization of Complex Systems*, Hanse Institute of Advanced Studies, Delmenhorst, Germany. Ed. A. Pelster, G. Wunner, Springer, 2013. (to be published)

[4] C. Gruber, O. Luongo. Cosmographic analysis of the equation of state of the universe through Padé approximations. Accepted for publication in Phys. Rev. D, 2013. arXiv:1309.3215 [gr-qc].

[5] C. Gruber, H. Kleinert. Observed Cosmological Reexpansion in Minimal QFT with Bose and Fermi Fields. Submitted to Gen. Rel. Grav., 2013.

[6] C. Gruber, A. Pelster. Bose-Einstein condensates in white dwarfs. In preparation, 2013.

Acknowledgments

Even though a PhD ends with a thesis carrying the name of one person alone, there are many people without whom the dissertation in this form wouldn't have been possible. Since I cannot put everyone on the front page, I'd like to credit some of them here.

Many thanks go to my supervisor Prof. Dr. Dr. h.c. mult. Hagen Kleinert, who has guided me in my scientific development within the last years, and shaped my understanding and perception of physics. His lively mind and his interconnected and all-embracing knowledge have been a great inspiration, and I would like to thank him for taking me on as a student and dedicating his time to me.

I'd like to thank my collaborators for the cosmography part of this thesis, Dr. Orlando Luongo, Dr. Alejandro Aviles and Prof. Dr. Hernando Quevedo, who I had the opportunity to meet through the scientific exchanges of my PhD funding program. The work together was a big pleasure and created transnational and transoceanic connections. In particular, I want to thank Orlando for his many ideas and initiative spirit, which made the collaborations possible.

Further, I would like to thank Prof. Dr. Axel Pelster, who mainly supervised me during the last year of my PhD. I have profited very much from his founded knowledge and didactic skills, and am grateful for his teaching me a thorough way of approaching physical problems, questioning and checking every step for physical justification.

I got the opportunity to stay at the University of Oldenburg on the invitation of Prof. Dr. Jutta Kunz-Drolshagen for a few weeks to intensively work on the BEC project of my thesis and enjoyed the hospitality of and scientific exchange with her working group on field theory as well as the Graduate College for Models of Gravity associated with the Universities of Oldenburg and Bremen. Moreover I would like to express my gratitude to ICRANet and its center in Pescara under the direction of Prof. Dr. Remo Ruffini, where I had the privilege to stay for six months during my PhD. In particular, the work and discussions with Prof. Dr. She-Sheng Xue and Prof. Dr. Jorge Rueda were very much appreciated. Further, I'd like to thank D.ssa Federica Di Berardino for her invaluable help, her amazing managing skills and her friendship during my stay.

I'm very grateful for having been chosen to receive the Erasmus Mundus PhD scholarship from the European Commission. I have profited very much from the lively exchange

of ideas between physicists from all over the world and all the possibilities for cross-field connections drawn in the many scientific schools, meetings and conferences offered by the program. Our coordinator Prof. Dr. Pascal Chardonnet has faced a big task in managing the administrative procedures and scientific activities, and I would like to thank him very much for his efforts. Ultimately, I would like to thank Prof. Dr. Dieter Breitschwerdt from the Technical University Berlin for agreeing to be the second referee for this thesis and a member of my PhD defense commission, and fulfilling all the duties connected to this position.

However, life has more than just the scientific aspects to offer - and therefore I'd like to thank with all my heart my companions during the last three-and-some years, who have shared with me the pleasures and hardships of a PhD and have made my life so much more pleasant: in Berlin, my fellow PhD colleagues at the MPI in Golm, who have contributed so much to an even work-life balance, exploring Berlin together with me over the years; as well as my friends from my working group and the various guests to the institute at FU Berlin, with who I have spent many hours drinking tea in the kitchen and an occasional beer in a pub, philosophizing about life and physics. I have enjoyed many interesting schools and conferences in various places, which has allowed me to get to know my fellow PhD colleagues from the EM and IRAP PhD programs, studying in other European cities. The colorful collection of people from all over the world has been the most wonderful environment to work and study and a fascinating occasion for cultural exchange, and I'm grateful for everyone I had the pleasure to meet and become friends with during these past few years.
Finally I'd like to thank my family in Austria, in particular my sister, who is always so much more proud of me than I'd ever be, and my parents, who invariably support me in my endeavors wherever they may lead me, and always offer me a safe haven in their home.

Thank you all.